

A BIOCHEMICAL, PHYSIOLOGICAL AND
STRUCTURAL CHARACTERIZATION OF AzoC,
A NOVEL AZOREDUCTASE
FROM *CLOSTRIDIUM PERFRINGENS*

By

JESSICA MARIE MORRISON

Bachelor of Science in Biology
Saginaw Valley State University
University Center, Michigan
2010

Bachelor of Science in Medical Technology
Saginaw Valley State University
University Center, Michigan
2010

Submitted to the Faculty of the
Graduate College of the
Oklahoma State University
in partial fulfillment of
the requirements for
the Degree of
DOCTOR OF PHILOSOPHY
May, 2015

A BIOCHEMICAL, PHYSIOLOGICAL AND
STRUCTURAL CHARACTERIZATION OF AzoC,
A NOVEL AZOREDUCTASE
FROM *CLOSTRIDIUM PERFRINGENS*

Dissertation Approved:

Dr. Gilbert H. John

Dissertation Adviser

Dr. Babu Z. Fathepure

Dr. Wouter D. Hoff

Dr. Erika I. Lutter

Dr. Edralin A. Lucas

ACKNOWLEDGEMENTS

Very little science is done these days without collaboration. The work in this Dissertation could not have been possible without the time and help of others. I would like to thank Dr. Gilbert John, first and foremost, for his guidance and support over these years. In addition, the support and feedback from my committee (Dr. Babu Fathepure, Dr. Erika Lutter, Dr. Edralin Lucas, Dr. William Picking and Dr. Wouter Hoff) has been so very valuable.

I would like to thank the DNA/Protein Core Facility in the Biochemistry Department, specifically Dr. Steve Hartson and Janet Rogers, for their help with mass spectroscopy of metabolites and proteins. In addition, I would like to thank Dr. Mark Payton in the Statistics Department for his help with statistical analysis of large data sets and Dr. Jason Belden and Shane Morrison in the Zoology Department for their help with HPLC. I would also like to thank Dr. David Jacobs in the Chemistry Department for his help with LC-MS experiments and Dr. Wendy Picking's lab for their help with Circular Dichroism. Chapter IV would not have been possible with the collaborative efforts of the Molecular Biophysics class (Shuo Dai, Jie Ren, Amanda Taylor and Mitchell Wilkerson) and Dr. Aihua Xie in the Physics Department.

I am grateful for the financial support through the National Science Foundation Graduate Research Fellowship Program (Grant 1144467) and Teaching Assistant support provided by the Department of Microbiology and Molecular Genetics.

I would like to acknowledge all of the undergraduates who have passed through Dr. John's laboratory through the years and thank them for their support: John Cooper, Nyssa Cullin, Shelby Rice, Cassandra Camp, Bryan Fritz, Robin Sherman, Amber Anderson, Lindsey Berger, Sara Greenlee, Jantzen Matli, Chad Muncrief, Keely Redhage, Lauren Lowe-Thompson, Roberta Reed, Natasha Anderson, Dalton Delaney, Emily Grubbs and Marla Ichord.

Finally, I would like to thank my family for their support and trust in my decision to go to Graduate School and move across the country. My husband, Shane, has been so supportive and I couldn't be happier sharing this intensely crazy journey with him.

Name: JESSICA MARIE MORRISON

Date of Degree: MAY, 2015

Title of Study: A BIOCHEMICAL, PHYSIOLOGICAL AND STRUCTURAL
CHARACTERIZATION OF AzoC, A NOVEL AZOREDUCTASE
FROM *CLOSTRIDIUM PERFRINGENS*

Major Field: MICROBIOLOGY, CELL AND MOLECULAR BIOLOGY

Abstract: Azo dyes are used throughout the paper, textile, food, beverage, pharmaceutical and cosmetic industries as artificial colorants and are characterized by the presence of an azo (double nitrogen) bond. Azoreductases are bacterially-produced enzymes which are capable of breaking these azo bonds and, in some cases, can result in the production of carcinogenic metabolites. *Clostridium perfringens*, a common inhabitant of both the human gut and the environment, is a bacteria that produces a significant amount of azoreductase activity. The gene that encodes for this azoreductase was characterized and given the name AzoC. AzoC is very novel, as compared to similarly functioning enzymes. AzoC has been shown to preferentially reduce large molecular weight sulfonated azo dyes, such as Direct Blue 15 (992.8 g/mol), with use of NADH and FAD as cofactors. The azoreduction is much increased under anaerobic conditions as compared to aerobic conditions (4-fold greater activity under anaerobic conditions). Interestingly, with certain azo dye and cofactor conditions, the presence of the cofactors alone can cause azo dye reduction. However, with the use of an azoreductase-free control in place, this can non-enzymatic activity can be accounted for. In addition, the structure of AzoC was found to be trimeric in nature, with the AzoC monomers being held together by disulfide bonding. The secondary structure of AzoC is consistent with that of other azoreductases, despite having low sequence identity. When the *azoC* gene was disrupted (knocked out) by intron insertion, results suggested the presence of additional enzymes capable of azoreduction. In addition, azo dye metabolites produced following azo dye reduction were found to slow *C. perfringens* generation time. AzoC was found to be released following *C. perfringens* exposure to sulfonated azo dyes and negatively charged sulfonated compounds. This enzyme was also found to localize to the Gram-positive periplasmic region of the *C. perfringens* cells. The results of this study serve to fill an important gap in the literature, providing the first information on a strictly anaerobic azoreductase, as well as a link between environmental azo dye exposure and the physiological state of *Clostridium perfringens* cells.

TABLE OF CONTENTS

Chapter	Page
I. LITERATURE REVIEW	1
General Human Microbial Flora	2
Normal Flora of the Human Gastrointestinal Tract	3
Metabolism of the Normal Intestinal Flora	6
Role of Intestinal Flora in Xenobiotic Metabolism and Carcinogenesis	6
Azo Dyes and Metabolism	8
Mutagenicity of Azo Dyes and Aromatic Amines	12
Azoreductase	13
Diversity of Azoreductases	15
Crystal Structures of Azoreductases	21
<i>Clostridium perfringens</i>	22
<i>Clostridium perfringens</i> Cell Structure	24
Protein Translocation Systems	26
<i>Clostridium perfringens</i> Cell Growth	28
<i>Clostridium perfringens</i> Azoreductase Function	29
Azoreductase Gene (AzoC)	30
Conclusion	31
II. IDENTIFICATION, ISOLATION AND CHARACTERIZATION OF A NOVEL AZOREDUCTASE FROM <i>CLOSTRIDIUM PERFRINGENS</i>	32
Abstract	32
Introduction	33
Background Information and Previous Work (Wright, 2007)	34
Materials and Methods	37
Azo Dyes	37
Purification of the Azoreductase Enzyme	38
Pure Enzyme Assays – Anaerobic and Aerobic Conditions	39
Pure Enzyme Assays – Cofactor Effect	41
Pure Enzyme Assays – Optimal Temperature	41
Pure Enzyme Assays – Optimal pH	41
Pure Enzyme Assays – Effect of Oxygen	42
Pure Enzyme Assays – Enzyme Kinetics	42
Results	42
Pure Enzyme Assays – Initial Work and Cofactor Effect	42
Pure Enzyme Assays – Optimal Temperature	45

Chapter	Page
Pure Enzyme Assays – Optimal pH.....	46
Pure Enzyme Assays – Effect of Oxygen.....	47
Pure Enzyme Assays – Enzyme Kinetics.....	49
Discussion.....	49
III. THE NON-ENZYMATIC REDUCTION OF AZO DYES BY FLAVIN AND NICOTINAMIDE COFACTORS UNDER VARYING CONDITIONS.....	53
Abstract.....	53
Introduction.....	54
Materials and Methods.....	56
Cofactors and Azo Dyes.....	56
Dye Reduction Assays – Cofactor Specificity.....	56
Purification of the Azoreductase (AzoC).....	58
Oxidized NAD ⁺ Assays.....	60
pH Assays.....	60
HPLC Analysis of Metabolites.....	61
Mass Spectroscopy Analysis of Metabolites.....	62
Results.....	62
Dye Reduction Assays – AzoC and Cofactors.....	62
NAD ⁺ Assays.....	68
pH Assays.....	69
Analysis of Metabolites.....	71
Discussion.....	72
IV. STRUCTURE AND STABILITY OF AN AZOREDUCTASE WITH AN FAD COFACTOR FROM THE STRICT ANAEROBE <i>CLOSTRIDIUM PERFRINGENS</i>	78
Abstract.....	78
Introduction.....	79
Materials and Methods.....	81
Sample Preparation.....	81
Liquid Chromatography – Mass Spectroscopy.....	83
Far-UV Circular Dichroism Spectroscopy.....	84
FTIR Spectroscopy.....	85
SDS-PAGE.....	86
MALDI-TOF Spectroscopy.....	86
Enzyme Activity Studies.....	87
Size Exclusion Chromatography.....	87
UV-Visible Spectroscopy.....	89
Bioinformatics Analysis.....	89
Results.....	90
Cofactor Identification.....	90

Chapter	Page
Secondary Structure Characterization.....	93
Multimeric State of AzoC.....	95
Thermal Stability of AzoC.....	97
Bioinformatics Analysis.....	100
Discussion.....	102
V. NON-CLASSICAL AZOREDUCTASE SECRETION IN <i>CLOSTRIDIUM PERFRINGENS</i> IN RESPONSE TO SULFONATED AZO DYE EXPOSURE AND THE GENERATION OF A Δ azoC KNOCKOUT MUTANT	107
Abstract.....	107
Introduction.....	108
Materials and Methods.....	111
Bacterial Strains and Azo Dyes	111
Creation of a Δ azoC Knockout Mutant	112
AzoC Purification and Antibody Production	115
SDS-PAGE	117
Western Blotting.....	117
Protein Extraction from <i>C. perfringens</i>	118
Non-Dividing Cells Exposed to Azo Dyes	119
Dividing Cells Exposed to Azo Dyes	120
Periplasmic Fraction	120
Azoreductase Enzyme Activity.....	121
Cell Lysis/Leakage Assays	122
Results.....	123
azoC Gene Inactivation: Creation of a Δ azoC Knockout Mutant.....	123
Exposure to Azo Dyes Causes Protein Release	124
AzoC is Released Upon Azo Dye Exposure.....	126
AzoC Release is Sulfonation-Specific	129
AzoC Release is Both Dye Concentration-Dependent and Time-Dependent.....	130
Additional Azoreductases are Present in <i>C. perfringens</i>	130
Discussion.....	133
VI. PRELIMINARY STUDIES ON THE GROWTH AND PHYSIOLOGY OF <i>CLOSTRIDIUM PERFRINGENS</i> WILD TYPE AND Δ azoC KNOCKOUT MUTANT: AN AZO DYE EXPOSURE STUDY	139
Abstract.....	139
Introduction.....	140
Materials and Methods.....	141
Bacterial Strains, Media and Azo Dyes	141
azoC Gene Knockout	143
Bacterial Growth and Azo Dye Reduction by Whole Cell Cultures	144
Results.....	145

Chapter	Page
Azo Dye Reduction.....	145
Effect of Azo Dyes on Cell Growth.....	158
Discussion.....	162
VII. FINAL DISCUSSION.....	167
REFERENCES	170

LIST OF TABLES

Table	Page
1. Characteristics of Biochemically-Tested Azoreductases	15
2. Crystal Structure Details of Azoreductases	21
3. Specific Activities of Other Dyes in the Presence of AzoC and Albumin	45
4. AzoC Temperature and Oxygen Condition Comparisons	46
5. Fold-Increases of Temperature and Oxygen Condition Comparisons.....	46
6. HPLC Retention Times of Azo Dye Metabolites Produced Under Different Conditions	72
7. Secondary Structural Characterization of AzoC Using Circular Dichroism and FTIR Spectroscopy	94
8. Enzymatic Specific Activities of Reduced and Oxidized Forms of AzoC	96
9. Secondary Structural Characteristics of Other Azoreductases as Compared to Oxidized AzoC.....	103
10. Percentage of Azo Dye Reduction Occurring over Time for Each Bacterial Strain (<i>C. perfringens</i> Wild Type, <i>C. perfringens</i> Δ azoC Knockout and <i>B.</i> <i>infantis</i>) in Each Media Type (BHI, CMM, PBSG), as Compared to Pure AzoC	146
11. Specific Activity for Each Bacterial Strain (<i>C. perfringens</i> Wild Type, <i>C.</i> <i>perfringens</i> Δ azoC Knockout and <i>B. infantis</i>) in Each Media Type (BHI, CMM, PBSG).	158
12. Early and Late Log Phase Comparison for BHI Media for Both <i>C. perfringens</i> Wild Type Cells and <i>C. perfringens</i> Δ azoC Knockout Mutant.	162

LIST OF FIGURES

Figure	Page
1. General Anatomy of the Human Gastrointestinal Tract and the Normal Flora.....	4
2. Cytochrome P450 Reaction Scheme.....	6
3. Generalized Drug Metabolism Scheme.....	7
4. Azo Dye Structures and Molecular Weights.....	9
5. Azoreductase Activity Scheme.....	10
6. Influence of Functional Groups on Azo Bond Reduction.....	11
7. Molecular Phylogenetic Analysis of Azoreductases by the Maximum Likelihood Method.....	20
8. Cell Envelope Structure of a Gram-positive Bacteria, Similar to <i>C. perfringens</i>	25
9. Region View of CPE0915 in the <i>C. perfringens</i> Chromosome.....	35
10. PCR Amplification of the <i>azoC</i> ORF and SDS-PAGE Analysis of AzoC.....	37
11. Effect of Cofactors on Direct Blue 15 Reduction by AzoC.....	44
12. Effect of Temperature on Direct Blue 15 Reduction.....	46
13. Effect of pH on Direct Blue 15 Reduction.....	47
14. Effect of Oxygen on AzoC Specific Activity.....	48
15. Effect of Oxygen on Direct Blue 15 Reactivation.....	48
16. Predicted Ping-Pong Bi Bi Reaction for AzoC in the Absence of Oxygen (A) and in the Presence of Oxygen (B).....	51
17. FAD and NADH Cofactors as Compared to AzoC.....	63
18. Diversity in Terms of Dye Reduction as Visualized by the Different Dyes.....	64
19. Anaerobic and Aerobic Cofactor Dye Reduction Comparison.....	66
20. Cofactor Dye Reduction as Compared to an Azoreductase (AzoC).....	68
21. Comparison of the Effect of NADH and NAD ⁺ on Dye Reduction.....	69
22. Effect of pH on Cofactor Dye Reduction.....	70
23. Direct Blue 15 Breakdown and Resultant Metabolites Predicted.....	71
24. Orbitrap Mass Spectrum Data.....	73
25. Mass Spectrometry to Identify the Cofactor of AzoC.....	91
26. MALDI-TOF Spectroscopy of AzoC.....	92
27. Secondary Structural Characterization of AzoC Using Circular Dichroism and FTIR Spectroscopy.....	94
28. Determination of the Multimeric State of AzoC.....	95
29. FTIR Spectroscopy of AzoC Structure and Thermal Stability.....	98
30. Thermal Stability of AzoC.....	100
31. Bioinformatics Study of AzoC.....	101
32. Structures of Azo Dyes and Chemicals Tested.....	112

Figure	Page
33. Confirmation of Δ azoC Knockout.....	124
34. Protein Release Due to Azo Dye Exposure	125
35. Azo Dye-Induced AzoC Release in Extracellular, Intracellular and Periplasmic Fractions.....	127
36. Sulfonated Compound-Induced Release of Proteins	129
37. Concentration Dependence of Protein Release in <i>C. perfringens</i>	131
38. Wild Type and <i>C. perfringens</i> Δ azoC Enzyme Assays of Azo Dye-Induced Release Proteins.....	132
39. Proposed Model of AzoC Release upon Sulfonated Compound Exposure	138
40. Generation Time of <i>C. perfringens</i> Wild Type, <i>C. perfringens</i> Δ azoC Knockout Mutant and <i>B. infantis</i> in Different Media Types	159

CHAPTER I

LITERATURE REVIEW

Most of the organisms on Earth are microorganisms and they are invisible to the naked eye. Despite their small size, these microorganisms play central roles in the web of life. Evidence has shown that the lives of all macro life forms (humans, animals, plants) are intimately tied to the activities of these microorganisms (Madigan *et al*, 2009).

Microorganisms are very diverse in nature. Due to their overall diversity and adaptability, microorganisms can be found in a variety of locations such hydrothermal vents deep in the ocean floor, the glaciers of the Arctic and on and within other organisms, including humans, animals and plants. Microorganisms generally fall into one of three domains, Bacteria, Archaea or Eukarya. Though there are major differences between the domains, members of Archaea are typically found in more extreme environments than Bacteria and are often called "extremophiles", for their proclivity towards extreme environments (Madigan *et al*, 2009). Bacteria, though not as extreme, are found in a wide variety of environments, from the soil to animal guts, and often live in complex communities with the other domains (Archaea and Fungi). In these complex communities, microorganisms often link metabolic processes in a way such that the waste products of one species may be the nutrient or energy source for another species.

Microorganisms have vast metabolic capacities in terms of the way in which they acquire energy. They can use different electron sources for energy, including organic compounds like

glucose (chemoorganotrophs), inorganic compounds like hydrogen (chemolithotrophs), and the sun (phototrophs). Microorganisms have different catabolic systems such as aerobic respiration (oxygen as the terminal electron acceptor), anaerobic respiration (inorganic compound other than oxygen as the terminal electron acceptor), and fermentation (organic compounds), and in some cases, they can switch between the different systems based on the environmental conditions.

Because of their vast metabolic capacities, microorganisms play valuable roles in the environments that they reside in. Besides their role in nutrient cycling and the global biogeochemical cycle, microorganisms play a big role environmentally in terms of bioremediation. In bioremediation, the unique metabolic capacities of certain species of microorganisms are used to clean up environmental pollution that is usually anthropogenic and recalcitrant in the environment. These types of microorganisms are also commonly used to clean up wastewater treatment plant effluent, which would otherwise typically require harsh chemicals to treat.

In addition to their use in bioremediation in the environment, microorganisms have also been exploited for their metabolic capacities in other industries. Fermenters, for example, have been exploited for years by the beverage industry and more recently the biofuel industry to produce alcohols. The nitrogen-fixating capacity of certain environmental microorganisms has also been used by farmers for generations to improve crop yields. More recently, microorganisms have been used in biotechnology and genetic engineering to produce products of commercial interest and for gene expression and have revolutionized the way in which molecular biology research is applied.

General Human Microbial Flora

Before birth, humans are generally free of microorganisms. However, during the birthing process, a baby is first exposed to the mother's normal flora via mother's birth canal. From birth to death, humans are exposed to microorganisms, which results in the human body having more bacteria cells on/in their bodies than human cells. As all body surfaces (skin and mucous membranes: mouth,

respiratory tract, gastrointestinal tract, urogenital tract) become colonized by microorganisms, these bacteria can interact amongst themselves or with the human host (Madigan *et al*, 2009).

Many microorganisms are only able to survive on the human surface for a short period of time and are referred to as the transient microbial flora, whereas those that have more of a permanent residence are known as the normal flora (Madigan *et al*, 2009; Tortora *et al*, 2012). The normal flora of an organism can be beneficial to the host and often do not cause problems unless they move from their normal habitat or can take advantage of a host's compromised immune system (Ahmad *et al*, 2010). Benefits of the normal flora that colonize the human body include the prevention of the colonization of harmful microbes (pathogens) by way of sequestering nutrients from these pathogens or by producing antimicrobial compounds which are harmful to the pathogens (Ahmad *et al*, 2010). The normal flora can also aid in the digestion of food in the intestine and stimulate the immune system (Ahmad *et al*, 2010).

Normal Flora of the Human Gastrointestinal Tract

The gastrointestinal tract is home to the largest number of microorganisms in the human body as well as the most diversity overall with as many as 500 different species of bacteria (Finegold *et al*, 1975; Madigan *et al*, 2009; Moore & Holdeman, 1974; Whitman *et al*, 1998). Interestingly, 10^{14} colony forming units of bacteria is 10 times more than the number of human cells in the body (Finegold *et al*, 1975; Moore & Holdeman, 1974; Whitman *et al*, 1998). The human gastrointestinal tract starts at the mouth, goes through the esophagus, into the stomach, followed by the small intestine and large intestine (Figure 1) (Madigan *et al*, 2009). The environment of the gastrointestinal tract changes dramatically from start to finish and each different environmental condition is able to support different types of microorganisms (Madigan *et al*, 2009). The role of the normal flora in the gastrointestinal tract is to aid in the digestion of food, to enhance the body's immune system, and to serve as an antagonist against pathogenic intestinal bacteria (Madigan *et al*, 2009).

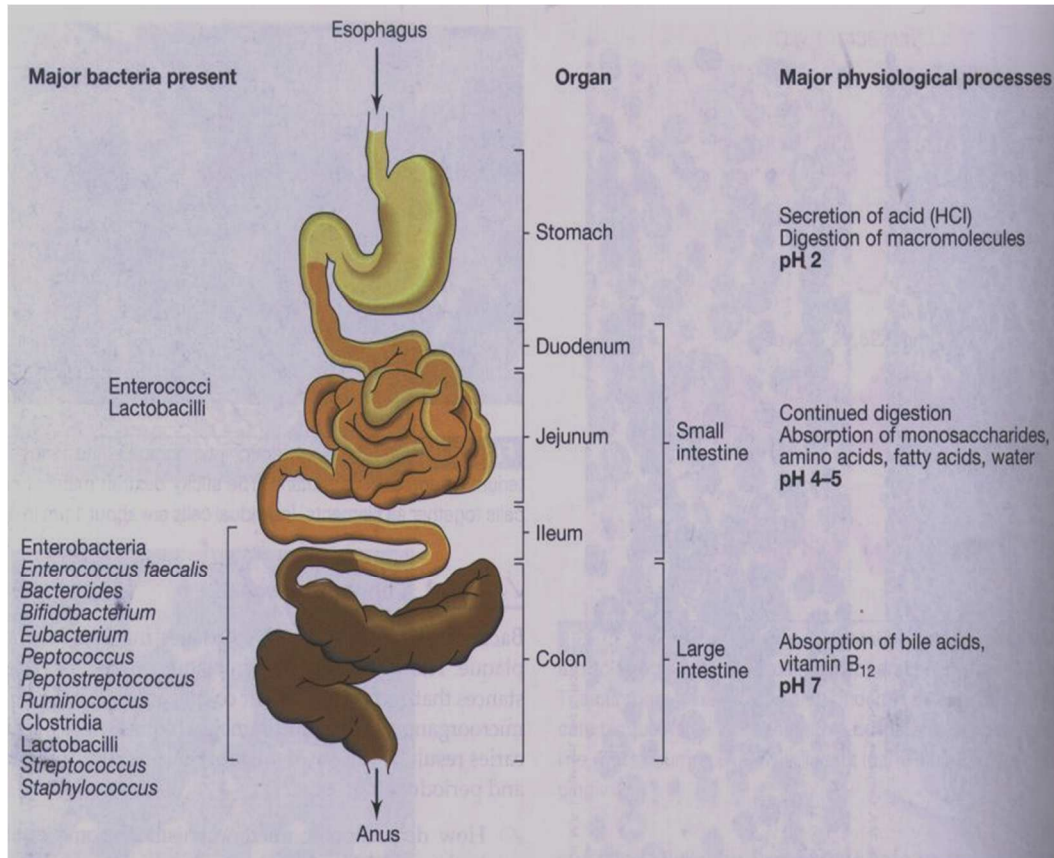


Figure 1. General Anatomy of the Human Gastrointestinal Tract and the Normal Flora (Madigan *et al*, 2009).

Microbes enter the gastrointestinal tract through the food we eat, the water we drink, and the air we breathe. Saliva is one of the main sources of bacteria entering the gastrointestinal tract; saliva can contain millions of bacteria per milliliter (Tortora *et al*, 2012). The first hurdle for microorganisms to entering our gastrointestinal tract is the low pH and overall harsh environment of the stomach (Madigan *et al*, 2009). The low pH condition of the stomach can inactivate some microorganisms, while others are able to survive (*Helicobacter*, *Lactobacilli* and *Streptococci*) and enter the intestines (Ahmad *et al*, 2010; Borriello, 2000; Savage, 1977). Following the stomach, the small intestine begins with the duodenum, which also features a low pH, many of the same bacteria as found in the stomach, and other Gram-positive bacteria (Arumugam *et al*, 2011; Claesson *et al*, 2009; Madigan *et al*, 2009; Savage, 1977). In the jejunum and ileum, though, the pH is increased (4-5) and features as many as 10^5 to 10^7 colony forming units per gram of digested material (Madigan *et al*,

2009). Here, the Gram-positive bacteria begin to be outnumbered by Gram-negative bacteria and aerobic bacteria begin to be outnumbered by anaerobic bacteria (Arumugam *et al*, 2011; Borriello, 2000; Claesson *et al*, 2009; Madigan *et al*, 2009). The large intestine is the most heavily populated region of the gastrointestinal tract by far, containing more than 100 billion bacteria per gram of fecal material (Borriello, 2000; Madigan *et al*, 2009; Tortora *et al*, 2012). Here we also find the most bacterial species diversity of all of the gastrointestinal tract, primarily due to the area being rich in nutrients for the bacteria, having a relatively neutral pH, and being more stagnant than the other areas of the gastrointestinal tract (Madigan *et al*, 2009; Savage, 1977). Because of the low availability of oxygen, we see microorganisms of varying degrees of oxygen tolerance (Macfarlane & Gibson, 1994). In the colon, Gram-negative bacteria (such as *Escherichia coli*) outnumber Gram-positive bacteria and microorganisms capable of anaerobic respiration (such as *Clostridium perfringens*) outnumber strictly aerobic microorganisms (Arumugam *et al*, 2011; Borriello, 2000; Claesson *et al*, 2009; Madigan *et al*, 2009).

The diversity of the normal flora in the gastrointestinal tract is constantly fluctuating and changing, based on diet and medications. People being treated with antibiotics, for example, dramatically reduce the number of normal flora in their gastrointestinal tract which makes them more prone to infections by opportunistic pathogens (Madigan *et al*, 2009). Foods and supplements can provide a means of probiotics, which increases the colonization of lost normal gut flora thereby providing a health benefit (Madigan *et al*, 2009). Probiotics can also provide a means to increase bacterial diversity of the normal gut flora, as probiotic products such as yogurts and milk contain many different species of *Lactobacillus*, *Lactococcus*, *Streptococcus* and *Bifidobacterium* (Gueimonde *et al*, 2004).

Metabolism of the Normal Intestinal Flora

The relationship between the human gastrointestinal tract and the normal microbial flora that inhabit it is more than just a commensal relationship; rather, the relationship is mutualistic. In the colon, the microbes benefit from human host as the intake and digestion of food fuels their metabolism and survival and in turn microbes metabolize and produce vitamins which are necessary for human survival (Madigan *et al*, 2009). For example, vitamins B₁₂ and K are considered essential because they cannot be synthesized by humans (Madigan *et al*, 2009). Additionally, there are steroids produced by our liver and released into our intestine which are not absorbed by our bodies until they are modified and activated by the normal intestinal flora (Gill *et al*, 2006; Guarner & Malagelada, 2003). Because of the overall diversity of microorganisms within our gastrointestinal tract, there is a great diversity of metabolic capabilities of the bacteria residing in our gut (Roberfroid *et al*, 1995).

Role of Intestinal Flora in Xenobiotic Metabolism and Carcinogenesis

Intestinal microflora play a key role in xenobiotic metabolism through a process called enterohepatic circulation (Hanninen *et al*, 1987). The normal gut flora has a wide variety of metabolic capabilities, as they can utilize enzymes to either directly reduce xenobiotic compounds or to reduce the transformed metabolites produced by cytochrome P450 (Figures 2 and 3) (Chung, 1997). In some cases, these microbial enzymes can detoxify toxic compounds (in a way similar to cytochrome P450); however, in other cases, these microbial enzymes can produce compounds more toxic than the original compound through deconjugation reactions (Figure 3) (Chung, 1997).

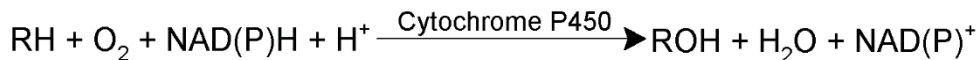


Figure 2. Cytochrome P450 Reaction Scheme (Gandolfi, 1991; Iwasaki *et al*, 2010; Roland *et al*, 1993).

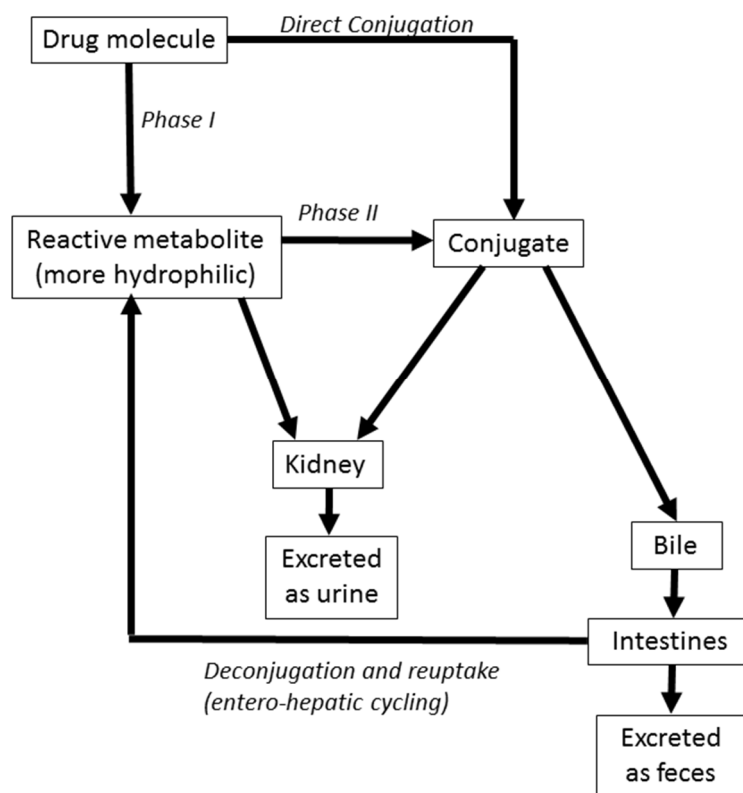


Figure 3. Generalized Drug Metabolism Scheme.

Xenobiotics are molecules which are foreign to the host and are often encountered by the gastrointestinal tract as anthropogenic components of foods or beverages consumed (Chung, 1997). Since xenobiotics are foreign to the host, these chemicals and often their metabolites are sometimes toxic and/or mutagenic in nature to the host. Enzymes of the host gastrointestinal tract, as well as those produced by the normal gut flora, can be both beneficial and deleterious when it comes to dealing with these anthropogenic compounds (Chung, 1997).

Regarding enterohepatic cycling, cytochromes such as P450 are part of a supergene family that plays a major role through the oxidative metabolism of xenobiotics and other drugs and their clearance from the body (Iwasaki *et al*, 2010). This supergene family is composed of mono-oxygenases which are of mixed function and are present in many tissues (Iwasaki *et al*, 2010). The

cytochromes in the liver, specifically cytochrome P450, are the most involved in the metabolism and detoxification of xenobiotic compounds through Phase I and Phase II reactions (Figure 3) (Chung, 1997; Iwasaki *et al*, 2010). In the liver, cytochrome P450 utilizes two protons and two electrons from NADPH to oxidize the xenobiotic compound (Figure 2) and a second enzyme, flavin monooxygenase modifies the xenobiotic to expose functional groups for modification and conjugation (Figure 3) (Gandolfi, 1991; Hanninen *et al*, 1987; Roland *et al*, 1993). What prevents the removal of the modified molecule is the deconjugation process, normally driven by the flora in the intestines (Figure 3). The deconjugated molecule can be toxic and reabsorb or recirculate, and is called enterohepatic cycling (Figure 3). This recirculation can occur several times, which can cause increasing levels of toxicity or detoxification in the body.

Azo Dyes and Metabolism

Humans have been using natural dyes for centuries. However, in 1856, William Henry Perkin accidentally laid the groundwork for synthetic dyes (Saratale *et al*, 2010). Though W.H. Perkin did not directly develop azo dyes, his work with synthetic organic pigments laid the foundation for a synthetic compound that we use to this day (Saratale *et al*, 2010). Azo dyes are organic synthetic colorants which are used widely by the textile, paper, cosmetic, pharmaceutical and food industries and are the most important dye currently used in the textile industry (Chen, 2006; Chung *et al*, 1992). Azo dyes are characterized by the presence of one or more double nitrogen bonds ($-N=N-$, azo bond) and aromatic rings, as shown in Figure 4 (Pandey *et al*, 2007). The presence of the chromophore, the azo bond, is what allows azo dyes to absorb light in the visible spectrum and gives the dyes their color (Saratale *et al*, 2010). Azo dyes are classified based on the presence of various functional groups, as well as the number of azo bonds present in the molecule.

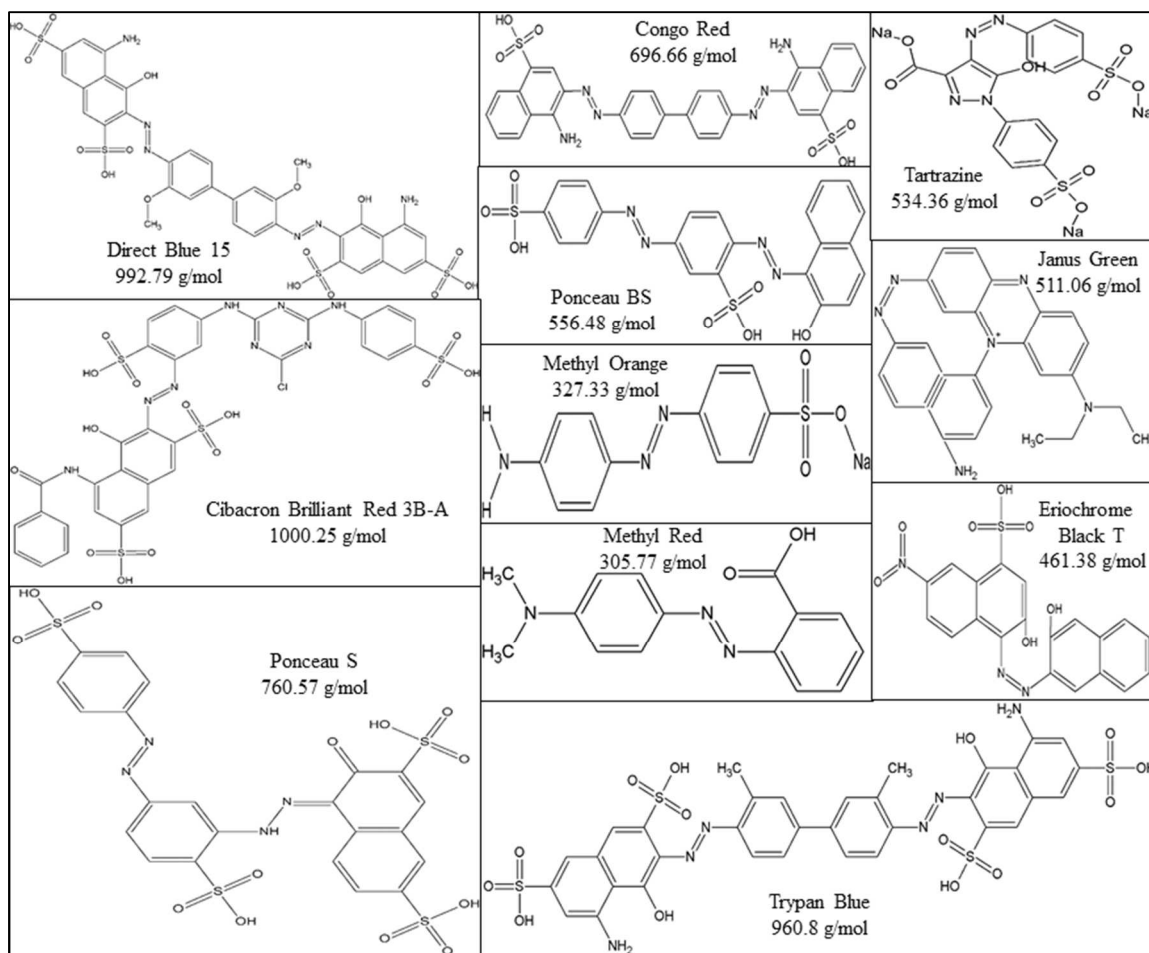


Figure 4. Azo Dye Structures and Molecular Weights.

Azo dyes are recalcitrant in the environment because of the lack of similar natural compounds. Interestingly, only one natural compound containing an azo group is known, 4,4'-dihydroazobenzene, from the *Agaricus xanthodermus* mushroom (Gill & Strauch, 1984). It was recently estimated that yearly world dye production was around 1 million tons, about half of this being contributed to azo dyes (Pandey *et al.*, 2007). Because of azo dye loss through rather inefficient dyeing processes, azo dyes often enter the environment through wastewater streams, as wastewater treatment plants are generally not efficient at removing azo dyes from wastewater (Pandey *et al.*, 2007). It is estimated that as much as 280,000 tons of azo dyes are discharged into wastewater treatment plants every year (Saratale *et al.*, 2010).

For years, wastewater treatment plant workers had issues with the removal of azo dyes from their wastewater streams (Saratale *et al*, 2010). Using the physicochemical methods that are characteristic of wastewater treatment streams, azo dyes are not completely removed and generate a multitude of secondary waste products themselves that have their own pollution issues (Saratale *et al*, 2010). This process, in some cases, can produce secondary waste products that are more harmful than the original presence of the azo dyes in the wastewater (Saratale *et al*, 2010). When it was found that microorganisms were capable of reducing these dyes, a bioremediation approach was sought in order to provide the most eco-friendly option for the removal of azo dyes from textile wastewater treatment streams (Saratale *et al*, 2010).

Many types of both microorganisms and macroorganisms are capable of metabolizing azo dyes. In fact, fungi, yeast, algae, plants, bacteria and humans are all capable of breaking down these dyes (Saratale *et al*, 2010). In bacteria, this metabolic process features the reductive cleavage of the azo bond of the dye, which in turn releases the aromatic amines which were used to form the azo dye (Figure 5) (Chen, 2006; Saratale *et al*, 2010). In mammals, the breakdown of azo dyes is catalyzed by liver enzymes, such as cytochrome P450, as previously mentioned for other xenobiotic compounds (Chung *et al*, 2000; Rafii & Cerniglia, 1995).

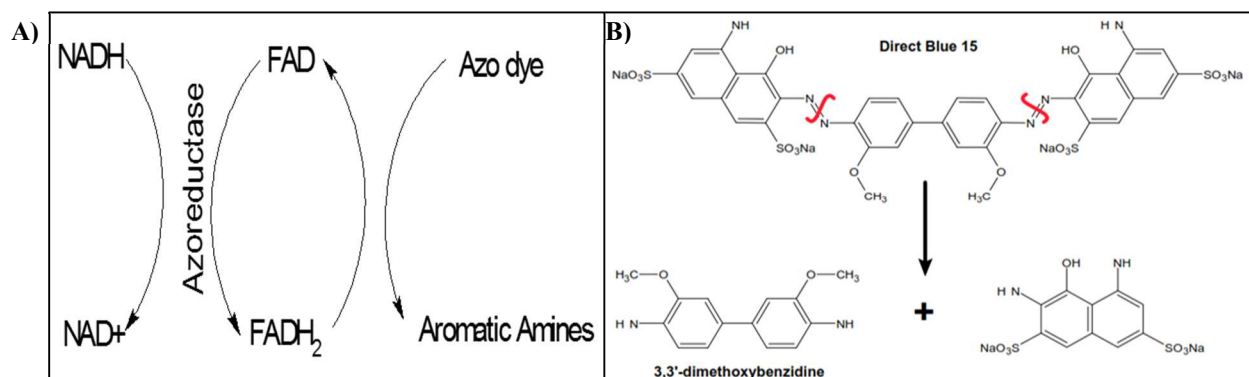


Figure 5. Azoreductase Activity Scheme. **A)** Generalized azo dye breakdown, **B)** Enzymatic breakdown of Direct Blue 15

The ability of an azo dye to be reduced ultimately depends on the structure of the azo dye. The number of azo bonds and size of the dye play a major role in determining whether an azo dye will be metabolized, however, the primary factor in azo dye reduction is in the characteristics of the functional groups surrounding the azo bond (Bardi & Marzona, 2010; Chen, 2006). Specifically, the electron density surrounding the azo bond (Bardi & Marzona, 2010; Chen, 2006). The reduction of the azo bond has been shown to be facilitated by the presence of electron-withdrawing groups surrounding the azo bond, such as $-\text{NO}_2$ and $-\text{SO}_3\text{H}$ (Bardi & Marzona, 2010; Chen, 2006). Having such a functional group in the para position to the azo bond reduces the electron density around the azo bond making it easier to be reduced (Figure 6) (Bardi & Marzona, 2010; Chen, 2006; Hsueh & Chen, 2008). In addition, steric hindrance and sheer size of functional groups in the ortho position can decrease dye reduction (Figure 6) (Hsueh & Chen, 2008).

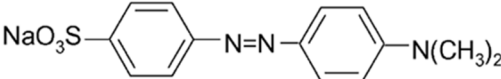
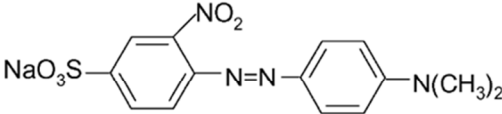
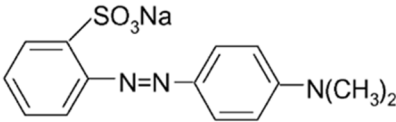
<p>Methyl Orange 4-(4'-dimethylaminophenylazo) benzenesulfonic acid sodium salt [p-MO] $\lambda_{f_{\max}} = 465\text{nm}$</p>		<p>V ($\mu\text{M}/\text{min}/\text{g cell}$)</p> <p>3.13</p>
<p>4-(4'-dimethylaminophenylazo) -2-nitro-benzenesulfonic acid sodium salt [o-NO₂-p-MO] $\lambda_{f_{\max}} = 440\text{ nm}$</p>		<p>1.08</p>
<p>2-(4'-dimethylaminophenylazo) benzenesulfonic acid sodium salt [o-MO] $\lambda_{f_{\max}} = 440\text{ nm}$</p>		<p>1.54</p>

Figure 6. Influence of Functional Groups on Azo Bond Reduction. Figure modified from Hsueh et al (Hsueh & Chen, 2008). Three derivatives of Methyl Orange are shown, along with their specific activity (V).

Azoreductase activity of bacteria in the human gastrointestinal tract was greatly advanced by accomplishments made by researchers at the National Center for Toxicological Research (Rafii *et al*, 1990). These researchers created a large-scale semi-continuous culture system containing human intestinal microflora and exposed them to the azo dye Direct Blue 15 (Rafii *et al*, 1990). Through this system, these researchers were able to isolate intestinal bacteria which were capable of reducing the azo dye and, in the process, greatly advance our knowledge of the bacteria that produce this enzyme (Chung *et al*, 1992; Rafii *et al*, 1990).

Mutagenicity of Azo Dyes and Aromatic Amines

It is well-known that aromatic amines are notorious for being carcinogenic in nature, especially those containing moieties of toluene, aniline, naphthalene and benzidine (Chung, 1997; Vineis & Pirastu, 1997). In fact, there are many studies which show an increased prevalence for bladder cancer in individuals who have worked in or near an azo dye manufacturing facility (Bulbulyan *et al*, 1995; Cartwright, 1983; Chung, 1997; Chung *et al*, 2000; Dillon *et al*, 1994; Sontag, 1981; Vineis & Pirastu, 1997). Specifically, the aromatic amines accumulate in the bladders of these individuals as they are awaiting clearance from the body and host cell mutagenesis occurs (Bulbulyan *et al*, 1995; Chung *et al*, 2000; Vineis & Pirastu, 1997). Aside from bladder cancer, the azo dye metabolites have also been linked to causing contact dermatitis (when in contact with azo textile dyes), liver nodules, splenic carcinomas as well as stomach, kidney and skin cancer (Brown & Devito, 1993; Dillon *et al*, 1994; Sontag, 1981). To cause such toxicity and cancer, it is thought that, like its parent azoreductase, the aromatic amines undergo metabolic activation to become highly reactive ions (Brown & Devito, 1993). These highly reactive ions, being very electrophilic, can bind to both DNA and RNA, causing tumors induced by genetic mutation (Brown & Devito, 1993). The ability of azo dyes and their metabolites to persist in the environment, coupled with their inherent toxicity and carcinogenicity, makes these compounds a concern to both human health and environmental health.

The reduction of azo dyes by normal gastrointestinal tract flora has been well-studied in many bacteria in both whole cell culture studies (*Enterobacter aerogenes*, *Bacteroides*, *Clostridium*, *Fusobacterium*, *Ruminococcus*, *Salmonella*, *Staphylococcus*, *Streptococcus*, *Proteus*, *Lactobacillus* and *Eubacillus*) and in pure enzyme studies (direct purification or heterologously expressed from bacteria such as *E. coli*, *Bacillus subtilis*, *Enterococcus faecium*, *Enterococcus faecalis* and *Pseudomonas aeruginosa*) (Chen *et al*, 2004; Chung *et al*, 1992; Macwana *et al*, 2010; Nakanishi *et al*, 2001; Punj & John, 2009; Sugiura *et al*, 2006; Wang *et al*, 2007). As azo dyes are used widely as artificial colorants in our food, beverage and pharmaceutical products, the normal flora of the human gastrointestinal tract encounter these dyes very often (Goldin, 1990). Because the normal flora of the gastrointestinal tract are able to reduce these azo dyes to aromatic amines, it is no surprise that the ingestion of these dyes has been linked to several types of cancer in humans (Bulbulyan *et al*, 1995; Cartwright, 1983; Chung, 1997; Chung *et al*, 2000; Chung *et al*, 1992; Dillon *et al*, 1994; Sontag, 1981; Vineis & Pirastu, 1997).

Azoreductase

The first recorded azoreductase discovery from a pure culture was in 1982 by Zimmerman in *Pseudomonas* KF46 (now known as *Xenophilus azovorans*) (Zimmermann *et al*, 1982). This particular enzyme was found to be capable of reducing the azo dye, Orange II, by use of NADH or NADPH as electron donors and was monomeric in nature (30 kDa) (Zimmermann *et al*, 1982). Two years later, Zimmerman discovered another azoreductase in *Pseudomonas* K24 (now known as *Pigmentiphaga kullae*) capable of reducing Orange I (Zimmermann *et al*, 1984). This additional azoreductase was also monomeric in structure, though much smaller than the Orange II azoreductase (21 kDa versus 30 kDa) (Zimmermann *et al*, 1984; Zimmermann *et al*, 1982). Neither azoreductase showed any antigenic cross-reactivity, suggesting that they have very different protein sequences (Zimmermann *et al*, 1984). Both of these azoreductases were shown to be flavin-independent, as in

no exogenous flavin was required for azoreduction to occur (Zimmermann *et al*, 1984; Zimmermann *et al*, 1982).

The first record of flavin-dependent azoreductases being studied was in 1992 by Ghosh (Ghosh *et al*, 1992). Ghosh studied the azoreductases of *Shigella dysenteriae* type 1 (Ghosh *et al*, 1992). Two azoreductases were identified in this bacterium and they were very different in nature. Azoreductase I was a dimer (28kDa) whereas Azoreductase II was a monomer (11kDa) (Ghosh *et al*, 1992). Additionally, the azoreductases showed differential dye specificity, as Azoreductase I was able to reduce the azo dye Amaranth, but Azoreductase II was not (Ghosh *et al*, 1992). Azoreductase II, however, could reduce Ponceau SX, Tartrazine and Orange II (Ghosh *et al*, 1992). Ghosh also identified azoreductase proteins in *E. coli* K12 which also had differential substrate specificities from the *Shigella* azoreductases (Ghosh *et al*, 1993; Ghosh *et al*, 1992).

In 2001, the first heterologous expression of an azoreductase occurred with the azoreductase that was discovered in *Bacillus* OY1-2, a soil bacterium (Suzuki *et al*, 2001). This represented a huge step forward in the field as pure azoreductases were now able to be efficiently purified and tested. The pure azoreductase was shown to have broad dye specificity and to utilize NADPH as an electron donor without the addition of exogenous flavin (Suzuki *et al*, 2001). Several years later, an azoreductase isolated from *Rhodobacter sphaeroides* was shown to have a Ping-Pong Bi-Bi reaction mechanism (Bin *et al*, 2004). In the Ping-Pong Bi-Bi mechanism, 2 moles of NADH are used to reduce 1 mole of azo dye via a flavin cofactor (Bin *et al*, 2004).

The breakthrough in the field of intestinal azoreductase research came in 2001 when Nakanishi's group was studying an enzyme that they had predicted to be an acyl carrier protein (acp) phosphodiesterase from *E. coli* (Nakanishi *et al*, 2001). This enzyme, though, was shown not to have any phosphodiesterase activity, but rather had high azoreductase activity (Nakanishi *et al*, 2001). Similarly, an acp phosphodiesterase in *Pseudomonas aeruginosa* was found to have azoreductase

activity but not phosphodiesterase activity (Wang *et al*, 2007). Both purified azoreductase enzymes required the addition of exogenous flavin cofactor (FMN) for azoreductase activity to occur (Nakanishi *et al*, 2001; Wang *et al*, 2007). The requirement for the exogenous addition of flavin cofactor is azoreductase-dependent and may not be required by all azoreductases, as witnessed by the *Bacillus* azoreductase detailed above. Additionally, all azoreductases have been shown to utilize a nicotinamide cofactor for enzyme activity, though it may be NADH or NADPH or either depending on the azoreductase. Again, the azoreductase reaction in *Pseudomonas* was shown to function by a Ping-Pong bi-bi reaction (Nakanishi *et al*, 2001).

Diversity of Azoreductases

All aerobic azoreductases which have been biochemically studied in their pure forms to date are shown in Table 1. It can be seen from Table 1 that there is great diversity amongst biochemically-tested azoreductases in terms of substrate specificity, multimeric state and cofactors utilized. However, it is important to note that all but one of the azoreductases in Table 1 are from aerobic or facultative anaerobes. Only one azoreductase from a strictly anaerobic bacteria is well-characterized (Table 1).

Table 1. Characteristics of Biochemically-Tested Azoreductases

Organism	ID (PDB or Accession #)	Dyes Tested	Optimal Dye	Cofactors	Polymeric State	(An)aerobe / Source	Reference
<i>Bacillus anthracis</i> strain Sterne	3P0R	N/D	N/D	N/D	Monomer	Facultative anaerobe / Environment	(Filippova <i>et al</i> , 2010)
<i>Bacillus anthracis</i> strain Ames Ancestor	3U7I	N/D	N/D	FMN NADH	Tetramer	Facultative anaerobe / Environment	(Zhang <i>et al</i> , 2011)
<i>Bacillus sp.</i> OY1-2	BAB13746, Q9FAW5	Methyl Red, Acid Red 88, Sumifix Red B, Acid Orange 7, Reactive Black 5	Acid Red 88	NADPH	N/D	Facultative anaerobe / Environment	(Suzuki <i>et al</i> , 2001)
<i>Bacillus amyloliquefaciens</i> strain AB	ACF17423	Direct Red 28	Direct Red 28	NADH	N/D	Facultative anaerobe / Environment	(Bafana <i>et al</i> , 2008)
<i>Bacillus sp.</i> B29	BAF02597	Methyl Red, Orange I, Orange II, Orange G, Acid Red 88, 1-(2-pyridylazo)-2-naphthol, New coccin, Sunset Yellow FCF	Methyl Red	FMN NADH	Dimer	Facultative anaerobe / Environment	(Ooi <i>et al</i> , 2007)

Organism	ID (PDB or Accession #)	Dyes Tested	Optimal Dye	Cofactors	Polymeric State	(An)aerobe / Source	Reference
<i>Bacillus sp.</i> B29	BAH36887	Methyl Red, Ethyl Red, Methyl Orange, Orange I, Orange II, Orange G, Acid Red 88, New coccin, Sunset Yellow FCF	Methyl Red, Ethyl Red	FMN NADH	Dimer	Facultative anaerobe / Environment	(Ooi <i>et al</i> , 2009)
<i>Bacillus sp.</i> B29	BAH36886	Methyl Red, Ethyl Red, Methyl Orange, Orange I, Orange II, Orange G, Acid Red 88, 1-(2-pyridylazo)-2-naphthol, New coccin, Sunset Yellow FCF	Methyl Red, Ethyl Red	FMN NADH	Dimer	Facultative anaerobe / Environment	(Ooi <i>et al</i> , 2009)
<i>Bacillus subtilis</i> Strain ISW1214	BAB85976	Azobenzene, p-aminobenzene, Mordant Orange I, Methyl Red, Acid Orange 52, Reactive Yellow 17, Acid Yellow 23, Reactive Orange 16, Reactive Red 22, Reactive Orange I, Reactive Red 2, Direct Red 80, Direct Brown 44, Reactive Red 120, Congo Red, 6.42Reactive Black 5, Reactive Red 180, Acid Red 88, Acid Orange 10, Acid Orange 7	Methyl Red	NADPH	N/D	Facultative anaerobe / Environment	(Sugiura <i>et al</i> , 2006)
<i>Bacillus subtilis</i> strain ATCC 6633	BAB85974	Azobenzene, p-aminobenzene, Mordant Orange I, Methyl Red, Acid Orange 52, Reactive Yellow 17, Acid Yellow 23, Reactive Orange 16, Reactive Red 22, Reactive Orange I, Reactive Red 2, Direct Red 80, Direct Brown 44, Reactive Red 120, Congo Red, Reactive Black 5, Reactive Red 180, Acid Red 88, Acid Orange 10, Acid Orange 7	Reactive Red 22, Methyl Red	NADPH	N/D	Facultative anaerobe / Environment	(Sugiura <i>et al</i> , 2006)
<i>Bacillus sp.</i>	ACI12881	Methyl orange, Flame orange, Ammonium-azo-I, alizarin yellow R, Methyl Red, Janus Green, Citrus Yellow, Orange G, Ponceau BS, Ruby Red, Basic Blue 41, Nitro-naphthyl-DMA, Orange I, Orange II, BHQ-10	BHQ-10	FMN NADPH	Tetramer	Facultative anaerobe / Environment	(Johansson <i>et al</i> , 2011)

Organism	ID (PDB or Accession #)	Dyes Tested	Optimal Dye	Cofactors	Polymeric State	(An)aerobe / Source	Reference
<i>Bacillus subtilis</i>	O32224	N/D	N/D	FMN NADH	Dimer	Facultative anaerobe / Environment	(Nishiya & Yamamoto, 2007)
<i>Bacillus subtilis</i> subsp. <i>subtilis</i> str. 168	O07529	Azobenzene, p-aminobenzene, Mordant Orange I, Methyl Red, Acid Orange 52, Reactive Yellow 17, Acid Yellow 23, Reactive Orange 16, Reactive Red 22, Reactive Orange I, Reactive Red 2, Direct Red 80, Direct Brown 44, Reactive Red 120, Congo Red, Reactive Black 5, Reactive Red 180, Acid Red 88, Acid Orange 10, Acid Orange 7	Reactive Red 22	NADPH	N/D	Facultative anaerobe / Environment	(Sugiura <i>et al.</i> , 2006)
<i>Escherichia coli</i> K12	2D5I, 2Z9C, 2Z98, 1V4B, P41407	Methyl red, Ethyl red, Ponceau SX, Menadione (QR)	Methyl Red, Ethyl Red, Menadione (QR)	FMN NADH	Dimer	Facultative anaerobe / Gut	(<i>Ito et al.</i> , 2005; <i>Ito et al.</i> , 2006; <i>Ito et al.</i> , 2008; <i>Nakanishi et al.</i> , 2001)
<i>Yersinia pestis</i> CO92	4ESE	N/D	N/D	FMN NADH	Monomer	Facultative anaerobe / Gut	(Tan <i>et al.</i> , 2012)
<i>Enterococcus faecalis</i>	2HPV, AAR38851, Q831B2	Methyl Red, Orange II, Amaranth, Orange G, Ponceau BS, Ponceau S, Menadione (QR)	Methyl Red, Menadione (QR)	FMN NADH	Tetramer	Facultative anaerobe / Gut	(Chen <i>et al.</i> , 2004; Liu <i>et al.</i> , 2007)
<i>Pseudomonas aeruginosa</i>	2V9C, 3LT5, 3R6W, 15595982	Methyl Red, Orange II, Orange G, Ponceau BS, Ponceau S, PAABSA, Amaranth	Methyl Red	FMN NADPH	Tetramer	Facultative anaerobe / Gut	(Ryan <i>et al.</i> , 2010; Wang <i>et al.</i> , 2007)
<i>Pseudomonas aeruginosa</i>	15597158	Methyl Red, PAABSA, Orange G, Orange II, Amaranth, Ponceau BS, Ponceau S	Ponceau BS	FMN NADPH	Tetramer	Facultative anaerobe / Gut	(Ryan <i>et al.</i> , 2010)
<i>Pseudomonas aeruginosa</i>	15598419	Methyl Red, PAABSA, Orange G, Orange II, Amaranth, Ponceau BS, Ponceau S	Methyl Red	FMN NADPH	Tetramer	Facultative anaerobe / Gut	(Ryan <i>et al.</i> , 2010)
<i>Enterococcus faecium</i> strain ATCC 6569	ACX30669	Methyl Red, Congo Red, Acid Red 88, Ponceau BS, Orange II, Direct Blue 15, Ponceau S, Tartrazine, Amaranth	Methyl Red	FMN NADH	N/D	Facultative anaerobe / Gut	(Macwana <i>et al.</i> , 2010)
<i>Staphylococcus cohnii</i>	ACF54629	Acid red B, Acid scarlet GR, Direct Blue 15, Acid Yellow G, Acid Orange II	Acid Red B	None	N/D	Facultative anaerobe / Skin	(Yan <i>et al.</i> , 2012)
<i>Shewanella decolorationis</i> strain S12	ABM97417	Fast Acid Red GR, Reactive Brilliant Blue	Reactive Brilliant Blue	N/D	N/D	Facultative anaerobe/ Environment	(Xu <i>et al.</i> , 2005)

Organism	ID (PDB or Accession #)	Dyes Tested	Optimal Dye	Cofactors	Polymeric State	(An)aerobe / Source	Reference
<i>Rhodobacter sphaeroides</i>	AAN17400	Reactive Brilliant Red K-2BP, Reactive Brilliant Red X-3B, Reactive Yellow X-6G, Red I, Red II, Red III	Reactive Brilliant Red X-3B, Red II, Red III	N/D	N/D	Facultative anaerobe / Environment	(Song <i>et al</i> , 2003)
<i>Geobacillus stearothermophilus</i> Strain IFO13737	BAB85975	Azobenzene, p-aminazobenzene, Mordant Orange I, Methyl Red, Acid Orange 52, Reactive Yellow 17, Acid Yellow 23, Reactive Orange 16, Reactive Red 22, Reactive Orange I, Reactive Red 2, Direct Red 80, Direct Brown 44, Reactive Red 120, Congo Red, Reactive Black 5, Reactive Red 180, Acid Red 88, Acid Orange 10, Acid Orange 7	Methyl Red	N/D	N/D	Facultative anaerobe / Environment	(Sugiura <i>et al</i> , 2006)
<i>Pigmentiphaga kullae</i>	AAO39146	Orange I	Orange I	N/D	N/D	Aerobe / Environment	(Blumel & Stolz, 2003)
<i>Pigmentiphaga kullae</i>	ADD80733	Methyl Red, Amaranth, Ponceau BS, Ponceau S, Orange II, Orange G, Magneson II, 1-(4-nitrophenylazo)-2-naphthol, 1-(4-nitrophenylazo)-resorcinol	Orange I	NADPH Flavin-free	Monomer	Aerobe / Environment	(Chen <i>et al</i> , 2010)
<i>Staphylococcus aureus</i> strain ATCC 25923	AAT29034, Q50H63	Orange II, Amaranth, Methyl Red, Ponceau BS, Ponceau S	Methyl Red	FMN NADPH	Tetramer	Facultative anaerobe / Skin	(Chen <i>et al</i> , 2005a)
<i>Xenophilus azovorans</i>	Q8KU07, AAM92125	Orange II, Violet N, Acid Orange 8, Acid Orange 12, Ponceau BS, Acid Red 88, Sunset Yellow FD6, Sudan I, Sudan II, Sudan III, Sudan IV, Orange G, Acid Red 18, Amaranth, Acid Black 52, Acid Red 151, 1-(2-pyridylazo)-2-naphthol, calconcarboxylic acid, calmagite	Orange II	NADPH	N/D	Facultative anaerobe / Environment	(Blumel <i>et al</i> , 2002)
<i>Clostridium perfringens</i> strain ATCC 3626	AGH15624	Direct Blue 15, Methyl Red, Tartrazine, Trypan Blue, Congo Red, Eriochrome Black T, Buffalo Black NBR, Janus Green, Cibacron Brilliant Red 3B-A, Ponceau S, Ponceau BS, Methyl Orange	Direct Blue 15	FAD NADH	Trimer	Strict anaerobe / Sheep intestine	(Morrison <i>et al</i> , 2012)

Azoreductase activity has been shown to occur nonenzymatically under anaerobic conditions (Stolz, 2001). Stolz describes a process that is dependent on reduced flavins, many of which he states will react directly with either oxygen or the azo dyes themselves (Stolz, 2001). Previous studies have shown that under anaerobic conditions, the reduced flavins can shuttle electrons to the azo dye and cause non-enzymatic reduction of the azo bond (Roxon *et al*, 1967; Russ *et al*, 2000; Stolz, 2001). However, reduced flavins are only prevalent in the cytoplasm of the cell, so the azoreduction must occur intracellularly in order for this process to occur (Stolz, 2001). With the highly polar nature of some of the most frequently tested azo dyes, it seems that transport of the azo dyes into the cytoplasm would be a major rate limiting factor (Stolz, 2001). However, one could search the available genomes of anaerobic microorganisms to find that they do in fact contain putative azoreductases. A common strategy is to use the gene sequence of the *E. coli* azoreductase (AzoR) as a query to perform a BLAST search to find azoreductase genes. In addition, the original *acp* phosphodiesterase primers have been used to search genomes for other potential azoreductases.

Since the gene that encodes for an azoreductase was isolated and characterized from *Clostridium perfringens*, an observation regarding whether anaerobic bacteria contain unique azoreductases compared to aerobic bacteria can be made. It can be noted from the phylogenetic tree shown in Figure 7 that the sequence for the azoreductase of *C. perfringens* strain ATCC 3626 is very different from the other azoreductases that have been studied in pure form. As detailed in Table 1, no other azoreductases from strict anaerobes have been studied, suggesting a possible explanation for the differences seen. When comparing similarity of AzoC to the two azoreductases that it falls nearest to on the tree, *Staphylococcus aureus* strain ATCC 25923 and *Staphylococcus cohnii*, it can be determined that AzoC has only 19.4% identity with *Staphylococcus cohnii* and only 17.5% identity with *Staphylococcus aureus* strain ATCC 25923 (determined with Mega5 and http://www.bioinformatics.org/sms2/ident_sim.html) (Tamura *et al*, 2011).

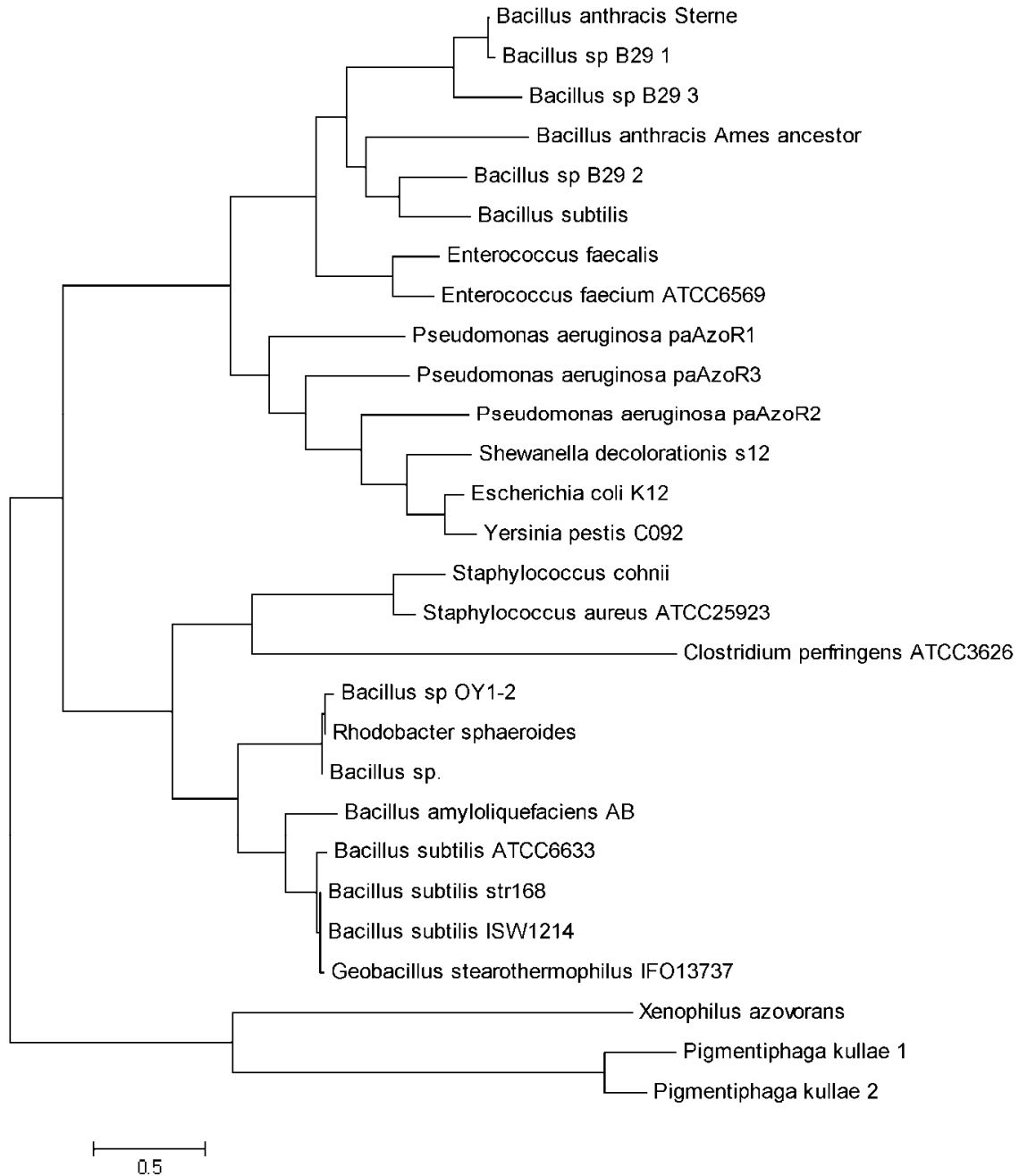


Figure 7. Molecular Phylogenetic Analysis of Azoreductases by the Maximum Likelihood Method. The evolutionary history was inferred by using the Maximum Likelihood method based on the JTT matrix-based model (Jones *et al*, 1992). The tree with the highest log likelihood (-6205.9679) is shown. Initial tree(s) for the heuristic search were obtained automatically as follows. When the number of common sites was < 100 or less than one fourth of the total number of sites, the maximum parsimony method was used; otherwise BIONJ method with MCL distance matrix was used. The tree is drawn to scale, with branch lengths measured in the number of substitutions per site. The analysis involved 28 amino acid sequences. All positions containing gaps and missing data were eliminated. There were a total of 141 positions in the final dataset. Evolutionary analyses were conducted in MEGA5 (Tamura *et al*, 2011).

In 1990, Fatemeh Rafii and colleagues showed that several strict anaerobic bacteria (*Eubacterium hadrum*, *Eubacterium spp.*, *Clostridium clostridiiforme*, *Butyrivibrio spp.*, *Bacteriodes spp.*, *Clostridium paraputrificum*, *Clostridium nexile* and *Clostridium spp.*) were capable of reducing azo dyes in culture studies (Rafii *et al*, 1990). Two years later, Dr. Rafii determined that the azoreductases from these various strictly anaerobic bacteria had immunological homology, suggesting that they share common regions within their sequence (Rafii *et al*, 1992). As more azoreductase genes are identified from anaerobic bacteria, the data in Table 1 will include more anaerobic azoreductases, thereby, supporting the idea that both aerobic and anaerobic azoreductase do exist.

Crystal Structures of Azoreductases

To date, only five azoreductases from aerobic and facultative anaerobes have been crystallized and their three-dimensional structures determined, as detailed in Table 2. To date, no pure azoreductases from strictly anaerobic bacteria have had their structures determined. The first azoreductase structure was AzoR of *E. coli*, which was crystallized and its structure solved in 2006 (PBD 2D5I) (Ito *et al*, 2006). The crystal structure of AzoR revealed the active site of the protein in complex with Methyl Red, its preferred azo dye substrate (Ito *et al*, 2008). The three-dimensional structure of AzoR also shows that the protein has a Rossmann fold structure with five parallel β -sheets flanked by six α -helices (Ito *et al*, 2006). AzoR is also homodimeric in nature, with each monomer having a flavodoxin-like fold holding FMN at the dimer interface (Ito *et al*, 2006). Site-directed mutagenesis studies have suggested that conformational active site changes are responsible for differential substrate specificity (Ito *et al*, 2008).

Table 2. Crystal Structure Details of Azoreductases.

Organism (Azoreductase Name)	PDB ID No.	Characteristics	Multimeric State	Cofactor	Reference
<i>E. coli</i> (AzoR)	2D5I	Rossmann Fold	Dimer	FMN	(Ito <i>et al</i> , 2006)
<i>E. faecalis</i> (AzoA)	2HPV	Rossmann Fold	Dimer	FMN	(Liu <i>et al</i> , 2007)
<i>B. anthracis</i>	3P0R	Rossmann Fold	Monomer	N/D	(Filippova <i>et al</i> , 2010)
<i>P. aeruginosa</i> (paAzoR1)	2V9C	Rossmann Fold	Tetramer	FMN	(Wang <i>et al</i> , 2007)
<i>Y. pestis</i>	4ESE	Rossmann Fold	Dimer	FMN	(Tan <i>et al</i> , 2012)

After AzoR was crystallized, the azoreductases from *E. faecalis* (AzoA, PDB 2HPV) and *Pseudomonas aeruginosa* (paAzoR1, PDB 2V9C) had their crystal structures solved in 2007 (Liu *et al*, 2007; Wang *et al*, 2007). These three-dimensional structures were very similar to that of AzoR, showing a Rossmann fold structure and bound FMN cofactor in a flavodoxin fold (Liu *et al*, 2007; Wang *et al*, 2007). Both AzoA and paAzoR1 are homomultimers, though AzoA is a homodimer and paAzoR1 is a homotetramer (Liu *et al*, 2007; Wang *et al*, 2007). The azoreductases of *Bacillus anthracis* (PDB 3P09) and *Yersinia pestis* (PDB 4ESE) have also been solved, but not intensively studied as they were both the result of high-throughput Structural Genomics projects (Filippova *et al*, 2010; Tan *et al*, 2012). However, both show the characteristic Rossmann fold; additionally, the azoreductase from *Yersinia pestis* was shown to be homodimeric in nature and in complex with FMN in a flavodoxin fold (Filippova *et al*, 2010; Tan *et al*, 2012).

The study of *C. perfringens* and its azoreductase activity is at its infancy. The role of azoreductase in *C. perfringens* is unknown, as its impact on the host or its surrounding normal flora population is not fully understood. In addition, the structure and function of the current AzoC is not fully known. Improving our understanding of these unknowns will have implications in human health as well as in the environment.

Clostridium perfringens

Clostridium perfringens (*C. perfringens*) is a large, Gram-positive bacillus (Ahmad *et al*, 2010). *C. perfringens* is a strict anaerobe and forms endospores under poor environmental conditions (Ahmad *et al*, 2010). *C. perfringens* is ubiquitous and found everywhere from the soil to the colon of the gastrointestinal tract of humans (Ahmad *et al*, 2010). *C. perfringens* is a part of the normal flora of the gastrointestinal tract, though it can be an opportunistic pathogen if the conditions are appropriate, as the bacteria produces three types of toxins (α -toxin, β -toxin and an enterotoxin) (Ahmad *et al*, 2010). *C. perfringens* can be a contaminant in food products and can cause enterocolitis

and food poisoning when ingested in large quantities (Ahmad *et al*, 2010). Most often, *C. perfringens* is found as a contaminant in meat, specifically beef, food products (Angelotti *et al*, 1962; Hall & Angelotti, 1965). *C. perfringens* is capable of sugar, starch, pectin and cellulose fermentation, producing large quantities of hydrogen and carbon dioxide gas and is a common cause of both gas gangrene and cellulitis (Ahmad *et al*, 2010; Madigan *et al*, 2009). The α -toxin and β -toxin produced by this medically-important bacterium are hemolytic in nature and cause acute infections that have lytic effects on many types of cells (Ahmad *et al*, 2010). *C. perfringens* has a diverse metabolic capacity, as it is able to undergo both anaerobic respiration and fermentation (Ahmad *et al*, 2010). Some strains of *C. perfringens* contain catalase, peroxidase and superoxide dismutase, but still require the environment to have low oxygen tension and a low oxidation-reduction potential (Gregory *et al*, 1978).

Clostridium perfringens strains are grouped into five different types, based on their production of the four toxins of *C. perfringens*, including α -toxin, β -toxin, γ -toxin and ι -toxin (Shimizu *et al*, 2002a). The complete genome of *C. perfringens* strain 13, which produces α -toxin (Type A strain) and is isolated from the soil, is known (Shimizu *et al*, 2002a). The complete genome of *C. perfringens* strain SM101 is also known, which is an enterotoxin-producing food poisoning isolate (Myers *et al*, 2006). *C. perfringens* strain ATCC 13124 also has its complete genome known (Myers *et al*, 2006). In contrast, *C. perfringens* strain ATCC 3626, an intestinal isolate from a lamb, produces β -toxin (Type B strain). The genome sequencing of *C. perfringens* ATCC 3626 is not yet complete. Investigation of the available genome of *C. perfringens* strain ATCC 3626 shows that this particular strain is significantly different than the other genome-sequenced *C. perfringens* strains, including the well-studied *C. perfringens* strain 13, strain SM101 and strain ATCC 13124. As calculated by the National Center for Biotechnology Information (NCBI), the dendrogram featuring all genome-sequenced *C. perfringens* strains shows that *C. perfringens* strain ATCC 3626 is located on a separate clade from the three other genome-sequenced *C. perfringens* strains, suggesting that the

not-often-studied *C. perfringens* strain ATCC 3626 is quite unique. Additionally, *C. perfringens* strain ATCC 3626 has a much larger genome size (3.80 Mb) compared to *C. perfringens* strain 13 (3.0 Mb), *C. perfringens* strain SM101 (2.96 Mb) and *C. perfringens* strain ATCC 13124 (3.26 Mb). *C. perfringens* strain ATCC 3626 also has many more genes (3710) than *C. perfringens* strain 13 (2840), *C. perfringens* strain SM101 (2765) and *C. perfringens* strain ATCC 13124 (3016). *C. perfringens* strain ATCC 3626 also has many more proteins (3301) than *C. perfringens* strain 13 (2723), *C. perfringens* strain SM101 (2619) and *C. perfringens* strain ATCC 13124 (2876). Additionally, the numbers for *C. perfringens* will only rise, as its genome sequencing is not yet complete.

***Clostridium perfringens* Cell Structure**

C. perfringens stains purple during a Gram stain and is thus a Gram-positive bacteria. A schematic of the cell envelope structure is shown in Figure 8. The cell structure of *C. perfringens* is comprised of a cell membrane, which encompasses the cytoplasm. Extracellular to the cell membrane of a Gram-positive bacteria lies the periplasmic space (Forster & Marquis, 2012). The periplasmic space consists of proteins and lipoteichoic acid that is anchored to the cell membrane (Forster & Marquis, 2012; Matias & Beveridge, 2008). Though this area between the cell membrane and cell wall is often referred to as a periplasmic space, it is technically an inner-wall zone (it is 30 nm thick) and is not as thick as a typical Gram-negative cell wall periplasmic space (Forster & Marquis, 2012).

The Gram-positive bacterial cell wall is a very dynamic structure that undergoes constant remodeling (Forster & Marquis, 2012; Xia *et al*, 2010). This region is 25-50 nm thick and is composed of peptidoglycan, wall teichoic acid polymers and a variety of amino acids; additionally, the peptidoglycan in Gram-positive bacteria is composed of disaccharide glycan chains of various lengths that are linked by short proteins (Forster & Marquis, 2012). It has been suggested that proteins as large as 25 kDa can freely cross the cell wall to the extracellular environment, but this

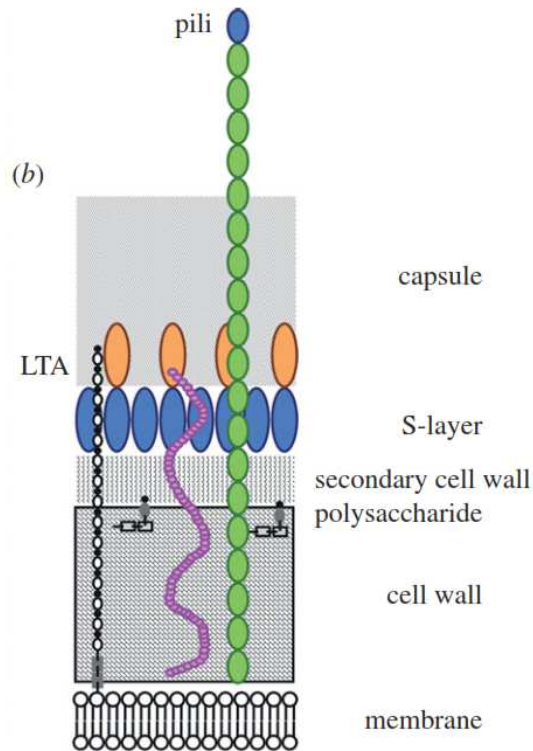


Figure 8. Cell Envelope Structure of a Gram-positive Bacteria, Similar to *C. perfringens*. LTA (Lipoteichoic acid) (Schneewind & Missiakas, 2012).

estimate largely depends on the length of the glycan chains of peptidoglycan, the level of cross-linking between these chains, pH and turgor pressure; it is by no means an unregulated event (Forster & Marquis, 2012).

The cell wall of *C. perfringens* (formerly *C. welchii*) was studied in 1966 by B. T. Pickering (Pickering, 1966). In particular, the cell wall was found to contain alanine, 2,6-diaminopimelic acid, glutamic acid, glycine, glucosamine, muramic acid, galactosamine, mannosamine, ethanolamine, rhamnose, galactose and phosphorus (Pickering, 1966). The structure of the cell wall was found to consist of 1 - 4-linked N-acetylglucosamine (NAG) and N-acetylmuramic acid (NAM) residues (Pickering, 1966). To the NAM and NAG, through the carboxyl group of muramic acid, a peptide composed of D- and L-alanine, D-glutamic acid, L-lysine and glycine is linked (Pickering, 1966). L-lysine can also be found to be substituted by 2,6-diaminopimelic acid (Pickering, 1966). In the cell wall model provided by B.T. Pickering, the hexapeptide crossbridge is predicted to be in the

following order: L-Ala-D-Glu(Gly)-L-Lys(DAP)-D-Ala-D-Ala-D-Glu (Pickering, 1966). The peptidoglycan structure of *Clostridium* is known to be substantially different between vegetative and spore-forming cells, suggesting that this bacterium enters a structurally-unique “non-growth” state (Humann & Lenz, 2009).

In addition to the major cell wall components described above, *C. perfringens* also contains many important surface and cell wall proteins, as studied recently in *C. perfringens* strain ATCC 13124 (Alam *et al*, 2009). Many of the proteins found on the surface of this strain of *C. perfringens* were found to be immunogenic and are potential vaccine candidates for this medically-important bacterium (Alam *et al*, 2009). In addition, these S-layer proteins could also serve as a mechanism of rapid diagnosis of *C. perfringens* infections (Alam *et al*, 2009; Sara & Sleytr, 2000). Proteins located on the surface of *C. perfringens* strain ATCC 13124 include ornithine carbamoyltransferase, cystathione beta-lyase, choloylglycine hydrolase, serine proteinase and rhomboid-family proteins, including many other proteins predicted to have functions in metabolism (including amino acid transport and metabolism or lipid metabolism) (Alam *et al*, 2009). In *C. difficile*, the *secA2* gene is required for the assembly of the S-layer (Schneewind & Missiakas, 2012). *C. perfringens* is also known to have a functional two-component system (BceRS) that functions in signal transduction in response to stressors (Jordan *et al*, 2008).

Protein Translocation Systems

The cell membrane is the main hurdle of proteins crossing to the extracellular environment. Six protein translocation systems have been studied in Gram-positive bacteria to date (the Secretion translocation system, the twin arginine transporter, the fimbriin-protein exporter, the flagella export apparatus, phage-inserted holins and the ESAT-6.WXG100 secretion system) (Forster & Marquis, 2012). The protein translocation systems of *C. perfringens* have not been studied, though in close relatives *C. tetani*, *C. difficile* and *C. acetobutylicum*, the secretion translocation (Sec) system seems

to be the most common way that proteins are excreted into the extracellular environment (Berks *et al*, 2005; Bruggemann *et al*, 2003; Desvaux *et al*, 2005; Schneewind & Missiakas, 2012). In *C. difficile*, two separate *secA* genes have been identified, one of which (*secA2*), seems to be directly responsible for the protein secretion related to the creation of the S-layer (Schneewind & Missiakas, 2012). The twin arginine translocation system (Tat) has been found to be absent from all *Clostridium* genomes so far (Bruggemann *et al*, 2003).

Interestingly, in the previously mentioned recent study on the cell-surface proteins of *C. perfringens* strain ATCC 13124, several of the surface proteins found were predicted to be cytoplasmic in nature due to function or lack of signal peptide (Alam *et al*, 2009). Additionally, this phenomenon has been found in an increasing number of proteins throughout Gram-positive bacteria (Alam *et al*, 2009; Bukau & Horwich, 1998; Cole *et al*, 2005; Severin *et al*, 2007; Shimizu *et al*, 2002b; Walz *et al*, 2007). In fact, in a previous study it was shown in *C. perfringens* that the culture supernatant following late exponential phase contained proteins that were predicted to be intracellular and that did not contain signal sequences (Shimizu *et al*, 2002b). ESAT-6 secretions are known to support the secretion of proteins that do not contain a signal peptide sequence (Pallen, 2002). ExPortal systems may also play a role but these have not been thoroughly studied in *C. perfringens* (Rosch & Caparon, 2004).

Despite the overwhelming support for translocated proteins without signal peptide sequences, the mechanism by which these proteins are able to exit the cell without a signal peptide sequence is yet unknown (Bendtsen *et al*, 2005; Wang *et al*, 2013; Wickner & Schekman, 2005). Some authors have recently suggested piggy-backing on proteins with signal sequences as a possible mechanism of transport for non-signal peptide sequence proteins (Wickner & Schekman, 2005). In *E. coli*, environmental extracellular stress on the cell wall can cause proteins to selectively escape from the intracellular space due to a stress response (Vazquez-Laslop *et al*, 2001). Non-classical protein secretion appears to be tightly regulated and influenced by specific stimuli and may represent a stress

response (Wang *et al*, 2013). Therefore, the main aim of this non-classical protein secretion pathway may be to protect the cell from the undesirable effects of the stressor or may aid in bacterial virulence (Wang *et al*, 2013). As previously mentioned, *C. perfringens* does have a functioning BceRS two-component system for stress response (Jordan *et al*, 2008). However, there does not appear to be any signal or motif that is consistent with these non-classically secreted proteins, making prediction of these proteins difficult (Bendtsen *et al*, 2005).

***Clostridium perfringens* Cell Growth**

The growth and nutritional requirements of *C. perfringens* were determined almost immediately upon the discovery of the species, as it was an important food contaminant (Fuchs & Bonde, 1957). In most cases, *C. perfringens* requires complex media to grow, suggesting that the species possesses a very simplistic metabolic system and cannot synthesize many components required for growth and survival (Caldwell, 2000; Fuchs & Bonde, 1957). The generation time of *C. perfringens* can be as rapid as 7.4 minutes under optimal conditions (37 to 45°C, rich media), confirming the role of this bacterium as a contaminant in meat and poultry products and a common cause of food-borne illness (Shimizu *et al*, 2002a; Smith & Schaffner, 2004; Willardsen *et al*, 1979).

C. perfringens is a strictly anaerobic bacterium that is capable of anaerobic respiration and fermentation (Madigan *et al*, 2009). The recent genome sequencing of *C. perfringens* strain 13 has shown that *C. perfringens* is capable of utilizing a variety of sugars as a carbon source, including fructose, galactose, glycogen, lactose, maltose, mannose, raffinose, starch and sucrose, both via culture studies and the presence of the necessary glycolytic genes within the genome (Shimizu *et al*, 2002a; Sneath, 1986). *C. perfringens* was determined to have the complete set of enzymes necessary for both glycolysis and glycogen metabolism, but is lacking the genes necessary for the tricarboxylic acid (TCA) cycle or any respiratory chain related proteins (Shimizu *et al*, 2002a). Additionally, all of the genes responsible for anaerobic fermentation are present in the *C. perfringens* genome, resulting

in the production of lactate, alcohol, acetate and butyrate, which have been found in culture studies (Shimizu *et al*, 2002a; Sneath, 1986). Fermentation results in the production of hydrogen gas and carbon monoxide, both of which are necessary for the creation of an anaerobic environment in host tissues and are directly responsible for the growth and survival of *C. perfringens* in the host (Shimizu *et al*, 2002a). In addition to the typical fermentation pathways, genes necessary for amino acid fermentation are also found in *C. perfringens*, specifically for the fermentation of serine and threonine (Shimizu *et al*, 2002a). *C. perfringens* is capable of switching between anaerobic respiration and fermentation based on the electron acceptor present in the environment.

***Clostridium perfringens* Azoreductase Function**

Rafii and colleagues were instrumental in the initial culture studies of strictly anaerobic intestinal bacteria. In their initial studies, they isolated several species and strains of bacteria which they found to be capable of reducing the azo dye, Direct Blue 15, on a non-denaturing SDS gel assay (Rafii & Cerniglia, 1990). Among these bacteria that seemed to possess an azoreductase was *C. perfringens* (Rafii & Cerniglia, 1990). Based on the single zone of Direct Blue 15 clearing on the gel, it was predicted that *C. perfringens* only contained one azoreductase enzyme, which Rafii and colleagues proceeded to extract from the gel and purify (Rafii & Cerniglia, 1990). Upon purification and analysis on an SDS-PAGE gel, it was determined that the putative azoreductase was actually dimeric in nature (Rafii & Cerniglia, 1990). The putative azoreductase did not require the exogenous addition of a flavin cofactor for activity, but interestingly did require the absence of oxygen (Rafii & Cerniglia, 1990; Rafii *et al*, 1990). Culture studies suggested that the azoreductase production was constitutive and extracellular, a finding which was confirmed by immunoelectron microscopy with gold-labeled antibodies to the putative azoreductase (Rafii & Cerniglia, 1990; Rafii & Cerniglia, 1993; Rafii *et al*, 1990). Rafii's azoreductase was found to be antigenically similar to a putative azoreductase from *Eubacterium*, which suggested the presence of a conserved domain in azoreductases (Rafii *et al*, 1992).

In their last publication (1999), the Rafii group attempted to rescue and characterize this putative azoreductase gene in a fragment of DNA, however, their study was not complete (Rafii & Coleman, 1999). In 2007, Cristee Wright studied this fragment and upon looking deeper into the 3.8kB fragment that Rafii had suggested contained the azoreductase, Wright found that this fragment contained a number of open reading frames, none of which were expected to code for an azoreductase enzyme (Wright, 2007). However, given the high azoreductase activity against Direct Blue 15 seen in Rafii's culture studies, there is a high probability that there is a functioning azoreductase present in *C. perfringens* (Rafii & Cerniglia, 1990; Rafii *et al*, 1990; Wright, 2007). In her thesis, Cristee Wright was able to identify a candidate for the azoreductase of *C. perfringens* (Wright, 2007).

Azoreductase Gene (AzoC)

Wright identified the gene for the azoreductase of *C. perfringens* strain ATCC 3626 through searching the available *C. perfringens* genome for sequence homology to both the nucleic acid and protein sequences from known bacterial azoreductases from *E. coli*, *Staphylococcus aureus*, *Enterococcus faecalis* and *Bacillus OYI-2* in hopes that there would be a conserved domain which aids in conferring azoreductase activity (Wright, 2007). Wright cloned and expressed her NAD(P)H-dependent FMN reductase (which contained an FMN-reductase domain) gene in *E. coli*, but was unable to obtain pure protein (Wright, 2007). Initial studies with mixed protein showed high azoreductase activity against Direct Blue 15, consistent with the culture studies (Wright, 2007). Pure enzyme studies with AzoC would be needed to confirm that this gene encodes for azoreductase activity in *C. perfringens* strain ATCC 3626.

Conclusion

Very little information is known about azoreductases that originate from strictly anaerobic bacteria. Much of the information comes from whole cell culture studies of strict anaerobes isolated from the human gastrointestinal tract. The purpose of this study is to fully characterize the azoreductase of *C. perfringens* strain ATCC 3626 in terms of enzyme structure and function in order to fill the gap in the literature regarding azoreductases originating from strictly anaerobic bacteria.

CHAPTER II

IDENTIFICATION, ISOLATION AND CHARACTERIZATION OF A NOVEL AZOREDUCTASE FROM *CLOSTRIDIUM PERFRINGENS*

The following chapter is based off of a publication in the journal *Anaerobe* (2012, **18**:229-234) and appears here with the journal's permission.

Abstract

Azo dyes are used widely in the textile, pharmaceutical, cosmetic and food industries as colorants and are often sources of environmental pollution. There are many microorganisms that are able to reduce azo dyes by use of an azoreductase enzyme. It is through the reduction of the azo bonds of the dyes that carcinogenic metabolites are produced thereby a concern for human health. The field of research on azoreductases is growing, but there is very little information available on azoreductases from strict anaerobic bacteria. In this study, the azoreductase gene was identified in *Clostridium perfringens*, a pathogen that is commonly found in the human intestinal tract. *C. perfringens* shows high azoreductase activity, especially in the presence of the common dye Direct Blue 15. A gene that encodes for a flavoprotein was isolated and expressed in *E.coli*, and further purified and tested for azoreductase activity. The azoreductase (known as AzoC) was characterized by enzymatic reaction assays using different dyes. AzoC activity was highest in the presence of two cofactors, NADH and FAD. A strong cofactor effect was shown with some dyes, as dye reduction occurred without the presence of the AzoC (cofactors alone). AzoC was shown

to perform best at a pH of 9, at room temperature, and in an anaerobic environment. Enzyme kinetics studies suggested that the association between enzyme and substrate is strong. The results show that AzoC from *C. perfringens* has azoreductase activity.

Introduction

Azo dyes are synthetic organic colorants used widely in the manufacture of textiles, pharmaceuticals, cosmetics, and a wide variety of foods. Each year, almost 1 million tons of azo dyes are produced worldwide (Suzuki *et al*, 2001). Most of the dyes are released into the environment as effluent in industrial wastewater and, because of their recalcitrance, persist there as pollutants (Nakanishi *et al*, 2001). In addition, azo dyes are linked to causing several types of cancers in humans (Rafii & Coleman, 1999).

Azoreductases cleave the azo linkage (N=N) of azo dyes in a reductive process that produces aromatic amines and decolorizes the dye (Nakanishi *et al*, 2001; Stolz, 2001). The genes encoding azoreductases have been cloned and characterized from a number of bacterial strains (Blumel & Stolz, 2003; Chen *et al*, 2005a; Chen *et al*, 2004; Nakanishi *et al*, 2001; Sugiura *et al*, 2006). The enzymes, reported to be flavoproteins, range from 19 - 30 kDa in size and require either NADH or NADPH as electron donors. Bacteria from the human intestinal tract can be exposed to azo dyes from environmental contamination and from consumption of dyes in foods and drugs (Dillon *et al*, 1994; Marmion, 1991). In the intestine, bacterial azoreductases reduce the dyes to their component aromatic amines. Some of these amines are carcinogenic and mutagenic to humans, causing cancer of the kidney, bladder, stomach, and liver (Brown & Devito, 1993; Chung *et al*, 2000; Rafii & Coleman, 1999). Several species of intestinal bacteria with azoreductase activity have been isolated and studied (Chung & Cerniglia, 1992; Gingell & Walker, 1971; Rafii *et al*, 1990; Song *et al*, 2003; Walker *et al*, 1971). Among those having high azoreductase activity is the anaerobic bacterium *Clostridium perfringens*.

C. perfringens is a Gram-positive, rod-shaped, anaerobic and spore-forming bacterium (Ahmad *et al*, 2010). Some strains contain catalase, peroxidase, and superoxide dismutase but still require low oxygen tension and low oxidation reduction potential. *C. perfringens* is considered a pathogen as it produced enterotoxins that cause a range of symptoms from mild enterotoxaemia to fatal gas gangrene (Ahmad *et al*, 2010). The bacterium possesses both anaerobic respiration and fermentative capabilities, which provides it with a diverse metabolic capacity (Ahmad *et al*, 2010). One major metabolic activity found is azoreductase. The current study isolated an azoreductase gene from the chromosome of *C. perfringens*, expressed the gene in *Escherichia coli*, and purified and characterized the enzyme activity using several azo dyes. This is the first time a flavoprotein from *C. perfringens* has been identified as having azoreductase activity.

Background Information and Previous Work (Wright, 2007)

To determine if *C. perfringens* cultures were able to efficiently reduce azo dyes, Direct Blue 15 was added to the culture and at approximately 4 hours the dye was completely reduced, which suggested that the organism contained an azoreductase. No dye reduction was seen in the accompanying control. Other dyes besides Direct Blue 15 were also tested, along with dye only controls; over a period of 12 hours, most of the other dyes were reduced under the control conditions, without the presence of the whole cells. Direct Blue 15 showed no reduction under these control conditions, but a great reduction in the presence of the whole cells.

tblastn and tblastp software (National Center for Toxicological Research) were used to search the *C. perfringens* chromosome for proteins showing homology to the deduced nucleotide and amino acid sequences of the azoreductases from *E. coli*, *Enterococcus faecalis*, *Staphylococcus aureus* and *Bacillus* OY1-2. Since the nucleotide and amino acid sequences of known azoreductases revealed no conserved sequences based on primary alignments, a more

rigorous screening method was implemented. A list of known bacterial azoreductases and their conserved domains was obtained from the Universal Protein Resource (UniProt) Knowledgebase. The putative azoreductase gene from *C. perfringens* was identified by first identifying bacterial azoreductase conserved domains which were found to be homologous to either an FMN_reductase or a flavodoxin_2 conserved region. The Protein Family Database (PFAM) was used to identify proteins with these conserved domains within the *C. perfringens* chromosome and also to compare their function(s) to that of known azoreductases. Using PFAM, a single putative NAD(P)H-dependent FMN reductase having a conserved FMN_reductase domain was identified in the *C. perfringens* chromosome. The gene, annotated as a hypothetical protein was designated *azoC* for the purpose of the study. Analysis of the gene coordinates revealed the ORF to be part of an operon with four other ORFs – two hypothetical proteins with unknown function, a probable anaerobic ribonucleotide reductase, and a hypothetical protein thought to be involved in 2'-deoxyribonucleotide metabolism (Figure 9).

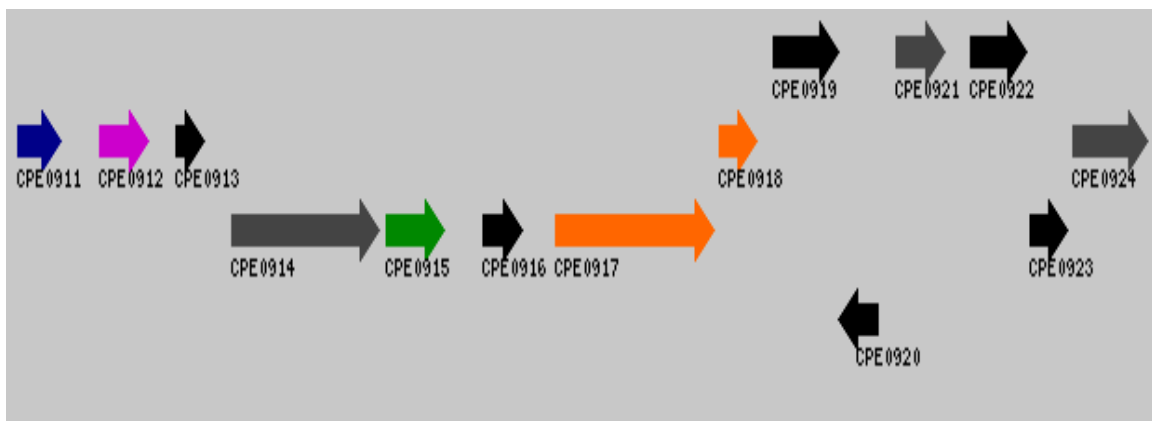


Figure 9. Region View of CPE0915 in the *C. perfringens* Chromosome (Institute). CPE0911 – glutathione peroxidase; CPE0917 – probable anaerobic ribonucleotide reductase; CPE0912, CPE0913, CPE0916, CPE0918, CPE0919, CPE0920, CPE0922, CPE0923 – hypothetical proteins; CPE0914, CPE0915, CPE0921, CPE0924 – conserved hypothetical proteins. CPE0915 represents the putative *azoC*.

C. perfringens strain ATCC 3626 was grown on sheep blood agar plates in an anaerobic jar for 3 days at 37°C and used to inoculate 10 mL of anaerobic brain heart infusion broth (BHI) in an anaerobic chamber. The broth culture was used for the preparation of chromosomal DNA. Genomic DNA was extracted from a fresh 10 mL culture of *C. perfringens* strain ATCC 3626 according to the Masterpure Gram Positive DNA Purification Kit (Epicentre Biotechnologies). The *azoC* open reading frame was amplified using *C. perfringens* genomic DNA as template. The forward primer (*flavoF3*) included an XhoI site before the start codon: 5'-CGGCC TCGAG ATGAA AGTAT TATTA GTTA - 3'. The reverse primer (*flavo0915r*) included a BamHI site downstream of the *azoC* ORF: 5' – GTGAA AGGAT CCTTA TCTAA TAAAA TTAGT TCTTT CTCTT TC - 3'.

Template DNA and primers for the control reaction were provided in the TOPO TA cloning kit (Invitrogen). PCR was carried out in a Perkin Elmer 480 DNA thermal cycler. Conditions for amplification were followed as outlined in the TOPO TA cloning manual (Invitrogen) - one cycle of 2 min at 94°C, 25 cycles with each cycle consisting of 1 min at 94°C, 1 min at 55°C, and 1 min at 72°C, and a final extension of 7 min at 72°C. The products were analyzed on a 1% agarose gel after staining with ethidium bromide.

The PCR product containing the *azoC* ORF was directly cloned into pCR 2.1-TOPO TA vector (Invitrogen) and sequenced. The TOPO clone and pET15b (Novagen) were each cleaved by sequential digestion with XhoI and BamHI restriction enzymes, each time at 37°C for 12 hours. The 721 bp product (Figure 10A) from cleavage of the TOPO clone was purified using the QIAquick Gel Extraction Kit (QIAGEN) and ligated between the XhoI and BamHI sites of pET15b in a reaction containing 0.1 U T4 DNA ligase and carried out at 4°C for 16 hours. A 2 µl volume of the ligation mixture was used to transform 20 µl of NovaBlueDE3 *E. coli* cells (Novagen). Following plasmid extractions, positive clones were confirmed by PCR with the insert specific primers *flavoF3* and *flavo0915r* and by simultaneous cleavage with XhoI and

BamHI. The recombinant DNA (pAzoC) was used to transform BL21pLysS *E. coli* cells, which were deficient in protease activity, and used for expression of the azoreductase. The induced protein produced a band at 22.6 kDa based on the SDS-PAGE gel (Figure 10B).

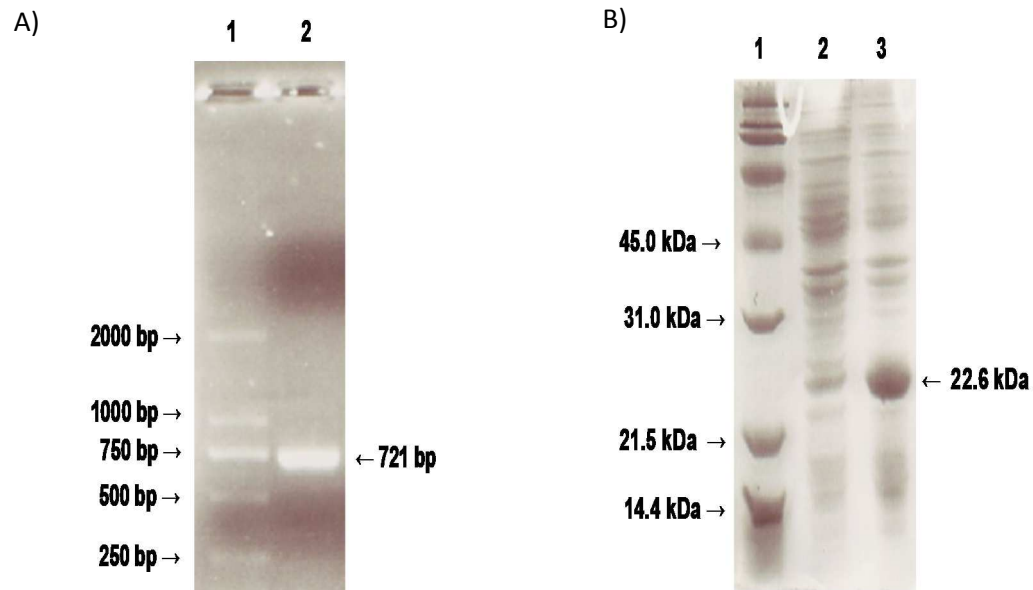


Figure 10. PCR Amplification of the *azoC* ORF and SDS-PAGE Analysis of AzoC. **A)** PCR Amplification of *azoC* ORF. Lane 1: Mid-Range Marker (Thermo Scientific), Lane 2: *azoC* ORF. **B)** SDS-PAGE Analysis of AzoC. Lane 1: Protein Standard (Pierce), Lane 2: Uninduced AzoC, Lane 3: Induced (1 mM IPTG, 3 hrs, 37°C) AzoC.

Materials and Methods

Azo Dyes

Azo dyes were purchased from the following companies: Direct Blue 15 (MP Biomedicals), Methyl Red (Acros Organics), Tartrazine (Sigma-Aldrich), Trypan Blue (Kodak), Congo Red (Sigma-Aldrich), Eriochrome Black T (MCB), Buffalo Black NBR (Allied Chemical), Janus Green (Sigma-Aldrich) and Cibacron Brilliant Red 3B-A (Sigma-Aldrich).

Purification of the Azoreductase Enzyme

The *E. coli* cells containing the pAzoC (as prepared above) were inoculated into a 5 mL LB broth containing ampicillin (100 µg/mL) and incubated overnight with shaking at 200 rpm at 37°C. The cells were transferred to a large flask containing 1 L LB broth containing ampicillin (100 µg/mL) and incubated shaking at 200 rpm at 37°C until the OD₆₀₀ of the culture was at 0.6. The cells were then induced with isopropyl-beta-D-thiogalactopyranoside (IPTG, 1 mM final concentration) for an additional 3 hours. This culture was then centrifuged (6000 x g, 10 minutes, 4°C) to pellet the cells. The supernatant was discarded as bacterial waste and the pellets were stored at -20°C until protein purification could occur.

The pellet was thawed and resuspended in 10 mL of a lysis/wash buffer (20% glycerol, 50 mM sodium monobasic phosphate, 750 mM sodium chloride and 20 mM imidazole in double-distilled water, pH 8.0). Lysozyme (0.1 mg/mL final concentration) was added to each of the pellets and incubated on ice for 30 minutes. Cell pellets were sonicated with a Sonic 300 dismembranator with an intermediate tip and relative output of 60%. Sonication occurred in 10 intervals of 5 seconds each. The cell suspension remained on ice when not being sonicated to ensure that the protein was not denatured by the heat generated by sonication. The suspension was centrifuged (10,000 x g, 30 minutes, 4°C) to pellet the cell debris and to leave the protein in solution.

The supernatant was subjected to nickel-nitrilotriacetic acid (Ni-NTA) slurry (Clon-Tech) in a 1:1 ratio of supernatant to slurry in a glass frit column (Kimble-Chase Flex Column). The Histidine-tag of the protein allows for this purification procedure to be effective. All steps were carried out at 4°C to ensure that the protein did not denature during the process. The samples were incubated at 4°C for 1 hour on a BioDancer orbital shaker (New Brunswick Scientific) at medium speed to ensure that the His-tagged protein would stick to the Ni-NTA resin. Following protein

exposure to the column, the excess solution was drained from the column (pre-wash fraction) and the resin was washed with lysis/wash buffer until the effluent from the column was clear (wash fractions). Following washing, the protein was eluted from the resin by exposing the resin to elution buffer (20% glycerol, 50 mM sodium monobasic phosphate, 750 mM sodium chloride, 250 mM imidazole, double-distilled water, pH 8.0). At least four elutions were carried out to ensure that all protein was eluted from the resin. Elutions were saved and stored at -20°C.

All elutions were analyzed with an SDS-PAGE gel. SDS-PAGE analysis was performed as described previously (Laemmli, 1970). Protein samples were prepared for analysis directly following protein purification by adding a 1X concentration of SDS-PAGE loading buffer (4X loading buffer = 0.06 M TRIS-HCl pH 6.8, 10% (v/v) glycerol, 2% (w/v) SDS, 0.0025% (w/v) bromophenol blue). Beta-mercaptoethanol (5%) was used to denature disulfide bonds. Protein samples were boiled for 15 minutes and then loaded (20 μ L) onto a 12.5% SDS-PAGE gel. Coomassie blue was used for staining and the protein bands were visualized and photographed in comparison to a 250 kDa protein ladder (New England Biolabs). Protein concentration was determined with a Nanodrop spectrometer, using the Molar Extinction Coefficient of the protein (0.880) to determine the protein concentration. The Molar Extinction Coefficient was determined by using the NCBI database. All samples were concentrated using an Amicon Ultrafiltration cell under Nitrogen pressure and a Millipore filter (Regenerated Cellulose membrane, NMWL 10,000) to achieve a protein concentration of between 2 and 5 mg/mL.

Pure Enzyme Assays – Anaerobic and Aerobic Conditions

Assays for azoreductase activity for the pure AzoC protein were carried out both anaerobically and aerobically. All experiments were performed in triplicate. Enzyme reactions were carried out in a 1.5 mL-polystyrene cuvette (Sigma-Aldrich) with a total reaction volume of 1 mL. The buffer used in most cases (except for specific pH experiments) was 25 mM TRIS, pH

9.0. Although different azo dyes were tested the final concentration tested was consistently 20 μM . Experiments were performed to determine the optimal enzyme concentration in the reaction by altering the concentration of the protein and once the optimal AzoC concentration was found, different cofactors were tested (NADH and NADPH). The concentration of NADH (Acros Organics) was also altered in experiments to determine optimal conditions for dye reduction (10 mM NADH). FAD (Sigma-Aldrich) and FMN (Sigma-Aldrich) were both tested as cofactors and FAD was found to be an essential component to the azoreductase function of AzoC at an optimal concentration of 2 mM.

Reactions were prepared by mixing the appropriate buffer, azo dye, water and the enzyme together in the cuvette and bubbling with nitrogen at a rate of 1 nitrogen bubble per second for 10 minutes. Immediately following the nitrogen bubbling, mineral oil was added to the top of the cuvette to prevent the introduction of oxygen into the newly anaerobic system. Aerobic experiments were performed without the nitrogen bubbling step and without the addition of mineral oil. To begin the reaction, 10 mM NADH and 2 mM FAD were mixed together separately and then added to the reaction and mixed together carefully as to not introduce oxygen into the system. The reaction was scanned using a Shimadzu UV-1650 PC spectrophotometer. Each azo dye was scanned prior to the reaction with the spectrophotometer to determine the optimal absorbance for each dye (all dye absorption values were above 340 nm and extinction coefficients were used in determining the final concentration of dyes). In some cases, an absorbance was selected that was not the optimal due to interference by the absorbance of FAD, which is orange in color. The absorbencies tested were as follows: Direct Blue 15 (602.5 nm), Cibacron Brilliant Red 3B-A (534.00 nm), Congo Red (531.00 nm), Tartrazine (425.00 nm), Janus Green (597.50 nm), Trypan Blue (533.50 nm), Buffalo Black NBR (614.50 nm), Methyl Red (430.00 nm) and Eriochrome Black T (527.50 nm). Dye concentration was interpolated from absorbencies by making standard curves of dye concentrations to find the extinction coefficient.

This was determined to be a spectrophotometer-specific equation of a best fit line. Experiments were also done to determine the optimal order of the addition of reactants to the system where each of the components (dye, AzoC, cofactors) were added last in separate experiments.

Pure Enzyme Assays – Cofactor Effect

To determine the effect of the cofactor on the enzyme reaction, experiments were performed that lacked the azoreductase and contained a protein control, albumin (Sigma-Aldrich). The protein control would serve to show whether the azoreductase was causing the reduction of the dye or if the cofactors and the presence of a protein was causing the reduction. Experiments were also performed that did not contain a protein and showed the effects of the cofactors themselves. In the case of the protein control, 138 µg of albumin was added to the reaction in place of AzoC. For the cofactor controls, only NADH and FAD were added to the reaction; no protein was present in these experiments.

Pure Enzyme Assays – Optimal Temperature

To determine the optimal temperature for the azoreductase enzyme to work, experiments were carried out at several different temperatures (25°C/room temperature, 30°C, 37°C, 45°C and 60°C). Prior to the reaction taking place, all components except for the cofactors were incubated in their cuvette in a water bath to reach the desired temperature. The cuvette was moved to the spectrophotometer to begin the experiment with the cofactors and then promptly moved back to the water bath. The absorbance was recorded every 5 minutes until the reading reached a plateau.

Pure Enzyme Assays – Optimal pH

To determine the optimal pH for AzoC to work, several different pH buffers were prepared to test azoreductase activity: sodium acetate pH 4.0 and 5.0, potassium phosphate pH 6.0 and 7.0, TRIS pH 8.0 and 9.0, sodium bicarbonate pH 10.0 and 11.0, and potassium chloride

pH 12.0. Enzyme experiments were conducted as described above by only changing the pH of the buffer used.

Pure Enzyme Assays – Effect of Oxygen

Since AzoC is from an anaerobic organism, there was curiosity as to the effect of oxygen on the protein itself. To study this, anaerobic and aerobic experiments were performed and compared as mentioned above. In another experiment, an anaerobic reaction at the optimal conditions was prepared and taken to complete dye reduction. Following dye reduction, the cuvette was bubbled again (in one case with Nitrogen and in another case with Oxygen). Dye and cofactors were added into the reaction and the cuvette scanned. This provides an understanding of the regeneration of the enzyme in the presence of oxygen as compared to anaerobically.

Pure Enzyme Assays – Enzyme Kinetics

A brief study of the enzyme kinetics was performed by taking one component of the experiment (dye, FAD, NADH) and changing the concentration of that component while keeping the others constant. The optimal conditions were 20 μ M dye, 10 mM NADH and 2 mM FAD. During the kinetics experiments, the optimal concentration of one of these components was tested by either increasing or decreasing in hopes of finding a saturation point for the enzyme. Results were graphed and analyzed by a Lineweaver-Burke plot to determine K_m and V_{max} .

Results

Pure Enzyme Assays – Initial Work and Cofactor Effect

Bacterial azoreductases require NADH and/or NADPH as an electron donor and the cofactor FMN and/or FAD can serve as a prosthetic group. AzoC was determined to be NADH-dependent as it demonstrated the highest activity, with NADPH showing no significant dye reduction activity when tested as an electron donor for the reaction for the reduction of Direct

Blue 15 (p-value >0.05, 95% confidence). FAD and FMN were also tested and the results showed that neither are acceptable for the reduction Direct Blue 15 by themselves (less than 10% dye reduction occurs) with AzoC, producing non-significant dye reduction (p-value >0.05, 95% confidence). However, when these flavin cofactors are combined with NADH a great reduction occurs, with up to 100% of the dye being reduced (Figure 11). This produces a statistically significant azo dye reduction at a 95% confidence interval (p-value <0.001). Comparing FMN by itself to FMN/NADH, the cofactor combination of FMN/NADH showed a five-fold increase in dye reduction, a result that is statistically significant at a 95% confidence interval (p-value <0.001). FAD/NADH compared to FAD by itself showed an 8.5-fold increase in dye reduction when the cofactor combination of FAD/NADH was used, which is also statistically significant at a 95% confidence interval (p-value <0.001).

Controls that test the reducing effects of the cofactors themselves on the dye were implemented to understand what effect the enzyme is playing compared to the cofactors. Although FMN/NADH produced the overall greatest drop in Direct Blue 15 absorbance, the control (without AzoC) showed just as much activity (Figure 11), resulting in non-significant dye reduction by FMN/NADH (p-value >0.05, 95% confidence). This was not the case with FAD/NADH, which showed great activity with AzoC, but significantly less activity when without AzoC (Figure 11). In contrast to FMN/NADH, the FAD/NADH combination with AzoC shows significant dye reduction over its non-enzymatic control at a 95% confidence interval (p-value <0.001). Due to this fact, the FAD/NADH combination was used in testing. Interestingly, the greatest reduction of the dye occurred when NADH and FAD were mixed together and added last to the reaction mixture, thus allowing time for the azo dye substrate to interact with AzoC prior to the addition of the cofactor mixture.

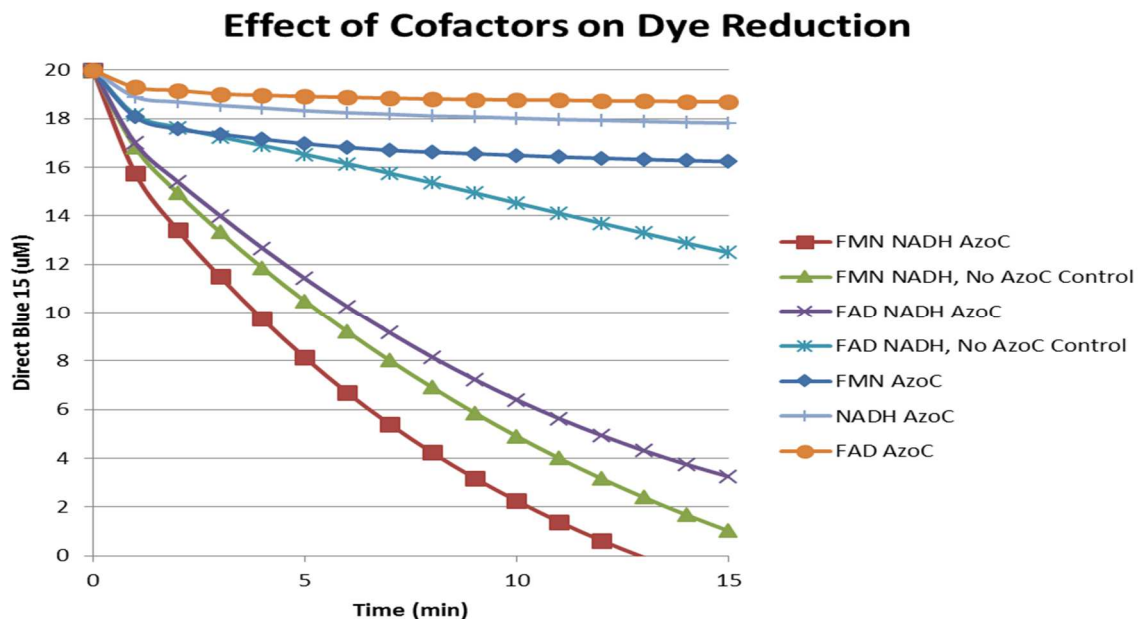


Figure 11. Effect of Cofactors on Direct Blue 15 Reduction by AzoC. Comparison of FAD/NADH with AzoC and FAD/NADH without AzoC shows a significant difference in dye reduction in the reaction with the enzyme (p-value <0.001, 95% confidence). Comparison of FMN/NADH with AzoC and FMN/NADH without AzoC does not show a significant difference in dye reduction between the reaction with the enzyme and the non-enzymatic control (p-value >0.05, 95% confidence).

Upon further examination of the dye reduction by AzoC, a cofactor effect was noticed. With Direct Blue 15, the presence of FMN/NADH alone was enough to reduce the dye, making dye reduction with AzoC, FMN/NADH insignificant over the FMN/NADH cofactors alone (p-value >0.05, 95% confidence) (Figure 11). When no protein was present, a slight reduction in dye absorbance occurred with FAD/NADH (less than 35% dye reduction) but a large reduction for FMN/NADH (100% dye reduction) suggesting that the reduction in dye was caused by the cofactors themselves. However, the FAD/NADH required the presence of the protein to produce significant Direct Blue 15 reduction and the presence of any protein, as shown by the albumin control in Table 3 (p-value <0.05, 95% confidence). This was not the case with the individual cofactors (FMN or NADH) themselves, but only occurred when the two cofactors were mixed together and added to the reaction. Other dyes were also tested with AzoC and this cofactor effect was also seen with some of the other dyes. A similar effect was observed with other dyes (Janus

Green, Cibacron Brilliant Red 3B-A and Eriochrome Black T) as the specific activity was not significantly different for the albumin control and AzoC (Table 3, unhighlighted rows, p-value >0.05, 95% confidence). Significantly, Direct Blue 15 undergoes the greatest reduction by AzoC, compared to other azo dyes tested when taking the non-AzoC containing control and therefore the effect of the cofactors into account (Table 3).

Table 3. Specific Activities of Other Dyes in the Presence of AzoC and Albumin. Specific activity is provided as mean \pm standard deviation across triplicates (n=3) for both AzoC and Albumin (control). Highlighted rows represent statistically significant differences at a 95% confidence interval (p-value <0.05)

Dye	Specific Activity with AzoC ($\mu\text{M dye/min/mg AzoC}$)	Specific Activity with Albumin ($\mu\text{M dye/min/mg Albumin}$)
Direct Blue 15	0.144 \pm 0.019	0.095 \pm 0.029
Tartrazine	0.002 \pm 0.002	0.001 \pm 0.000
Methyl Red	0.004 \pm 0.004	0.002 \pm 0.001
Buffalo Black NBR	0.072 \pm 0.015	0.053 \pm 0.002
Janus Green	0.015 \pm 0.005	0.018 \pm 0.004
Cibacron Brilliant Red 3B-A	0.128 \pm 0.035	0.134 \pm 0.006
Congo Red	0.089 \pm 0.040	0.037 \pm 0.017
Eriochrome Black T	0.056 \pm 0.001	0.056 \pm 0.002
Trypan Blue	0.130 \pm 0.042	0.099 \pm 0.025

Pure Enzyme Assays – Optimal Temperature

Between the five temperatures tested, no significant difference in dye reduction was seen (p-value >0.05, 95% confidence) (Figure 12). The optimal temperature of AzoC was between 30°C and 37°C (Figure 12). It appears that temperatures that are near body temperature are the most optimal. Interestingly, when comparing the cofactor effect at 37°C versus 25°C, the cofactor effect is less of a factor at 25°C, suggesting that 25°C is actually the more optimal temperature to use in experimentation (Tables 4 and 5). AzoC at 37°C showed a 2.0-fold increase over its control, while AzoC at 25°C showed a 2.4-fold increase over its control.

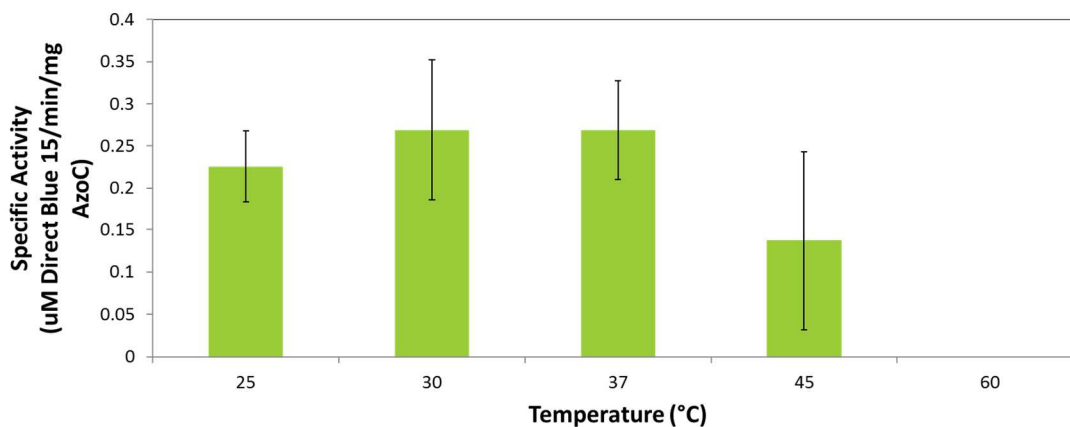


Figure 12. Effect of Temperature on Direct Blue 15 Reduction. Specific activity is provided as mean \pm standard deviation (error bars) across triplicates (n=3) for the four temperatures tested. Protein precipitation occurred at 60°C, making testing dye reduction not possible. No significant differences are found between the five temperatures tested (p-value >0.05, 95% confidence).

Table 4. AzoC Temperature and Oxygen Condition Comparisons. Specific Activity is provided as the mean across triplicates (n=3), with “SD” representing the standard deviation of the triplicate samples. Oxygen state is anaerobic unless noted otherwise.

Condition	Specific Activity (µM Direct Blue 15/min/mg AzoC)	SD
Aerobic AzoC 25°C	0.051	0.042
Albumin 25°C	0.095	0.029
Albumin 37°C	0.136	0.052
AzoC 37°C	0.269	0.058
AzoC 25°C	0.226	0.042

Table 5. Fold Increases of Temperature and Oxygen Condition Comparisons.

Fold Increases	
AzoC 37°C/AzoC 25°C	1.2
AzoC 25°C/Albumin 25°C	2.4
AzoC 25°C/Aerobic AzoC 25°C	4.4
AzoC 37°C/Albumin 37°C	2.0

Pure Enzyme Assays – Optimal pH

The optimal pH of the reaction was determined to be pH 9.0 (Figure 13). Upon further investigation of the protein, it was found that the pI of the protein is 8.72 which corresponds to

the optimal pH. Due to the high variability at the increased pH, pH 9 was found to be the most statistically significant (p-value <0.05, 95% confidence).

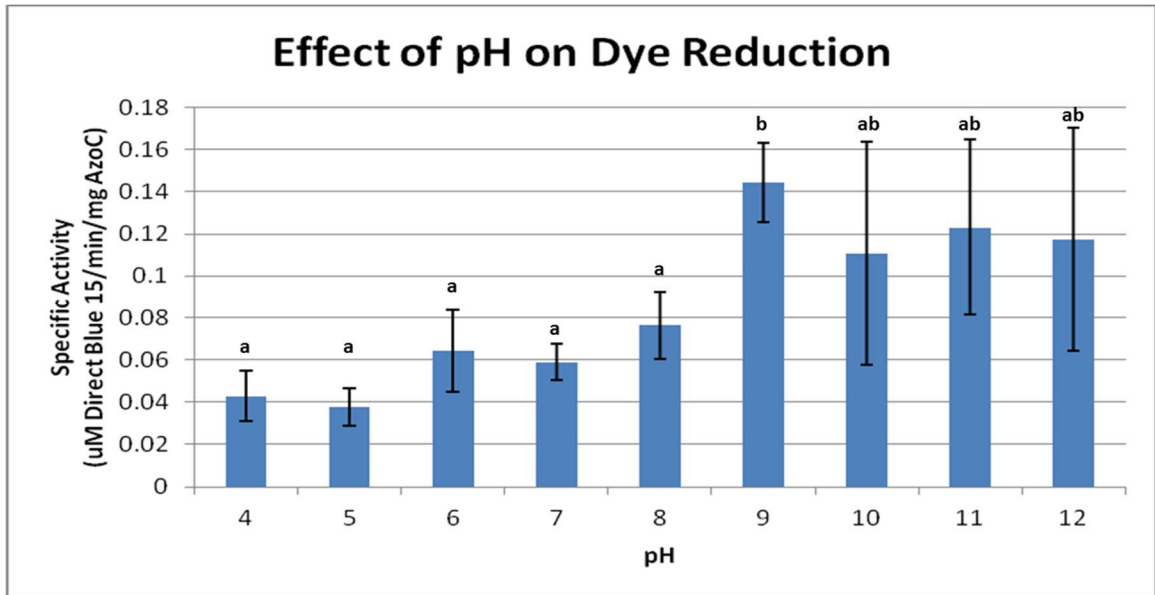


Figure 13. Effect of pH on Direct Blue 15 Reduction. Specific activity is provided as mean \pm standard deviation (error bars) across triplicates (n=3) for the various pH conditions tested. Letters represent comparisons of the different specificity activity measurements at the noted pH values; two means with the same letter are not significantly different at a 95% confidence interval (p-value >0.05).

Pure Enzyme Assays – Effect of Oxygen

When AzoC was exposed to oxygen, the specific activity was greatly reduced when compared to the anaerobic experiment, as a four-fold increase was seen with the anaerobic sample (Table 5, Figure 14). This suggests AzoC is sensitive to oxygen, which has been reported by others (Bragger *et al*, 1997). This sensitivity may be due to oxygen oxidizing the cofactor thereby inhibiting the enzyme reaction (Chang *et al*, 2001). In addition, oxygen may be a preferable electron acceptor over the azo groups (Chung & Stevens, 1993; Srinivasan & Viraraghavan, 2010). Using the same sample reaction, anaerobic activation followed by aerobic activation and finally anaerobic reactivation produced activities that were high, low and high, suggesting that oxygen may outcompete the dye for electrons, as mentioned above (Figure 15).

However, it is possible that the oxygen is oxidizing both the cofactors and dyes. On the other hand, without oxygen, an azo compound will act as sole oxidant, and its reduction rate will be controlled solely by the rate of formation of the electron donor (reduced flavin nucleotides). It must also be noted that, under aerobic conditions, dye reduction does still occur, however, the reduction occurs at a much slower rate than the anaerobic dye reduction reaction.

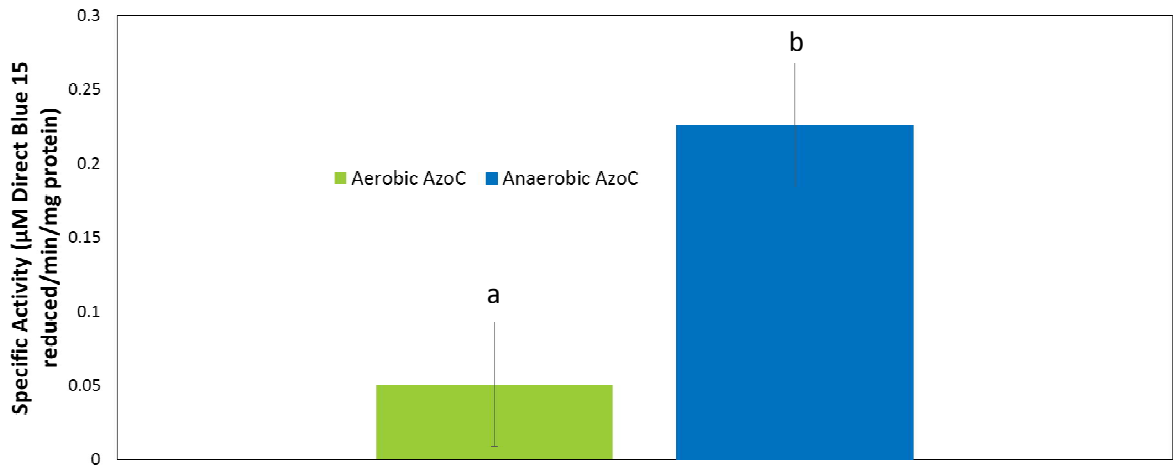


Figure 14. Effect of Oxygen on AzoC Specific Activity. Specific activity is provided as mean \pm standard deviation (error bars) across triplicates ($n=3$) for the conditions tested (aerobic and anaerobic). Letters represent comparisons of the different specificity activity measurements at the noted oxygen states; two means with the same letter are not significantly different at a 95% confidence interval (p -value >0.05).

Effect of Oxygen on AzoC Reactivation

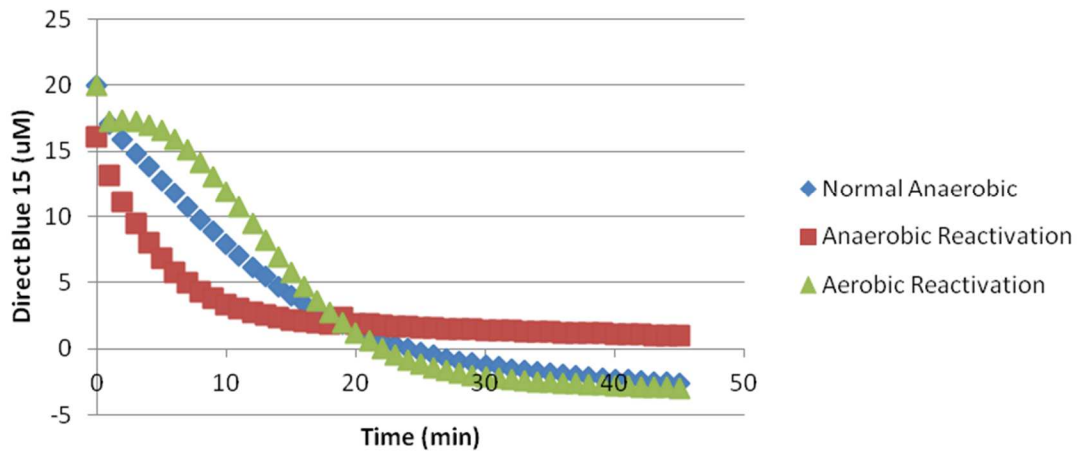


Figure 15. Effect of Oxygen on AzoC Reactivation.

Enzyme kinetics experiments were completed to determine the K_m and V_{max} values for azo dye, FAD and NADH. The data suggest that the reaction specificity between the enzyme and substrates is strong, producing K_m values of 0.005 μM , 0.00018 mM, and 0.0081 mM when the dye concentration, FAD concentration, and NADH concentrations were altered, respectively. V_{max} values were 0.42 μM Direct Blue 15/min/mg AzoC, 0.012 mM FAD/min/mg AzoC, and 0.26 mM NADH/min/mg AzoC.

Discussion

The goal of this study was to characterize the enzyme predicted to be the cause of the azoreductase activity of *C. perfringens*. In a previous study, Cristee Wright analyzed a 3.8 kb fragment of *C. perfringens* DNA that had been shown to exhibit minimal activity, however no gene for azoreductase was found within this DNA fragment (Wright, 2007). Cristee Wright used information from known bacterial azoreductases and located an open reading frame in the *C. perfringens* chromosome that coded for a putative azoreductase (Wright, 2007). The protein, AzoC, was overexpressed in *E. coli* and the activity of the cell-free extract was tested on the common azo dye Direct Blue 15. These results suggest that AzoC reduces Direct Blue 15 in a NADH-dependent process under anoxic conditions.

The protein was successfully purified using Ni-NTA affinity chromatography. Out of the variety of dyes tested, Direct Blue 15 was the most greatly reduced by the enzyme. It was also found that, besides needing NADH for reduction, FAD is also essential for the enzyme to reach its full azoreductase potential. FMN did produce a great reduction in dye absorbance when combined with NADH and AzoC, but it also produced a similar drop in absorbance when not in the presence of AzoC, suggesting that this combination of cofactors is actually reducing the dye. The cofactors used in the experiment (FAD and NADH) were shown to have a great effect on

some dyes (specifically Janus Green, Cibacron Brilliant Red 3B-A and Eriochrome Black T) suggesting that in some cases it is possible for the cofactors themselves to be able to reduce dye absorbance. Thus, cofactors only or in the presence of a protein control should always be used as a control to make sure that the dye reduction that is occurring is due to the azoreductase enzyme being tested and not due to other components of the reaction.

The optimal conditions for the azoreduction reaction were found and are unexpected. The optimal pH was found to be at pH 9, which is unusual for an intestine-dwelling organism like *C. perfringens*. However, the pI of AzoC was found to be 8.72, which corresponds to the optimal pH. This suggests that AzoC may not be acting to its full potential within the intestinal tract. Though the enzyme seemed to work best at 30-37°C, the controls told a different story, as there was a strong cofactor effect at these increased temperatures. The optimal temperature was found to be at 25°C, which is also unusual for an intestine-dwelling organism. However, *C. perfringens* is also commonly found outside of the body and in the soil (Ahmad *et al*, 2010). These optimal conditions were shown to be just that by enzyme kinetics studies that showed high specificity in enzyme and substrate binding and reaction time.

AzoC was found to have a greater reducing potential for the dye when under anaerobic conditions than aerobic conditions and may be sensitive to oxygen in some way, which has been reported by others (Bragger *et al*, 1997). This sensitivity may be due to oxygen oxidizing the cofactor thereby inhibiting the enzyme reaction (Chang *et al*, 2001). In addition, oxygen may be a preferable electron acceptor over the azo groups of the azo dyes (Chung & Stevens, 1993; Srinivasan & Viraraghavan, 2010). However, it is possible that the oxygen is oxidizing both the cofactors and dyes. When in the presence of oxygen, there appears to be competition between the oxygen and the azo dye for reduction by the azoreductase, thus it was found that performing experiments under anaerobic conditions gave the best results and faster reduction times for Direct Blue 15. On the other hand, without oxygen, an azo compound will act as sole oxidant, and its

reduction rate will be controlled solely by the rate of formation of the electron donor (reduced flavin nucleotides). A schematic of the predicted Ping-Pong Bi Bi reaction for AzoC is shown in Figure 16. In absence of oxygen, Figure 16A is expected, whereas in the presence of oxygen, Figure 16B is expected.

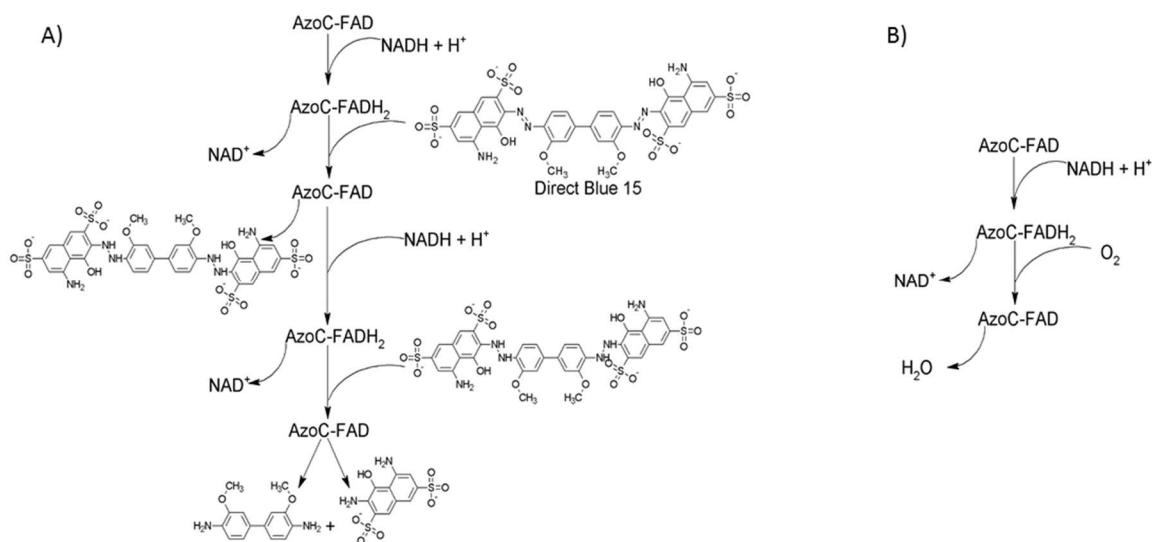


Figure 16. Expected Ping-Pong Bi Bi Reaction for AzoC in the Absence of Oxygen (A) and in the Presence of Oxygen (B).

Researchers suggest several mechanisms by which anaerobic bacteria are able to reduce azo dyes. One hypothesis is that these organisms possess true azoreductases that are specific in their function. Another hypothesis, and perhaps the most popular, is that reduced electron carriers (e.g. flavins) mediate reduction by a redox mechanism in which azo dyes are non-specific electron acceptors. Since our protein works best in the presence of a flavin (FAD), it can be suggested that the second mechanism is that which fits our AzoC.

In conclusion, our results showed that AzoC from *Clostridium perfringens* has azoreductase activity. Optimal conditions for the enzyme were found to be pH 9.0 and at room temperature (25°C) and with the cofactors NADH and FAD. A cofactor effect was observed during experimentation, suggesting that an experimental condition containing the cofactors

themselves and the dye, without the azoreductase, should be used as a control to understand the effect that the cofactors have on dye reduction. AzoC was also found to be oxygen sensitive, as AzoC performs enzymatically better under anoxic conditions than in the presence of oxygen. To our knowledge, this is the first study in which the ORF for a putative azoreductase or flavoprotein was rescued from a strict anaerobe, as well as cloned, expressed, purified, and characterized as to have azoreductase activity.

CHAPTER III

THE NON-ENZYMATIC REDUCTION OF AZO DYES BY FLAVIN AND NICOTINAMIDE COFACTORS UNDER VARYING CONDITIONS

The following chapter is based off of a publication in the journal *Anaerobe* (2013, **23**:87-96) and appears here with the journal's permission.

Abstract

Azo dyes are ubiquitous in products and often become environmental pollutants due to their anthropogenic nature. Azoreductases are enzymes which are present within many bacteria and are capable of breaking down the azo dyes via reduction of the azo bond. Often, though, carcinogenic aromatic amines are formed as metabolites and are of concern to humans. Azoreductases function via an oxidation-reduction reaction and require cofactors (a nicotinamide cofactor and sometimes a flavin cofactor) to perform their function. Non-enzymatic reduction of azo dyes in the absence of an azoreductase enzyme has been suggested in previous studies, but has never been studied in detail in terms of varying cofactor combinations, different oxygen states or pH's, nor has the enzymatic reduction been compared to azoreduction in terms of dye reduction or metabolites produced, which was the aim of this study. Reduction of azo dyes by different cofactor combinations was found to occur under both aerobic and anaerobic conditions and under physiologically-relevant pH's to produce the same metabolites as an azoreductase. These results show that, in some cases, the non-enzymatic reduction by the cofactors was found to be equal to that seen with the azoreductase, suggesting that all dye reduction in these cases is

due to the cofactors themselves. This study details the importance of the use of a cofactor-only control when studying azoreductase enzymes.

Introduction

Azoreductases are enzymes that have been linked to several types of cancers in humans (Chung *et al*, 2006). These enzymes are found within bacteria residing in the human intestinal tract where they convert azo dyes to carcinogenic metabolites (Ryan *et al*, 2010). Globally, more than 2000 different varieties of azo dyes are produced, which accounts for more than 50% of total dye production (Ryan *et al*, 2010). These dyes are used in foods, beverages, cosmetics, textiles, papers, pharmaceuticals and many other industries and are classified by the presence of a double nitrogen (azo, R-N=N-R) bond (dos Santos *et al*, 2007; Ryan *et al*, 2010). Environmentally, these dyes are seen as a recalcitrant pollutant present in waste water treatment streams produced from various industrial dyeing processes (Saratale *et al*, 2011).

Azo dyes are generally not harmful to humans, however, when broken down enzymatically by azoreductases, carcinogens are produced in some cases (Bardi & Marzona, 2010; Chung & Cerniglia, 1992). Azoreductases cleave the azo bond of azo dyes, releasing potentially toxic aromatic amines (Ryan *et al*, 2010). Of the thousands of azo dyes on the market, over 500 of them contain carcinogenic aromatic amines within their chemical formulation and are thus the dyes with which we are concerned about (Chung *et al*, 2006). Azoreductases have been identified in many bacteria of the human intestinal tract, including *Escherichia coli*, *Enterococcus faecalis*, *Enterococcus faecium*, *Clostridium perfringens*, and many others (Chen *et al*, 2004; Ghosh *et al*, 1993; Macwana *et al*, 2010; Rafii *et al*, 1997). Because azo dyes can enter our bodies through ingestion, it is likely that the reductive cleavage of azo dyes and the release of carcinogens in the intestinal tract can be linked to cancer in humans.

AzoC, an azoreductase that originates from the strictly anaerobic bacterium *Clostridium perfringens*, was recently isolated and biochemically characterized (Chapter 2), representing the first complete study of a pure azoreductase from a strict anaerobe (Morrison *et al*, 2012). *Clostridium perfringens*, while a strictly anaerobic bacteria, is able to survive in a vegetative state under atmospheric conditions of oxygen (Jean *et al*, 2004). Although a study by Rafii and Coleman (1999) suggested the presence of another azoreductase in *Clostridium perfringens*, that particular enzyme was tested and showed minimal activity (Morrison *et al*, 2012; Rafii & Coleman, 1999; Wright, 2007). AzoC is the only proven azoreductase in *Clostridium perfringens* and is different from that of Rafii and Coleman (1999) (Morrison *et al*, 2012; Rafii & Coleman, 1999; Wright, 2007). We have previously shown (Chapter 2) AzoC to have high enzymatic activity with Direct Blue 15, a large sulfonated azo dye (0.27 U/mg AzoC, where one unit of enzyme activity is defined as the amount of enzyme required to decolorize 1 μ mol of dye per minute) and with FAD and NADH as the optimal cofactors for the reaction (Morrison *et al*, 2012). The specific activity, along with determined K_m and V_{max} values ($K_m = 5$ nM, $V_{max} = 0.42$ U/mg protein) is comparable to azoreductases in the literature and suggests that AzoC is a strong and specific azoreductase (Morrison *et al*, 2012).

Azoreductases require cofactors to perform the oxidation-reduction reaction necessary to break the azo bond. Specifically, azoreductases require either nicotinamide adenine dinucleotide (NADH) or nicotinamide adenine dinucleotide phosphate (NADPH) as an electron donor, and a flavin cofactor, such as flavin mononucleotide (FMN) or flavin adenine dinucleotide (FAD) for electron transfer (Feng *et al*, 2012). In Chapter 2, it was noted that, under some circumstances, the cofactors necessary for AzoC to function were able to reduce azo dyes in the absence of an azoreductase (Morrison *et al*, 2012). Another study showed similar effects, but focused primarily on the non-enzymatic reduction of azo dyes by NADH at a relatively basic pH and did not evaluate the effects of alternative cofactors, or combinations of cofactors (such as a nicotinamide

cofactor and a flavin cofactor combined) (Nam & Renganathan, 2000). Because there are varied azoreductase reaction requirements, it is important to determine the effect of cofactors on azo dye reduction at varied temperatures, pH's, oxygen states, and with a variety of relevant and commonly tested azo dyes. This is the first study that provides a comprehensive look at the effect of NADH, NADPH, FMN and FAD on the reduction of azo dyes both aerobically and anaerobically and at different physiologically relevant pH values.

Materials and Methods

Cofactors and Azo Dyes

The cofactors used were purchased from the following companies: FAD (TCI America), FMN (Sigma-Aldrich), NADH (Acros Organics), NADPH (Applichem), NAD⁺ (Sigma-Aldrich).

The azo dyes were purchased from the following companies: Direct Blue 15 (MP Biomedicals), Methyl Red (Acros Organics), Tartrazine (Sigma-Aldrich), Trypan Blue (Kodak), Congo Red (Sigma-Aldrich), Eriochrome Black T (MCB), Janus Green (Sigma-Aldrich), Cibacron Brilliant Red 3B-A (Sigma-Aldrich), Ponceau S (Fluka), Ponceau BS (Sigma-Aldrich), Methyl Orange (Allied Chemicals).

Dye Reduction Assays – Cofactor Specificity

Assays with the cofactors (FAD, FMN, NADH and NADPH) were carried out both aerobically and anaerobically. All experiments were performed in triplicate in 1.5 mL polystyrene cuvettes (Sigma-Aldrich) with a total reaction volume of 1 mL. Although different azo dyes were tested in each case, the final dye concentration was consistently 20 μ M prepared in deionized water. The buffer was 25 mM potassium phosphate, pH 7.0. Flavin cofactors (FMN and FAD) were tested at a final concentration of 2 mM, while nicotinamide cofactors (NADH and NADPH) were tested at 10 mM, as determined to be optimal in Chapter 2; all cofactors were prepared in

deionized water (Morrison *et al*, 2012). All reactions were performed in a Shimadzu UV-1650PC spectrophotometer.

Each azo dye was scanned prior to the reaction to determine the optimal absorbance for each dye in the reaction mixture (dye absorbencies were above 340 nm and extinction coefficients were used in determining the concentration of the dyes at the conclusion of the reaction). In the case of the blue-absorbing dyes, such as Methyl Red and Tartrazine, an absorbance was selected that was not optimal in an effort to limit interference by the flavin cofactors, which absorb around 450 nm. The absorbencies for each azo dye tested were as follows: Cibacron Brilliant Red 3B-A (534.0 nm), Congo Red (531.0 nm), Direct Blue 15 (602.5 nm), Eriochrome Black T (527.5 nm), Janus Green (597.5 nm), Trypan Blue (533.5 nm), Methyl Red (430.0 nm), Tartrazine (425.0 nm), Ponceau S (515.5 nm), Ponceau BS (505.0 nm), Methyl Orange (465.5 nm). Dye concentration was interpolated from a plot of dye absorbance to time by making a standard curve of dye concentration to find the extinction coefficient. The extinction coefficient was determined to be spectrophotometer-specific and dependent on a line of best fit.

To identify the effect of the cofactor(s) on the dye absorbance, the cofactors were tested by themselves (NADH only, NADPH only, FMN only, FAD only) and in combinations (NADH/FMN, NADH/FAD, NADPH/FMN, NADPH/FAD), under aerobic and anaerobic conditions. All reaction conditions were performed by mixing the buffer, appropriate azo dye and deionized water together in the cuvette. Reactions were initiated by the addition of the appropriate cofactor(s). Cofactors in combination were mixed together prior to and after the addition to the reaction. Reaction absorbance was scanned every minute up to fifteen minutes at an absorbance appropriate for the specific azo dye. Additional steps were required for the anaerobic reactions, which involved bubbling the cuvette with nitrogen for ten minutes at a rate of one bubble per second. Mineral oil was then added to the top of the cuvette in an effort to prevent the introduction of oxygen into the reaction mixture. The reaction was initiated through the

addition of the appropriate anaerobically prepared cofactor(s), by piercing the oil overlay with a pipette tip and mixing carefully with an inoculating loop.

For comparison to the cofactor dye reductions samples, similar reaction conditions and methods were tested with the addition of AzoC (144 μg). The following mixtures were tested: AzoC with NADH only, NADPH only, FMN only, and FAD only and in combinations, AzoC with NADH/FMN, NADH/FAD, NADPH/FMN and NADPH/FAD. All reactions were performed in triplicate.

Purification of the Azoreductase (AzoC)

NovaBlue (DE3) *E. coli* cells containing the AzoC-containing plasmid and subsequent His-tag were prepared by Cristee Wright (see Chapter 2) (Wright, 2007). The *E. coli* cells containing pAzoC were inoculated into a 5 mL LB broth containing ampicillin (100 $\mu\text{g}/\text{mL}$ final concentration) and incubated overnight at 37°C while shaking at 200 rpm. This overnight culture was transferred to a large Erlenmeyer flask containing 1 L LB broth with ampicillin (100 $\mu\text{g}/\text{mL}$ final concentration) and incubated at 37°C with shaking at 200 rpm until an OD_{600} of 0.6 was reached. The cultures were then induced with isopropyl-beta-D-thiogalactopyranoside (IPTG, 1 mM final concentration) for an additional 3 hours while remaining at 37°C with shaking at 200 rpm. To pellet the cells, the culture was centrifuged (6000 x g, 10 minutes, 4°C). The supernatant was discarded as bacterial waste and the pellet was stored frozen at -20°C until further purification could occur.

To continue purification of AzoC, the cell pellet from above was thawed and resuspended in 10 mL of lysis/wash buffer (20% glycerol, 50 mM sodium monobasic phosphate, 750 mM sodium chloride, 20 mM imidazole, deionized water, pH 8.0). To lyse cells, lysozyme (0.1 mg/mL final concentration) was added to each pellet and incubated on ice for 30 minutes. Following incubation, cell suspensions were sonicated using a Sonic 300 dismembrator with an

intermediate tip and relative output of 60%. Sonication occurred for 10 times, 5 seconds each time, placing the cell suspension on ice in between sonications to cool the cell suspension and ensure that the heat generated was not denaturing the protein. The cell suspension was centrifuged (10,000 x g, 30 minutes, 4°C) to pellet the cell debris. The protein-containing supernatant was stored at 4°C until further purification can occur and the pellet was discarded as bacterial waste.

To purify the protein, the protein-containing supernatant was applied to a nickel-nitrilotriacetic acid (Ni-NTA) resin slurry (Clon-Tech) in a 1:1 ratio of unpure protein to resin in a glass frit column (Kimble-Chase Flex Column). The hexa-histidine tag on the induced AzoC protein allowed for AzoC to interact with the Ni²⁺ of the resin and ultimately allowed for pure AzoC to be isolated from the other protein contaminants. All purification steps occurred at 4°C to ensure that the protein did not denature. After applying the protein-containing supernatant to the Ni-NTA resin slurry in the glass frit column, the mixture was allowed to incubate horizontally on-column for at least 1 hour at 4°C while shaking at medium speed on a BioDancer orbital shaker (New Brunswick Scientific). This incubation ensures that AzoC in solution will interact with and bind to the Ni-NTA resin. Following this incubation, excess solution was drained from the column as the pre-wash fraction and the resin was washed with lysis/wash buffer until the effluent draining off of the column was clear (saved as wash fractions). After washing occurred, the pure protein was eluted from the Ni-NTA resin by exposure of the resin to an elution buffer (20% glycerol, 50 mM sodium monobasic phosphate, 750 mM sodium chloride, 250 mM imidazole, deionized water, pH 8.0). At least four elutions were carried out to ensure that all protein was eluted from the column. Elutions were saved and stored frozen at -20°C until further analysis could occur.

AzoC-containing elutions were analyzed via SDS-PAGE gel. SDS-PAGE gel analysis was performed as described previously (Laemmli, 1970). AzoC-containing samples were

prepared for this analysis directly following their purification by adding a 1X concentration of the SDS-PAGE loading buffer (4X loading buffer stock = 0.06 M TRIS-HCl pH 6.8, 10% (v/v) glycerol, 2% (w/v) SDS, 0.0025% (w/v) bromophenol blue). Beta-mercaptoethanol (5%) was used to denature disulfide bonds. To ensure protein unfolding, samples were boiled for at least 15 minutes prior to loading onto a 12.5% SDS-PAGE gel (20 μ L sample loaded per lane).

Coomassie blue was used for SDS-PAGE gel staining and the AzoC-containing protein bands were visualized and photographed in comparison to a 250 kDa protein ladder (New England Biolabs). A Nanovue Spectrometer was utilized to determine the protein concentration by use of the molar extinction coefficient of AzoC (0.880). The molar extinction coefficient was obtained through the NCBI database. The protein was concentrated between 2-10 mg/mL using an Amicon Ultrafiltration cell system (Nitrogen pressure and a NMWL 10,000 Millipore regenerated cellulose membrane). Protein was stored frozen at -20°C when not in use.

Oxidized NAD⁺ Assays

To test the specificity and function of the cofactors, reduced NADH and oxidized NAD⁺ were tested. Because Cibacron Brilliant Red 3B-A seems to have the most dramatic cofactor-effect, it was the dye used in this study. The azo dye reaction with Cibacron Brilliant Red 3B-A was tested aerobically and anaerobically with NAD⁺ only, and the combination of NAD⁺ and FAD. These experiments were performed in the absence of any protein, including AzoC.

pH Assays

In an effort to understand the physiological importance of the cofactor-only studies and the dependence of pH on the cofactor effect, the cofactor reaction mixtures were tested at different pHs: pH 6.0 (potassium phosphate buffer), pH 5.0 (sodium acetate buffer), pH 4.0 (sodium acetate buffer), pH 3.0 (sodium citrate buffer). Rumen fluid (pH ~8.5) was also tested and prepared for the experiments by spinning in a centrifuge (10,000 x g, 30 minutes, 4°C) to

remove debris. These pH-dependent experiments were conducted as described above by only changing the pH of the buffer used. The azo dye reaction mixtures were tested both aerobically and anaerobically for all pH values in the same manner as described previously.

HPLC Analysis of Metabolites

In an effort to understand the relative identities of the metabolites produced by the reaction with AzoC versus the reaction with the cofactors, the metabolites produced by both reactions were extracted and analyzed via HPLC and the metabolites spectra were compared.

Reactions were scaled up 10-fold in an effort to produce concentrated metabolites that were detectable with HPLC spectroscopy. Reactions were prepared aerobically and anaerobically either with the cofactors only (FAD/NADH) or with AzoC (1.44 mg) and cofactors (FAD/NADH). Reactions containing only the cofactors were prepared to a 2 mL volume in a test tube with 25 mM dye (Direct Blue 15), 50 mM NADH, 10 mM FAD, 25 mM potassium phosphate buffer pH 7.0, and deionized water to the desired volume. Anaerobic reactions were bubbled with nitrogen for twenty minutes at a bubble rate of one bubble per second and then overlaid with mineral oil. Reactions were incubated at 37°C. Controls were prepared by heat-denaturing both AzoC and cofactors. These control reactions were set-up as described above following the heat-denaturation.

After incubation, samples were extracted using three equal volumes of ethyl acetate (HPLC grade). Extractions were dried using sodium sulfate and concentrated under a gentle stream of nitrogen and gentle heating. Solvent was exchanged to methanol for HPLC analysis. An extraction control was also prepared, using a sample containing only Direct Blue 15. Separation of the metabolites produced was accomplished by use of an HPLC (Thermo Scientific) with an Alltima C18 column (150 mm x 4.6 mm, Alltech). Metabolites and retention times were determined by using a UV-VIS spectrophotometer set at 280 nm. A gradient elution was utilized

at 10% HPLC-grade methanol (90% reagent-grade water) for 5 minutes, followed by 30% methanol for 5 minutes, 40% methanol for 5 minutes, 50% methanol for 5 minutes, 60% methanol for 5 minutes and 100% methanol for 20 minutes to flush the column. 10% methanol was held for 3 minutes prior to the injection of a new sample. Flow rate was set at 0.8 mL/min. Each sample (100 μ L) was loaded onto the column, and dilutions of the test sample were prepared in methanol if deemed necessary for the accurate detection of metabolites.

Mass Spectroscopy Analysis of Metabolites

To determine the molecular weight of the dye metabolites produced by both the azoreductase and the cofactors only, samples prepared as described above were analyzed by infusion of the sample, diluted in a 66:33 Methanol/water mixture, directly into an LTQ Orbitrap XL mass spectrometer (Thermo Scientific) via a New Objective nanospray ion source. MS spectra were collected at a nominal resolution of 100,000. Mass spectra were analyzed using Xcalibur (Thermo Scientific) and had a 5-10 ppm mass accuracy.

Results

Dye Reduction Assays – AzoC and Cofactors

AzoC shows high enzymatic activity with Direct Blue 15 as a substrate. As shown in Figure 17, AzoC reduces the dye completely over a period of 15 minutes. When compared to its control (cofactors only), the dye reduction with AzoC is significantly greater (p-value <0.001, 95% confidence). However, when looking at Cibacron Brilliant Red 3B-A, the dye reduction profile is almost identical between the azoreductase and the cofactor only control (p-value >0.05, 95% confidence). This suggests that, in this particular case, the dye reduction seen with Cibacron Brilliant Red 3B-A is not significantly different between the azoreductase and the cofactor-only control, suggesting that the cofactors are responsible for all dye reduction. This provides the basis for the study in this Chapter.

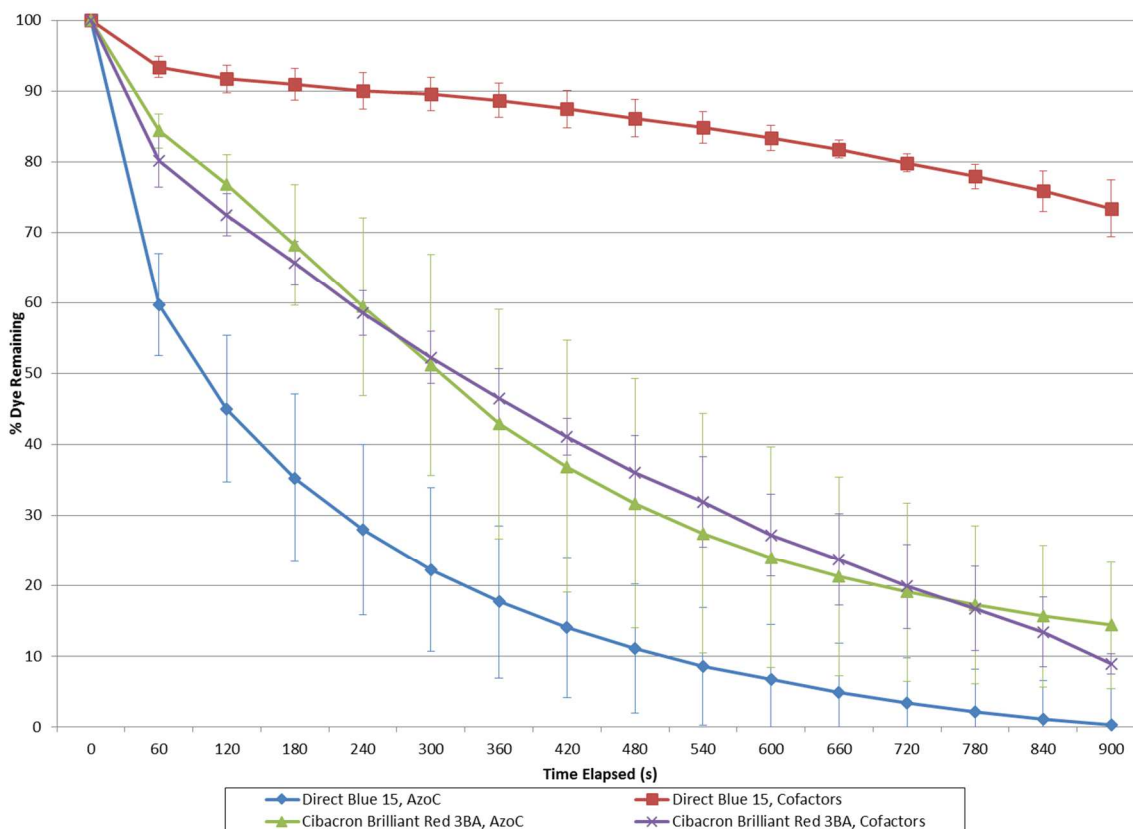


Figure 17. FAD and NADH Cofactors as Compared to AzoC. Reactions were performed with FAD and NADH in both the presence and absence of an azoreductase enzyme, AzoC, under anaerobic conditions and are compared for two different azo dyes (Direct Blue 15 and Cibacron Brilliant Red 3B-A). Experimental conditions, including dye concentration, were consistent. The percentage of dye remaining (% dye remaining) is plotted as a mean and the error bars represent standard deviation across triplicate (n=3) samples. Comparing the % dye reduced between Cibacron Brilliant Red 3B-A, with and without AzoC, there is not a significant difference in dye reduction (p-value >0.05, 95% confidence). However, with Direct Blue 15, the comparison of with and without AzoC shows a significant difference in dye reduction (p-value <0.001, 95% confidence).

Eleven azo dyes of varying characteristics (molecular weight, number of azo bonds, sulfonation) were tested (Figure 18). Single cofactor effects on dye reduction (FAD only, NADH only, etc) were not observed, as only a combination of two different cofactors showed significant reduction (Figure 18). There is great diversity amongst the dyes when it comes to reduction by the varying cofactor combinations. Cibacron Brilliant Red 3B-A was the best performing dye using the FAD/NADH and FMN/NADH combination as nearly 100% of the dye was reduced for both combinations. There was no specificity for dye reduction based on the number of azo bonds,

as seen with Direct Blue 15 (diazo) and Cibacron Brilliant Red 3B-A (monoazo) which had the highest degree of reduction (Figure 18). However, an increase in dye reduction based on the increase in the molecular weight of the dyes was noticed. Simple linear regressions were performed to assess the impact of molecular weight on dye reduction for each cofactor. For all of the cofactor combinations, there was a statistical significance between dye reduction and molecular weight at 95% confidence (FAD/NADH p-value=0.001, $R^2=0.6618$; FAD/NADPH p-value=0.0495, $R^2=0.1188$; FMN/NADH p-value=0.001, $R^2=0.6608$; FMN/NADPH p-value=0.001, $R^2=0.3839$); thus, in all cofactor combinations tested, the amount of dye reduction increased as the molecular weight of the dye increased.

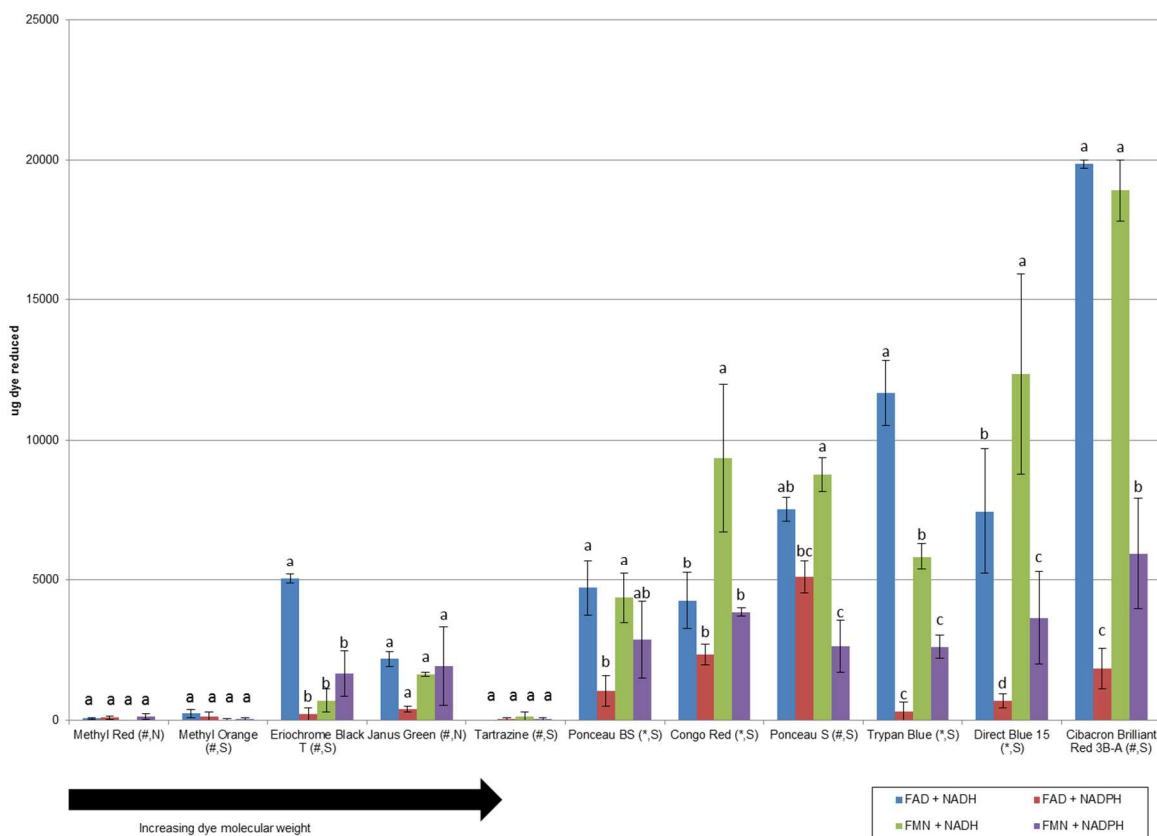


Figure 18. Diversity in Terms of Dye Reduction as Visualized by the Different Dyes. Reactions were performed with varying cofactor combinations (see key) with cofactors only under anaerobic conditions. Experimental conditions, including dye concentration, were kept consistent. Error bars represent standard error for triplicate samples (n=3). Letters (a,b,c) represent comparisons of the different cofactor combinations within a given dye; two means within the same dye with the same letter are not significantly different at a 95% confidence level. Dyes are shown in increasing molecular weight from left to right. (# = monoazo dye, * = diazo dye, N = non-sulfonated, S = sulfonated)

Four cofactor combinations were tested and each showed a high degree of diversity, as visualized by the letters above the bars in Figure 18. When comparing the flavin cofactor (FMN and FAD) and the same nicotinamide cofactor, a complex and varied degree of dye reduction occurred. In the cases of Eriochrome Black T and Trypan Blue, dye reduction is greater with FAD compared to FMN, a significant difference as reflected by the 95% confidence level. On the other hand, in the case of Congo Red, the dye reduction with FMN is significantly better than FAD at the 95% confidence level. For the combination of FMN/NADPH compared to the combination of FAD/NADPH, dye reduction is significantly better with FMN for Direct Blue 15 and Cibacron Brilliant Red 3B-A, while dye reduction is significantly better with FAD for Ponceau S at 95% confidence.

When comparing the nicotinamide cofactors (NADH and NADPH) to the same flavin cofactor, NADH combinations are consistently higher than NADPH with the specific dyes tested, as seen in Figure 18. Specifically, the FMN/NADH combination is significantly higher (95% confidence) with Congo Red, Ponceau S, Trypan Blue, Direct Blue 15 and Cibacron Brilliant Red 3B-A. In contrast, the FAD/NADH combination is significantly higher (95% confidence) with Eriochrome Black T, Ponceau BS, Trypan Blue, Direct Blue 15 and Cibacron Brilliant Red 3B-A.

Figure 19 examines the characteristics of the dyes, cofactor choice and its preferred oxygen state (aerobic or anaerobic) for dye reduction. There are two cases in which an oxygen-rich environment was significantly more conducive to dye reduction. For Ponceau BS (FMN/NADH) and Congo Red (FAD/NADH), the dye reduction occurred significantly better in the presence of oxygen than under anaerobic conditions (95% confidence). There are three cases in which an anaerobic environment was significantly more conducive to larger dye reduction by the FAD/NADH cofactor combinations: Cibacron Brilliant Red 3B-A, Direct Blue 15, and Trypan Blue. An opposite effect was seen with the intermediate size dyes (Congo Red and Ponceau BS) as an aerobic environment was significantly more ideal. However, the choice of

cofactor was different as Congo Red/ FAD and Ponceau BS/FMN were preferred. There was not a correlation between oxygen state and cofactor combination, suggesting that the ability of the cofactors to reduce dye is not dependent on the oxygen state. Finally, no preference for dye sulfonation occurred, as both aerobic and anaerobic environments support dye reduction.

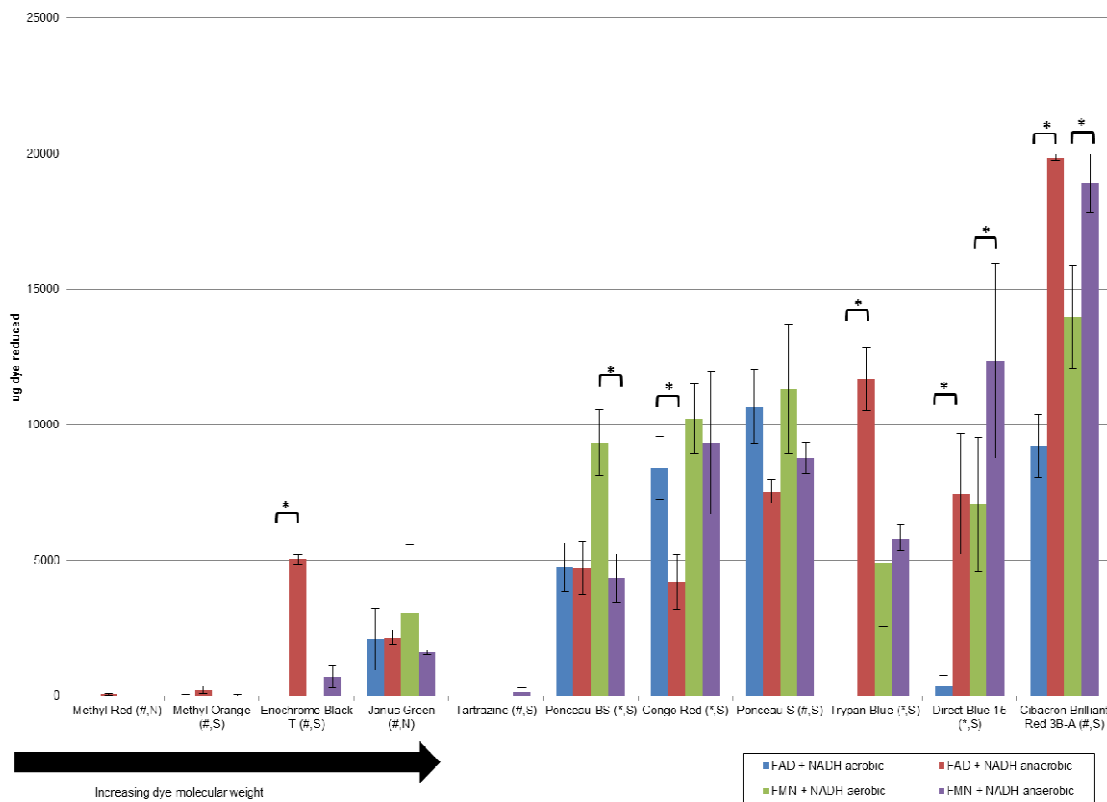


Figure 19. Anaerobic and Aerobic Cofactor Dye Reduction Comparison. Reactions were performed with varying cofactor combinations (see key) with cofactors only under both aerobic and anaerobic conditions. Experimental conditions, including dye concentration, were kept consistent. Error bars represent standard error for triplicate samples (n=3). Dyes are shown in increasing molecular weight from left to right. Asterisks (*) represent cases in which there is a significant difference between the two bars (p-value < 0.05, 95% confidence).

When the dye reduction produced by an azoreductase (AzoC)/cofactor combination is compared to the dye reduction produced by the cofactors alone, it can be seen that the addition of AzoC increased the dye reduction of the larger dyes (Congo Red, Ponceau S, Trypan Blue and Direct Blue 15) with FAD or FMN in combination with NADH, as seen in Figure 20. The only

exception was Cibacron Brilliant Red 3B-A. Interestingly, for Eriochrome Black T, a smaller dye, the addition of AzoC resulted in a decrease in dye reduction for FAD/NADH, which was significant at a 95% confidence level.

In some cases, dye reduction by the cofactors is not significantly different than the dye reduction produced by the azoreductase, such as the case with both the FMN/NADH combination (Methyl Orange, Methyl Red, Tartrazine, Eriochrome Black T, Janus Green and Cibacron Brilliant Red 3B-A) and FAD/NADH combination (Methyl Orange, Methyl Red, Tartrazine, Janus Green, Ponceau BS and Cibacron Brilliant Red 3B-A). In these cases, the fact that the azoreductase is not reducing the azo dye significantly better than the cofactors themselves suggests that all or most of the dye reduction that we are seeing with the azoreductase is due to the presence of the cofactors.

All of the four largest dyes (not including Cibacron Brilliant Red 3B-A) do not show a preference for cofactor combination. However, this does not hold for the next heaviest dye, Ponceau BS, as the azoreductase in this case seems to favor FMN. There is not a correlation between number of azo bonds and dye reduction by azoreductase and/or cofactors (Figure 20). All of the cases where the dye reduction by the azoreductase was significantly higher than the cofactors the dyes were sulfonated. The exception was Eriochrome Black T (sulfonated), which was reduced significantly more by the cofactors alone. Ultimately, some dyes were not significantly reduced under any experimental conditions, with or without cofactors or azoreductase, including Methyl Red, Methyl Orange and Tartrazine.

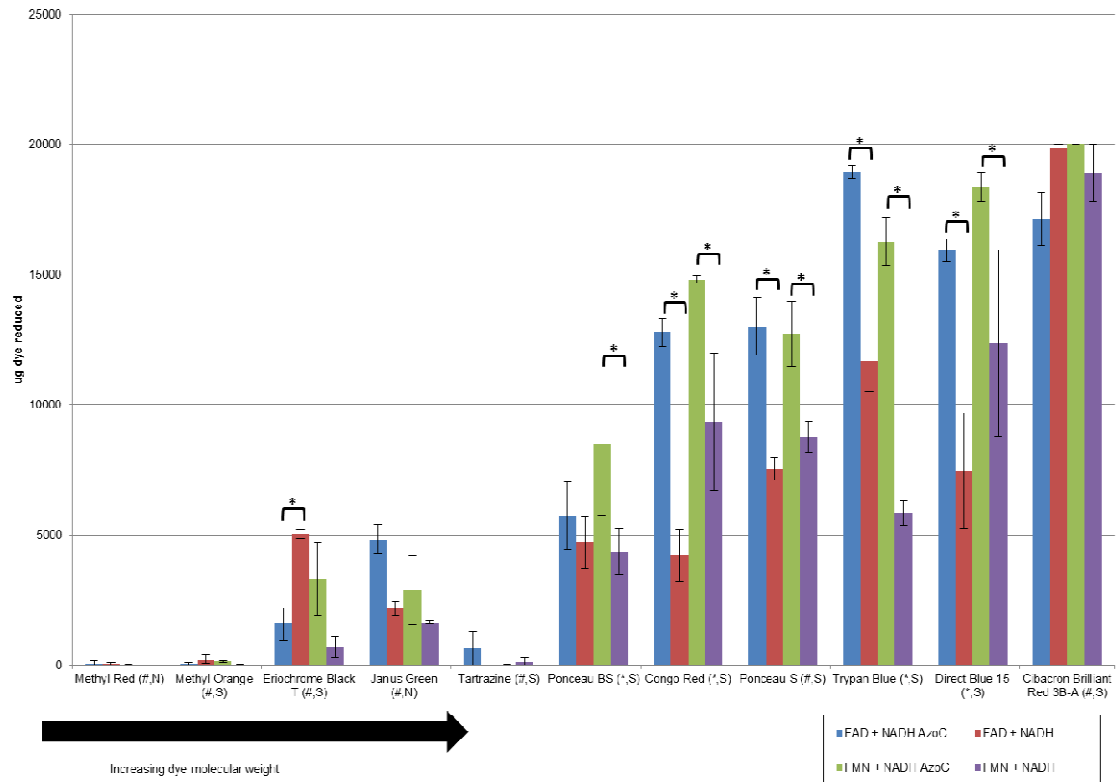


Figure 20. Cofactor Dye Reduction as Compared to an Azoreductase (AzoC). Reactions were performed with varying cofactor combinations (see key) with cofactors only under anaerobic conditions with and without AzoC. Experimental conditions, including dye concentration, were kept consistent. Error bars represent standard error for triplicate samples (n=3). Dyes are shown in increasing molecular weight from left to right. Asterisks (*) represent cases in which there is a significant difference between the two bars (p-value < 0.05, 95% confidence).

NAD⁺ Assays

The importance of a reduced form (NADH) of the cofactor, without AzoC, in dye reduction was shown compared to the oxidized (NAD⁺) form (Figure 21). When NADH and NAD⁺ are acting alone with Cibacron Brilliant Red 3B-A, both aerobically and anaerobically, no dye reduction is produced. However, when comparing the NADH/FAD combination to the NAD⁺/FAD combination, the difference is significant to a 95% confidence (p-value < 0.001). Aerobically, NADH/FAD reduces 18-fold greater dye than NAD⁺/FAD. The difference in

reduction is greater anaerobically, where NADH/FAD reduces 22-fold greater dye than NAD⁺/FAD, suggesting the possible inhibition of oxygen.

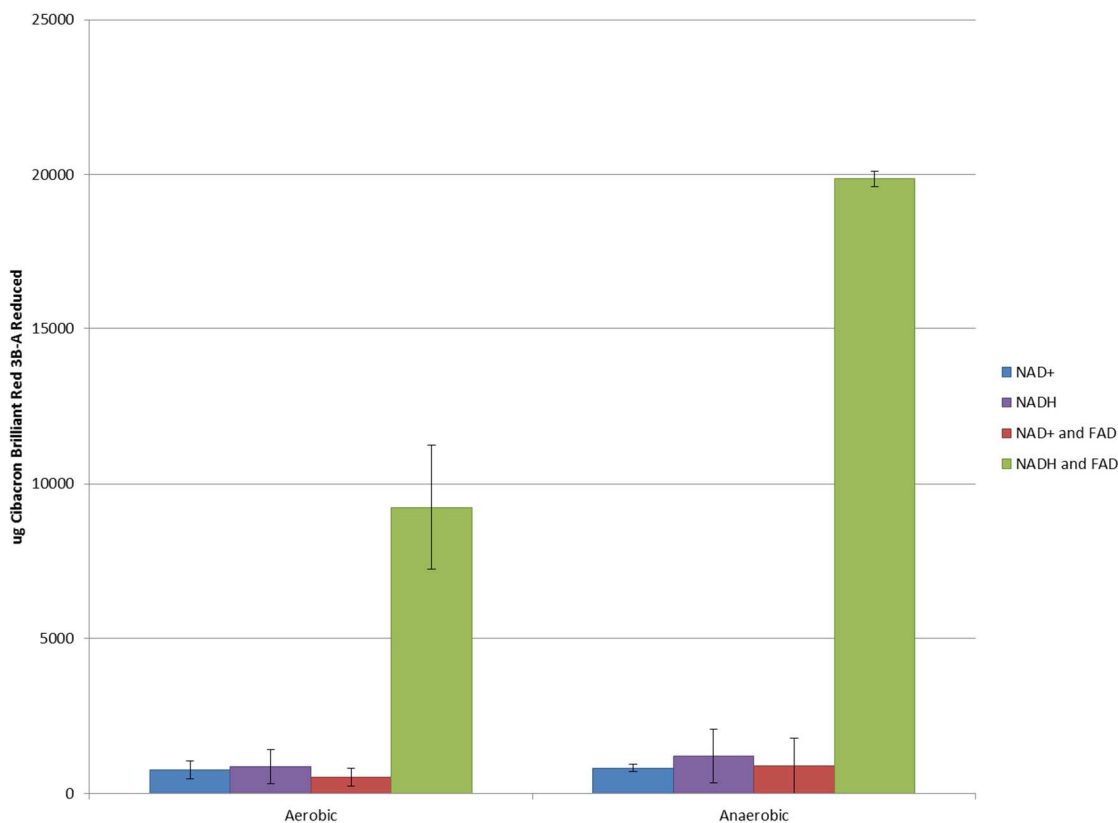


Figure 21. Comparison of the effect of NADH and NAD⁺ on dye reduction. Reactions were performed with varying cofactor combinations (see key) with cofactors only under anaerobic conditions with and without FAD. Experimental conditions, including dye concentration, were kept consistent. Error bars represent the standard error for triplicate samples (n=3).

pH Assays

To further evaluate the differences between NADPH and NADH, pH was studied as a variable using Cibacron Brilliant Red 3B-A (Figure 22). For the cofactor combination of FAD/NADH, both aerobically and anaerobically, an optimal pH for this cofactor effect was not found, as differences between the different pH values tested are not significant to 95% confidence. For the cofactor combination of FAD/NADPH, lower pH values tend to be favored, especially aerobically, as the dye reduction at pH 3 is significantly higher (at 95% confidence)

than at the other pH values tested. For the cofactor combination of FMN/NADH, both aerobically and anaerobically an optimal pH for this cofactor effect was not found, as differences between the different pH values tested are not significant to a 95% confidence level. For the cofactor combination of FMN/NADPH, lower pH values tend to be favored, as the dye is reduced significantly better (to a 95% confidence level) at a decreased pH. Overall, more dye is reduced with a flavin cofactor and NADH than with a flavin cofactor and NADPH, both aerobically and anaerobically between pH 8.5 and 4.0. However, as pH decreases to 3, the amount of dye reduced by a flavin cofactor and NADPH is higher than the flavin cofactor with NADH.

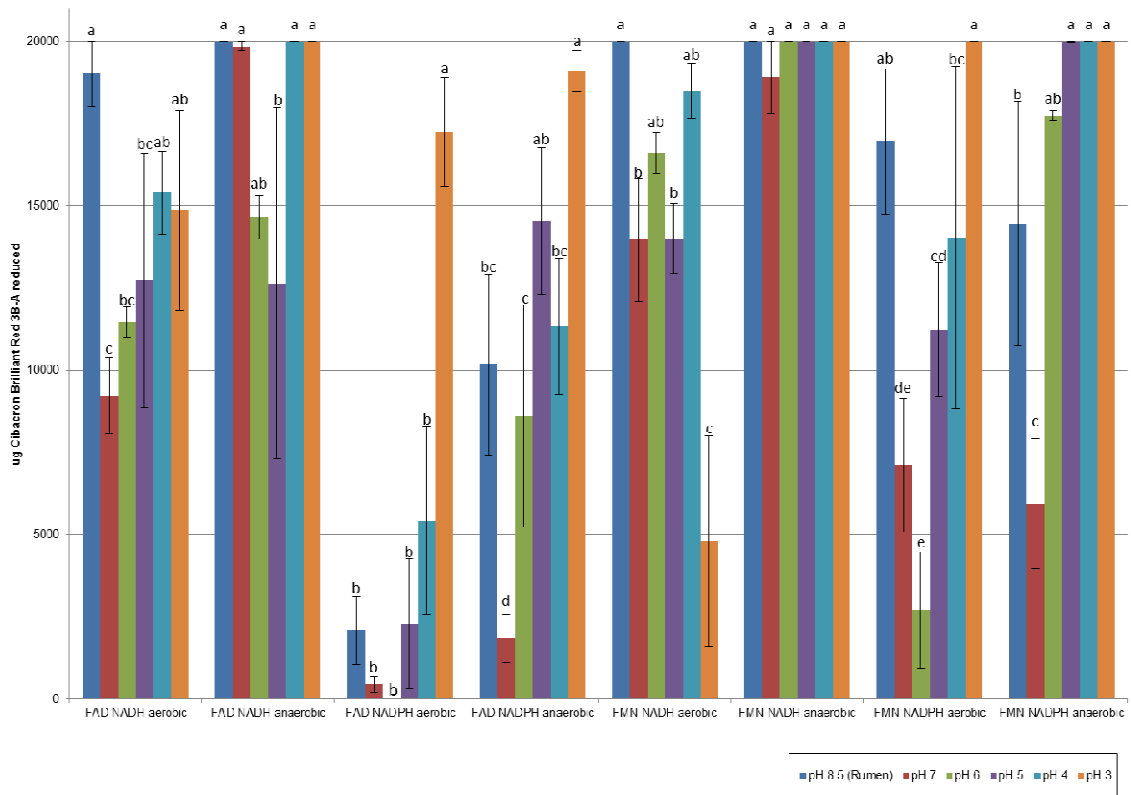


Figure 22. Effect of pH on Cofactor Dye Reduction. Reactions were performed with varying cofactor combinations (see key) with cofactors only under both aerobic (A) and anaerobic (B) conditions. Experimental conditions, including dye concentration, were kept consistent. Error bars represent standard error for triplicate samples (n=3). Letters represent comparisons of the different cofactor combinations within a given dye; two means within the same dye with the same letter are not significantly different at a 95% confidence level.

Analysis of Metabolites

To determine if the decolorization of the dye by the cofactors results in the generation of metabolites similar to an AzoC reaction, the metabolites produced by the cofactor reaction were compared to the metabolites produced by the azoreductase reaction. Figure 23 shows the expected metabolites from the reduction of Direct Blue 15, a dye that was more readily reduced.

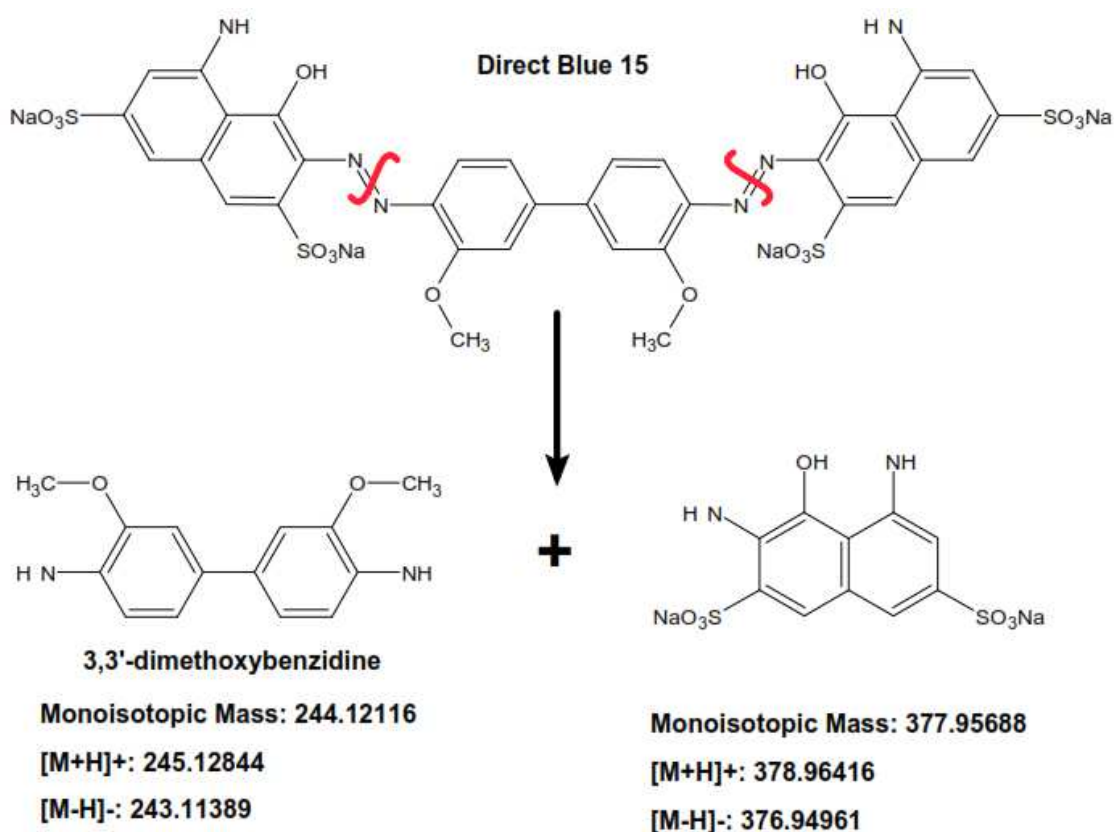


Figure 23. Direct Blue 15 Breakdown and Resultant Metabolites Predicted. Monoisotopic masses calculated based on molecular formula of metabolites. [M+H]⁺ represents the monoisotopic mass with the addition of one proton and [M-H]⁻ represents the monoisotopic mass with the subtraction of one proton.

HPLC analysis showed that each sample separated into two distinct peaks, the column retention times of which are shown in Table 6. The similarity in the retention times suggests the metabolites for the azoreductase and cofactor are the same.

Table 6. HPLC Retention Times of Azo Dye Metabolites Produced under Different Conditions. Retention times are given in minutes for the peaks that were visualized by UV-VIS at 280nm.

Condition	Retention Time (min)	
	Peak 1	Peak 2
AzoC, aerobic	12.246	12.919
Cofactors, aerobic	12.243	12.893
AzoC, anaerobic	12.299	12.929
Cofactors, anaerobic	12.273	12.853

Mass spectroscopy analysis of the dye metabolites is shown in Figure 24. In all of the conditions tested, the mass spectra are consistent with the 3,3'-dimethoxybenzidine metabolite being present in the [M+H]⁺ form (monoisotopic mass 245.128 m/z). The other metabolite at 377.956 m/z was not able to be seen in any of the mass spectra, however, this may be due to improper ionization conditions for that particular compound.

Discussion

The goal of this paper was to provide a comprehensive study of the effect of NADH, NADPH, FMN and FAD on the reduction of azo dyes both aerobically and anaerobically as compared to the reduction of dyes seen with an azoreductase. In Chapter 2, it was noted that, the cofactors necessary for AzoC to function were able to reduce azo dyes in the absence of AzoC.

A significant amount of diversity was noted amongst the cofactor-mediated reduction of the eleven diverse azo dyes tested. There does not appear to be a correlation between the number of azo bonds or sulfonation and the ability of the azo dye to be reduced by the all cofactors, as can be seen by the lack of an apparent correlation in Figure 18. However, there is a statistically significant correlation between the molecular weight of the dye and reduction, as larger dyes were more readily reduced compared to smaller dyes (95% confidence level). This correlation will need to be further examined with a larger sample set of dyes to confirm whether this correlation is relevant or if it is an artifact of the particular dyes tested.

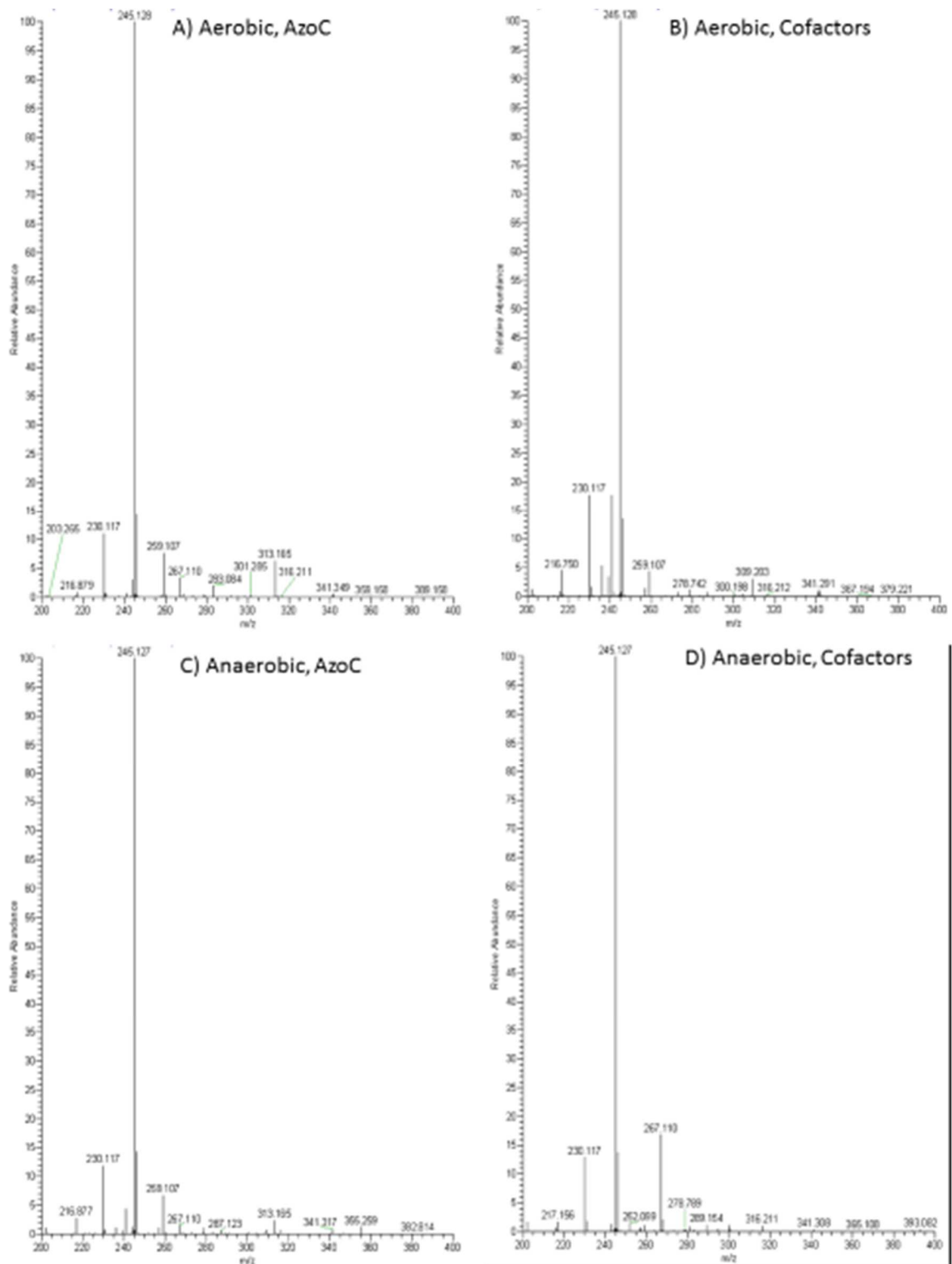


Figure 24. Orbitrap Mass Spectrum Data. **A)** Aerobic AzoC, **B)** Aerobic Cofactors, **C)** Anaerobic AzoC, **D)** Anaerobic Cofactors.

In all, four cofactor combinations were tested, as well as all of the cofactors alone. None of the cofactors alone were able to reduce the azo dyes, however, when in combination, dye reduction was significant (95% confidence level). The combination of a flavin cofactor with NADH consistently reduces azo dyes better than the same flavin cofactor with NADPH (Figure 18). Regarding the flavin cofactors, a varied outcome for dye reduction occurred. First, there is a significant outcome (95% confidence level) that shows that combinations with FMN favor larger dyes. In contrast, for FAD there is a preference for both smaller dyes as well as larger dyes. Figure 18 also provides an interesting finding regarding the degree of complete dye reduction as most dyes were not completely reduced by the cofactors alone, while only Cibacron Brilliant Red 3B-A was completely reduced. It is known that NADP(H) binds to redox proteins and controls the redox potential of flavin cofactors (Murataliev & Feyereisen, 2000). Therefore, it is likely that the redox potential changes that occur for each flavin cofactor are different, resulting in different redox differences for different azo dyes. Clinically, elevated cellular NADH levels have been shown to be associated with ethanol consumption (alcoholic liver disease) and diabetes (glomerular dysfunction) (Hagymasi *et al*, 2001; Ido *et al*, 1997; Seronello *et al*, 2010; Sorrell & Tuma, 1985; Tilton *et al*, 1992). It is possible that such an increased amount of cofactor in such an environment could be favorable for the generation of carcinogenic metabolites in these patients and is thus of clinical interest.

There was not a significant correlation between oxygen state and cofactor combination in terms of dye reduction, but there were significant differences between cofactors and oxygen states. Most dyes were reduced under anaerobic states with either flavin cofactor (95% confidence level) (Figure 19). The two exceptions were Congo Red and Ponceau BS, in which the former preferred an aerobic FAD combination and the latter preferred an aerobic FMN combination. This difference in oxygen state for dye reduction suggests that the dyes that prefer anaerobic conditions may be more readily affected by changes in oxygen levels. In addition,

larger molecular weight dyes seem to have a preference for anaerobic environments compared to moderate and small size dyes, suggesting oxygen changes the oxidation state of the larger dyes more readily thereby allowing reduction of the dye. Additionally, while the azoreduction reaction under aerobic conditions has the possibility of producing superoxide via semi-quinone radicals formed with the reduction of some azo dyes, this is not expected to occur in the absence of oxygen such as how AzoC was tested (Moller & Wallin, 2000).

The effect of added azoreductase to the cofactor combinations was significant (95% confidence level) in some cases (Figure 20). In the case of Methyl Orange, Methyl Red, Tartrazine, Janus Green and Cibacron Brilliant Red 3B-A, dye reduction with AzoC was not significantly different than the dye reduction seen with the cofactors alone (95% confidence level). This suggests that, for these particular dyes, the dye reduction is originating from the cofactors alone, or that AzoC may not be able to reduce these dyes. Enzyme specificity is also important as the larger dye (Cibacron Brilliant Red 3B-A) may not specifically bind to azoreductase. For Eriochrome Black T, it was noted that dye reduction with the cofactors alone was significantly better than that with the azoreductase. Eriochrome Black T has a unique structural characteristic in that it contains two fused-rings which are adjacent to the azo bond (Figure 4), which may allow AzoC more structural inhibition compared to the other nonfused-ring dyes and suggests that steric constraints may restrict the breakdown of the azo bond by the azoreductase but not by the cofactors. All of the azo dyes which were reduced significantly better by the azoreductase (95% confidence level) were large molecular weight dyes, which may suggest these dyes are better suited to have a binding pocket in the azoreductase than the smaller azo dyes.

It is hypothesized that reduction potential will play a role in the likelihood of the azo dye to be reduced, as azo dyes are reduced by oxidation-reduction reactions (Chung & Stevens, 1993). It is thought that if the reduction potential of the various azo dyes were more positive than

that of the flavin cofactor, electrons could be transferred from the nicotinamide cofactor ($E_0' = -0.320\text{V}$) to the flavin cofactor ($E_0' = -0.219\text{V}$) and to the azo dye ($E_0' > -0.219\text{V}$) which will be reduced (Zille *et al*, 2004). Literature have shown that this is true for reactions involving an azoreductase, so it is likely the same for non-enzymatic reaction involving the cofactors since a transfer of electrons is taking place (Zille *et al*, 2004). This will need to be investigated further to confirm that dye reduction potential does in fact show a correlation to the ability of the dye to be reduced by the cofactors.

The effects of pH changes on dye reduction were complex as various degrees of dye reduction occurred based on cofactors and oxygen states (Figure 22). What we did observe in terms of significance (95% confidence level) was each reaction set (i.e. cofactor combination and oxygen state) shows the low performing NADPH having more reduction at lower pHs (3-4) than higher pHs (7, 8.5). The rumen fluid (pH 8.5) may have contributed other factors which are difficult to account for that have resulted in an increase in reduction in some cases. For NADH, there were less differences seen between the basic and acidic conditions, as in some cases the results at pH 3 were not significantly different than those at pH 7. These observations are physiologically relevant, as azoreduction in the human body tends to occur in the ileum and colon of the intestinal tract where pH values of these regions ranges from 4-7 (Fallingborg, 1999; Wright, 2007). This suggests that dye reduction within the intestines may be by cofactors as well as azoreductases, with NADH reducing at both high and low pH values and NADPH reducing at decreased pH values. It is possible that the interactions between the excess phosphate group in NADPH may be helping or hindering the interactions between the nicotinamide cofactor and the azo dye. There is great diversity in the literature as to whether NADH or NADPH are preferred electron donors; in many cases, both NADH and NADPH work (Ghosh *et al*, 1992; Huang *et al*, 1979; Idaka *et al*, 1987; Wang *et al*, 2007; Zimmermann *et al*, 1982). Also, it should be noted that a reduced form of the nicotinamide cofactor is necessary for dye reduction to occur (Figure 21).

This is as expected, as when NADH is present in its oxidized state (NAD⁺), the proper electron flow cannot occur and therefore dye reduction does not occur (Figure 21).

The cofactors were found to produce the same dye metabolites as the azoreductase, as shown by HPLC and MS analytical studies, which suggests that dye reduction occurs by the same type of oxidation-reduction reaction, causing the breakdown of the azo bond. The presence of the 3,3'-dimethoxybenzidine metabolite conclusively shows that, in all conditions tested, both of the azo bonds of Direct Blue 15 have been broken. The outcome of our results suggests the importance of having a cofactor-only control within azoreductase studies as the azo bond can be reduced without the azoreductase, and the metabolites generated are identical to what is observed with enzyme reduced dye metabolism (Table 6 and Figure 24).

The goal of this Chapter was to offer an inclusive study of the effect of redox cofactors on the reduction of azo dyes under varying oxygen states as compared to an azoreductase reaction. In conclusion, the results showed that combinations of cofactors (a nicotinamide cofactor plus a flavin cofactor) are able to non-enzymatically reduce azo dyes by breakage of the azo bond under both aerobic and anaerobic conditions and at physiologically-relevant pH values. When compared to an azoreductase, this non-enzymatic reduction was found to be equal to azoreductase activity in some cases, suggesting the importance of cofactor-only reactions occurring for *in vitro* conditions. It is thought that this non-enzymatic reaction undergoes reduction potential changes for the dyes and cofactors. To our knowledge, this is the first study which provides a comprehensive look at the effect of NADH, NADPH, FMN and FAD on the reduction of azo dyes both aerobically and anaerobically as compared to an azoreductase.

CHAPTER IV

STRUCTURE AND STABILITY OF AN AZOREDUCTASE WITH AN FAD COFACTOR FROM THE STRICT ANAEROBE *CLOSTRIDIUM PERFRINGENS*

The following chapter is based off of a publication in the journal *Protein and Peptide Letters* (2014, **21**:523-534) and appears here with the journal's permission.

Abstract

Azoreductase enzymes present in many microorganisms exhibit the ability to reduce azo dyes, an abundant industrial pollutant, to produce carcinogenic metabolites that threaten human health. All biochemically-characterized azoreductases, around 30 to date, have been isolated from aerobic bacteria, except for AzoC, the azoreductase of *Clostridium perfringens*, which is from a strictly anaerobic bacterium. AzoC is a recently biochemically-characterized azoreductase. The lack of structural information on AzoC hinders the mechanistic understanding of this enzyme. In this Chapter, the biophysical characterization of the structure and thermal stability of AzoC by using a wide range of biophysical tools is reported: Liquid Chromatography-Mass Spectrometry (LC-MS), Circular Dichroism Spectroscopy, Fourier-transform Infrared (FTIR) Spectroscopy, SDS-PAGE, Size Exclusion Chromatography, MALDI-TOF and UV-visible spectroscopy. It was found that the flavin cofactor of AzoC is FAD, while all other structurally-known azoreductases employ FMN as a cofactor. The secondary structure of AzoC has 16% less α -helix structures, 5% more β -sheet structures and 11% more turn and unordered than the average of structurally-known

azoreductase that has 10-14% sequence similarities with AzoC. It was also found that oxidized AzoC is trimeric, which is unique amongst structurally known azoreductases. In contrast, reduced AzoC is monomeric, despite similarities in catalytic activity and thermal stability of oxidized and reduced AzoC. These results show that the use of FTIR spectroscopy is crucial for characterization of the β -sheet content in AzoC, illustrating the need for complementary biophysical tools for secondary structural characterization of proteins.

Introduction

Azo dyes are used extensively in industry, including pharmaceuticals, textiles, foods, beverages and cosmetic products (Chen *et al*, 2009). From the 700,000 tons of azo dyes used annually, 35,000 to 70,000 tons of them are discharged into the environment as pollutants (Chen *et al*, 2009). Azoreductase enzymes present in many microorganisms exhibit the ability to reduce azo dyes to produce carcinogenic metabolites that threaten human health (Priya *et al*, 2011). In Chapter 2, AzoC, an azoreductase from the strictly anaerobic bacterium, *Clostridium perfringens*, was isolated and biochemically characterized (Morrison *et al*, 2012). It was found in Chapter 2 that this azoreductase has strong and enzymatic specific activity with an azo dye substrate (0.27 μ moles Direct Blue 15/min/mg AzoC) (Morrison *et al*, 2012). The rate of dye decolorization, along with K_m and V_{max} values ($K_m = 5$ nM, $V_{max} = 0.42$ μ M dye/min/mg protein), is comparable to aerobic azoreductases in the literature, suggesting that AzoC is a strong and specific azoreductase (Morrison *et al*, 2012). Of the approximately 30 azoreductases that have been biochemically characterized, AzoC is the only one originating from a strictly anaerobic bacterium.

Azoreductases require cofactors for their catalytic function in an oxidation-reduction reaction. All azoreductases require a nicotinamide cofactor (NADH or NADPH) and most of them also preferentially and selectively utilize a flavin cofactor (FAD or FMN) (Abraham &

John, 2007; Ooi *et al*, 2012). Due to the inherent appearance of yellow color and the necessity for additional flavin cofactor for enzyme activity, AzoC has been shown to be a flavoprotein (Morrison *et al*, 2012). However, the identity of the flavin cofactor of AzoC remains unknown. A method is reported in this Chapter for rapid and accurate determination of the flavin cofactor of an azoreductase.

To date, all information available on azoreductase structure originates from aerobic bacteria; there is no structural information available from azoreductases isolated from strictly anaerobic bacteria (Correia *et al*, 2011; Filippova *et al*, 2010; Ito *et al*, 2006; Liu *et al*, 2007; Tan *et al*, 2012; Wang *et al*, 2007). With three-dimensional structures of five azoreductases known, azoreductases from aerobic microorganisms show significant structural similarity, specifically amongst those bacteria found in the human intestine (Ito *et al*, 2008). Also, while amongst aerobic azoreductases sequence similarity is low, azoreductases share structural topology and similarity which make the enzymes behave in a similar manner (Liu *et al*, 2007). Because *Clostridium perfringens* is also an inhabitant of the intestine, AzoC may be structurally similar to the aerobic azoreductases, even if it may not be similar in protein sequence. Based on these facts, it is expected that AzoC will show structural similarity to aerobic azoreductases, which will be tested experimentally in this proposal. Fourier Transform Infrared spectroscopy (FTIR) and circular dichroism (CD) spectroscopy are established techniques for the elucidation of a protein's secondary structure (Arrondo *et al*, 1993; Kelly & Price, 2000). The combined use of FTIR and CD spectroscopic approaches to study the enzyme's secondary structure is used for the first time here. Because very little is known about anaerobic azoreductases, the information provided by the secondary structure of an anaerobic azoreductase would represent a step forward in the field and would provide an understanding of the similarities and differences between the structures of aerobic and anaerobic azoreductases. The use of biophysical methods to characterize the AzoC

enzyme, to determine the identity of the cofactor of AzoC, and to determine the multimeric state and thermal stability of AzoC are also reported in this Chapter.

Materials and Methods

Sample Preparation

NovaBlue (DE3) *E. coli* cells harboring the AzoC-containing plasmid (with Histidine-tag and IPTG-triggered induction) were prepared by Cristee Wright (see Chapter 2) (Morrison *et al*, 2012; Wright, 2007). These *E. coli* cells were inoculated into a 5 mL LB broth and grown overnight at 37°C with orbital shaking at 200 rpm. The 5 mL LB broth also contained ampicillin (100 µg/mL final concentration) to select for the AzoC-plasmid containing *E. coli* cells. Following overnight growth, this 5 mL culture was transferred to a 1 L LB broth (containing 100 µg/mL ampicillin) and incubated at 37°C with orbital shaking at 200 rpm until an optical density of 0.6 (OD₆₀₀ = 0.6) was reached. Upon reaching the desired optical density, the *E. coli* culture was induced with isopropyl-beta-D-thiogalactopyranoside (IPTG, 1 mM final concentration) for at least 3 hours with incubation at 37°C and orbital shaking at 200 rpm. Following the IPTG-triggered induction, cells were pelleted by centrifugation (6,000 x g, 10 minutes, 4°C). The supernatant was discarded as bacterial waste and the cell pellet was stored frozen (-20°C) until further purification steps could be taken.

To rescue the induced AzoC from the *E. coli* cells, the cell pellet from the previous step was thawed and resuspended in 10 mL of lysis/wash buffer (20% glycerol, 50 mM sodium monobasic phosphate, 750 mM sodium chloride, 20 mM imidazole, deionized water, pH 8.0). To lyse the cells, lysozyme (0.1 mg/mL final concentration) was added to the cell suspensions and suspensions were incubated for 30 minutes on ice. Following this incubation, cells were lysed by sonication by using an intermediate tip on a Sonic 300 dismembrator with a relative output of 60%. Ten sonication cycles occurred, with 5 seconds in each cycle. To ensure that the released

protein did not denature due to the increased temperature caused by the sonication procedure, the cell suspension was placed on ice in between sonication cycles. To pellet the cell debris and separate out the protein-containing supernatant, the cell suspension was centrifuged (10,000 x g, 30 minutes, 4°C). The supernatant containing the protein was stored at 4°C until further purification could occur. The pellet was discarded as bacterial waste.

The protein-containing supernatant from the previous step was applied to a nickel-nitriloacetic acid (Ni-NTA) resin slurry (Clon-Tech) housed in a glass frit column (Kimble-Chase Flex Column). The hexa-histidine tag on AzoC allows for the protein to interact with the Ni²⁺ resin and allows for contaminants to be washed from the column and is ultimately what allows for AzoC to be purified. All protein purification steps occurred at 4°C to make sure that the protein did not denature during the process. Once the protein-containing supernatant was mixed with the Ni-NTA resin in the column, the mixture in the column was allowed to incubate for at least 1 hour at 4°C while orbitally shaking at medium speed on a BioDancer orbital shaker (New Brunswick Scientific). This incubation allows the Histidine-tag of AzoC adequate time to interact with and bind to the Ni²⁺ of the Ni-NTA resin. Following incubation, excess supernatant was drained from the column as the pre-wash fraction. The resin was then washed with lysis/wash buffer on column until the effluent leaving the column was clear (these washes were saved as wash fractions). After washing, the pure AzoC was eluted from the Ni-NTA column by exposing the resin to an elution buffer (20% glycerol, 50 mM sodium monobasic phosphate, 750 mM sodium chloride, 250 mM imidazole, deionized water, pH 8.0). A minimum of four elutions were completed to ensure that all protein was eluted from the column. The elutions were saved and stored frozen (-20°C) until they could be further analyzed.

SDS-PAGE (see detailed procedure below) was used to analyze the purity of the proteinaceous elutions and a Nanovue Spectrophotometer (GE Life Sciences) was utilized to determine the protein concentration by use of the molar extinction coefficient of AzoC (0.880).

The molar extinction coefficient was determined through use of the NCBI database. Protein concentration and buffer switching was completed by use of an Amicon Ultrafiltration cell under Nitrogen pressure and a Millipore regenerated cellulose membrane (NMWL 10,000) for large volumes, Amicon Ultra 15 filter (NMWL 10,000) for medium-sized volumes by centrifugation and Amicon Ultra 0.5 filter (NMWL 10,000) for small volumes by centrifugation. Protein was stored at -20 °C when not being actively used and otherwise kept in an ice bath. Throughout experiments, buffers were kept as consistent as possible in order to minimize any buffer-related effects on AzoC.

For liquid chromatography mass spectroscopy (LC-MS), protein prior to cofactor extraction was concentrated to 10 mg/mL in 50 mM potassium phosphate buffer (pH 7.5). For CD spectroscopy, AzoC was concentrated to 0.8 mg/mL in 50 mM potassium phosphate buffer (pH 7.5). For FTIR spectroscopy (both secondary structure and thermal stability studies), AzoC was prepared to a concentration of 10 mg/mL in 50 mM potassium phosphate buffer (pH 7.5) in D₂O. D₂O was used to minimize H₂O absorption in the Amide I region. For MALDI-TOF spectroscopy, AzoC was prepared to a concentration of 10 mg/mL in 20 mM TRIS (pH 7.5) and 10 mM NaCl buffer. For size exclusion chromatography, protein was concentrated to 10 mg/mL in potassium phosphate buffer (pH 7.5).

Liquid Chromatography-Mass Spectroscopy

For LC-MS, protein samples were prepared by heat denaturing 10 mg/mL AzoC in deionized water. Heat denaturation of AzoC occurred for 1 hour at 100°C to release the cofactor. The denatured protein was removed by pelleting and with an Amicon Ultra 15 (NMWL 10,000). A 0.45 µm filter was used to remove any particulate matter. Rescued cofactor was concentrated under a gentle stream of Nitrogen and gentle heating.

FMN (Sigma-Aldrich) and FAD (TCI America) standards were prepared in deionized water to 1 mM concentration. All measurements were performed in an LCMS 2010 EV (Shimadzu). The stationary phase of the LC was Shimadzu Premier C₁₈ 3 μm 4.6 mm × 100 mm; the mobile phase was a mixture of methanol and water at a flow rate of 0.3 ml/min. Each measurement was performed with 5 μl sample injection. The sample was eluted with 50% methanol for 5 min, followed by an increase in the methanol concentration from 50% to 95% within 2 min. Finally, 95% methanol was used as the mobile phase until the measurement was finished. All elutions from the LC were analyzed by a mass spectrometer with an electrospray ionizer combined with a single quadrupole analyzer. All negatively charged molecules within a 50 to 1000 m/z range were detected using scanning mode.

Far-UV Circular Dichroism Spectroscopy

CD spectra were collected using a Jasco J-815 CD spectrometer. Spectra were collected at 20 °C in the far-UV range (260-190 nm) using a step mode of 0.2 nm, bandwidth of 1.00 nm and a 50 nm/minute scan rate. Quartz cuvettes with a 1 mm pathlength were used. For secondary structure determination, an average of three scans was obtained for each spectrum at 20 °C. Solvent spectra were also obtained under the same conditions and were subtracted from the sample spectra. Thermal unfolding was followed by monitoring the ellipticity at 208 nm and 222 nm from 20°C to 90°C at a temperature ramp of 15°C/hour.

The spectra were converted to mean residue ellipticity (AzoC molecular mass of 25,070 Da, 228 amino acids) and the secondary structural content was deconvoluted using the online server Dichroweb with the SP175 reference data set and the CDSSTR algorithm (Compton & Johnson, 1986; Lees *et al*, 2006; Whitmore & Wallace, 2004). Thermal unfolding analysis data were plotted using the Matlab program (unfoldprotein.m), which uses a Savitsky-Golay filter (least squares polynomial regression) to smooth the denaturation profile and to minimize the error

due to baseline correction (White). The maximum of the first derivative corresponds to the melting temperature (John & Weeks, 2000; Kelly *et al*, 2005; Mergny & Lacroix, 2003).

FTIR Spectroscopy

Single beam spectra of AzoC and buffer were measured using Bruker IFS 66v FTIR spectrometer with a rapid-scan option at 4 cm^{-1} spectral resolution. A 9-reflection diamond attenuated total reflection (ATR) cell (DuraSamplIR II from SensIR Technologies, LLC) with temperature control was employed for this study. The temperature of the sample was regulated using a circulating unit (RTE-111 from NESLAB). The AzoC sample was first thermally stabilized at 20°C for 30 minutes prior to data collection. The rapid-scan mirror velocity of 200 kHz (6.330 cm/s) was used to increase the speed of data collection by 10-fold as compared to the normal mirror velocity. The single beam FTIR spectra were collected in the mid-infrared spectral region from 800 cm^{-1} to 4000 cm^{-1} with 1024 scans each and six repeated measurements for signal averaging at each temperature from 20°C to 90°C with 10°C intervals. The rate of temperature ramp from 20°C to 90°C was strictly controlled at $10^{\circ}\text{C}/15$ minutes for both AzoC and buffer.

All infrared absorption spectra of AzoC and potassium phosphate buffer were calculated from single beam spectra with the empty diamond ATR cell as reference. After averaging over six repeated measurements with a total of 6144 scans, the resulting statistical noise in the Amide I region is less than 0.063 mOD, far smaller than the infrared absorption signals in Amide I (~ 80 mOD). The infrared spectra from the AzoC protein were calculated by subtracting the buffer spectra in the corresponding temperature measured in the same manner as the protein spectra. To compare the spectral shapes of AzoC, Amide I bands were normalized by the total band area. Small contamination of water vapor signals was removed by subtracting the pure water vapor

spectra. The secondary derivative spectra of infrared absorption were computed with smoothing over 13 points of data.

SDS-PAGE

SDS-PAGE analysis was performed as described previously (Laemmli, 1970). Before SDS-PAGE analysis, 15 μ L of a purified protein sample (~10 mg/mL) was mixed with 5 μ L of SDS-PAGE loading buffer, which consists of 0.06 M TRIS-HCl pH 6.8, 10% (v/v) glycerol, 2% (w/v) SDS, 0.0025% (w/v) bromophenol blue, to the protein. Tris(2-carboxyethyl)phosphine (TCEP) was added as a reducing agent to reduce disulfide bonds at a concentration of 20 mM to one sample for reduced AzoC, whereas deionized water was added to the same volume of another purified AzoC sample for oxidized AzoC (Gray, 1993). TCEP was used for this study instead of the more common beta-mercaptoethanol because TCEP does not contain sulfur atoms which cause FTIR interference in regions of interest to this study. In addition, both AzoC samples were boiled for 15 minutes to denature. Each denatured AzoC protein sample (20 μ L) was loaded onto a 12.5% SDS-PAGE gel. Coomassie blue was used for staining and the protein bands for reduced and oxidized AzoC were visualized and photographed in comparison to a 250 kDa protein ladder (New England Biolabs).

MALDI-TOF Spectroscopy

To determine molecular weight of AzoC samples, purified protein sample was mixed with sinapinic acid solution. The size of the protein was measured using the linear mode in an Applied Biosystem DE-PRO MALDI-TOF Mass Spectrometer. The instrument was calibrated by external standards, apo-myoglobin and bovine serum albumin. Sensitivity of the measurement was ± 50 D.

Enzyme Activity Studies

An enzyme activity study to determine the differences in enzymatic specific activity between the reduced and oxidized AzoC was carried out as follows. Enzyme runs were carried out in 1.5 mL polystyrene cuvettes (Sigma-Aldrich) in triplicate with a total reaction volume of 1 mL. Reaction components (with the exception of the cofactors) were mixed together prior to the initiation of the reaction and included 25 mM TRIS (pH 9.0) buffer, 20 μ M Direct Blue 15, purified AzoC (144 μ g) and deionized water to make the total reaction volume. In the oxidized assay, AzoC was used as is, but in the reduced case, the AzoC sample was reduced with 1 mM TCEP. To prepare an anaerobic system, the cuvette was bubbled with nitrogen for 10 minutes at a bubble rate of 1 bubble per second. Following bubbling, the system was immediately overlaid with mineral oil. To begin the enzymatic reaction, 10 mM NADH and 2 mM FAD (which were premixed together) were added carefully to prevent the introduction of oxygen to the system and quickly mixed with an inoculating loop. The reaction was scanned at room temperature using a UV-1650 PC spectrophotometer (Shimadzu) at 602.5 nm. Direct Blue 15 was scanned prior to this reaction and its optimal absorbance was determined to be at 602.5 nm. Direct Blue 15 concentration was interpolated from its absorbance by making a standard curve of dye concentration to determine the extinction coefficient of Direct Blue 15. This is a spectrophotometer-specific equation of a best fit line. This data was utilized to calculate specific activity values for the oxidized and reduced AzoC samples with Direct Blue 15.

Size Exclusion Chromatography

A standard curve of protein molecular weight markers (Gel Filtration Standard #151-1901, Bio-Rad) was used to calibrate a size exclusion chromatography (SEC) column (Kostanski *et al*, 2004; Lemaire *et al*, 1989; Morl, 1981; Striegel *et al*, 2009). In addition, the protein standard was supplemented with Bovine Serum Albumin (BSA) as an additional standard (MP

Biomedicals, 5.0 mg). The SEC column (1 m x 1 cm, Kontes FlexColumn) was loaded with Bio-Gel P100 resin (Bio-Rad). Flow rate through the column was controlled by using a Microperpex Peristaltic Pump (LKB) set to a speed of 99, which resulted in a flow rate of 0.5 mL/min. Fractions were collected with a ISCO automatic fraction collector set to change collection tubes (13 x 100 mm borosilicate glass disposable culture tubes, Fisher Scientific) every 10 minutes, resulting in 5.0 mL fraction volume per tube. The fraction collector was started immediately as 0.5 mL of each protein sample (both standard and unknowns) was put onto the column. Data was collected by measuring the absorbance of each fraction in a UV-1650 PC spectrophotometer (Shimadzu) at 280 nm.

To determine the multimeric nature of reduced AzoC with non-covalent interactions, size exclusion chromatography (SEC) was performed. For reduced AzoC, the concentrated protein sample was treated with 1mM TCEP prior to loading on the column. For oxidized AzoC, the protein sample was treated with the same amount of deionized water. Samples were loaded on the column and analyzed as described above.

The elution volume of thyroglobulin was used to calculate void volume (V_0). Protein samples (standards and unknowns) left the column in multiple subsequent fractions, therefore the weighted average of elution volume (V_e), based on sample absorbance at 280 nm, and were used. Weighted protein standard values were used to create a standard curve. The elution volumes of the standards (V_e) were divided by the elution volume of thyroglobulin (V_0) to obtain V_e/V_0 , which is plotted against the log of the protein standards' molecular weights.

The SEC data from the standard proteins were fit to a straight line, $\text{Log}_{10}MW = -0.280 \cdot (V_e/V_0) + 2.740$, using non-linear least squares fitting (PSI-Plot). Based on the experimental V_e/V_0 values of reduced and oxidized AzoC, their molecular weights were estimated by use of the

linear equation of the Log_{10}MW versus V_e/V_0 . The errors on the molecular weight of reduced and oxidized AzoC were calculated based on 95% of confidence (PSI-Plot).

UV-Visible Spectroscopy

A sample of AzoC in 50 mM potassium phosphate buffer (pH 7.5) was scanned from 300-500 nm using a Shimadzu UV-1601PC UV/Visible Spectrophotometer using a quartz cuvette (Shimadzu Corporation). The absorption maxima at 450 nm is due to the presence of FAD in the molecule and $11300 \text{ M}^{-1}\text{cm}^{-1}$ was used as the literature value for the bound extinction coefficient of FAD (Axley *et al*, 1997). Peak absorbance at 450 nm was converted to a molarity value for FAD using the specified extinction coefficients and path length of the instrument (1 cm). Because FAD also absorbs in the 280 nm range (where protein concentration would be determined), a standard of the same molarity that was determined for FAD was used as a blank to measure protein concentration in a way such that all absorbance at 280 nm due to FAD was subtracted and the true absorbance due to protein could be determined. The extinction coefficient for AzoC was calculated using the full AzoC sequence at the ProtParam tool at the ExPASy website (<http://web.expasy.org/protparam/>) to be $19940 \text{ M}^{-1}\text{cm}^{-1}$ and a molarity value for AzoC was calculated (Wilkins *et al*, 1999). The molar value of AzoC was compared to the molar value of FAD to determine the relative ratio of FAD per AzoC. TCEP was added as a reducing agent to reduce disulfide bonds (5 mM TCEP) to understand the ratio in reduced form. Following disulfide bond reduction with TCEP, the sample was passed through an Amicon Ultra 0.5 (NMWL 10,000) filter to remove any unbound FAD.

Bioinformatics Analysis

Sequences and structures were obtained for other azoreductases whose crystal structures are known through the Protein Databank (www.pdb.org) (Berman *et al*, 2000). Secondary structures of other crystallized azoreductase proteins were obtained through the Protein Databank

(www.pdb.org) and analyzed for the percentage of each secondary structural element using PYMOL (Berman *et al*, 2000; Goldin, 1990; PyMOL). Sequence alignments were performed using Clustal Omega using the default parameters (Goujon *et al*, 2010; Sievers *et al*, 2011). Sequence identities were generated by using the Sequence Manipulation Suite (<http://www.bioinformatics.org/sms2>) (Stothard, 2000). Mega 5 was utilized for molecular phylogenetic analysis to generate a maximum likelihood tree (Tamura *et al*, 2011). The JTT matrix-based model was used with the highest log likelihood (-2385.4617) (Jones *et al*, 1992). Initial trees for the heuristic search were obtained automatically as follows: when the number of common sites was <100 or less than one fourth of the total number of sites, the maximum parsimony method was used; otherwise, BIONJ method with MCL distance matrix was used.

Results

Cofactor Identification

To identify the chemical identity of the flavin cofactor of AzoC, the native protein was heat denatured to release its cofactor, and protein-free cofactor extract was prepared for analysis using LC-MS. As seen in Figure 25, the mass spectrum of the AzoC cofactor is consistent with that of the FAD standard. The FMN standard (Figure 25A) shows a single strong peak at m/z 455 and is considered to be FMN⁻ and is not present in the mass spectrum of AzoC cofactor (Figure 25C). The FAD standard, on the other hand, (Figure 25B) shows three significant peaks. The peak of m/z 784 is considered to be the FAD⁻ peak and the peak of m/z 392 is considered to be the FAD²⁻ peak and both are present in the mass spectrum of the AzoC cofactor (Figure 25C). Between the FAD standard (Figure 25B) and the AzoC cofactor (Figure 25C), the only difference was in a peak of significant intensity with a higher m/z . The peak of m/z 807 in the FAD standard was determined to be a Na⁺ adduct peak (presumably from the manufacturing of FAD) while the peak of m/z 822 in the AzoC cofactor was determined to be a K⁺ adduct peak (most likely a

remnant of the protein being in a potassium phosphate buffer). Based on these results we conclude that AzoC contains FAD as its flavin cofactor.

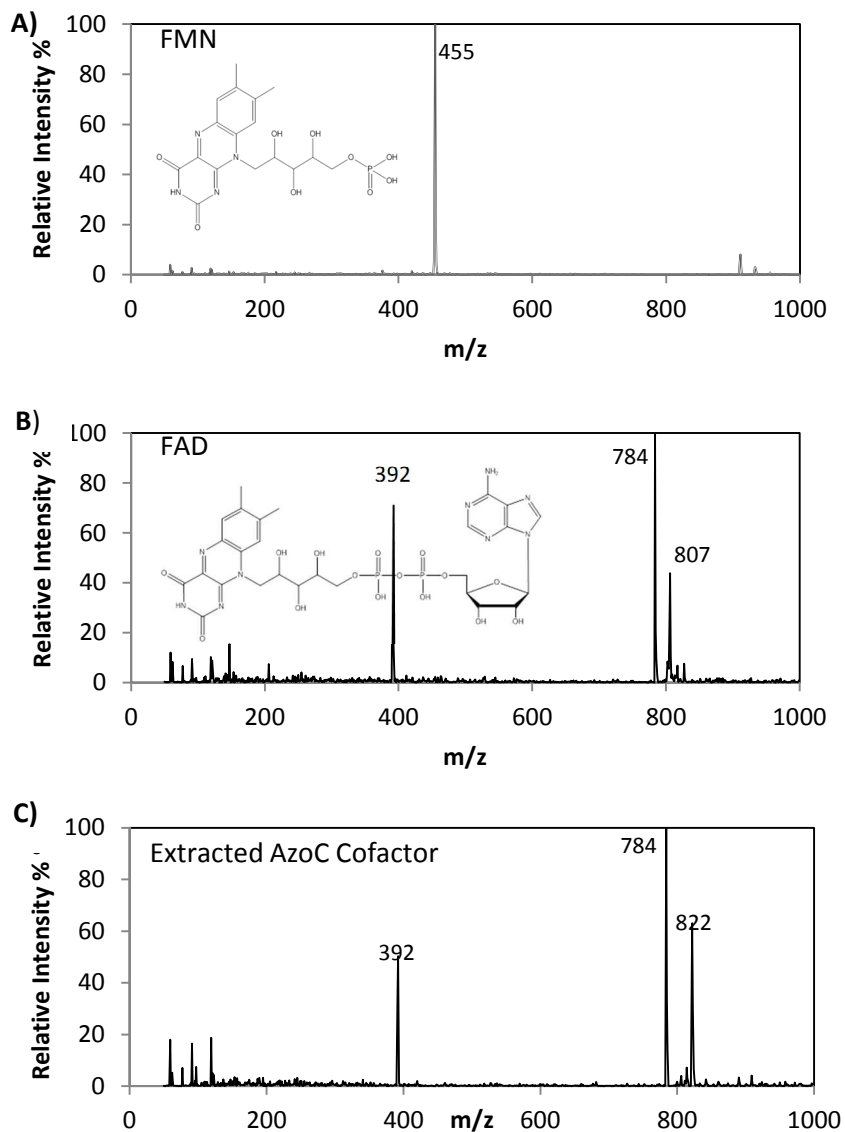


Figure 25. Mass Spectrometry to Identify the Cofactor of AzoC. **(A)** Mass spectrum of FMN standard (1 mM). The peak at m/z 455 is considered to be FMN⁻¹. **(B)** Mass spectrum of FAD standard (1 mM). The peak at m/z 784 is FAD⁻¹, m/z 392 is FAD⁻², and m/z 807 a Na-FAD adduct. **(C)** Mass spectrum of AzoC cofactor. The peak at m/z 784 is consistent with FAD⁻¹, m/z 392 is consistent with FAD⁻², and m/z 807 is consistent with a K-FAD adduct.

The FAD content of the enzyme was determined by measuring the absorbance of AzoC at 450 nm and converting to a molarity value by use of the extinction coefficient of bound FAD from the literature, $11300 \text{ M}^{-1}\text{cm}^{-1}$ (Axley *et al*, 1997). Throughout the process it was noted that the maximum absorbance of the flavin did not change upon heat denaturation of AzoC. The AzoC concentration was determined to be $92.8 \mu\text{M}$ (± 2.5) and the FAD concentration was determined to be $96.7 \mu\text{M}$ (± 3.9). Based on the molarity of AzoC and FAD in the sample, the ratio between AzoC and FAD is calculated to be approximately 1:1, which suggests that each AzoC binds to 1 FAD.

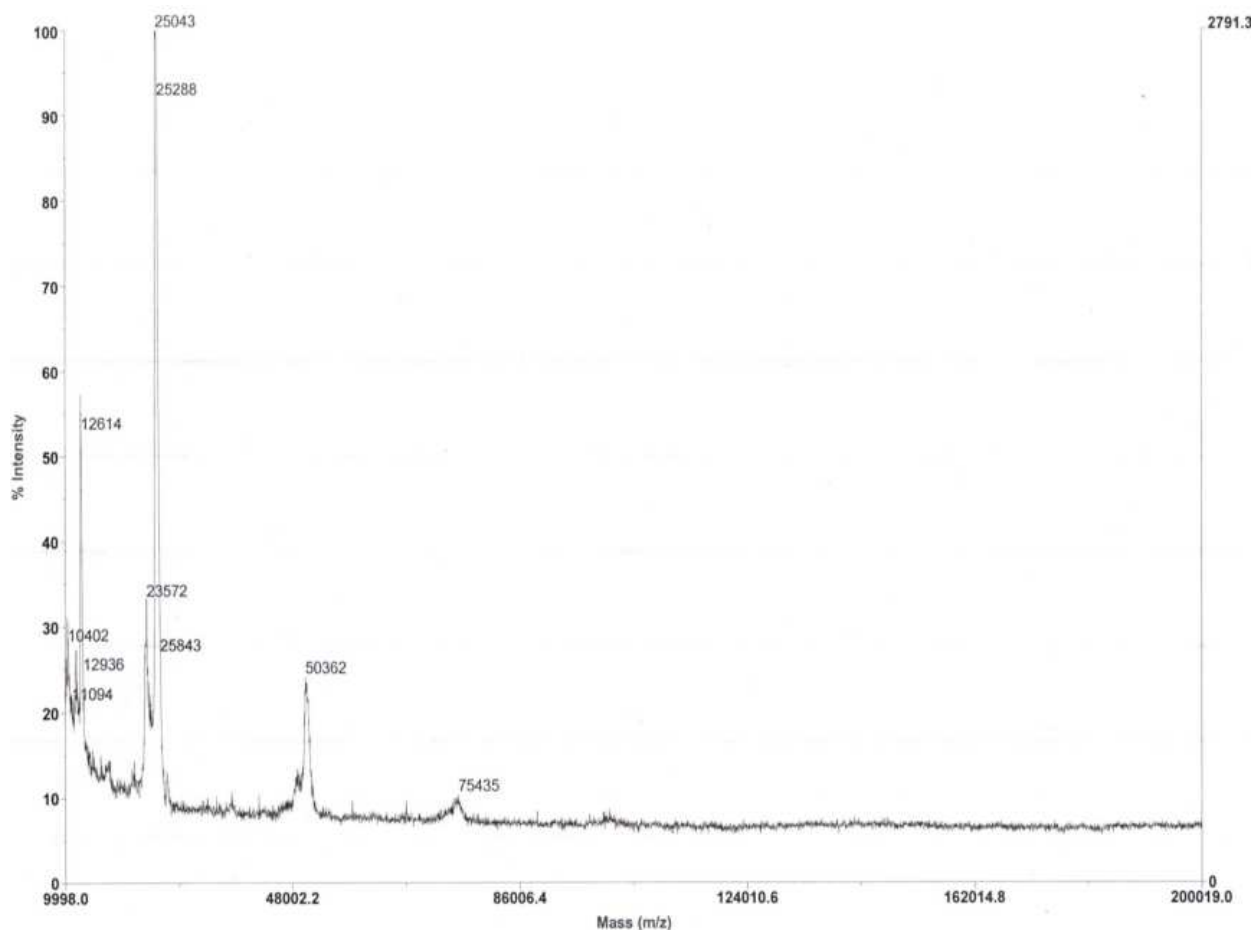


Figure 26. MALDI-TOF spectroscopy of AzoC. The intense peak at m/z 25,043 Da (± 50 Da), is consistent with the molecular weight of AzoC (25,067.8 Da). The mid-sized peak at m/z 50,362 Da (± 50 Da) is consistent with 2X the molecular weight of AzoC and thus represents a dimeric AzoC. The small peak at m/z 75,435 Da (± 50 Da) is consistent with 3X the molecular weight of AzoC and thus represents a trimeric AzoC. Absent from these three peaks is the mass of the cofactor (785.55 Da).

MALDI-TOF spectroscopy showed an intense peak at m/z 25,043 Da (\pm 50 Da), which is consistent with the molecular weight of AzoC (25,067.8 Da) and thus represents the monomeric form of AzoC (Figure 26). Absent from this peak is the mass of the cofactor (785.55 Da), which suggests that the ionization required for MALDI-TOF is enough to dissociate the cofactor. Therefore, the cofactor is bound through non-covalent interactions with AzoC.

Secondary Structure Characterization

Two experimental techniques were utilized to study the secondary structure of AzoC. In far UV-CD, the double minima present at 208 nm and 222 nm suggest the prevalence of significant α -helical regions (Figure 27A) (Tiffany & Krimm, 1969). Secondary structural components were estimated from the spectrum as seen in Figure 27A by the use of the on-line server Dichroweb with the SP175 reference data set and the CDSSTR algorithm (Compton & Johnson, 1986; Lees *et al.*, 2006; Whitmore & Wallace, 2004).

AzoC appears to contain a significant portion of α -helix structures as well as a significant amount of unordered structure (Table 7). The NRMSD (normalized root mean square deviation) is significantly low (0.059 for oxidized AzoC and 0.069 for reduced AzoC), suggesting a goodness of fit in the structural prediction. Because CD spectroscopy is relatively insensitive to β -sheet structures (Whitmore & Wallace, 2008), FTIR spectroscopy was employed to characterize the secondary structure of AzoC in order to achieve more accurate estimate of the β -sheet structures of AzoC (Figure 27B).

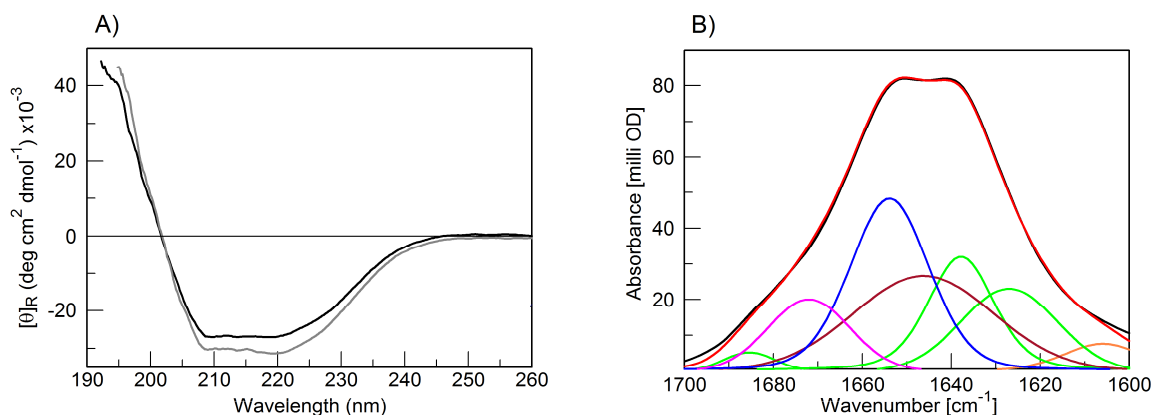


Figure 27. Secondary Structural Characterization of AzoC Using Circular Dichroism and FTIR Spectroscopy. **A)** CD spectroscopy of AzoC. The far-UV CD spectra were recorded at 20 °C at a scan rate of 50 nm/minute with a resolution of 0.2 nm. Spectra are an average of two consecutively scanned samples, corrected for solvent spectra. **B)** Secondary structure analysis of AzoC at 20 °C by employing FTIR absorption spectroscopy in Amide I region. FTIR absorption spectrum of AzoC (black), multi-band overall fitting of Amide I and side chains (red), and individual bands for α -helix (blue, 1653.9 cm^{-1}), β -sheet (green, 1627.0, 1637.8, 1685.4 cm^{-1}), turn (pink, 1672.0 cm^{-1}), unordered structure (dark red, 1646.3 cm^{-1}), and side chains (orange, 1605.9 cm^{-1}).

Table 7. Secondary Structural Characterization of AzoC Using Circular Dichroism and FTIR Spectroscopy. The Combination is based on a weighted average of the CD and FTIR spectroscopic data.

Technique	α -helix (%)	β -sheet (%)	Turn (%)	Unordered (%)
CD	37	5	17	41
FTIR	29	32	13	26
Combination (CD + FTIR)	33	23	15	29

The stretching frequency of the backbone carbonyl C=O (Amide I) is sensitive to the geometry and hydrogen bonding interactions of the protein backbone, and has been widely used to characterize the secondary structures of proteins (Arrondo *et al*, 1993; Barth & Zscherp, 2002; Decatur, 2006; Pelton & McLean, 2000). Spectral fitting with combined Gaussian and Lorentzian spectral shapes using OPUS software (Bruker Optics) are shown in Figure 27B and revealed that AzoC contains 29% α -helix, 32% β -sheet, 13% turn, and 26% unordered structure, as summarized in Table 7. The presence of β -sheets is identified from both the infrared absorption spectra and in the secondary derivatives of infrared absorption (a large peak at 1638 cm^{-1}). The overall secondary structural determination of AzoC shown in Table 7 is based on the weighted averaging of the CD and FTIR spectroscopic data.

Multimeric State of AzoC

The molecular weight of AzoC is 25.1 kDa based on its sequence. Figure 28A shows that, in the presence of this disulfide-bond reducing agent TCEP, SDS-PAGE analysis reveals a molecular weight of ~25 kDa from reduced AzoC, consistent that of monomer AzoC. However, when TCEP is absent from the SDS-PAGE, AzoC appears to be ~75 kDa in size. Thus, the molecular weight of the oxidized AzoC is approximately three times of the molecular weight of AzoC monomer. The SDS-PAGE data of AzoC with and without TCEP (Figure 28A) reveal that oxidized AzoC is a trimer which is held together by inter-molecular disulfide bonds.

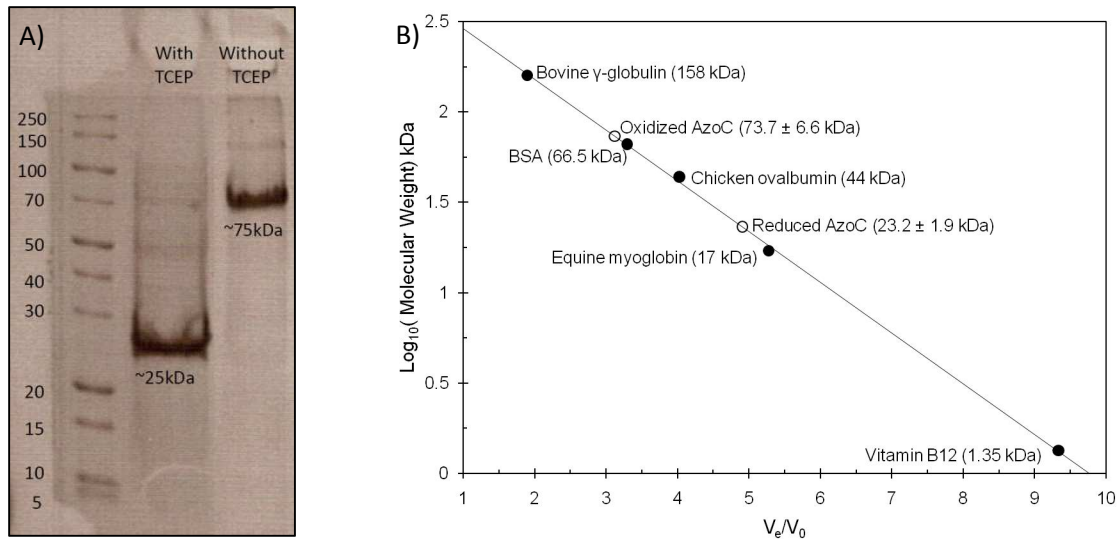


Figure 28. Determination of the Multimeric State of AzoC. **A)** SDS-PAGE of AzoC in reduced (with TCEP) and oxidized forms. **B)** Size exclusion chromatography of oxidized and reduced AzoC as compared to standards. X-axis (V_e/V_0) was calculated dividing the elution volumes of the standards (V_e) by the elution volume of thyroglobulin (V_0) to obtain V_e/V_0 , which is plotted against the log of the standards' molecular weights. The fitted function was $\text{Log}_{10}MW = a(V_e/V_0) + b$, where $a = -0.280$ and $b = 2.740$. AzoC sample molecular weights were estimated by the equation of the line. Oxidized AzoC is predicted to be 73.7 ± 6.6 kDa. Reduced AzoC is predicted to be 23.2 ± 1.9 kDa. PSI Plot (non-linear least squares fitting) was used to calculate error (PSI-Plot).

SEC was performed to determine the multimeric nature of reduced AzoC with non-covalent interactions. As shown in Figure 28B, the linear relationship between the molecular weight of proteins and V_e/V_0 was obtained from the SEC data of standard proteins. This linear

relationship was used to find the unknown molecular weight of oxidized and reduced AzoC based on their V_e/V_0 values under identical SEC conditions. The errors in the molecular weight analysis were derived from 95% of confidence based on the accuracy of the least square fitting. For V_e/V_0 of 3.11, the molecular weight of the oxidized AzoC is 73.7 ± 6.6 kDa, which is consistent with trimeric AzoC (75.2 kDa). For V_e/V_0 of 4.90, the molecular weight of the reduced AzoC is 23.2 ± 1.9 kDa, which is consistent with monomeric AzoC (25.1 kDa).

As previously detailed, the FAD content of the monomeric (reduced) enzyme was determined by measuring the absorbance of AzoC at 450 nm and converting to a molarity value to be compared to the above results for the trimeric (oxidized) enzyme. The AzoC concentration was determined to be $88.3 \mu\text{M} (\pm 2.6)$ for the reduced sample and the FAD concentration was determined to be $92.7 \mu\text{M} (\pm 3.2)$. Based on the molarity of AzoC and FAD in the sample, the ratio between AzoC and FAD is calculated to be approximately 1:1, which suggests that each AzoC binds to 1 FAD. As the ratio (1:1) was the same in both the oxidized and reduced form, it is suggested that each monomer of AzoC binds to one FAD molecule.

Looking at the enzymatic specific activity of reduced (monomeric) AzoC versus the oxidized (trimeric) AzoC, the different forms do not significantly affect specific activity. The enzymatic specific activity of the monomeric form is not significantly different (p-value >0.05, 95% confidence) than the trimeric form in terms of Direct Blue 15 reduction (Table 8).

Table 8. Enzymatic Specific Activities of Reduced and Oxidized Forms of AzoC. Enzymatic Specific Activity is provided as the mean across triplicates (n=3), “±” the standard deviation of the triplicate samples.

	Enzymatic Specific Activity (μg Direct Blue 15 reduced/min/mg AzoC)
Reduced (Monomer)	0.107 ± 0.032
Oxidized (Trimer)	0.100 ± 0.035

Thermal Stability of AzoC

FTIR spectroscopy was utilized to study the thermal stability of AzoC. The results, shown in Figure 29, reveal distinctive structural transitions in the temperature range of 20°C-90°C. AzoC is thermally stable from 20°C to 40°C. Initial thermal denaturation of AzoC starts above 40°C before reaching 50°C, which is consistent with AzoC being from *Clostridium perfringens*, an inhabitant of the human intestine (37°C). Adsorption of AzoC to the ATR diamond surface was observed between 40°C-70°C. Adsorption is detected through changes in the total Amide I band area (Figures 29A, 29B and 29C) as well as the peak at 1616 cm⁻¹ (Figure 29D). This particular peak shows up at a temperature between 40°C-50°C and because of the principle of ATR cell measurement, the IR beam will penetrate into the sample a small depth. The growing peak at 1616 cm⁻¹, then, must come from adsorption to the surface of the ATR cell. The adsorption process is normally invisible in the normal transmission spectroscopy as used in CD spectroscopy. The use of the ATR cell makes it possible to observe this adsorption process. The concurrent processes of adsorption and initial denaturation indicate that AzoC adsorption might be triggered by its partial unfolding.

The denaturation of AzoC was detected through changes in the secondary structure using both secondary derivatives and difference spectra of AzoC as shown in Figures 29D and 29E. As the temperature increases, both α -helix and native β -sheet structures are reduced (1653 & 1637 cm⁻¹) and a new denatured form of β -sheet structure (1616 cm⁻¹) begins to accumulate. Upon reaching 90°C, AzoC forms a combination of highly unordered structures (~1646 cm⁻¹) and the denatured form of β -sheet (1616 cm⁻¹). The mid-point melting temperature from FTIR studies is around 65°C.

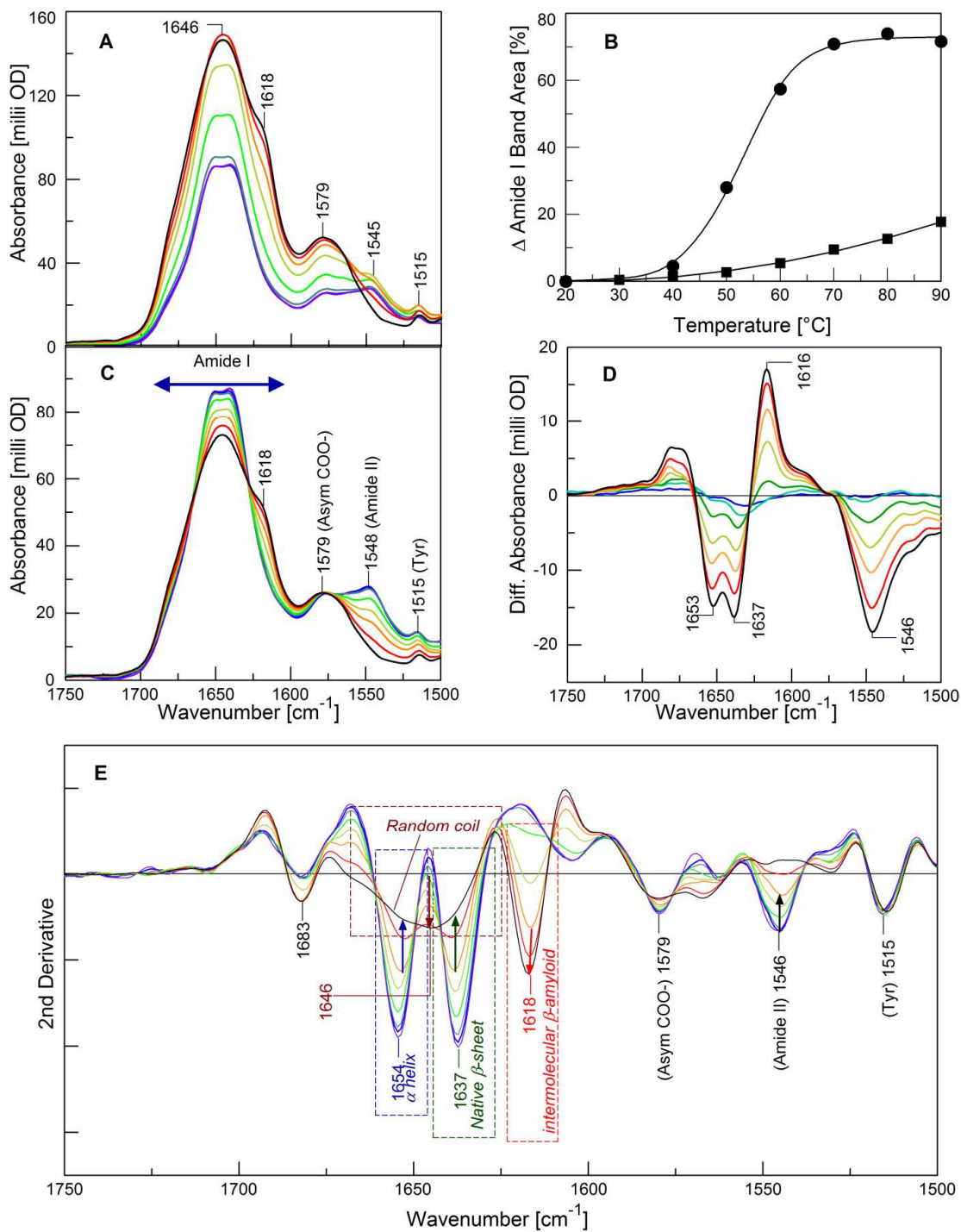


Figure 29. FTIR Spectroscopy of AzoC Structure and Thermal Stability. **(A)** FTIR absorption spectra of AzoC at 20 $^{\circ}\text{C}$ (purple), 30 $^{\circ}\text{C}$ (blue), 40 $^{\circ}\text{C}$ (cyan), 50 $^{\circ}\text{C}$ (green), 60 $^{\circ}\text{C}$ (olive), 70 $^{\circ}\text{C}$ (orange), 80 $^{\circ}\text{C}$ (red), and 90 $^{\circ}\text{C}$ (black) without normalization; **(B)** Temperature dependences of AzoC Amide I band area increases (related to AzoC concentration): squares for AzoC increases due to water evaporation and circles for AzoC increases due to adsorption; **(C)** AzoC spectra after normalization (20 $^{\circ}\text{C}$ -90 $^{\circ}\text{C}$ as color coded in A); **(D)** Difference infrared absorption spectra (30 $^{\circ}\text{C}$ -90 $^{\circ}\text{C}$) in comparison with 20 $^{\circ}\text{C}$ spectrum; and **(E)** Secondary derivatives of absorption spectra. Arrows indicate the direction of changes as the temperature increases.

In addition to protein denaturation, FTIR spectroscopy is sensitive to protein unfolding based on the solvent exposure of the backbone using the Amide II signal of CNH stretching. Upon solvent exposure, the backbone CNH is exchanged to CND, causing the depletion of the Amide II signal around 1548 cm^{-1} . FTIR data (Figure 29C) shows that at 90°C , the AzoC backbone is fully solvent exposed (either transiently or steadily). However, even as high as 80°C , part of the AzoC backbone remains protected from H/D exchange (solvent exposure). These results provide insight into the nature of AzoC unfolding upon thermal denaturation based on the fact that the backbone CNH is partially protected as high as 80°C . Based on a simple two-state model that consists of a native state and an unfolded state, the AzoC population in the unfolded state increases as temperature increases. The backbone CNH groups can be transiently solvent exposed during the thermal equilibrium between the folded and unfolded states, thus resulting depletion of the Amide II band due to H to D exchange at much lower temperature prior to thermal denaturation. The fact that the backbone CNH is partially protected as high as 80°C may suggest a novel unfolding mechanism.

Multimers of a protein are often more stable than monomers (Creighton, 1992). CD spectroscopy was used to determine the unfolding temperatures of the protein in its oxidized (trimeric) and reduced (monomeric) forms to understand if the trimeric form of AzoC aids in stability. Denaturation profiles were plotted with increasing temperature for two fixed wavelengths (208 nm and 222 nm), which correspond to the α -helix structures as observed in the CD absorption spectra (Figure 30). Analysis of the CD spectroscopic data revealed that the melting (i.e. unfolding) temperature of the AzoC monomer is slightly lower than that of the trimeric AzoC, as shown in Figure 30. However, the difference is small and not significant (p-value >0.05 , 95% confidence); the monomer unfolds at a 3-5 $^{\circ}\text{C}$ lower temperature than the trimer.

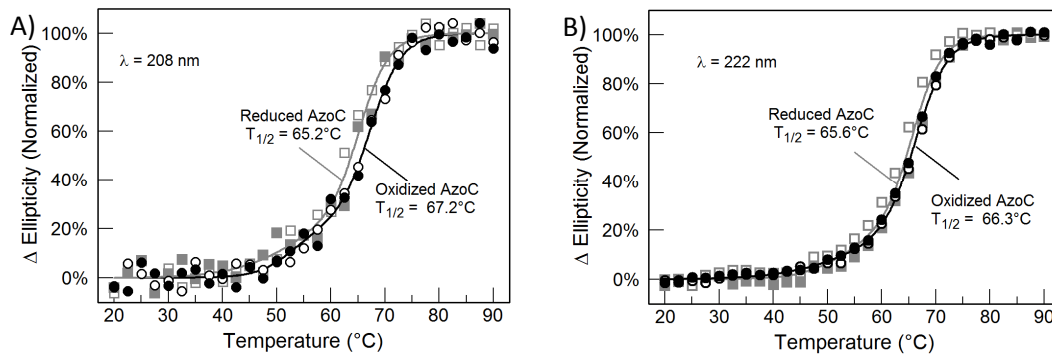


Figure 30. Thermal Stability of AzoC. Denaturation curves of oxidized (trimeric) AzoC (black circles) and reduced (monomeric) AzoC (grey squares) at (A) 208nm and (B) 222nm. Open and filled circles represent two replicates for oxidized (trimeric) AzoC at the given wavelength. Open and filled squares represent two replicates for reduced (monomeric) AzoC at the given wavelength. Values on the graph represent calculated thermal melting temperatures for oxidized (trimeric) AzoC and reduced (monomeric) AzoC. $T_{1/2}$ represents the temperature at 50% Δ Ellipticity during the thermal denaturation of AzoC.

Bioinformatics Analysis

Bioinformatics analysis (Figure 31) shows a very low level of sequence similarity between AzoC from *C. perfringens* and other azoreductases whose three-dimensional structures have been determined. As shown in the sequence alignment in Figure 31A, only seven residues are identical amongst the six sequences compared (<3%), while a slightly higher amount is conserved in terms of a strongly similar amino acid substitution (<10%), and a lower amount is weakly conserved in terms of a weakly similar amino acid substitution (<5%) (classifications of substitutions based on the Clustal Omega matrix). From looking at the alignment in Figure 31A, it is clear that the five sequences of azoreductases having their three-dimensional structures known are very similar to each other in sequence but very different from AzoC. None of the conserved amino acid residues are AzoC's eight cysteines, which is highly unique for an azoreductase; of the other five azoreductases studied here, only the azoreductase from *Pseudomonas aeruginosa* has a cysteine (1) (Wang *et al*, 2007). Though not highly conserved, the eight cysteines of AzoC are critical for disulfide bond formation.

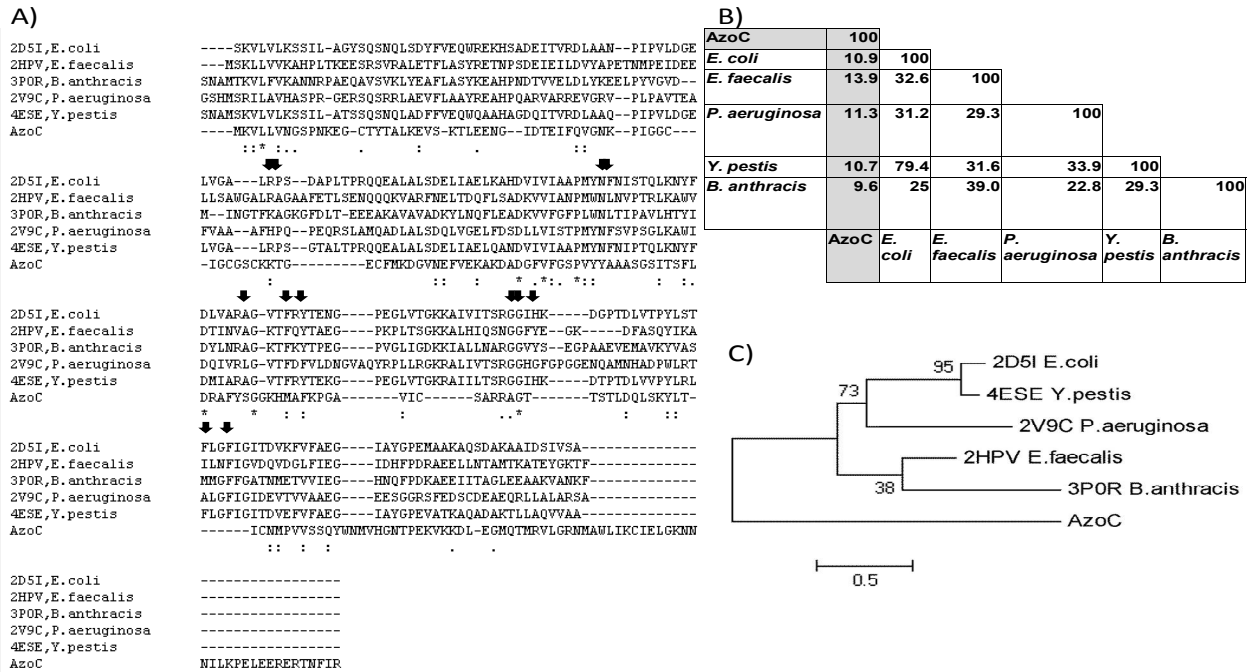


Figure 31. Bioinformatics Study of AzoC. **A)** Clustal Omega alignment of crystallized azoreductases and AzoC (“*” = same amino acid, “:” = strongly similar amino acid substitution, “.” = weakly similar amino acid substitution) (Goujon *et al.*, 2010; Sievers *et al.*, 2011). The code for each of the first five azoreductases represents the PDB identification number from which the sequence was accessed, followed by the organism of origin for each azoreductase. Arrows above amino acids are used to signify those amino acids discussed in the text. **B)** Sequence identities and similarities between the crystallized azoreductases and AzoC (Stothard, 2000). Values represent the percent sequence similarity and identity between the two samples in matrix format. **C)** Molecular phylogenetic analysis by Maximum Likelihood method. The percentage of trees in which the associated taxa clustered together is shown next to the branches. Evolutionary analyses were conducted in MEGA5 (Tamura *et al.*, 2011).

As shown by the crystal structure of the azoreductase of *E. coli*, Asn-97, Phe-98, Gly-141, Gly-142 and His-144 are essential for coordination of the flavin cofactor (Ito *et al.*, 2008). As seen in Figure 31A, Asn-97, Gly-141 and Gly-142 are identical amongst the five azoreductases with their structures known. Only Gly-142 is identical when AzoC is compared as well and Gly-141 is weakly conserved (an Ala in AzoC). Phe-98 and His-144 are slightly conserved amongst the five structurally-known azoreductases, and completely variant in AzoC. In *E. coli*, Arg-59, Phe-98, Ala-112, Phe-118, Phe-159 and Phe-162 are critical to the active site of the azoreductase (Ito *et al.*, 2008). As seen in Figure 31A, Arg-59 is conserved amongst the structurally-known azoreductases and AzoC and Phe-98 is identical between all azoreductases in Figure 31A.

However, Ala-112 shows high conservation amongst the structurally-known azoreductases in small, hydrophobic residues whereas AzoC shows a polar residue. Similarly, Phe-118 is identical amongst all of the structurally-known azoreductases, but is a Met in AzoC. Phe-159 and Phe-162 are highly conserved and identical, respectively, amongst the structurally-known azoreductases but are absent in AzoC.

As suggested by the sequence alignment, sequence identity between AzoC and the structurally-known azoreductases is very low, as shown in Figure 31B. When comparing AzoC to the other azoreductases, the values range from 9.6% to 13.9%. However, when comparing between the five azoreductases with their structures known, the values are much higher (range 22.8% to 79.4%) going as high as 79.4% between *E. coli* and *Y. pestis*. When this similarity is viewed as a phylogenetic tree, AzoC is seen as in the outgroup when compared to the azoreductases that have their structures known (Figure 31C), again showing its low level of sequence similarity with these other azoreductases.

Discussion

In this Chapter, the use of biophysical methods to characterize the AzoC enzyme is reported, including (1) a determination of the identity of the cofactor of AzoC, (2) a determination of the approximate secondary structure of AzoC and (3) a determination of the polymeric state and stability of AzoC. In Chapter 2, the azoreductase protein from *Clostridium perfringens*, AzoC, has been successfully identified, isolated and characterized AzoC. Because of the absence of structural information about azoreductases from strictly anaerobic microorganisms, a structural analysis of AzoC is necessary to fill in the literature gap and provide an understanding of the degree of similarity between aerobic and anaerobic azoreductases.

The cofactor of AzoC has been identified to be FAD (Figure 25). The use of FAD by AzoC is unique amongst azoreductases studied, as most azoreductases seem to prefer FMN

(Table 9) (Ito *et al*, 2006; Liu *et al*, 2007; Tan *et al*, 2012; Wang *et al*, 2007). While *Clostridium perfringens* cells contain both FAD and FMN, our results show that FAD is preferred (Semde *et al*, 1998). FMN is a much smaller molecule than FAD and may be preferred based on size constraints in the flavin cofactor coordination site. Asn-97, Phe-98, Gly-141, Gly-142 and His-144 have been shown to be important in flavin coordination in *E. coli* and are well conserved amongst the azoreductases of known structure but not as well conserved in AzoC (Figure 31A) (Ito *et al*, 2008). Because all of the structurally-known azoreductases require FMN, whereas AzoC requires FAD, it is hypothesized that the low similarity in this region is due to AzoC's requiring FAD as a cofactor and thus variant amino acids to coordinate it. Additionally, presented in this Chapter is a simplified and conclusive method for the rapid determination of the flavin cofactor for an azoreductase protein. In this Chapter it has also been shown that AzoC has an FAD attached non-covalently in a 1:1 ratio. A 1:1 ratio of flavin cofactor to azoreductase monomer is consistent with the other azoreductases studied here (Ito *et al*, 2006; Liu *et al*, 2007; Tan *et al*, 2012; Wang *et al*, 2007).

Table 9. Secondary Structural Characteristics of Other Azoreductases as Compared to Oxidized AzoC.

Organism	PDB ID No.	α -helix (%)	β -sheet (%)	Turn + Unordered (%)	Multimeric State	Cofactor	Reference
<i>E. coli</i>	2D5I	44	16	40	Dimer	FMN	(Ito <i>et al</i> , 2006)
<i>E. faecalis</i>	2HPV	51	19	30	Dimer	FMN	(Liu <i>et al</i> , 2007)
<i>B. anthracis</i>	3P0R	52	17	31	Monomer	N/D ^a	(Filippova <i>et al</i> , 2010)
<i>P. aeruginosa</i>	2V9C	49	20	31	Tetramer	FMN	(Wang <i>et al</i> , 2007)
<i>Y. pestis</i>	4ESE	48	19	33	Dimer	FMN	(Tan <i>et al</i> , 2012)
Average ^b		49	18	33			
<i>C. perfringens</i>		33	23	44	Trimer	FAD	This Chapter
Difference ^c		-16	+5	+11			

^a N/D = cofactor not determined.

^b The averaged secondary structural components from the five structurally-known azoreductases.

^c The calculated difference between the *C. perfringens* azoreductase and the average of the five structurally-known azoreductases.

The secondary structure of AzoC was determined by use of both CD and FTIR spectroscopic techniques. Both CD and FTIR spectroscopies identified a large fraction of α -helices in AzoC, and are consistent regarding the turn structures (Table 7). The large discrepancy in β -sheet content is largely due to the relative insensitivity of CD spectroscopy to β -sheet as has been detailed by Whitmore and Wallace (Whitmore & Wallace, 2008). Overall, β -sheets are more highly variable because they can be in variable orientations with different twists and related phi/psi angles and can be overall less intense than α -helices when seen by CD spectroscopy (Whitmore & Wallace, 2008). In proteins with high α -helical content, like AzoC, it is likely that the contribution of α -helices to the spectrum can overshadow that of the β -sheets in CD spectroscopy (Whitmore & Wallace, 2008). In FTIR spectroscopy, the strong presence of β -sheet is clearly identified from both the infrared absorption spectra and in the secondary derivatives of infrared absorption (a large peak at 1638 cm^{-1}). Therefore, FTIR spectroscopy is more sensitive to β -sheet structural characterization than CD spectroscopy. Because CD spectroscopy is relatively insensitive to β -sheet structures, whereas FTIR spectroscopy does not have this issue, it is hypothesized that the combination of CD and FTIR spectroscopies will lead to more accurate protein secondary structure determination (Whitmore & Wallace, 2008). The combined CD and FTIR spectroscopic data provides a more reliable secondary structure characterization of AzoC, as summarized in Table 7. Shown here is a simple, novel method for determination of protein secondary structure and thermal stability by the combined use of CD and FTIR spectroscopic techniques.

AzoC was shown to be a trimer held together by disulfide bonds under oxidized conditions. Disulfide bond connections between monomers in azoreductases is unique to AzoC to the author's knowledge; the presence of 8 cysteines is also unique to AzoC when compared to the azoreductases of known structure (Figure 31A and Table 9). Of the structurally-known azoreductases, AzoC is the only known trimer and is thus structurally unique in multimeric form

(Table 9). The trimeric form, however, does not seem to be significantly more stable or enzymatically active than the monomer (Table 8 and Figure 30). In terms of enzymatic specific activity, the enzyme activity of the oxidized (trimeric) protein is not significantly different than that of the reduced (monomeric) protein, suggesting that AzoC functions equally well as an azoreductase whether a monomer or a trimer (Table 8). Since the nature of the cytoplasmic environment where the azoreductase is produced is highly reducing (strictly anaerobic), it is not expected that the disulfide bonds that form the trimer would occur naturally inside the cell (Derman *et al*, 1993; Gilbert, 1990; Hwang *et al*, 1992). However, if the protein is found to be secreted into the extracellular environment, the trimer can be formed (Beebe *et al*, 1990; Pollitt & Zalkin, 1983). It is also possible that the formation of the disulfide bonds may play a role in an oxygen-protection mechanism, an observation which has been noticed in other strictly anaerobic Gram-positive bacteria (Daniels *et al*, 2010; Vita *et al*, 2008). However, future work would be needed to study this further. Thermal stability studies with CD and FTIR were largely very consistent in terms of the determination of protein melting temperature. Overall, the thermal stability studies with FTIR of AzoC showed an interesting result. The backbone CNH appears to be partially protected and not completely unfolded at temperatures as high as 80°C, suggesting an unfolding mechanism that may be more complex than the typical two-state mechanism for AzoC.

Along with having low sequential similarity (Figure 31B), utilization of a different flavin cofactor and a unique multimeric state (Table 9), AzoC also shows differences secondary structural characteristics when compared with the azoreductases that have their crystal structures known. All of the azoreductases examined in this Chapter contain significant α -helical character, with much less β -sheet structure. When compared to the average azoreductase, AzoC contains 16% less α -helices, 5% more β -sheets and 11% more unordered structure. Also, the ratio of α -helix to β -sheet is 1.5 in AzoC, whereas the same ratio is approximately 2.5 in the structurally known azoreductases. AzoC contains a significant amount of unordered loop structures that is

higher than the structurally-known azoreductases. In this way, AzoC is significantly different than the other azoreductases (Table 9).

CHAPTER V

NON-CLASSICAL AZOREDUCTASE SECRETION IN *CLOSTRIDIUM PERFRINGENS* IN RESPONSE TO SULFONATED AZO DYE EXPOSURE AND THE GENERATION OF A Δ *azoC* KNOCKOUT MUTANT

Abstract

Clostridium perfringens, a strictly anaerobic microorganism and inhabitant of the human intestine, has been shown to produce an azoreductase enzyme (AzoC), an NADH-dependent flavin oxidoreductase. This enzyme reduces azo dyes into aromatic amines, which can be carcinogenic. A significant amount of work has been completed on the activity of AzoC. Despite this, much is still unknown, including whether azoreduction of these dyes occurs intracellularly or extracellularly. In addition to this, to date, a gene knockout mutant for any azoreductase in bacteria has not been completed. The Sigma-Aldrich TargeTron Gene Knockout System was utilized for targeted specific gene disruption by Group II intron insertion within the *azoC* gene of the *C. perfringens* genome. A physiological study of *C. perfringens* involving the effect of azo dye exposure was completed to fill the literature gap. Through exposure studies, azo dyes were found to cause cytoplasmic protein release, including AzoC, from *C. perfringens* in dividing and non-dividing cells. Sulfonation (negative charge) of azo dyes proved to be the key to facilitating protein release of AzoC and was found to be azo-dye-concentration-dependent. Additionally, AzoC was found to localize to the Gram-positive periplasmic region. Using the Δ *azoC* knockout mutant, the presence of additional azoreductases in *C. perfringens* was suggested. These results

support the notion that the azoreduction of these dyes may occur extracellularly for the commensal *C. perfringens* in the intestine.

Introduction

Bacterial azoreductases are enzymes which are capable of reducing azo dyes into their component amines (Levine, 1991). Azo dyes are common synthetic colorants which are used in many industries spanning foods and beverages to textiles and paper products (Chen, 2006; Chung *et al*, 1992). Azo dyes possess a namesake azo bond (-N=N-), which makes them capable of being reduced into their component aromatic amines by the azoreductase enzyme (Stolz, 2001). These aromatic amine metabolites have been found to be carcinogenic in many cases (Rafii & Coleman, 1999). Aside from being a threat to human health, azo dyes are also frequently found as environmental pollutants, an end result of industrial processing applications (Chen, 2006; Chung *et al*, 1992; Stolz, 2001).

Azoreductases have been studied in a large variety of bacteria, including those important for both the environment and human health (Blumel & Stolz, 2003; Chen *et al*, 2005a; Chen *et al*, 2004; Nakanishi *et al*, 2001; Sugiura *et al*, 2006). The azoreductase from *Clostridium perfringens* (AzoC) has recently been characterized and several unique attributes have been revealed, as detailed in Chapters 2-4 (Morrison *et al*, 2014; Morrison & John, 2013; Morrison *et al*, 2012). First, AzoC is significantly different from other well-studied azoreductases in terms of its sequence and structure (see Chapter 4). The azoreductase with the highest sequence identity with AzoC is AzoA from *Enterococcus faecalis*, which shares only 13% amino acid sequence identity (Morrison *et al*, 2014). AzoC possesses a trimeric structure with each monomer non-covalently bound to a redox cofactor, flavin adenine dinucleotide (FAD). The FAD cofactor is unique amongst other azoreductases studied to date, where all other studied azoreductases utilize flavin mononucleotide (FMN). AzoC monomers are held together by disulfide bonding forming a

trimeric structure; no other trimeric azoreductases have been determined to date (Morrison *et al*, 2014). Second, AzoC is the only azoreductase from a strict anaerobe, as other azoreductases are from aerobic-respiring microorganisms. Thus, *in vivo* and *in vitro* optimal AzoC enzyme activity requires reduced levels of oxygen (Morrison *et al*, 2014; Morrison & John, 2013; Morrison *et al*, 2012). Third, AzoC has a very different substrate preference compared to other highly studied azoreductases (Chen *et al*, 2005a; Chen *et al*, 2004; Feng *et al*, 2010; Macwana *et al*, 2010; Maier *et al*, 2004; Morrison *et al*, 2012). AzoC prefers large molecular weight, sulfonated azo dyes (e.g. Direct Blue 15 and Ponceau BS), whereas other azoreductases tend to prefer smaller molecular weight non-sulfonated azo dyes (e.g. Methyl Red and Methyl Orange) (Chen *et al*, 2005a; Chen *et al*, 2004; Feng *et al*, 2010; Macwana *et al*, 2010; Maier *et al*, 2004; Morrison *et al*, 2014; Morrison & John, 2013; Morrison *et al*, 2012).

Although the literature is replete with azoreductase studies, physiological information on whether the interaction of azoreductase and azo dyes occurs intracellularly or extracellularly is largely lacking, and what is there is controversial. The literature has contrasting views on whether azoreductase activity occurs intracellular (Feng *et al*, 2010) or extracellular (Maier *et al*, 2004; Stolz, 2001) or both, depending on the specific azo dye and its chemical characteristics (Punj & John, 2008).

The enzyme would need to be able to exit the cell if the azo dye and azoreductase were to interact extracellularly. Classical protein secretion systems are complex structures involved in translocating and excreting proteins (Schneewind & Missiakas, 2012). These systems in *C. perfringens* have not been studied. However, in closely related taxa (*C. tetani* and *C. acetobutylicum*) the secretion translocation system (Sec) is the most common mechanism for protein excretion into the extracellular environment via Sec-dependent protein signal sequences (Bruggemann *et al*, 2003; Desvaux *et al*, 2005). Other translocation systems such as the twin arginine translocation system (Tat) have not been reported to date in any *Clostridium* species

(Berks *et al*, 2005; Desvaux *et al*, 2005). Previous research has shown that AzoC does not contain a signal peptide and is therefore predicted to be an intracellular azoreductase by its sequence (Morrison *et al*, 2014; Morrison *et al*, 2012).

Extracellular to the cell membrane of Gram-positive bacteria lies a small periplasmic space (Forster & Marquis, 2012; Navarre & Schneewind, 1999). This Gram-positive periplasmic space consists of proteins and lipoteichoic acid that are anchored to the cell membrane (Forster & Marquis, 2012; Matias & Beveridge, 2008). Technically, the periplasmic space is an inner-wall zone (30 nm thick) which is significantly less than a typical Gram-negative cell wall periplasmic space (Forster & Marquis, 2012). Beyond the periplasmic space are surface proteins that are covalently linked to the peptidoglycan. Interestingly, in a recent study of the cell-surface proteins of *C. perfringens* strain ATCC 13124, several of the extracellular surface proteins that were identified were actually predicted to be intracellular in nature due to function or lack of a signal peptide (Alam *et al*, 2009).

This phenomenon has been frequently observed in an increasing number of proteins throughout Gram-positive bacteria (Alam *et al*, 2009; Bukau & Horwich, 1998; Cole *et al*, 2005; Severin *et al*, 2007; Shimizu *et al*, 2002a; Shimizu *et al*, 2002b; Walz *et al*, 2007). In fact, a study in *C. perfringens* strain 13 showed that the extracellular culture supernatant following late exponential phase contained non-signal sequence proteins that were predicted to be intracellular (Shimizu *et al*, 2002a; Shimizu *et al*, 2002b). The mechanism by which these proteins are able to exit the cell without a signal sequence is yet to be described and is commonly referred to as non-classical protein secretion (Wickner & Schekman, 2005). A recent study in *E. coli* has suggested that environmental extracellular stress on the cell wall can cause proteins to selectively release from the intracellular space (Vazquez-Laslop *et al*, 2001). Despite not having a signal peptide, it is possible that a signal response or non-covalent interaction may cause AzoC to translocate

across the membrane, non-covalently associate with the cell wall, and eventually exist under the right conditions as extracellular azoreductase.

To garner a complete look at the effect of AzoC on *C. perfringens* strain ATCC 3626, AzoC will be knocked out. To our knowledge, this is the first knockout of an azoreductase gene completed, as well as the first recorded gene knockout in *C. perfringens* strain ATCC 3626. Other important genes have been knocked out in other strains of *C. perfringens* by the use of a Targetron Gene Knockout kit, optimized for this particular bacteria (Chen *et al*, 2007; Chen *et al*, 2005b; Gupta & Chen, 2008; Heap *et al*, 2010a; Heap *et al*, 2010b; Heap *et al*, 2007; Li & McClane, 2008; Li & McClane, 2010).

The goals of this Chapter are to create a Δ *azoC* knockout mutant, to use azo dye exposure studies to understand the physiological effects of azo dye exposure on *C. perfringens* and to analyze AzoC protein release in this bacteria to determine the cellular location of azoreductase activity.

Materials and Methods

Bacterial Strains and Azo Dyes

Clostridium perfringens strain ATCC 3626 was grown anaerobically, under static growth conditions (non-shaking) in Brain Heart Infusion (BHI) broth (Difco Laboratories) at 37°C, unless otherwise noted.

The following azo dyes were used during this investigation: Direct Blue 15 (MP Biomedicals), Methyl Red (Acros Organics), Ponceau BS (Sigma-Aldrich), Methyl Orange (Allied Chemicals). Sodium benzene sulfonate served as the non-azo dye compound and was purchased from TCI America. Chemical compound structures can be seen in Figure 32.

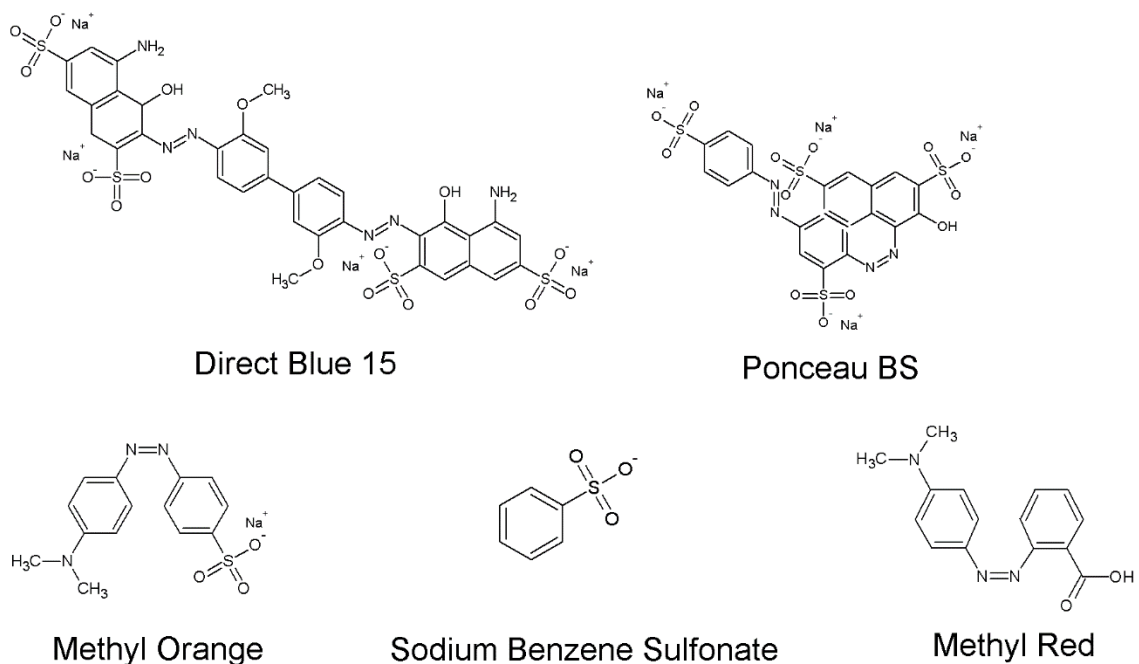


Figure 32. Structures of Azo Dyes and Chemicals Tested. Direct Blue 15 represents a high molecular weight (992.80 g/mol) sulfonated azo dye. Ponceau BS represents a mid-molecular weight (556.48 g/mol) sulfonated azo dye. Methyl Orange represents a small molecular weight (327.33 g/mol) sulfonated azo dye. Sodium benzene sulfonate (non-azo dye) shares similar structures to azo dyes in terms of sulfonation. Methyl Red represents a small molecular weight (305.77 g/mol) non-sulfonated azo dye.

Creation of a Δ azoC Knockout Mutant

A Δ azoC knockout mutant was created by inactivating the *azoC* gene in *C. perfringens* by the insertion of a group II intron using the TargeTron (Sigma-Aldrich) insertional mutagenesis system with a *Clostridium*-modified protocol and plasmid (Chen *et al*, 2005b). The Sigma TargeTron algorithm (www.sigma-genosys.com/targetron/) was utilized to identify optimal intron insertion sequence sites within the *azoC* gene sequence. An intron was targeted in the sense orientation between nucleotides 228 and 229 of the *azoC* open reading frame, as this particular region has the highest score (9.72) and the lowest E-value (0.028). Low E-values correspond to the highest efficiency designs (Chen *et al*, 2005b). The *azoC*-specific targeting primers used for this process were: IBS (5'-AAAAA AGCTT ATAAT TATCC TTAAGG GGACG CAGAT GTGCG CCCAG ATAGG GTG-3'), EBS1d (5'-CAGAT TGTAC AAATG TGGTG ATAAC

AGATA AGTCG CAGAT GGTA A CTTAC CTTTC TTTGT-3'), EBS2 (5'-TGAAC GCAAG TTTCT AATTT CGGTT TCCTT CCGAT AGAGG AAAGT GTCT-3'), and a Targetron-provided EBS Universal Primer. Primers were diluted upon receipt to the following concentrations: IBS (100 μ M), EBS1d (100 μ M), EBS2 (20 μ M), EBS Universal Primer (20 μ M). The four primers were used to create a Primer Master Mix by mixing 2 μ L of each primer to 20 μ L in water for total Primer Master Mix volume.

A 50 μ L total volume PCR reaction, with the aim of retargeting the provided intron to be specific for targeting the *azoC* gene, was set-up by using 1 μ L of the four Primer Master Mix, 1 μ L of the Targetron-kit provided Intron PCR template, and 25 μ L JumpStart REDTaq ReadyMix (Sigma-Aldrich), with water to volume. The PCR reaction consisted of an initial denaturation of 30 seconds at 94°C, 30 cycles of denaturation (15 seconds at 94°C), annealing (30 seconds at 55°C) and extension (30 seconds at 72°C), followed by a final extension of 2 minutes at 72°C. PCR was performed in an MJ Researcher PTC-100 Programmable Thermal Cycler. The PCR reaction was run on a 4% agarose gel to confirm that a 350 bp band was present, as it is the expected product of the PCR-retargeting procedure. Following confirmation, the PCR product was purified using the GenElute PCR Clean-up Kit (Sigma-Aldrich).

A double restriction enzyme digestion was performed to cut the intron PCR product from above to produce cohesive ends to be able to be ligated into the *Clostridium*-specific vector. HindIII (20 U/ μ L) and BsrGI (10 U/ μ L) were added in a double digestion reaction that included 200 ng of purified PCR product, 2 μ L of 10X Restriction Enzyme Buffer (compatible with both HindIII and BsrGI), 1 μ L each of HindIII and BsrGI, and water to a 20 μ L total reaction volume. The reaction was completed in an MJ Researcher PTC-100 Programmable Thermal Cycler for 30 minutes at 37°C, 30 minutes at 60°C and 10 minutes at 80°C. The same double restriction enzyme digestion was also performed on the *Clostridium*-specific pJIR750ai plasmid to produce cohesive ends.

Ligation of the cut pJIR750ai plasmid and *azoC*-targeted intron was performed by using the Quick-Link T4 DNA Ligation Kit (Sigma-Aldrich). Briefly, 40 ng of the HindIII/BsrGI-cut pJIR750ai plasmid and 6 μ L of the HindIII/BsrGI-cut intron PCR product were added together and mixed with 10 μ L of the provided Quick-Link Buffer A and 2 μ L of the provided Quick-Link Buffer B for a total reaction volume of 20 μ L. The components were mixed together and heated to 60°C for 30 seconds, followed by cooling on ice for 1 minute. Quick-Link Ligase was then added (1 μ L) and mixed. The reaction was allowed to progress for 30 minutes at room temperature.

This plasmid, pJIR750aiAzoC, was electroporated into *C. perfringens* strain ATCC 3626 (Gupta & Chen, 2008). Briefly, 0.2 mL of the *C. perfringens* strain ATCC 3626 cells were inoculated into the bottom of a tube of 10 mL fluid thioglycollate media for an overnight culture at 37°C, without shaking (Gupta & Chen, 2008). The overnight culture (0.2 mL) was used to inoculate 10 mL TGY broth (30 g/L trypticase, 10 g/L yeast extract, 20 g/L glucose, 1 g/L l-cysteine) for a second overnight culture at 37°C, without shaking (Gupta & Chen, 2008). The *C. perfringens* cells were harvested by centrifugation (6000 x g, 10 minutes, 4°C) and washed twice with SMP buffer (270 mM sucrose, 1 mM MgCl₂, 7 mM sodium phosphate buffer, pH 7.3) (Gupta & Chen, 2008). Following washing, *C. perfringens* cells were resuspended in 400 μ L of SMP buffer and placed into a 0.2 cm Gene Pulser cuvette (Bio-Rad) with 5 μ g of the pJIR750aiAzoC plasmid (Gupta & Chen, 2008). The cuvette was electroporated with a single pulse of 2.5 kV at 25 μ F capacitance and 200 Ω resistance using a Gene Pulser Xcell Electroporation System (Bio-Rad) (Gupta & Chen, 2008). Following the electroporation, the cells were rescued into 3 mL of warmed TGY broth, making sure to rinse the cuvette with additional TGY broth to recover any additional cells (Gupta & Chen, 2008). The electroporated cells were incubated at 37°C without shaking for 3 hours (Gupta & Chen, 2008).

Transformants were selected by anaerobic growth on BHI agar plates containing chloramphenicol (15 µg/mL). Selected transformants were grown in 10 mL anaerobic BHI cultures containing chloramphenicol (15 µg/mL) and their genomic DNA was extracted using a Genomic DNA Purification Kit (Wizard). Following genomic DNA extraction, PCR was utilized to confirm the presence of intron insertion within the *azoC* gene by using AzoC-sequence specific primers: *azoC*-F (5'-CGGCC TCGAG ATGAA AGTAT TATTA GTTA-3'), *azoC*-R (5'-GTGAA AGGAT CCGCT GATTA AAATT AACTT TGATA TATTT CAC-3') (see Chapter 2) (Morrison *et al*, 2012; Wright, 2007). PCR was carried out in a MJ Research PTC-100 Programmable Thermal Cycler. Conditions for amplification were as follows: one cycle of 2 minutes at 94°C, 25 cycles with each cycle consisting of 1 minute at 94°C, 1 minute at 55°C, and 1 minute at 72°C, and a final extension of 7 minutes at 72°C. The PCR amplicon was observed by 0.8% (w/v) agarose gel electrophoresis and ethidium bromide staining using a 1 Kb ladder (Promega) and 100 bp ladder (Fermentas GeneRuler).

AzoC Purification and Antibody Production

E. coli (DE3) NovaBlue cells harboring an AzoC-containing plasmid and required His-tag were prepared by Cristee Wright (see Chapter 2) (Morrison *et al*, 2012; Wright, 2007). These cells were inoculated into 5 mL of LB broth containing 100 µg/mL ampicillin. Cultures were incubated overnight at 37°C with shaking at 200 rpm. This culture, following overnight incubation, was transferred to 1 L of LB broth with 100 µg/mL ampicillin and incubated while shaking at 200 rpm until an OD₆₀₀ of 0.6 was reached. At this point, the culture was induced with isopropyl-beta-D-thiogalactopyranoside (IPTG) at a 1 mM concentration for 3 hours at 37°C and shaking at 200 rpm. Cultures were pelleted by centrifugation (6000 x g, 10 minutes, 4°C). The supernatant was discarded while the pellet was stored frozen at -20°C until AzoC purification could occur.

The cell pellet from above was thawed and resuspended in 10 mL of lysis/wash buffer (20 mM imidazole, 750 mM sodium chloride, 50 mM sodium monobasic phosphate, 20% glycerol, deionized water, pH 8.0). Following resuspension, cells were lysed by the addition of lysozyme (0.1 mg/mL final concentration); following lysozyme addition, cells were incubated on ice for 30 minutes. Cells suspensions were then sonicated using a Sonic 300 dismembrator with an intermediate tip with relative output set at 60%. Sonication occurred 10 times, 5 seconds each, with placing the cells on ice in between sonications to ensure that any proteins released did not denature. Following sonication, the cell suspension was centrifuged (10,000 x g, 30 minutes, 4°C) to pellet cell debris. The proteinaceous supernatant was stored at 4°C until further purification could occur, while the cell debris pellet was discarded.

AzoC purification occurred as follows. The proteinaceous supernatant from the previous step was introduced to a nickel-nitrilotriacetic acid (Ni-NTA) resin suspension (UBP-Bio) in a glass frit column (Kimble-Chase Flex Column). The Histidine tag of the AzoC protein is what allows for AzoC to interact with the Ni²⁺ on the resin and is what allows for this protein purification procedure to succeed. All of the steps of the purification procedure occurred at 4°C to make sure that AzoC did not denature during the process. Following the application of AzoC to the Ni-NTA resin, the mixture was allowed to incubate, in the column, at 4°C while shaking horizontally at medium speed on a BioDancer orbital shaker (New Brunswick Scientific). This hour-long incubation allows adequate time for the histidine tag of AzoC to interact with the Ni²⁺ bound to the resin in the column. Following incubation, solution was drained from the column and the resin in the column was washed with lysis/wash buffer until the solution leaving the column was clear. Pure AzoC was eluted from the column by exposure of the resin to elution buffer (250 mM imidazole, 750 mM sodium chloride, 50 mM sodium monobasic phosphate, 20% glycerol, deionized water, pH 8.0). Elutions were carried out until the yellow-colored AzoC was eluted from the column. The elutions were saved and stored frozen at -20°C.

Purified AzoC (1 mg at a 100 µg/mL concentration) was used by Thermo Fisher Scientific Custom Services (Rockford, IL) to produce a rabbit anti-AzoC polyclonal antibody. In short, a total of four immunizations of AzoC were administered to two rabbits on a 90-day protocol. Injections were given at four separate subcutaneous sites to foster an immune system reaction to generate the anti-AzoC antibody. A total of four bleeds for antibodies were taken during the 90-day protocol, along with a terminal bleed following the 90 days. Thermo Fisher Scientific Custom Services provided us with approximately 90 mL of AzoC-active sera per rabbit immunized.

SDS-PAGE

Protein fractions were analyzed by SDS-PAGE gel electrophoresis. SDS-PAGE analysis was performed as previously described (Laemmli, 1970). Prior to analysis by SDS-PAGE, 15 µL of protein sample was mixed with 5 µL of SDS-PAGE loading buffer (0.06 M TRIS-HCl pH 6.8, 10% (v/v) glycerol, 2% (w/v) SDS, 0.0025% (w/v) bromophenol blue). Beta-mercaptoethanol was added as a reducing agent (5%) to denature disulfide bonds. Prepared samples were boiled for 15 minutes and then the total volume was loaded onto a 12.5% SDS-PAGE gel. For protein analysis, following gel run, Coomassie blue was used as the protein stain and protein bands were visualized and photographed in comparison to an unstained protein molecular weight marker (14.4-116 kDa, Thermo Scientific). A pre-stained protein molecular weight marker was used for Western blotting gels (2-250 kDa, Bio-Rad).

Western Blotting

To observe the absence of the AzoC protein in the *ΔazoC* knockout mutants and the presence in the Wild Type cells, protein fractions extracted from the cells as described below were analyzed by Western Blotting with an anti-AzoC antibody. Following separation by SDS-PAGE, the proteins were transferred to an Immun-Blot PVDF Membrane (Bio-Rad) using a Mini

Trans-Blot Electrophoretic Transfer Cell (Bio-Rad) for 1 hour, chilled with an ice block, and set at 100 V. The membrane was washed three times with deionized water, and then blocked in TBS-3% (w/v) gelatin for 30 minutes at room temperature. Following blocking, the membrane was washed in TBS-0.05% (v/v) Tween (TBST). The membrane was then exposed to the primary antibody (rabbit-anti-AzoC) at a 1:1000 dilution in TBST-1% (w/v) gelatin for 1 hour at room temperature. Following primary antibody exposure, the membrane was washed twice with TBST. The membrane was exposed to a 1:300 dilution (in TBST-1% (w/v) gelatin) of horse radish peroxidase (HRP) conjugated with goat anti-rabbit IgG (H+L) secondary antibody (Bio-Rad) for 1 hour. Following secondary antibody treatment, the membrane was washed twice in TBST and once in TBS. To develop the Western blot, the membrane was exposed to 4-CN solution as per the manufacturer's instructions (Bio-Rad). The membranes were imaged using an Alpha Innotech Imager and corresponding software was used for image viewing. Due to the colorimetric reaction that occurs in the Western blot procedure, the Western blot results are qualitative only (detect the presence, not quantity of AzoC) (Levine *et al*, 2000; Patton, 2002; Westermeier & Marouga, 2005).

Protein Extraction from C. perfringens

C. perfringens (Wild Type strain ATCC 3626 and the *ΔazoC* knockout mutant) cultures in 5 mL anaerobic BHI broth were prepared and incubated overnight at 37°C. Overnight cultures were transferred to a total of 500 mL anaerobic BHI media and grown statically at 37°C until an OD₆₀₀ of 0.6 was reached. Optical density measurements were taken with a Shimadzu UV-1650PC spectrophotometer with a 1 cm path length. Cells were pelleted by centrifugation (6000 x g, 10 minutes, 4°C). The cell pellets were resuspended in 10 mL of TRIS buffer and prepared for lysis, in order to extract proteins. Lysozyme (0.1 mg/mL final concentration) was added and cells were incubated on ice for 30 minutes. Cells were then disrupted by sonication (performed 10 times, 5 seconds each, icing in between, at 60 Hz). The sonicated cells were pelleted by

centrifugation (10,000 x g, 30 minutes, 4°C). Supernatants were saved as the proteinaceous fraction.

Non-Dividing Cells Exposed to Azo Dyes

Azo dye exposure studies using non-dividing *C. perfringens* cells were performed and designed as previously described (Vazquez-Laslop *et al*, 2001). All compounds shown in Figure 32 were tested with *C. perfringens* strain ATCC 3626. Cultures of *C. perfringens* in 5 mL anaerobic BHI broth were prepared and incubated overnight at 37°C. These cultures were then transferred to a total of 500 mL anaerobic BHI and grown until an OD₆₀₀ of 0.6 was reached. Optical density measurements were taken with a Shimadzu UV-1650PC spectrophotometer with a 1 cm path length. Cells from the 500 mL culture were pelleted by centrifugation (6000 x g, 10 minutes, 4°C). The cell pellets were exposed to the dyes by resuspending the cell pellets in 10 mL of TRIS buffer (10 mM TRIS, pH 7.5) containing the appropriate azo dye or sodium benzene sulfonate (20 µM final concentration), and incubated for 10 minutes on ice. For time and concentration-dependence studies, exposure time points of 1 and 100 minutes and variant azo dye concentrations of 2 µM and 200 µM were also prepared and tested in the same manner. Tris buffer (10 mM TRIS, pH 7.5) without azo dye served as a no-dye-exposed control. Following the first exposure, cells were pelleted by centrifugation (6000 x g, 10 minutes, 4°C). The resultant extracellular supernatant was saved and analyzed for proteins. As a wash, the cell pellet was resuspended again in 10 mL of TRIS buffer (10 mM TRIS, pH7.5), incubated on ice for 10 minutes, and pelleted as before. The cell pellets were resuspended in 10 mL of TRIS buffer (10 mM TRIS, pH 7.5) and prepared for lysis, in order to extract the intracellular proteins. Lysozyme (0.1 mg/mL final concentration) was added and cells were incubated on ice for 30 minutes. Cells were then lysed by sonication (performed 10 times, 5 seconds each, icing in between, at 60 Hz). The sonicated cells were pelleted by centrifugation (10,000 x g, 30 minutes, 4°C). Supernatants were saved as the intracellular fractions.

Dividing Cells Exposed to Azo Dyes

To compare and understand any differences in protein release by dividing and non-dividing cells, actively growing cultures (dividing cells) were also tested for their response to azo dye exposure. Overnight *C. perfringens* cultures were inoculated into anaerobic BHI and grown until an OD₆₀₀ of 0.4 was reached (early log phase). The early-log phase culture (1 mL) was transferred to 10 mL anaerobic BHI containing 20 µM of the appropriate azo dye (Figure 32) or an equal volume of deionized water as a control and incubated. After 2.5 hours of incubation, mid-log phase (OD₆₀₀ of 0.6) cells were pelleted by centrifugation (6,000 x g, 10 minutes, 4°C). At this phase of growth (mid-log phase), a significant dye reduction was observed, and the resultant supernatant was saved as the extracellular fraction. Intracellular fractions were obtained by cell lysis as previously mentioned.

Periplasmic Fraction

In an effort to pinpoint the location of the azoreductase, the Gram-positive periplasmic region was isolated (Stal & Blaschek, 1985). This fraction was compared to the extracellular and intracellular fractions. To begin, *C. perfringens* cultures were grown anaerobically in modified Fluid Thioglycollate media (mFTM) (Stal & Blaschek, 1985). Following overnight growth, mFTM media with 0.4% (w/v) glycine was inoculated and incubated (500 mL culture) (Stal & Blaschek, 1985). Once cultures reached an OD₆₀₀ of 0.6, they were centrifuged (11,000 x g, 10 minutes, 4°C). Cell pellets were resuspended in 10 mL of TRIS buffer (10 mM TRIS, pH 7.5), with or without Direct Blue 15 azo dye (20 µM final concentration). To obtain the Gram-positive periplasmic fraction, the cell pellets were resuspended in a 10 mL anaerobic osmotically stable solution (50 mM TRIS, 0.5 M sucrose, 25 mM calcium chloride, 25 mM magnesium chloride, in mFTM) with 1 mg/mL lysozyme. Cells were incubated to allow them to form protoplasts. Following incubation and protoplast formation, cells were centrifuged (4,500 x g, 10 minutes,

25°C); at this point, the cell pellet and supernatant were separated. The supernatant, which contained cell wall debris, as well as the periplasmic region, was isolated and centrifuged further (10,000 x g, 30 minutes, 4°C) to remove cell wall debris and to isolate proteins from the Gram-positive periplasmic region. This supernatant was retained as the periplasmic fraction. For intracellular fractions, the previously formed protoplast cell pellet was resuspended in TRIS buffer (10 mM TRIS, pH 7.5) and sonicated 10 times, consisting of 5 seconds pulses each time, icing in between pulses and the setting at 60 Hz. The sonicated cells were pelleted by centrifugation (10,000 x g, 30 minutes, 4°C). The supernatant was saved as the intracellular fraction.

Azoreductase Enzyme Activity

Enzymatic activity was tested on all fractions (extracellular, periplasmic and intracellular). Proteins were concentrated to approximately 1 mg/mL using ammonium sulfate precipitation. Briefly, ammonium sulfate was mixed with supernatant to a final ammonium sulfate concentration of 80% (w/v) and mixed at room temperature for 15 minutes with vigorous stirring. Following precipitation, the solution was centrifuged (10,000 x g, 15 minutes, 4°C). The supernatant was discarded and pellet (precipitated protein) was resuspended in 1 mL of TRIS buffer (10 mM TRIS, pH 7.5).

Azoreductase enzyme activity was tested in a 1.5 mL polystyrene cuvette (Sigma-Aldrich), 50 µL of concentrated protein was added to the reaction mixture (final concentration 25 mM sodium phosphate, pH 7.0, and 20 µM of the appropriate azo dye). Deionized water was added to a final volume of 1 mL. To create an anaerobic environment, the reaction mixture was bubbled with nitrogen at a rate of 1 nitrogen bubble per second for 10 minutes. Immediately after bubbling, mineral oil was added to the cuvette/mixture to maintain an anaerobic environment for the duration of the experiment. To activate the reaction, a mixture of 10 mM NADH (Acros

Organics) and 2 mM FAD (Sigma-Aldrich) was added by penetrating the mineral oil layer as to limit the amount of introduced oxygen. This reaction was scanned at room temperature using a Shimadzu UV-1650PC spectrophotometer (1 cm pathlength) at a wavelength that was previously determined to be optimal for each azo dye: Direct Blue 15 (602.5 nm), Methyl Red (430.0 nm), Methyl Orange (425.0 nm), Ponceau BS (505.0 nm). Dye absorbance was followed over a period of 30 minutes. The concentration of the dye was determined from a standard curve of known dye concentrations vs absorbance based on the Beer-Lambert law. Each experiment was performed in triplicate.

Cell Lysis/Leakage Assays

To understand whether the observed protein release was the result of cellular lysis or membrane leakage, cell viability experiments were completed. First, to determine whether cells were lysing, as opposed to actively releasing protein, a lactate dehydrogenase (LDH) assay was performed. *C. perfringens* is known to produce LDH, an intracellular enzyme and a common predictor of cell lysis (Korzeniewski & Callewaert, 1983; Shimizu *et al*, 2002a). A Pierce LDH Cytotoxicity Assay Kit (Thermo Scientific) was utilized for this experiment. Collected concentrated fractions (extracellular, periplasmic, intracellular) following azo dye and control exposure were tested for LDH activity according to the manufacturer's instructions. A standard curve was generated by plotting known LDH concentrations against their absorbance values (A_{490}) to generate an equation of a line from which experimental LDH concentrations could be extrapolated. Experiments were performed in triplicate.

Second, to determine whether the *C. perfringens* cell membranes were leaking to release protein, a cell membrane viability assay was performed. The Trypan Blue method for cell viability testing is a tried and true method which can identify viable cells over non-viable cells with a leaky cell membrane (Strober, 2001; Tennant, 1964). By this method, cells with an intact

cell membrane exclude the large polar dye, whereas cells with a damaged or leaky cell membrane are stained blue (Strober, 2001; Tennant, 1964). *C. perfringens* cells following exposure to all azo dyes, sodium benzene sulfonate, or buffer (as a control) were resuspended in TRIS buffer (10 mM TRIS, pH 7.5). Cell suspensions were mixed (1:1 dilution) with 0.4% (w/v) Trypan Blue solution and dilutions were prepared to ensure countability (between 15 and 50 cells per 1 mm² grid). A hemocytometer was loaded and grids were visualized by Phase Contrast microscopy. The number of viable (unstained) and non-viable (blue) cells were counted, and the percent cell viability was calculated for four replicates.

To ensure that the *C. perfringens* cells were not forming endospores to interfere with the cell viability assays, endospore stains were performed on all cell samples. Endospore staining was performed as previously described (Schaeffer & Fulton, 1933).

Results

azoC Gene Inactivation: Creation of a Δ azoC Knockout Mutant

PCR analysis using the *azoC*-F and *azoC*-R primers confirmed the presence of the targetron in the middle of the *azoC* gene in *C. perfringens* knockout cells, as compared to the *azoC* gene in the Wild Type (Figure 33A). Sequencing of this ~1500 bp band confirmed that the intron was inserted at the correct location in the *azoC* gene.

To further confirm the absence of the AzoC protein in the *C. perfringens* Δ azoC knockout mutant, Western blot analysis was performed. As shown in Figure 33B, no production of AzoC was detected from the Δ azoC knockout mutant (Figure 33B, Lane 1), as compared to the Wild Type (Figure 33B, Lane 2) and AzoC pure protein positive control (Figure 33B, Lane 3). These results confirm the presence of a successful knockout of the *azoC* gene in *C. perfringens* strain ATCC 3626.

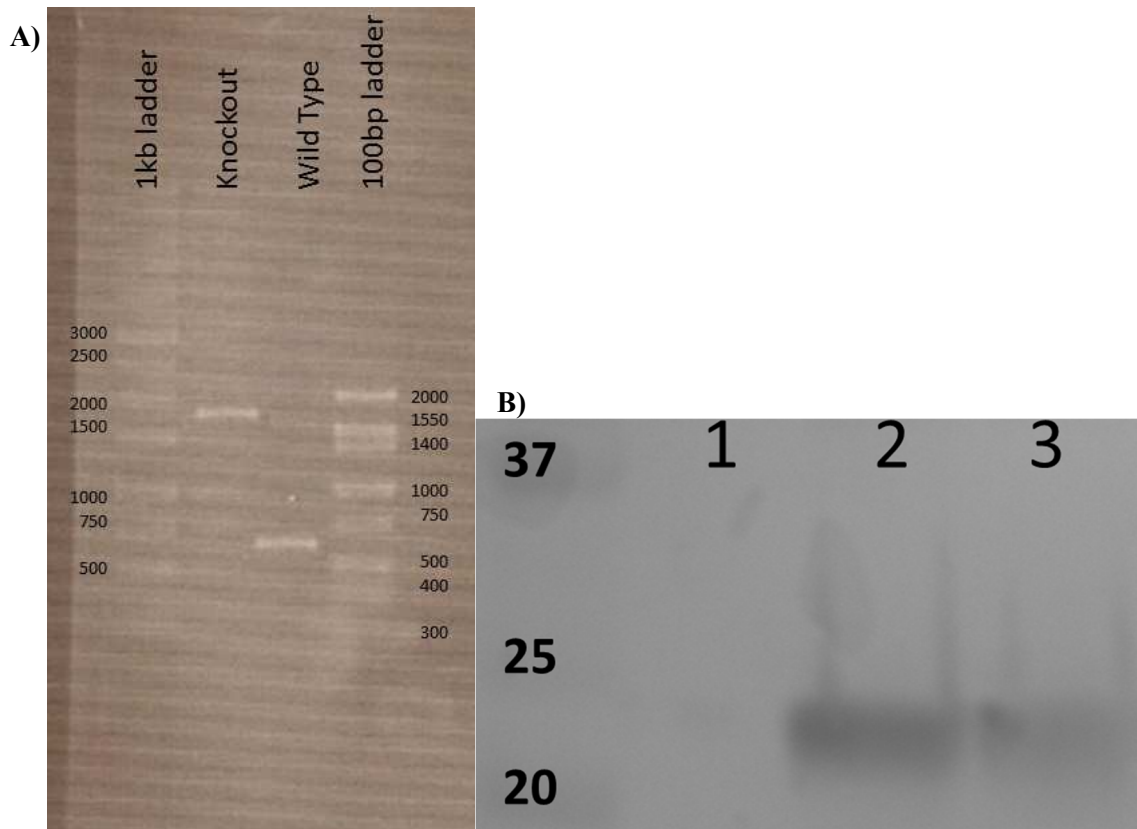
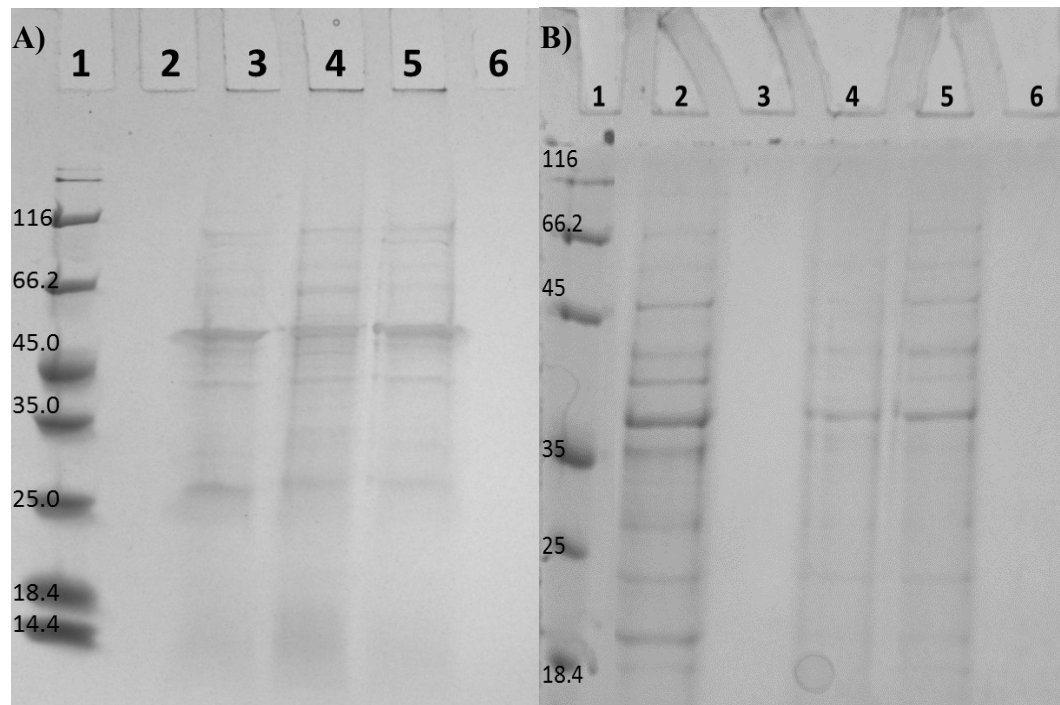


Figure 33. Confirmation of Δ azoC Knockout. **A)** Gel Electrophoresis following *azoC*-specific PCR for *C. perfringens* Wild Type strain and *C. perfringens* Δ azoC knockout mutant. Results are shown as compared to a 1 Kb ladder (Promega) and 100 bp ladder (Fermentas GeneRuler). **B)** Western blotting of protein from *C. perfringens* Δ azoC mutant and *C. perfringens* Wild Type, as compared to a Protein Molecular Weight Marker; Lane 1 – *C. perfringens* Δ azoC knockout mutant; Lane 2 – *C. perfringens* Wild Type; Lane 3 – Pure AzoC positive control. Western blot was probed with an anti-AzoC antibody. Due to the colorimetric reaction used in the Western blot procedure, this procedure is qualitative only (looking for the presence of AzoC) (Levine *et al.*, 2000; Patton, 2002; Westermeier & Marouga, 2005). Therefore, these Western Blots are only capable of looking for the presence of AzoC, not quantifying the enzyme.

Exposure to Azo Dyes Causes Protein Release

All results shown are from experiments with non-dividing cells, because the results from dividing and non-dividing cells were consistent. The exposure of certain azo dyes to *C. perfringens* caused a range of proteins (14 - 115 kDa) to be released (Figure 34A). Interestingly, the azo dyes that caused protein release (Direct Blue 15, Ponceau BS, and Methyl Orange) produced similar protein profiles in their extracellular fractions, whereas the control (buffer, no dye-exposure – Lane 2) and Methyl Red (Lane 6) exposure did not produce protein release



C) Sample	LDH Concentration (mU/mL)		Cell Viability (%)	Endospore Formation
	Intracellular	Extracellular		
Control (No dye)	474 ± 10.8	1.5 ± 1.9	93 ± 3	-
Direct Blue 15	471 ± 16.5	1.0 ± 1.1	94 ± 4	-
Ponceau BS	465 ± 16.4	1.3 ± 1.5	95 ± 4	-
Methyl Orange	466 ± 17.2	0.8 ± 1.2	93 ± 4	-
Methyl Red	479 ± 18.0	0.6 ± 1.1	92 ± 4	-
Sodium Benzene Sulfonate	472 ± 13.5	1.0 ± 1.5	95 ± 3	-

Figure 34. Protein Release Due to Azo Dye Exposure. **A)** SDS-PAGE protein profiles of extracellular supernatant non-dividing azo dye-exposed *C. perfringens* Wild Type cells. Lane 1 - Protein Molecular Weight Marker; Lane 2 - Control (buffer-exposed) extracellular supernatant; Lane 3 – Direct Blue 15-exposed extracellular supernatant; Lane 4 – Ponceau BS-exposed extracellular supernatant; Lane 5 – Methyl Orange-exposed extracellular supernatant; Lane 6 – Methyl Red-exposed extracellular supernatant. 20 µg of concentrated protein is shown loaded onto each lane on the gel. **B)** SDS-PAGE protein profiles of extracellular supernatant non-dividing azo dye-exposed *C. perfringens* *AzoC* knockout mutant cells. Lane 1 - Protein Molecular Weight Marker; Lane 2 - Direct Blue 15-exposed extracellular supernatant; Lane 3 – Control (buffer-exposed) extracellular supernatant; Lane 4 – Ponceau BS-exposed extracellular supernatant; Lane 5 – Methyl Orange-exposed extracellular supernatant; Lane 6 – Methyl Red-exposed extracellular supernatant. 20 µg of concentrated protein is shown loaded onto each lane on the gel **C)** Assays for Total Cell Lysis (Lactate Dehydrogenase, or LDH) and Cell Membrane Viability (Trypan Blue Assay). For LDH activity from concentrated samples (resulting from the extracellular matrix, or intracellular components), a standard curve with known LDH concentrations was used to generate an equation of a line with which experimental LDH concentrations were extrapolated. LDH activity is provided as mean ± standard deviation across triplicates (n=3) for both intracellular and extracellular samples. For the Trypan Blue assay, percentage of cell viability was calculated by dividing the number of viable cells by the total cell number. Percentage of cell viability is provided as the mean ± standard deviation across four replicate samples (n=4). For the endospore results, a “-” presents the absence of endospores, whereas a “+” would represent the presence of endospores.

profiles, as seen in the SDS-PAGE gel (Figure 34A). This suggests that these specific azo dyes caused *C. perfringens* to release proteins into the extracellular matrix. Exposure to azo dyes also showed that sulfonated azo dyes are critical for this protein release phenomenon. Direct Blue 15, Ponceau BS and Methyl Orange are all sulfonated azo dyes whereas Methyl Red, the only non-sulfonated azo dye tested, did not cause protein release (Figure 34A). The *C. perfringens* Δ azoC mutant also showed a similar protein release profile, thus demonstrating that the presence of the AzoC protein is not critical for the observed protein release seen here (Figure 34B).

Results indicate that the observed protein release following exposure to azo dyes (Figures 34A and 34B) is not caused from cell lysis due to the high viability of cells following azo dye exposure (>92%; Figure 34C). All extracellular samples were found to be negative for LDH activity (p-value >0.05, 95% confidence) and all intracellular samples were found to be positive for LDH activity (p-value >0.05, 95% confidence) (Figure 34C). Since LDH is a known intracellular enzyme in *C. perfringens*, these results demonstrate that the observed protein release profiles were caused by the azo dyes and are not the result of cell lysis (Korzeniewski & Callewaert, 1983; Shimizu *et al*, 2002a). Protein release was also not due to cell membrane leakage, as the percentage of viable cells in the azo dye-exposed samples was not statistically different than the percentage of viable cells in the non-dye-exposed control (p-value >0.05, 95% confidence) (Figure 34C). Additionally, the cells were not forming endospores (Figure 34C).

AzoC is Released Upon Azo Dye Exposure

The release of AzoC was demonstrated by testing the intracellular, periplasmic, and extracellular fractions of non-dividing cells exposed to Direct Blue 15 (Figure 35). AzoC has previously been shown to be specific for Direct Blue 15 (see Chapter 2) (Morrison *et al*, 2014; Morrison & John, 2013; Morrison *et al*, 2012). The specific detection of AzoC was confirmed by Western blot using anti-AzoC antibodies (Figure 35). Results suggest that AzoC is

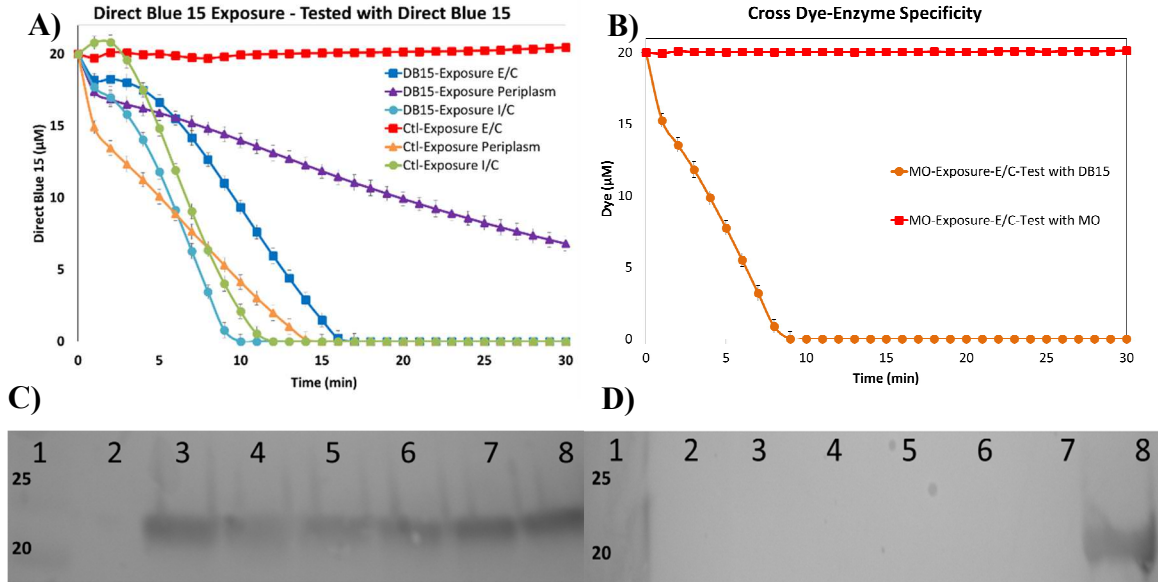


Figure 35. Azo-Dye-Induced AzoC Release in Extracellular, Intracellular and Periplasmic Fractions. **A)** Enzymatic assay of Wild Type *C. perfringens* released proteins following Direct Blue 15 exposure, tested for activity against Direct Blue 15. “DB15” represents the Direct Blue 15 exposed *C. perfringens* cells. “Ctl” represents the control (buffer, no azo dye exposure) condition. “E/C” represents the proteins released extracellularly following dye exposure and “I/C” represents intracellular proteins remaining inside the cell following exposure. Direct blue 15 dye reduction is plotted as mean \pm standard deviation (error bars) across triplicate samples (n=3) **B)** Enzymatic assay of Wild Type *C. perfringens* secreted proteins following Methyl Orange exposure, tested for activity against either Methyl Orange or Direct Blue 15. “MO” represents Methyl Orange exposed *C. perfringens* cells, as well as Methyl Orange enzymatic assay. “DB15” represents Direct Blue 15 enzymatic assay. “E/C” represents the proteins secreted extracellularly following dye exposure. Dye reduction is plotted as mean \pm standard deviation (error bars) across triplicate samples (n=3). **C)** Western blot of Wild Type *C. perfringens* released proteins following Direct Blue 15 exposure, probed with an anti-AzoC antibody, **D)** Western blotting of *C. perfringens* Δ azoC mutant released proteins following Direct Blue 15 exposure, probed with an anti-AzoC antibody. For both **C)** and **D)**, Lane 1 - Protein Molecular Weight Marker; Lane 2 - Control (buffer-exposed) extracellular supernatant; Lane 3 - Control (buffer-exposed) periplasmic component; Lane 4 - Control (buffer-exposed) intracellular fraction; Lane 5 - Direct Blue 15-exposed extracellular supernatant; Lane 6 - Direct Blue 15-exposed periplasmic component; Lane 7 - Direct Blue 15-exposed intracellular fraction; Lane 8 - Pure AzoC positive control. Note: Because of the colorimetric reaction that occurs between the secondary antibody (goat anti-rabbit IgG) that is conjugated to horse radish peroxidase and the alkaline phosphatase substrate solution, the Western Blots seen here are strictly qualitative, not quantitative (Levine *et al*, 2000; Patton, 2002; Westermeier & Marouga, 2005). Therefore, these Western Blots are only capable of looking for the presence of AzoC, not quantifying the enzyme.

physiologically translocated from the cytoplasm to the periplasm regardless of azo dye exposure (Figures 35A and 35C). All periplasmic fractions (regardless of exposure condition) showed the presence of AzoC in the periplasmic region both via enzyme activity studies against Direct Blue 15 (Figure 35A) and Western blotting (Figure 35C). The activity in the periplasmic fraction following control exposure was significantly higher than in the Direct Blue 15-exposed cells (p-value <0.001, 95% confidence). Extracellular release of AzoC does not occur until cells are exposed to sulfonated azo dyes, which is supported by subsequent enzyme activity against Direct Blue 15 and a positive reaction for AzoC on the Western blot (Figures 35A and 35C). The control (no dye exposure) does not show enzymatic activity against Direct Blue 15 or extracellular AzoC on the Western blot (Figures 35A and 35C). The activity in the extracellular fraction following Direct Blue 15-exposure was significantly higher than in the control-exposed cells (p-value <0.001, 95% confidence). A Western blot comparison of Wild type and Δ azoC mutant *C. perfringens* for the three fractions confirmed AzoC was not expressed in the Δ azoC mutant (Figures 35C and 35D). The activity in the intracellular fractions following either Direct Blue 15 or control exposure were not significantly different (p-value >0.05, 95% confidence).

To determine whether exposure to specific azo dyes induced the release of an azoreductase specific for that azo dye, fractions that were generated following exposure to one azo dye were tested for enzymatic activity against another azo dye (Figure 35B). When non-dividing *C. perfringens* cells were exposed to Methyl Orange, only intracellular fractions were able to reduce Methyl Orange (Figure 35B). It is hypothesized that exposure to Methyl Orange did not cause the release of Methyl Orange-specific azoreductase. However, the same Methyl Orange exposed extracellular fraction was able to reduce Direct Blue 15 (Figure 35B). Thus, a type of cross dye-enzyme event was observed in which the azo dye exposure from which proteins are released does not mean that the released proteins can reduce that specific azo dye.

AzoC Secretion is Sulfonation-Specific

As the mechanism of AzoC release was more closely examined, it appears as though sulfonation of the exposure compound was critical. Direct Blue 15, Ponceau BS, Methyl Orange, all sulfonated azo dyes, as well as sodium benzene sulfonate, a sulfonated non-azo dye, caused AzoC to be released (Figures 36A). However, Methyl Red, a non-sulfonated azo dye, as well as

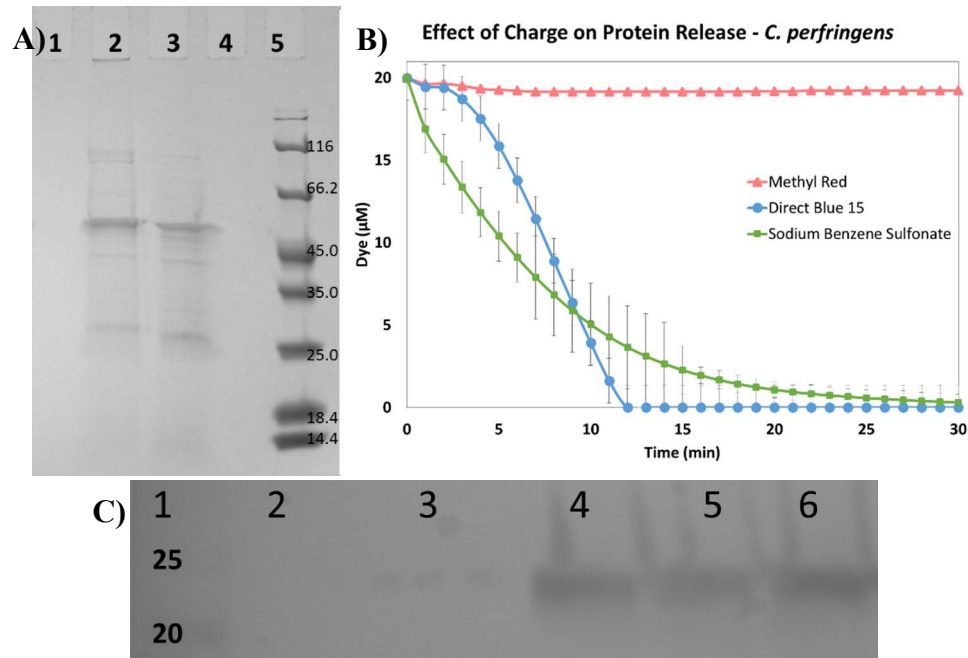


Figure 36. Sulfonated Compound-Induced Release of Proteins. **A)** SDS-PAGE protein profiles of extracellular supernatant from non-dividing azo dye-exposed *C. perfringens* Wild Type cells. Lane 1 - Methyl Red-exposed extracellular supernatant; Lane 2 - Direct Blue 15-exposed extracellular supernatant; Lane 3 - Sodium Benzene Sulfonate-exposed extracellular supernatant; Lane 4 - Control (buffer-exposed) extracellular supernatant; Lane 5 - Protein Molecular Weight Marker. 20 µg of concentrated protein is shown loaded onto each lane on the gel. **B)** Enzymatic assay of *C. perfringens* released proteins following sulfonated compound exposure. Proteinaceous extracellular supernatants following sulfonated compound (Direct Blue 15 and Sodium Benzene Sulfonate) exposure were tested for activity against Direct Blue 15 (y-axis, µM Dye remaining), proteinaceous extracellular supernatant following non-sulfonated compound (Methyl Red) exposure was tested for activity against Methyl Red (y-axis, µM Dye remaining). Dye reduction is plotted as mean ± standard deviation (error bars) across triplicate samples (n=3). **C)** Western blot of Wild Type *C. perfringens* released proteins following sulfonated compound exposure, probed with an anti-AzoC antibody. Lane 1 - Protein Molecular Weight Marker; Lane 2 - Control (buffer-exposed) extracellular supernatant; Lane 3 - Methyl Red-exposed extracellular supernatant; Lane 4 - Direct Blue 15-exposed extracellular supernatant; Lane 5 - Sodium Benzene Sulfonate-exposed extracellular supernatant; Lane 6 - AzoC positive control. Note: Because of the colorimetric reaction that occurs between the secondary antibody (goat anti-rabbit (IgG)) that is conjugated to horse radish peroxidase and the alkaline phosphatase substrate solution, the Western Blots seen here are strictly qualitative, not quantitative (Levine *et al.*, 2000; Patton, 2002; Westermeier & Marouga, 2005). Therefore, these Western Blots are only capable of looking for the presence of AzoC, not quantifying the enzyme.

the control buffer (no dye exposure), did not cause proteins to be released (Figures 36A). Likewise, the extracellular supernatant following Methyl Red exposure is not able to reduce Methyl Red (Figure 36B). However, the extracellular supernatant following sodium benzene sulfonate exposure reduces Direct Blue 15 to the same degree that the extracellular supernatant following Direct Blue 15 exposure does (p-value >0.05, 95% confidence) (Figure 36B). The presence of AzoC in all three sulfonated exposures was confirmed by a positive reaction for AzoC on the Western blot (Figure 36C). This suggested that sulfonation is key to protein release, with AzoC being one of the proteins that is released. Similar protein release was seen with the *C. perfringens* Δ azoC mutant, however, AzoC was absent (from Western Blots).

AzoC Release is Both Dye Concentration-Dependent and Time-Dependent

Results from the time- and concentration-dependence experiments showed a positive correlation between azo dye concentration and the percentage of dye reduction. Increased concentrations of Direct Blue 15 increased the percent azo dye reduction, until 100% azo dye reduction occurred (Figure 37). Specifically, at a 5 minute azo dye exposure, the increasing azo dye concentration showed an increase in the amount of dye reduced (Figure 37). A clear time dependence can also be observed for the concentrations tested until dye reduction reached steady state (Figure 37).

Additional Azoreductases are Present in C. perfringens

A comparison between Wild type and Δ azoC mutant *C. perfringens* in terms of their intracellular and extracellular fractions provided evidence for additional azoreductases (Figure 38). Specifically, exposure of the *C. perfringens* Δ azoC mutant to Direct Blue 15 produced an azoreductase reaction against Direct Blue 15 in the intracellular fraction. The presence of Direct Blue 15 reduction in the absence of AzoC, although significantly lower activity than in the same Wild type *C. perfringens* fractions (p-value <0.05, 95% confidence), suggested the presence of

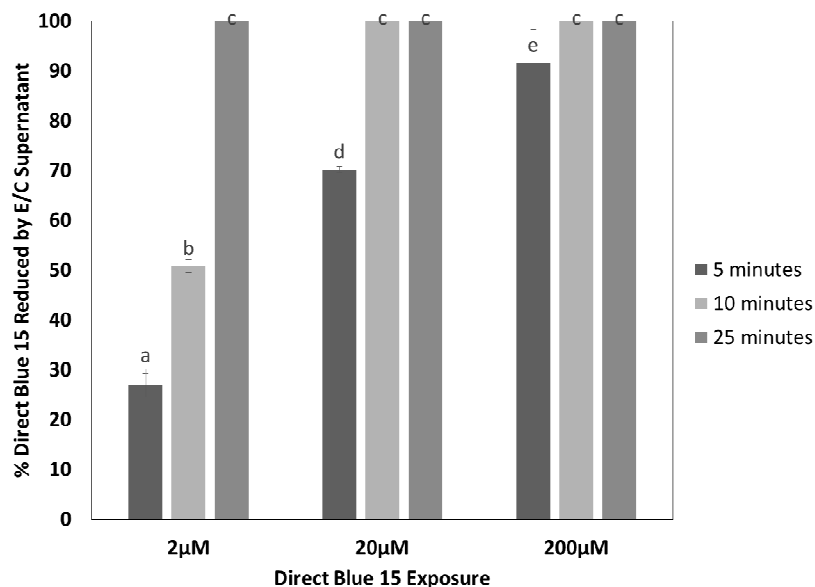


Figure 37. Concentration dependence of protein release in *C. perfringens*. Enzyme assay of three different concentrations of Direct Blue 15 at three different time points. The extracellular (“E/C”) supernatant from different dye concentration exposures and exposure time points were tested. Direct Blue 15 reduction was measured and the result is presented as percentage of Direct Blue 15 reduced. The percentage of Direct Blue 15 dye reduction is plotted as mean \pm standard deviation (error bars) across triplicate samples (n=3) for three concentrations. Letters represent comparisons of the different conditions; two means with the same letter are not significantly different at a 95% confidence level (p-value >0.05).

additional azoreductases in the *C. perfringens* intracellular fraction that were capable of Direct Blue 15 reduction (Figure 38A and Figure 38B). Additional evidence was seen while using Methyl Red, which is readily reduced when grown in *C. perfringens* cultures. Both Wild type and Δ azoC mutant *C. perfringens* intracellular fractions showed high activity against Methyl Red, while the extracellular fractions did not have the ability to reduce Methyl Red (Figure 38C and Figure 38D). This suggested that the *C. perfringens* Δ azoC mutant harbored active azoreductases specific for Methyl Red intracellularly, thereby support the presence of additional azoreductases in the cytoplasm of *C. perfringens*. Similar results were seen with intracellular fractions from Methyl Orange-exposed *C. perfringens* Δ azoC mutant (Figures 38E and 38F). These additional azoreductases are predicted to be cytoplasmic only, as the Gram-positive periplasmic region showed no significant azoreductase activity in both the control and Direct Blue 15 exposed *C. perfringens* Δ azoC mutant (p-value >0.05, 95% confidence) (Figures 38E and 38F).

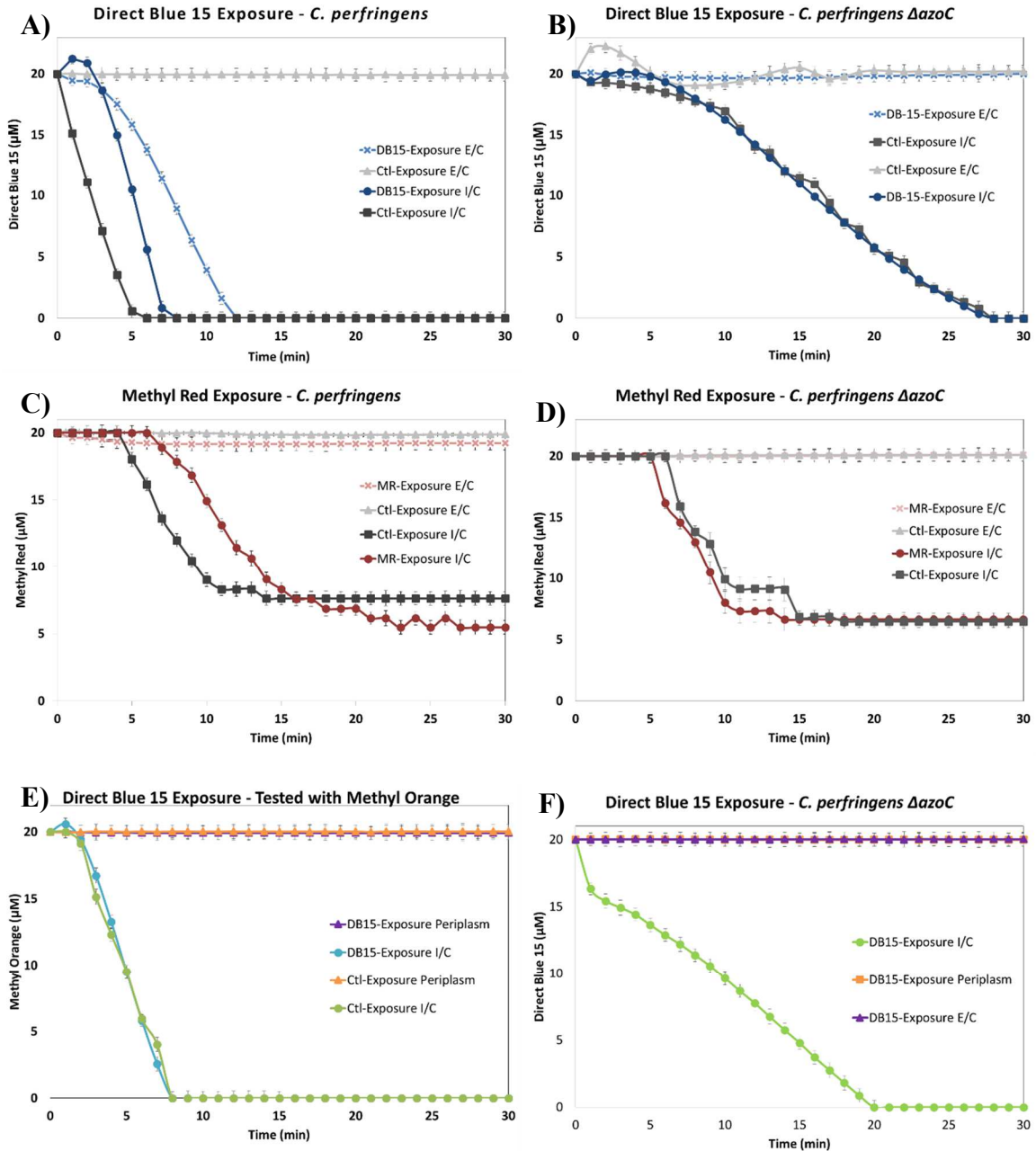


Figure 38. Wild Type and *C. perfringens* Δ azoC Enzyme Assays of Azo Dye-Induced Released Proteins. **A)** Wild Type *C. perfringens* proteins released (extracellular and intracellular fractions) following Direct Blue 15 exposure, **B)** *C. perfringens* Δ azoC proteins released following Direct Blue 15 exposure, **C)** Wild Type *C. perfringens* proteins released following Methyl Red exposure, **D)** *C. perfringens* Δ azoC proteins released following Methyl Red exposure, **E)** Enzymatic Activity of Wild Type *C. perfringens* proteins released following Direct Blue 15 exposure, tested for activity against Methyl Orange, **F)** Enzymatic Activity of *C. perfringens* Δ azoC proteins released following Direct Blue 15 exposure. For all enzyme activity figures (A-F), “DB15” or “MR” represents the Direct Blue 15 and Methyl Red exposed *C. perfringens* cells, respectively. “Ctl” represents the control (buffer, no azo dye exposure) condition. “E/C” represents extracellular proteins following exposure and “I/C” represents intracellular proteins following exposure. Dye reduction is plotted as mean \pm standard deviation (error bars) across triplicate samples (n=3).

Discussion

A successful gene knockout of the *azoC* gene has been completed, as shown by the Western blot in Figure 33B. AzoC is no longer a functioning enzyme in the *C. perfringens* Δ azoC cells. Previous gene knockouts in *C. perfringens* have shown the introduction of an intron into a gene of interest via the Targetron kit (as utilized here) are very stable and do not show any revertants back to the original genotype, due to the genetic change occurring in the genome of the bacteria (Chen *et al*, 2007; Chen *et al*, 2005b; Gupta & Chen, 2008; Heap *et al*, 2010a; Heap *et al*, 2010b; Heap *et al*, 2007; Li & McClane, 2008; Li & McClane, 2010).

Commensal *C. perfringens* in the intestine can be exposed to a number of environmental conditions (i.e. azo dyes), which can affect the permeability of the cell envelope, leading to the secretion of proteins. A full understanding of which environmental conditions control protein release is important for understanding how *C. perfringens* functions physiologically within our bodies. To help achieve this, a study of the effect of azo dyes on *C. perfringens*, with a particular focus on protein release, was conducted.

The current study has demonstrated that the charged groups on sulfonated azo dyes cause the release of AzoC and other proteins from the periplasmic/cell wall region to the exterior of *C. perfringens*. This phenomenon was shown to be sulfonation-specific (Figure 36); however, release is not reliant on the negative charge alone. For example, Methyl Red, typically thought of as a non-polar azo dye (pKa 4.8), is likely to have its hydroxyl groups negatively charged at the pH tested in this study (pH = 7.5) (Yamanaka *et al*, 1987). The sulfonated compounds tested (Direct Blue 15, Ponceau BS, Methyl Orange and sodium benzene sulfonate) have pKa's that also suggest that, at the pH tested, they would all have negatively charged sulfonated groups as well (ChemAxon, 2014; Oakes & Gratton, 1998). However, only the sulfonated negative charges caused protein release. Also, protein release was not limited to azo dyes, as the non-azo

dye/sulfonated compound sodium benzene sulfonate, was able to cause similar protein release (Figure 36). This suggests that the presence of a charged sulfonated group drives protein release rather than the actual azo bond. In addition, this phenomenon is not caused by either cell lysis or cell wall leakage (Figure 34C).

The charged nature of the sulfonated groups in the azo dyes and sodium benzene sulfonate as well as the charged nature of AzoC supports a possible ionic interaction with cell wall structures. This ionic interaction may result in neutralizing of the cell wall region, which could prevent proteins from ionic interaction with the now-neutral cell wall region, which would cause the release of proteins like as AzoC. Assuming that the sulfonation-mediated AzoC release decreases the amount of constitutive AzoC present in the cytoplasm, then it would be expected that less enzyme activity would be observed in the intracellular fractions of the azo dye exposed cells. Our results are consistent with this hypothesis where in the Direct Blue 15-exposed intracellular fractions, Direct Blue 15 was fully reduced at approximately 7.5 minutes. In the non-dye exposed control, the same reduction occurs in only 5 minutes (Figure 38A). Because faster azoreductase activity directly related to amount of azoreductase present, it can be understood that the intracellular fractions of the control cells contain significantly more azoreductase than the intracellular fractions of the cells that have been exposed to Direct Blue 15 (Morrison *et al*, 2012).

Dye interaction with the cell wall was demonstrated by showing a relationship between increasing azo dye concentration and azoreductase activity in the extracellular fractions. Exposure to increasing concentrations of Direct Blue 15 correlated with an increasing percentage of azo dye reduced, thereby supporting an azo dye concentration dependence for AzoC release into the extracellular fraction (Figure 37). Interestingly, at 200 μM Direct Blue 15 exposure concentration, the dye was reduced 100% for all exposure time points, suggesting the cell wall ionic interacting binding sites were fully saturated with dye, thereby maximizing the amount of

protein that was released. An interesting observation supporting a steady-state phenomenon based on a simple diffusion process for the proteins was seen. Intracellular and extracellular enzyme activities for dye-exposed cells were always equivalent which suggested that AzoC diffuses out of the cytoplasm until it reached equilibrium with the extracellular.

There appears to be no correlation between a specific azo dye exposure and a specific azoreductase released. Methyl Orange exposure caused proteins to be released, but the released proteins were not specific for azoreductase against Methyl Orange (Figure 35B). Rather, these proteins were specific for azoreduction against Direct Blue 15 (Figure 35B). On the other hand, Direct Blue 15-exposed cells caused proteins to be released that were specific for Direct Blue 15 (Figures 38A and 38E) (Morrison & John, 2013; Morrison *et al*, 2012).

The presence of additional azoreductase(s) in *C. perfringens* has been demonstrated. First, the presence of intracellular Direct Blue 15-specific azoreductase activity in the *C. perfringens* Δ azoC mutant (in the absence of AzoC) strongly suggests that there are additional intracellular azoreductase(s) present in *C. perfringens* that are also specific for Direct Blue 15 (Figure 38B). Second, using the *C. perfringens* Δ azoC mutant, Methyl Red is not reduced by extracellular proteins but is reduced by intracellular proteins in the wild type and *C. perfringens* Δ azoC mutant (Figure 38D). Third, the presence of proteins in the intracellular *C. perfringens* Δ azoC mutant that was specific for Methyl Orange suggests the presence of additional azoreductases (Figure 38E). These additional azoreductases appear to remain in the intracellular region and do not travel to the periplasm like AzoC (Figures 38E and 38F). Further, we have searched the available contigs of the *C. perfringens* strain ATCC 3626 genome, and have identified three additional putative azoreductases based on their sequence similarity to either AzoC, AzoM (*Enterococcus faecium*) or AzoR (*Escherichia coli*).

AzoC appears to localize to the Gram-positive periplasmic region as seen in the Western blot using an anti-AzoC antibody (Figure 35C). It is likely that surface proteins attached through ionic interaction to the peptidoglycan and/or wall- or lipo-teichoic acids make-up the periplasmic space thereby enabling AzoC to localize to this region. This observation begs the question as to how AzoC translocates across the cytoplasmic membrane. It was observed that AzoC localizes to the periplasmic region both in the presence and absence of azo dye exposure (Figure 35C) suggesting that translocation is a normal physiological event and not dependent on the presence of the azo dye.

Interestingly, as previously discussed, AzoC does not contain a signal peptide sequence, which predicts AzoC to be an intracellular enzyme by sequence alone (Morrison *et al*, 2014; Morrison *et al*, 2012). The translocation of proteins without a signal peptide sequence is not an uncommon phenomenon (Alam *et al*, 2009; Bukau & Horwich, 1998; Cole *et al*, 2005; Severin *et al*, 2007; Shimizu *et al*, 2002a; Shimizu *et al*, 2002b; Walz *et al*, 2007). In another *C. perfringens* strain (ATCC 13124) several predicted cytoplasmic proteins (also by their sequence) were shown to actually be translocated surface proteins (Alam *et al*, 2009). ESAT-6 secretions are known to support the secretion of proteins that do not contain a signal peptide sequence (Pallen, 2002). ExPortal systems may also play a role but these have not been studied in *C. perfringens* (Rosch & Caparon, 2004).

Despite the overwhelming support for translocated proteins without signal peptide sequences, the mechanism by which these proteins are able to exit the cell without a signal peptide is yet known (Wickner & Schekman, 2005). Authors have recently suggested piggy-backing on proteins containing signal sequences as a possible mechanism of transport for non-signal peptide proteins (Wickner & Schekman, 2005). In *E. coli*, environmental extracellular stress on the cell wall has been shown to cause proteins to selectively escape from the intracellular space due to a stress response (Vazquez-Laslop *et al*, 2001). Thus, despite not having

a signal peptide, it is possible that AzoC could translocate to the periplasmic space by a non-classical method.

The physiological processes of cell division and protein release can be linked (Navarre & Schneewind, 1999). Specifically, there is evidence that the cell division process in Gram-positive bacteria is linked to important proteins associated with the protein secretion machinery (Carlsson *et al*, 2006; DeDent *et al*, 2008; Frankel *et al*, 2010; Navarre & Schneewind, 1999). In *Streptococcus pyogenes*, it was found that pathogenically-important proteins are directed to different locations in the cell envelope by specific signal sequences during the events of cell division (Carlsson *et al*, 2006). In addition, in *E. coli* and *Saccharomyces cerevisiae*, only in actively-dividing cells were proteins released (Carlsson *et al*, 2006). Research with *Staphylococcus aureus* has shown that the SecA secretion system (as opposed to the TAT pathways) protein release during active cell division is crucial in this important pathogen (DeDent *et al*, 2008). More recently, ABI domains (transmembrane proteins) have been linked to this process and identified as crucial for protein translocation during cell division (Frankel *et al*, 2010). Despite the literature link in cell division being important for some protein translocation, we did not see the link here, as non-dividing cells exposed to sulfonated compounds behaved in a similar manner to the actively dividing cells.

Overall, the outcome of the study supports the following hypothesis. The negatively-charged sulfonated groups on the azo dyes compete with similarly charged azoreductases for positive charge sites in the cell wall. Thus, by saturating the sites with azo dyes thereby creating a neutralizing region on the cell wall, AzoC efficiently releases to the extracellular matrix. It is further hypothesized that there are other azoreductases that do not naturally translocate and have different dye specificities than AzoC. Lastly, we hypothesize that most azo dyes are too large (molecular mass greater than 500 Da) and too polar to penetrate the cell wall, thereby the release

of some azoreductases is likely an adaptive mechanism for *C. perfringens* in the intestine to be able to reach and reduce these dyes. A hypothetical schematic model is shown in Figure 39.

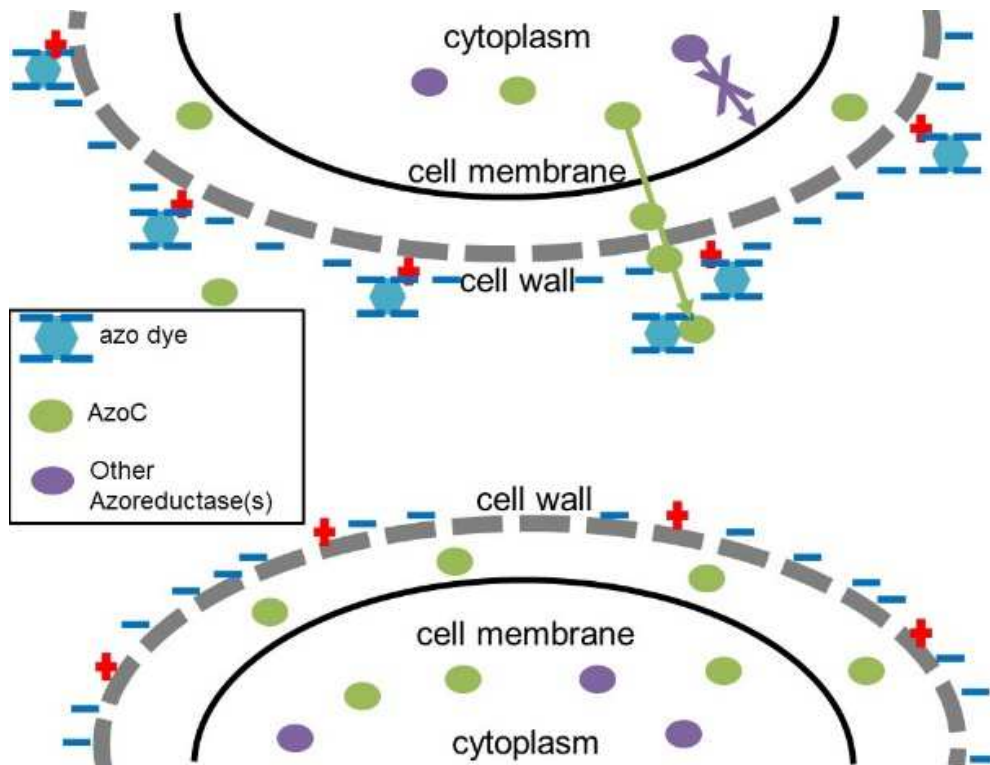


Figure 39. Proposed Model of AzoC Release Upon Sulfonated Compound Exposure. Hypothetical model predicting the interaction between sulfonated azo dyes and the *C. perfringens* cell wall that results in the release of AzoC from the cell and into the extracellular matrix.

In conclusion, this study demonstrated how sulfonated negatively charged compounds such as azo dyes enable the release of proteins, including AzoC, from the periplasmic space of *C. perfringens* strain ATCC 3626, resulting in an extracellular azoreductase reaction.

CHAPTER VI

PRELIMINARY STUDIES ON THE GROWTH AND PHYSIOLOGY OF *CLOSTRIDIUM* *PERFRINGENS* WILD TYPE AND Δ *azoC* KNOCKOUT MUTANT: AN AZO DYE EXPOSURE STUDY

Abstract

Clostridium perfringens, a strictly anaerobic microorganism and inhabitant of the human intestine, has been shown to produce the azoreductase enzyme, AzoC, an NAD(P)H-dependent flavin oxidoreductase. This enzyme reduces azo dyes into aromatic amines, which are carcinogenic in nature. A significant amount of work has been completed which focuses on the activity of this enzyme, however, few studies have been done that focus on the physiology of azo dye reduction. Dye reduction studies coupled with *C. perfringens* growth studies in the presence of ten different azo dyes were completed to compare the growth and activity of the *C. perfringens* Wild Type cells, the *C. perfringens* Δ *azoC* knockout mutant, and *Bifidobacterium infantis*, a non-azoreductase-producing control bacteria. The presence of azo dyes significantly increased the generation time of *C. perfringens* in rich media, an effect that was not seen in minimal media. In addition, azo dye reduction studies with the Δ *azoC* knockout suggests the presence of additional functional azoreductases in this important bacterium.

Introduction

Clostridium perfringens is a Gram-positive, spore-forming strict anaerobic bacteria that is ubiquitous in nature, found in a variety of locations such as soil and the human gastrointestinal tract (Ahmad *et al*, 2010). The bacterium is considered a medically-important bacterium that is capable of causing a number of infectious diseases that include food poisoning, antibiotic-associate diarrhea and gas gangrene (Ahmad *et al*, 2010). Various strains of *C. perfringens* are known and they differ based upon the specific type of toxin(s) produced (Ahmad *et al*, 2010). *C. perfringens* contains many genes and metabolic capabilities, one of which is azoreductase activity (Morrison *et al*, 2014; Morrison & John, 2013; Morrison *et al*, 2012).

Bacterial azoreductases are enzymes which are capable of reducing azo dyes into their component amines (Levine, 1991). Azo dyes are common synthetic colorants which are used in many industries spanning foods and beverages to textiles and paper products (Chen, 2006; Chung & Cerniglia, 1992). Azo dyes possess a namesake azo bond (-N=N-), which makes them capable of being reduced into their component aromatic amines by the azoreductase enzyme (Stolz, 2001). However, in many cases, these aromatic amines have been found to be carcinogenic in nature (Rafii & Coleman, 1999). On top of them being a threat to human health, azo dyes are also frequently found as environmental pollutants, a result of industrial processing application (Chen, 2006; Chung & Cerniglia, 1992; Stolz, 2001).

The azoreductase of *C. perfringens* strain ATCC 3626, AzoC, has been studied in the previous Chapters both biochemically and structurally. What is lacking from the study, though, is a look at the physiology in terms of the effect of the azo dyes on *C. perfringens*, as well as the effect of AzoC on *C. perfringens*. To our knowledge, only one other physiological study has been completed for an azoreductase, which was with *Enterococcus faecalis* (Punj & John, 2008).

Investigation of the genome of *C. perfringens* strain ATCC 3626 shows that this particular *C. perfringens* strain is significantly different than the other genome-sequenced *C. perfringens* strains, including the well-studied strain 13. As calculated by the National Center for Biotechnology Information (NCBI), the dendrogram featuring all genome-sequenced *C. perfringens* strains shows that *C. perfringens* strain ATCC 3626 is located on a separate clade from *C. perfringens* strain 13, suggesting that the *C. perfringens* strain ATCC 3626 is quite unique. Additionally, *C. perfringens* strain ATCC 3626 has a much larger genome size compared to *C. perfringens* strain 13 (3.8Mb versus 3.0Mb), as well as many more genes and proteins (3710 genes versus 2840 genes, 3301 proteins versus 2723 proteins). Additionally, the numbers for *C. perfringens* will only rise, as its genome sequence is not yet complete.

The goals of this Chapter are to utilize an AzoC gene knockout mutant in *C. perfringens* strain ATCC 3626 to understand the effect of the AzoC enzyme on the bacteria, as well as to complete a physiological study to understand the effect of azo dye exposure to *C. perfringens* strain ATCC 3626.

Materials and Methods

Bacterial Strains, Media and Azo Dyes

Clostridium perfringens strain ATCC 3626, both Wild Type and *AzoC* knockout strains (see Chapter 5), and *Bifidobacterium infantis* strain ATCC 15697 were grown anaerobically in Brain Heart Infusion (BHI) broth (Difco Laboratories) at 37°C. *B. infantis* was used as a non-azoreductase containing bacterial control for the experiments that follow. Clostridial minimal media (CMM) was prepared as previously detailed (Fuchs & Bonde, 1957). CMM consisted of the following at pH 7.0: Na₂HPO₄·12H₂O (6 g/L), KH₂PO₄ (1.5 g/L), NH₄Cl (1 g/L), NaCl (2.5 g/L), MgCl₂ (0.1 g/L), FeCl₂ (0.7 g/L), glucose (4 g/L), adenine (10 mg/L), biotin (0.4 µg/L), calcium pantothenate (200 µg/L), pyroxidine (800 µg/L), ascorbic acid (5 mg/L), L-tryptophan

(0.05 mM), and the following amino acids, all at 0.5 mM (DL-alanine, L-arginine, L-aspartic acid, L-cystine, L-glutamic acid, L-histidine, DL-isoleucine, L-leucine, DL-phenylalanine, DL-threonine, DL-tyrosine, DL-valine) (Fuchs & Bonde, 1957). Growth-arrest media (phosphate-buffered saline with glucose, PBSG) was prepared as previously detailed (Punj & John, 2008). PBSG consisted of the following, at pH 7.0: NaCl (137 mM), KCl (2.7 mM), NaPO₄ (10 mM), KH₂PO₄ (2 mM), cysteine (600 mg/L), glucose (6 mM) (Punj & John, 2008).

Azo dyes used were purchased from the following companies: Direct Blue 15 (MP Biomedicals), Methyl Red (Acros Organics), Tartrazine (Sigma-Aldrich), Trypan Blue (Kodak), Congo Red (Sigma-Aldrich), Eriochrome Black T (MCB), Cibacron Brilliant Red 3B-A (Sigma-Aldrich), Ponceau S (Fluka), Ponceau BS (Sigma-Aldrich), Methyl Orange (Allied Chemicals). Their structures can be seen in Figure 4.

Each individual azo dye was scanned prior experimenting to determine the optimal absorbance for each dye in the reaction mixture (dye absorbencies were above 340nm and extinction coefficients were used in determining the concentration of the dyes at the conclusion of the reaction). The absorbencies for each azo dye tested were as follows: Cibacron Brilliant Red 3B-A (534.00nm), Congo Red (531.00nm), Direct Blue 15 (602.50nm), Eriochrome Black T (527.50nm), Trypan Blue (533.50nm), Methyl Red (430.00nm), Tartrazine (425.00nm), Ponceau S (515.50nm), Ponceau BS (505.00nm), Methyl Orange (465.50nm). Dye concentration was interpolated from a plot of dye absorbance to time by making a standard curve of dye concentration to find the extinction coefficient. The extinction coefficient was determined to be spectrophotometer-specific and dependent on a line of best fit.

azoC Gene Knockout

As detailed previously in Chapter 5, the *azoC* gene in *C. perfringens* was inactivated by the insertion of a group II intron using the TargeTron (Sigma-Aldrich) insertional mutagenesis system with a *Clostridium*-modified protocol and plasmid (Chen *et al*, 2005b). The Sigma TargeTron algorithm (www.sigma-geosys.com/targetron/) was utilized to identify optimal intron insertion sequence sites within the *azoC* gene sequence. An intron was targeted in the sense orientation between nucleotides 228 and 229 of the *azoC* open reading frame. Primers used for this process were: IBS (5'-AAAAA AGCTT ATAAT TATCC TTAAA GGACG CAGAT GTGCG CCCAG ATAGG GTG-3'), EBS1d (5'-CAGAT TGTAC AAATG TGGTG ATAAC AGATA AGTCG CAGAT GGTA CTTAC CTTTC TTTGT-3'), EBS2 (5'-TGAAC GCAAG TTTCT AATTT CGGTT TCCTT CCGAT AGAGG AAAGT GTCT-3'). Following PCR to retarget the provided intron, the 350-bp fragment was inserted into pJIR750ai to construct an *azoC*-specific TargeTron plasmid. This plasmid, pJIR750aiAzoC, was electroporated into *C. perfringens* (Gupta & Chen, 2008). Transformants were selected by anaerobic growth on BHI agar plates containing 15 µg/mL chloramphenicol. Selected transformants were grown in 10 mL anaerobic BHI cultures containing 15 µg/mL chloramphenicol and their genomic DNA was extracted using a Genomic DNA Purification Kit (Wizard). Following genomic DNA extraction, PCR was utilized to confirm the presence of intron insertion within the *azoC* gene by using AzoC-sequence specific primers: *azoC*-F (5'-CGGCC TCGAG ATGAA AGTAT TATTA GTTA-3'), *azoC*-R (5'-GTGAA AGGAT CCGCT GATTA AAATT AACTT TGATA TATTT CAC-3') (Chapter 2) (Morrison *et al*, 2012; Wright, 2007). PCR was carried out in a MJ Research PTC-100 Programmable Thermal Cycler. Conditions for amplification were as follows: one cycle of 2 minutes at 94°C, 25 cycles with each cycle consisting of 1 minute at 94°C, 1 minute at 55°C, and 1 minute at 72°C, and a final extension of 7 minutes at 72°C. The PCR amplicon was observed by 0.8% (w/v) agarose gel electrophoresis and ethidium bromide staining.

Lack of AzoC protein expression by the AzoC deletion mutant (*ΔazoC*) was confirmed by Western blotting.

Bacterial Growth and Azo Dye Reduction by Whole Cell Cultures

Cultures of the bacteria (*C. perfringens* Wild Type strain ATCC 3626, *C. perfringens ΔazoC* knockout mutant, or *B. infantis*) were grown anaerobically, without shaking, overnight at 37°C in BHI. Each overnight culture (5 mL) was placed into a 100 mL anaerobic bottle of BHI. These larger cultures were allowed to grow until OD₆₀₀=0.4 (log phase). Once log phase was reached, the bacteria were pelleted and resuspended in the media (1 mL) to be used for the experiment (BHI, CMM or PBSG). The log phase bacteria (1 mL) was placed into an anaerobic test tube containing 9 mL of the experimental media and 20 μM of the azo dye of interest. All experiments were completed in triplicate. Initially (t=0) and after every hour for 6 hours, and after 24 hours, samples (1 mL) were taken from every tube. The 1 mL samples were centrifuged (5 minutes at 10,000 x g at 4°C) to pellet the cells. The supernatant from the centrifugation (containing the azo dye) was scanned in a UV-1601PC spectrophotometer at the wavelengths previously mentioned to be optimal for each dye to measure the dye reduction. This supernatant provides a measure of azo dye concentration and thus reduction over time. The pellet from the centrifugation (containing the bacterial cells) was resuspended in 1 mL sterile water and scanned at OD₆₀₀ to determine bacterial cell density. This resuspended pellet provides a measure of bacterial growth over time. The resuspended bacteria cells were lysed with lysozyme (0.1 mg/mL final concentration) by incubation on ice for 30 minutes. Following incubation, cells were sonicated with a Sonic 300 dismembrator with a small tip and relative output of 60%. In total, 10 sonication cycles occurred, with 5 seconds of sonication in each cycle, placing the sample on ice in between sonications. Following sonication, the sample was centrifuged (30 minutes at 10,000 x g, 4°C). The protein concentration in the supernatant (within the bacterial cells) was also determined following cell lysis by the Bradford method (Bradford, 1976).

To briefly summarize, each of the three bacterial strains (*C. perfringens* Wild Type ATCC 3626, *C. perfringens* Δ azoC knockout mutant, and *B. infantis*) were tested with the previously mentioned ten different azo dyes and three different media types of varying complexities. In addition, each experiment was performed in triplicate and samples were taken after set-up (t=0) and at every hour for 6 hours (t=1, 2, 3, 4, 5, 6) and after overnight incubation (t=24 hours). Each 1 mL sample taken provides a measure of dye absorbance, bacterial cell density, and protein concentration.

Results

Azo Dye Reduction

The results for the azo dye reduction by whole cell cultures can be simplified by grouping the azo dyes together by those which have experience a significant change in dye reduction by the Δ azoC knockout mutant versus the Wild Type cells.

First, Methyl Red (Table 10A), Methyl Orange (Table 10B), Tartrazine (Table 10D) and Cibacron Brilliant Red 3B-A (Table 10J) do not show a statistically significant effect on dye reduction in the absence of the *azoC* gene (*C. perfringens* Δ azoC knockout cells, p-value >0.05, 95% confidence). In all four cases, the dye reduction seen with the *C. perfringens* Δ azoC cells are not statistically different than what is seen with the Wild Type (p-value >0.05, 95% confidence). This suggests that AzoC is not important for the reduction of these four dyes. In all three out of the four cases, this is also confirmed by the pure AzoC results, showing insignificant Methyl Red (Table 10A), Methyl Orange (Table 10B) or Tartrazine (Table 10D) reduction by the pure AzoC enzyme (p-value >0.05, 95% confidence). Additionally, *B. infantis* does not show significant Methyl Red, Methyl Orange or Tartrazine reduction (Table 10A, 10B, 10D), consistent with its role as a non-azoreductase producing control bacteria (p-value >0.05, 95% confidence). Cibacron Brilliant Red 3B-A shows significant reduction by AzoC, as well as *B. infantis*, suggesting that

non-enzymatic reduction is the cause (Table 10J) (p-value <0.05, 95% confidence). This has been previously reported with Cibacron Brilliant Red 3B-A (Morrison & John, 2013). In addition to comparing the Wild Type and *ΔazoC* knockout mutant, the three different media types can also be compared.

Table 10. Percentage of Azo Dye Reduction Occurring Over Time for Each Bacteria Strain (*C. perfringens* Wild Type, *C. perfringens ΔazoC* Knockout, and *B. infantis*) in Each Media Type (BHI, CMM, PBSG), as Compared to Pure AzoC. Results for each azo dye are shown: Methyl Red (A), Methyl Orange (B), Eriochrome Black T (C), Tartrazine (D), Ponceau BS (E), Congo Red (F), Ponceau S (G), Trypan Blue (H), Direct Blue 15 (I), Cibacron Brilliant Red 3B-A (J). Average percent (%) dye reduction values are shown for each time point. “±” values represent the standard deviation of triplicate samples. “BHI” represents rich media, “CMM” represents minimal media and “PBSG” represents growth arrest media.

A) Methyl Red % Dye Reduction

		Time Point (hr)						
Bacteria	Media	1	2	3	4	5	6	24
Wild Type	BHI	32 ± 1.0	40 ± 3.7	60 ± 0.3	60 ± 2.6	60 ± 1.9	55 ± 0.5	55 ± 4.9
Wild Type	CMM	15 ± 0.9	17 ± 0.6	23 ± 3.9	29 ± 3.5	58 ± 1.9	58 ± 1.9	58 ± 1.9
Wild Type	PBSG	13 ± 5.7	14 ± 4.4	17 ± 5.1	29 ± 5.5	26 ± 0.3	30 ± 0.7	34 ± 4.4
<i>ΔazoC</i>	BHI	37 ± 0.9	40 ± 2.0	54 ± 3.2	53 ± 1.5	58 ± 1.9	58 ± 1.9	58 ± 1.9
<i>ΔazoC</i>	CMM	16 ± 2.0	19 ± 2.2	24 ± 8.1	28 ± 6.0	58 ± 7.2	59 ± 8.3	54 ± 7.0
<i>ΔazoC</i>	PBSG	12 ± 6.0	11 ± 3.2	15 ± 4.1	26 ± 1.4	25 ± 3.2	32 ± 1.2	36 ± 3.7
<i>B. infantis</i>	BHI	0 ± 0	0.2 ± 0.4	1.3 ± 2.3	3.2 ± 2.9	3.6 ± 1.5	3.3 ± 4.4	5.8 ± 3.0
<i>B. infantis</i>	CMM	0 ± 0	0 ± 0	0.4 ± 0.8	0 ± 0	0.7 ± 1.2	0.2 ± 0.4	0 ± 0
<i>B. infantis</i>	PBSG	0 ± 0	0.2 ± 0.4	0.8 ± 0.8	0.6 ± 1.0	0.1 ± 0.2	0.1 ± 0.2	0 ± 0
Pure AzoC ^a		3.1 ± 1.0						

^a Pure AzoC % dye reduction was calculated with pure enzyme after a period of 15 minutes

B) Methyl Orange % Dye Reduction

Bacteria	Media	Time Point (hr)						
		1	2	3	4	5	6	24
Wild Type	BHI	66 ± 3.7	90 ± 4.5	91 ± 4.4	100 ± 0	100 ± 0	100 ± 0	100 ± 0
Wild Type	CMM	0 ± 0	7.4 ± 1.2	63 ± 1.1	65 ± 3.7	72 ± 4.5	77 ± 2.1	84 ± 1.5
Wild Type	PBSG	6.6 ± 2.2	3.6 ± 2.3	3.2 ± 4.5	5.9 ± 5.1	8.6 ± 2.8	6.3 ± 2.9	7.5 ± 4.1
<i>ΔazoC</i>	BHI	53 ± 2.4	79 ± 2.2	88 ± 1.5	99 ± 1.2	96 ± 3.4	100 ± 0	100 ± 0
<i>ΔazoC</i>	CMM	0 ± 0	13 ± 5.3	65 ± 3.4	73 ± 0.7	72 ± 6.1	74 ± 4.4	73 ± 1.7
<i>ΔazoC</i>	PBSG	5.6 ± 3.2	4.0 ± 2.5	3.1 ± 3.2	6.2 ± 5.4	9.0 ± 1.6	9.1 ± 3.7	6.0 ± 5.1
<i>B. infantis</i>	BHI	0 ± 0	0 ± 0	2.7 ± 1.2	5.8 ± 3.9	7.9 ± 4.6	8.3 ± 5.4	14 ± 3.3
<i>B. infantis</i>	CMM	1.3 ± 1.2	1.5 ± 1.4	0 ± 0	0.7 ± 1.2	0.7 ± 1.2	0.8 ± 1.4	0.1 ± 0.2
<i>B. infantis</i>	PBSG	0 ± 0	0 ± 0	0 ± 0	0.3 ± 0.6	1.7 ± 2.3	0 ± 0	0.8 ± 1.4
Pure AzoC ^a		1.3 ± 1.2						

^a Pure AzoC % dye reduction was calculated with pure enzyme after a period of 15 minutes

C) Eriochrome Black T % Dye Reduction

Bacteria	Media	Time Point (hr)						
		1	2	3	4	5	6	24
Wild Type	BHI	20 ± 6.0	26 ± 9.8	34 ± 12	28 ± 2.0	31 ± 3.1	30 ± 8.9	31 ± 0.4
Wild Type	CMM	0 ± 0	0 ± 0	0 ± 0	0 ± 0	12 ± 3.8	13 ± 2.6	17 ± 5.7
Wild Type	PBSG	0 ± 0	0 ± 0	0 ± 0	0 ± 0	0 ± 0	0 ± 0	0 ± 0
<i>ΔazoC</i>	BHI	2.5 ± 2.9	1.1 ± 5.0	22 ± 5.7	30 ± 6.6	26 ± 6.9	21 ± 6.1	31 ± 7.3
<i>ΔazoC</i>	CMM	0 ± 0	0 ± 0	0 ± 0	0 ± 0	0 ± 0	11 ± 2.9	10 ± 4.5
<i>ΔazoC</i>	PBSG	0 ± 0	0 ± 0	0 ± 0	0 ± 0	0 ± 0	0 ± 0	0 ± 0
<i>B. infantis</i>	BHI	0 ± 0	1.1 ± 2.0	0 ± 0	0 ± 0	0 ± 0	0 ± 0	0 ± 0
<i>B. infantis</i>	CMM	2.3 ± 4.0	0.9 ± 1.1	3.2 ± 5.5	2.1 ± 3.6	2.5 ± 2.8	0 ± 0	2.7 ± 3.6
<i>B. infantis</i>	PBSG	9.1 ± 2.8	7.5 ± 7.9	4.6 ± 3.9	7.1 ± 5.7	6.2 ± 7.7	9.4 ± 3.4	4.6 ± 4.2
Pure AzoC ^a		38 ± 3.8						

^a Pure AzoC % dye reduction was calculated with pure enzyme after a period of 15 minutes

D) Tartrazine % Dye Reduction

		Time Point (hr)						
Bacteria	Media	1	2	3	4	5	6	24
Wild Type	BHI	9.0 ± 3.1	35 ± 3.6	57 ± 3.9	59 ± 2.8	59 ± 2.8	59 ± 2.8	59 ± 2.8
Wild Type	CMM	0.8 ± 1.5	1.5 ± 0.7	33 ± 1.4	59 ± 0.3	60 ± 2.9	85 ± 2.9	100 ± 0
Wild Type	PBSG	0 ± 0	0 ± 0	3.2 ± 0.5	4.5 ± 2.8	5.4 ± 4.8	4.4 ± 1.6	8.0 ± 4.3
<i>ΔazoC</i>	BHI	11 ± 2.5	38 ± 2.1	62 ± 1.4	62 ± 1.4	62 ± 1.4	62 ± 1.4	62 ± 1.4
<i>ΔazoC</i>	CMM	0 ± 0	0 ± 0	30 ± 2.3	56 ± 2.7	62 ± 2.0	85 ± 0.3	97 ± 0.8
<i>ΔazoC</i>	PBSG	0 ± 0	0 ± 0	2.9 ± 0.2	5.1 ± 4.8	5.0 ± 4.6	4.1 ± 2.0	8.3 ± 4.0
<i>B. infantis</i>	BHI	0 ± 0	0.2 ± 0.3	0.4 ± 0.7	0.1 ± 0.2	1.7 ± 1.5	3.0 ± 2.8	7.0 ± 1.8
<i>B. infantis</i>	CMM	0 ± 0	0 ± 0	0 ± 0	0.4 ± 0.7	0 ± 0	0 ± 0	0 ± 0
<i>B. infantis</i>	PBSG	1.9 ± 1.8	1.1 ± 1.9	1.3 ± 2.2	0 ± 0	1.7 ± 1.6	2.3 ± 2.0	1.3 ± 2.2
Pure AzoC ^a		1.8 ± 2.1						

^a Pure AzoC % dye reduction was calculated with pure enzyme after a period of 15 minutes

E) Ponceau BS % Dye Reduction

		Time Point (hr)						
Bacteria	Media	1	2	3	4	5	6	24
Wild Type	BHI	84 ± 5.8	85 ± 3.0	91 ± 4.6	95 ± 2.7	100 ± 0	100 ± 0	100 ± 0
Wild Type	CMM	0.8 ± 1.7	27 ± 0.7	74 ± 2.1	99 ± 1.8	100 ± 0	100 ± 0	100 ± 0
Wild Type	PBSG	5.4 ± 0.8	7.6 ± 3.5	11 ± 2.8	17 ± 2.9	22 ± 2.2	18 ± 0.5	28 ± 0
<i>ΔazoC</i>	BHI	42 ± 1.7	56 ± 7.9	77 ± 11	90 ± 3.2	98 ± 2.4	98 ± 0.5	100 ± 0
<i>ΔazoC</i>	CMM	1.3 ± 3.2	1.3 ± 2.9	40 ± 0.9	68 ± 1.9	100 ± 0	100 ± 0	100 ± 0
<i>ΔazoC</i>	PBSG	0 ± 0	2.1 ± 0.7	5.9 ± 1.0	7.9 ± 2.6	10 ± 2.6	12 ± 0.9	30 ± 2.5
<i>B. infantis</i>	BHI	0 ± 0	0.4 ± 0.6	0 ± 0	3.7 ± 3.2	6.8 ± 2.6	6.3 ± 1.4	11 ± 2.4
<i>B. infantis</i>	CMM	1.8 ± 1.3	3.0 ± 1.3	2.6 ± 0.3	2.8 ± 2.4	2.6 ± 2.3	1.2 ± 2.1	4.2 ± 2.4
<i>B. infantis</i>	PBSG	0.1 ± 0.2	2.9 ± 2.1	2.0 ± 1.9	1.8 ± 3.0	3.1 ± 2.7	1.8 ± 1.6	2.1 ± 3.0
Pure AzoC ^a		52 ± 20						

^a Pure AzoC % dye reduction was calculated with pure enzyme after a period of 15 minutes

F) Congo Red % Dye Reduction

Bacteria	Media	Time Point (hr)						
		1	2	3	4	5	6	24
Wild Type	BHI	0 ± 0	0 ± 0	22 ± 21	38 ± 17	37 ± 16	37 ± 16	38 ± 13
Wild Type	CMM	0 ± 0	0 ± 0	17 ± 2.4	32 ± 2.0	32 ± 4.6	29 ± 5.1	31 ± 0.8
Wild Type	PBSG	1.3 ± 1.5	3.4 ± 5.5	9.1 ± 1.2	5.1 ± 3.0	6.3 ± 2.3	6.3 ± 3.5	6.9 ± 0.9
<i>ΔazoC</i>	BHI	0 ± 0	0 ± 0	11 ± 1.9	20 ± 3.4	24 ± 2.1	23 ± 3.2	33 ± 3.3
<i>ΔazoC</i>	CMM	0 ± 0	0 ± 0	4.3 ± 3.7	23 ± 3.6	24 ± 2.0	23 ± 2.0	22 ± 3.9
<i>ΔazoC</i>	PBSG	0 ± 0	0 ± 0	2.9 ± 1.2	3.5 ± 1.2	4.6 ± 2.1	5.0 ± 2.1	7.9 ± 2.8
<i>B. infantis</i>	BHI	4.4 ± 7.6	9.1 ± 2.1	9.6 ± 8.0	5.4 ± 6.9	2.9 ± 5.1	1.6 ± 2.8	0 ± 0
<i>B. infantis</i>	CMM	0 ± 0	0.6 ± 1.1	1.5 ± 0.4	2.8 ± 2.4	3.9 ± 3.9	0.3 ± 0.4	1.8 ± 1.0
<i>B. infantis</i>	PBSG	1.0 ± 0.9	1.5 ± 2.5	1.2 ± 1.5	3.2 ± 2.8	3.1 ± 2.1	3.2 ± 1.4	5.4 ± 2.1
Pure AzoC ^a		59 ± 30						

^a Pure AzoC % dye reduction was calculated with pure enzyme after a period of 15 minutes

G) Ponceau S % Dye Reduction

Bacteria	Media	Time Point (hr)						
		1	2	3	4	5	6	24
Wild Type	BHI	78 ± 3.2	100 ± 0	100 ± 0	100 ± 0	100 ± 0	100 ± 0	100 ± 0
Wild Type	CMM	0 ± 0	59 ± 0.9	100 ± 0	100 ± 0	100 ± 0	100 ± 0	100 ± 0
Wild Type	PBSG	2.9 ± 0.2	4.3 ± 3.5	4.3 ± 0.5	4.4 ± 3.3	4.5 ± 0.5	7.3 ± 2.9	16 ± 0.8
<i>ΔazoC</i>	BHI	36 ± 2.0	59 ± 2.0	81 ± 2.1	82 ± 1.0	88 ± 0.8	89 ± 0.3	100 ± 0
<i>ΔazoC</i>	CMM	0 ± 0	0 ± 0	57 ± 3.1	100 ± 0	100 ± 0	100 ± 0	100 ± 0
<i>ΔazoC</i>	PBSG	0 ± 0	1.5 ± 0.8	2.7 ± 0.1	4.1 ± 2.6	4.3 ± 1.2	5.0 ± 0.6	18 ± 0.7
<i>B. infantis</i>	BHI	2.8 ± 4.9	2.7 ± 4.7	4.9 ± 3.2	4.7 ± 3.6	5.1 ± 3.3	4.8 ± 3.2	5.8 ± 3.9
<i>B. infantis</i>	CMM	0.7 ± 1.1	2.4 ± 0.3	2.7 ± 1.3	2.0 ± 2.4	1.0 ± 1.0	2.3 ± 2.4	3.5 ± 2.3
<i>B. infantis</i>	PBSG	0 ± 0	1.0 ± 1.0	0.9 ± 1.5	0.5 ± 0.9	0 ± 0	0.9 ± 0.8	0.4 ± 0.8
Pure AzoC ^a		86 ± 13						

^a Pure AzoC % dye reduction was calculated with pure enzyme after a period of 15 minutes

H) Trypan Blue % Dye Reduction

Bacteria	Media	Time Point (hr)						
		1	2	3	4	5	6	24
Wild Type	BHI	3.6 ± 4.4	8.7 ± 3.4	29 ± 1.8	68 ± 0.7	100 ± 0	100 ± 0	100 ± 0
Wild Type	CMM	0 ± 0	0 ± 0	4.4 ± 0.2	8.9 ± 1.8	14 ± 2.1	8.2 ± 2.2	100 ± 0
Wild Type	PBSG	0 ± 0	0 ± 0	0 ± 0	0 ± 0	0 ± 0	0 ± 0	0.2 ± 3.3
<i>AzoC</i>	BHI	1.3 ± 0.6	1.0 ± 0.7	4.7 ± 1.5	27 ± 1.7	51 ± 7.2	73 ± 1.9	100 ± 0
<i>AzoC</i>	CMM	0 ± 0	0 ± 0	3.6 ± 2.5	6.1 ± 0.5	12 ± 1.8	15 ± 0.6	100 ± 0
<i>AzoC</i>	PBSG	0 ± 0	0 ± 0	0 ± 0	0 ± 0	0 ± 0	0 ± 0	0 ± 0
<i>B. infantis</i>	BHI	0 ± 0	5.3 ± 2.2	11 ± 4.4	15 ± 4.3	21 ± 2.5	21 ± 4.4	21 ± 4.6
<i>B. infantis</i>	CMM	0.4 ± 0.8	0 ± 0	0.2 ± 0.3	0 ± 0	0 ± 0	0 ± 0	0.1 ± 0.1
<i>B. infantis</i>	PBSG	0.1 ± 0.1	0.7 ± 1.0	0.9 ± 1.5	0.3 ± 0.5	0.4 ± 0.8	0.7 ± 0.8	0.4 ± 0.8
Pure AzoC ^a		74 ± 23						

^a Pure AzoC % dye reduction was calculated with pure enzyme after a period of 15 minutes

I) Direct Blue 15 % Dye Reduction

Bacteria	Media	Time Point (hr)						
		1	2	3	4	5	6	24
Wild Type	BHI	17 ± 19	35 ± 14	94 ± 5	100 ± 0	100 ± 0	100 ± 0	100 ± 0
Wild Type	CMM	0 ± 0	0 ± 0	25 ± 0.8	33 ± 1.6	51 ± 1.1	80 ± 0.7	100 ± 0
Wild Type	PBSG	0 ± 0	0 ± 0	0 ± 0	1.3 ± 1.7	2.5 ± 2.7	1.8 ± 1.0	9.2 ± 4.8
<i>AzoC</i>	BHI	0 ± 0	0 ± 0	22 ± 4.9	33 ± 8.2	54 ± 5.7	76 ± 5.0	100 ± 0
<i>AzoC</i>	CMM	0 ± 0	0 ± 0	6.0 ± 0.7	18 ± 7.1	22 ± 5.7	51 ± 0.9	100 ± 0
<i>AzoC</i>	PBSG	0 ± 0	0 ± 0	0 ± 0	0 ± 0	0 ± 0	0 ± 0	5.4 ± 0.2
<i>B. infantis</i>	BHI	0 ± 0	4.6 ± 4.0	14 ± 0.3	17 ± 6.2	21 ± 1.5	20 ± 1.6	21 ± 0.5
<i>B. infantis</i>	CMM	0.1 ± 0.1	0.6 ± 1.1	1.1 ± 1.6	1.4 ± 2.4	0.2 ± 0.3	1.7 ± 1.6	0 ± 0
<i>B. infantis</i>	PBSG	1.1 ± 2.0	0.5 ± 0.6	1.4 ± 2.1	1.5 ± 1.9	1.5 ± 2.5	1.2 ± 1.2	1.5 ± 1.9
Pure AzoC ^a		84 ± 10						

^a Pure AzoC % dye reduction was calculated with pure enzyme after a period of 15 minutes

J) Cibacron Brilliant Red 3B-A % Dye Reduction

Bacteria	Media	Time Point (hr)						
		1	2	3	4	5	6	24
Wild Type	BHI	54 ± 0.9	100 ± 0	100 ± 0	100 ± 0	100 ± 0	100 ± 0	100 ± 0
Wild Type	CMM	1.9 ± 1.6	5.2 ± 2.2	73 ± 1.6	100 ± 0	100 ± 0	100 ± 0	100 ± 0
Wild Type	PBSG	0 ± 0	0 ± 0	0 ± 0	13 ± 1.7	12 ± 2.7	17 ± 1.0	19 ± 4.8
<i>ΔazoC</i>	BHI	47 ± 0.8	100 ± 0	100 ± 0	100 ± 0	100 ± 0	100 ± 0	100 ± 0
<i>ΔazoC</i>	CMM	0.9 ± 3.1	0.6 ± 3.4	64 ± 4.2	100 ± 0	100 ± 0	100 ± 0	100 ± 0
<i>ΔazoC</i>	PBSG	0 ± 0	0 ± 0	0 ± 0	18 ± 2.5	16 ± 3.5	17 ± 0.8	21 ± 6.5
<i>B. infantis</i>	BHI	0 ± 0	3.0 ± 3.5	16 ± 2.2	79 ± 1.8	100 ± 0	100 ± 0	100 ± 0
<i>B. infantis</i>	CMM	12 ± 3.1	91 ± 1.0	100 ± 0	100 ± 0	100 ± 0	100 ± 0	100 ± 0
<i>B. infantis</i>	PBSG	0.8 ± 1.4	0.9 ± 1.6	0.1 ± 0.2	0.6 ± 1.0	0 ± 0	0.1 ± 0.2	0 ± 0
Pure AzoC ^a		99 ± 1.3						

^a Pure AzoC % dye reduction was calculated with pure enzyme after a period of 15 minutes

Methyl Red is significantly reduced by both the *C. perfringens* Wild Type and *ΔazoC* mutant in rich (BHI) media (Table 10A) (p-value <0.05, 95% confidence). Within 3 hours, 60% of the dye added is reduced. This amount is reduced when both *C. perfringens* strains are grown in minimal media (CMM), as in the same 3 hours only 23% of the dye is reduced. However, the cells that are grown in CMM recovers activity against Methyl Red and by 5 hours has the same amount of dye reduced as in the rich media. This suggests that, because growth is slower in the minimal media, the azoreductases are still being produced, just at a reduced rate. The reduction rate is further reduced in the growth arrest media, as after 24 hours only 34% of the dye is reduced. Because the *C. perfringens* cells are not actively growing in the PBSG media, it can be reasoned that any dye reduction seen is the result of the already produced azoreductases. Thus, azoreductase production is constitutive in the *C. perfringens* cells.

Methyl Orange is significantly reduced by both the *C. perfringens* Wild Type and *ΔazoC* knockout mutant cells in rich (BHI) media (Table 10B) (p-value <0.05, 95% confidence). Within 4 hours, 100% of Methyl Orange added is reduced. This amount is significantly reduced when the

C. perfringens cells are grown in minimal media (CMM), as in the same 4 hours only 65% of the dye is reduced (p-value <0.05, 95% confidence). The cells that are grown in CMM slowly begin to recover activity but only achieves 84% Methyl Orange reduction after 24 hours. Like with Methyl Red, this suggests that, because growth is slower in the minimal media, the azoreductases are still being produced, just at a reduced rate. The reduction rate is even further reduced in the growth arrest media (PBSG), as after 24 hours only 7.5% of the dye is reduced. Because these *C. perfringens* cells are not actively growing the PBSG media, it can be reasoned that any dye reduction seen is the result of the already produced azoreductases. Because Methyl Orange reduction is so reduced in the growth arrest media, it could be that the azoreductase capable of Methyl Orange reduction is inducible, or that the mechanism by which enzyme meets dye is not functional in this growth arrest state in the Wild Type.

Tartrazine is significantly reduced by both the *C. perfringens* Wild Type and Δ azoC mutant in rich (BHI) media (Table 10D) (p-value <0.05, 95% confidence). Within 3 hours, 57% of the dye added is reduced. This amount is initially reduced when both *C. perfringens* strains are grown in minimal media (CMM), as in the same 3 hours only 33% of the dye is reduced. However, the cells that are grown in CMM recovers activity against Tartrazine and surpass the activity of the cells grown in BHI. At 24 hours of exposure, the Tartrazine has been reduced by 100% in both the Wild Type and Δ azoC mutant. This suggests that, because growth is slower in the minimal media, the azoreductases are still being produced, just at a reduced rate. The reduction rate is further reduced in the growth arrest media, as after 24 hours only 8% of the dye is reduced. Because the *C. perfringens* cells are not actively growing the PBSG media, it can be reasoned that any dye reduction seen is the result of the already produced azoreductases. Thus, azoreductase production is not constitutive in the *C. perfringens* cells.

Cibacron Brilliant Red 3B-A is a unique case. Previous research has shown that this dye is subject to non-enzymatic reduction (Morrison & John, 2013). The results presented in Table

10J serve to confirm this. In a very short period of time (2 hours), Cibacron Brilliant Red is reduced 100% in the rich media (BHI) in both strains of *C. perfringens*. In the minimal media (CMM), 100% dye reduction is also noticed, but at a slower rate (4 hours). *B. infantis*, the non-azoreductase-containing control bacteria shows a significant reduction of Cibacron Brilliant Red 3B-A as well, reaching 100% dye reduction in 5 hours, suggesting that this dye is subjected to non-enzymatic reduction (p-value <0.05, 95% confidence).

The remaining six azo dyes, Eriochrome Black T (Table 10C), Ponceau BS (Table 10E), Congo Red (Table 10F), Ponceau S (Table 10G), Trypan Blue (Table 10H) and Direct Blue 15 (Table 10I) show a significant effect on dye reduction with the absence of the *azoC* gene (p-value <0.05, 95% confidence). In all six cases, the dye reduction seen with the *C. perfringens* Δ *azoC* cells are significantly lower than what is seen with the Wild Type (p-value <0.05, 95% confidence). This suggests that AzoC is important for the reduction of these six dyes. In all of the six cases, this is confirmed by the pure AzoC results, showing strong Eriochrome Black T (Table 10C), Ponceau BS (Table 10E), Congo Red (Table 10F), Ponceau S (Table 10G), Trypan Blue (Table 10H) and Direct Blue 15 (Table 10I) reduction by the pure enzyme (p-value <0.05, 95% confidence). Additionally, *B. infantis* does not show significant strong reduction of any of these six dyes, suggesting that non-enzymatic reduction is not the case (Table 10C, 10E, 10F, 10G, 10H, 10I) (p-value >0.05, 95% confidence). In addition to comparing the Wild Type and Δ *azoC* knockout mutant, the three different media types can also be compared for these six dyes.

Eriochrome Black T is very slowly reduced by the *C. perfringens* Wild Type in rich (BHI) media (Table 10C). Within 24 hours, only 31% of Eriochrome Black T added is reduced. This amount is significantly reduced when the Wild Type is grown in minimal media (CMM), as in the same 24 hours only 27% of the dye is reduced (p-value <0.05, 95% confidence). This suggests that, because growth is slower in the minimal media, the azoreductases are still being produced, just at a reduced rate. Eriochrome Black T reduction is completely absent when in the

growth arrest media (PBSG) as significant dye reduction is not seen (p-value >0.05, 95% confidence). Because these Wild Type cells are not actively growing the PBSG media, it can be reasoned that any dye reduction seen is the result of the already produced azoreductases. Because Eriochrome Black T reduction is absent from the growth arrest media, it could be that the azoreductase capable of Eriochrome Black T reduction is possibly inducible, or that the mechanism by which enzyme meets dye is not functional in this growth arrest state in the Wild Type. With Eriochrome Black T, a strong difference between the Wild Type and the $\Delta azoC$ knockout mutant, as the Eriochrome Black T dye reduction results for the $\Delta azoC$ mutant in either media type are significantly different than the Wild Type (Table 10C) (p-value <0.05, 95% confidence). However, the reduction of the $\Delta azoC$ mutant seems to recover and catch up to that of the Wild Type, suggesting that there may be additional azoreductases that are capable of reducing Eriochrome Black T present. In addition, *B. infantis* does not show significant Eriochrome Black T reduction (p-value >0.05, 95% confidence).

Ponceau BS is very strongly reduced by the *C. perfringens* Wild Type in rich (BHI) media (Table 10E) (p-value <0.05, 95% confidence). Within 1 hour, 84% of the dye added is reduced. This amount is reduced when the Wild Type is grown in minimal media (CMM). However, the cells that are grown in CMM recovers activity against Ponceau BS and by 4 hours has the same amount of dye reduced as in the rich media. This suggests that, because growth is slower in the minimal media, the azoreductases are still being produced, just at a reduced rate. The reduction rate is further reduced in the growth arrest media, as after 24 hours only 28% of the dye is reduced. Because the *C. perfringens* cells are not actively growing the PBSG media, it can be reasoned that any dye reduction seen is the result of the already produced azoreductases. Thus, azoreductase production is constitutive in the *C. perfringens* cells. With Ponceau BS, a very strong difference between the Wild Type and the $\Delta azoC$ knockout mutant is seen, as the dye reduction results for the $\Delta azoC$ mutant in either media type are significantly different than the

Wild Type (Table 10E) (p-value <0.05, 95% confidence). However, the reduction of the *ΔazoC* mutant seems to recover and catch up to that of the Wild Type, suggesting that there may be additional azoreductases that are capable of reducing Ponceau BS present. In addition, *B. infantis* does not show significant Ponceau BS reduction (p-value >0.05, 95% confidence).

Congo Red is very slowly reduced by the *C. perfringens* Wild Type in rich (BHI) media (Table 10F). Within 4 hours, only 38% of the Congo Red added is reduced; after 24 hours, this amount of dye reduced does not increase. This amount is the same as when the Wild Type is grown in minimal media (CMM), suggesting that the change from a rich to a minimal media does not affect Congo Red reduction. Congo Red reduction is still present when in the growth arrest media (PBSG). Because these Wild Type cells are not actively growing the PBSG media, it can be reasoned that any dye reduction seen is the result of the already produced azoreductases. With Congo Red, a strong difference between the Wild Type and the *ΔazoC* knockout mutant, as dye reduction results for the *ΔazoC* mutant in either media type are significantly different than the Wild Type (Table 10F) (p-value <0.05, 95% confidence). However, the reduction of the *ΔazoC* mutant seems to recover and catch up to that of the Wild Type, suggesting that there may be additional azoreductases that are capable of reducing Congo Red present.

Ponceau S is very strongly reduced by the *C. perfringens* Wild Type in rich (BHI) media (Table 10G) (p-value <0.05, 95% confidence). Within 2 hours, 100% of the dye added is reduced. This amount is reduced when the Wild Type is grown in minimal media (CMM), as it takes the cells grown in CMM 3 hours to reach the same complete dye reduction. This suggests that, because growth is slower in the minimal media, the azoreductases are still being produced, just at a reduced rate. The reduction rate is further reduced in the growth arrest media. Because the *C. perfringens* cells are not actively growing the PBSG media, it can be reasoned that any dye reduction seen is the result of the already produced azoreductases. Thus, azoreductase production is constitutive in the *C. perfringens* cells. With Ponceau B, a significant difference between the

Wild Type and the *ΔazoC* knockout mutant is seen, as the dye reduction results for the *ΔazoC* mutant in either media type are significantly different than the Wild Type (Table 10G) (p-value <0.05, 95% confidence). However, the reduction of the *ΔazoC* mutant seems to recover and catch up to that of the Wild Type after an overnight incubation, suggesting that there may be additional azoreductases that are capable of reducing Ponceau S present. In addition, *B. infantis* does not any signs of Ponceau S reduction (p-value >0.05, 95% confidence).

Trypan Blue is strongly reduced by the *C. perfringens* Wild Type in rich (BHI) media (Table 10H) (p-value <0.05, 95% confidence). Within 5 hours, 100% of the dye added is reduced. This amount is significantly reduced when the Wild Type is grown in minimal media (CMM), as it takes the cells grown in CMM a full 24 hours to reach the same complete dye reduction (p-value <0.05, 95% confidence). This suggests that, because growth is slower in the minimal media, the azoreductases are still being produced, just at a reduced rate. The reduction rate is completely absent when the cell are grown in the growth arrest media. With Trypan Blue, a significant difference between the Wild Type and the *ΔazoC* knockout mutant is seen, as the dye reduction results for the *ΔazoC* mutant in either media type are significantly different than the Wild Type (Table 10H) (p-value <0.05, 95% confidence). However, the reduction of the *ΔazoC* mutant seems to recover and catch up to that of the Wild Type after an overnight incubation, suggesting that there may be additional azoreductases that are capable of reducing Trypan Blue present.

Direct Blue 15 is strongly reduced by the *C. perfringens* Wild Type in rich (BHI) media (Table 10I) (p-value <0.05, 95% confidence). Within 4 hours, 100% of the dye added is reduced. This amount is significantly reduced when the Wild Type is grown in minimal media (CMM), as it takes the cells grown in CMM a full 24 hours to reach the same complete dye reduction; at the 4 hours that the BHI-grown cells reach 100% dye reduction, the cells grown in CMM are only at a 33% dye reduction (p-value <0.05, 95% confidence). This suggests that, because growth is

slower in the minimal media, the azoreductases are still being produced, just at a reduced rate. The reduction rate is nearly absent when the cell are grown in the growth arrest media. With Direct Blue 15, a significant difference between the Wild Type and the *ΔazoC* knockout mutant is seen, as the dye reduction results for the *ΔazoC* mutant in either media type are significantly different than the Wild Type (Table 10I) (p-value <0.05, 95% confidence). However, the reduction of the *ΔazoC* mutant seems to recover and catch up to that of the Wild Type after an overnight incubation, suggesting that there may be additional azoreductases that are capable of reducing Direct Blue 15 present.

In addition to looking at the percentage of each dye reduced at different time points, a cumulative specific activity can be calculated for the total protein of the cell extracts for each of the strains tested in each media type.

Table 11 shows that, Methyl Red, Methyl Orange and Tartrazine do not show a significant difference in specific activity when comparing the *C. perfringens* Wild Type to the *C. perfringens ΔazoC* mutant in BHI, CMM, or PBSG (p-values >0.05, 95% confidence). This confirms the pure enzyme data as shown above, that AzoC is not important for the reduction of these three azo dyes. Table 11 also shows that Eriochrome Black T, Ponceau BS, Congo Red, Ponceau S, Trypan Blue and Direct Blue have significant differences in specific activity when comparing the *C. perfringens* Wild Type to the *C. perfringens ΔazoC* mutant in BHI, CMM, or PBSG (p-values <0.05, 95% confidence).

Table 11. Specific Activity for Each Bacterial Strain (*C. perfringens* Wild Type, *C. perfringens* Δ azoC knockout and *B. infantis*) in Each Media Type (BHI, CMM, PBSG). Average specific activity (nmol dye reduced/min/mg total protein) values are shown for each condition. “±” values represent the standard deviation of triplicate samples. “BHI” represents rich media, “CMM” represents minimal media and “PBSG” represents growth arrest media. “Wild Type” refers to the *C. perfringens* Wild Type, “ Δ azoC” refers to the *C. perfringens* Δ azoC knockout, and “*B. infantis*” refers to the control bacteria.

Condition	nmol dye reduced/min/mg total protein									
	Methyl Red	Methyl Orange	Eriochrome Black T	Tart-Razine	Ponceau BS	Congo Red	Ponceau S	Trypan Blue	Direct Blue 15	Cibacron Brilliant Red 3B-A
Wild Type	0.31 ± 0.019	0.68 ± 0.006	0.37 ± 0.053	0.57 ± 0.036	0.49 ± 0.011	0.46 ± 0.131	19.41 ± 1.648	0.75 ± 0.013	6.72 ± 1.326	2.52 ± 0.045
ΔazoC	0.31 ± 0.003	0.72 ± 0.011	0.27 ± 0.051	0.63 ± 0.014	0.36 ± 0.012	0.32 ± 0.055	3.56 ± 0.212	0.53 ± 0.024	2.42 ± 0.813	2.51 ± 0.060
<i>B. infantis</i>	0.01 ± 0.005	0.03 ± 0.007	0.01 ± 0.011	0.02 ± 0.004	0.03 ± 0.007	0.00 ± 0.000	0.01 ± 0.006	0.03 ± 0.007	0.04 ± 0.003	0.83 ± 0.024
Wild Type	3.54 ± 0.313	8.92 ± 0.821	0.12 ± 0.006	0.55 ± 0.015	1.59 ± 0.020	0.53 ± 0.032	17.84 ± 1.885	0.19 ± 0.132	1.80 ± 0.100	1.87 ± 0.039
ΔazoC	3.63 ± 0.361	8.32 ± 0.467	0.04 ± 0.013	0.50 ± 0.045	1.30 ± 0.017	0.31 ± 0.070	1.75 ± 0.045	0.18 ± 0.008	0.31 ± 0.005	1.93 ± 0.072
<i>B. infantis</i>	0.00 ± 0.000	0.00 ± 0.003	0.01 ± 0.008	0.00 ± 0.000	0.01 ± 0.008	0.02 ± 0.005	0.01 ± 0.011	0.00 ± 0.003	0.00 ± 0.000	3.76 ± 0.061
Wild Type	5.84 ± 0.473	1.26 ± 0.869	0.14 ± 0.240	1.67 ± 0.993	6.49 ± 0.594	0.97 ± 0.060	4.13 ± 0.079	1.42 ± 0.189	2.46 ± 0.995	3.44 ± 0.148
ΔazoC	5.49 ± 0.310	1.44 ± 0.521	0.12 ± 0.046	1.43 ± 0.744	0.61 ± 0.524	0.78 ± 0.099	0.26 ± 0.100	0.19 ± 0.111	0.45 ± 0.194	3.82 ± 1.74
<i>B. infantis</i>	0.06 ± 0.101	0.45 ± 0.780	0.16 ± 0.271	0.26 ± 0.443	0.11 ± 0.047	2.20 ± 0.152	0.20 ± 0.354	0.07 ± 0.120	0.35 ± 0.320	0.00 ± 0.000

Effect of Azo Dyes on Cell Growth

Looking first at rich media (BHI), it can be seen that *C. perfringens* Wild Type has a very fast generation time of less than 10 minutes in the absence of azo dyes (Figure 40A). The absence of the *azoC* gene (*C. perfringens* Δ azoC knockout mutant) does not have a significant effect on generation time over the Wild Type in the absence of dye, suggesting that AzoC does not play a role in basic growth processes (Figure 40A) (p-value >0.05, 95% confidence). In the absence of dye, the generation time of *B. infantis* is significantly higher than that of *C. perfringens* at around 20 minutes (Figure 40A) (p-value <0.05, 95% confidence). Significant generation time effects are not seen in any case with *B. infantis* in BHI media (Figure 40A) (p-value >0.05, 95% confidence).

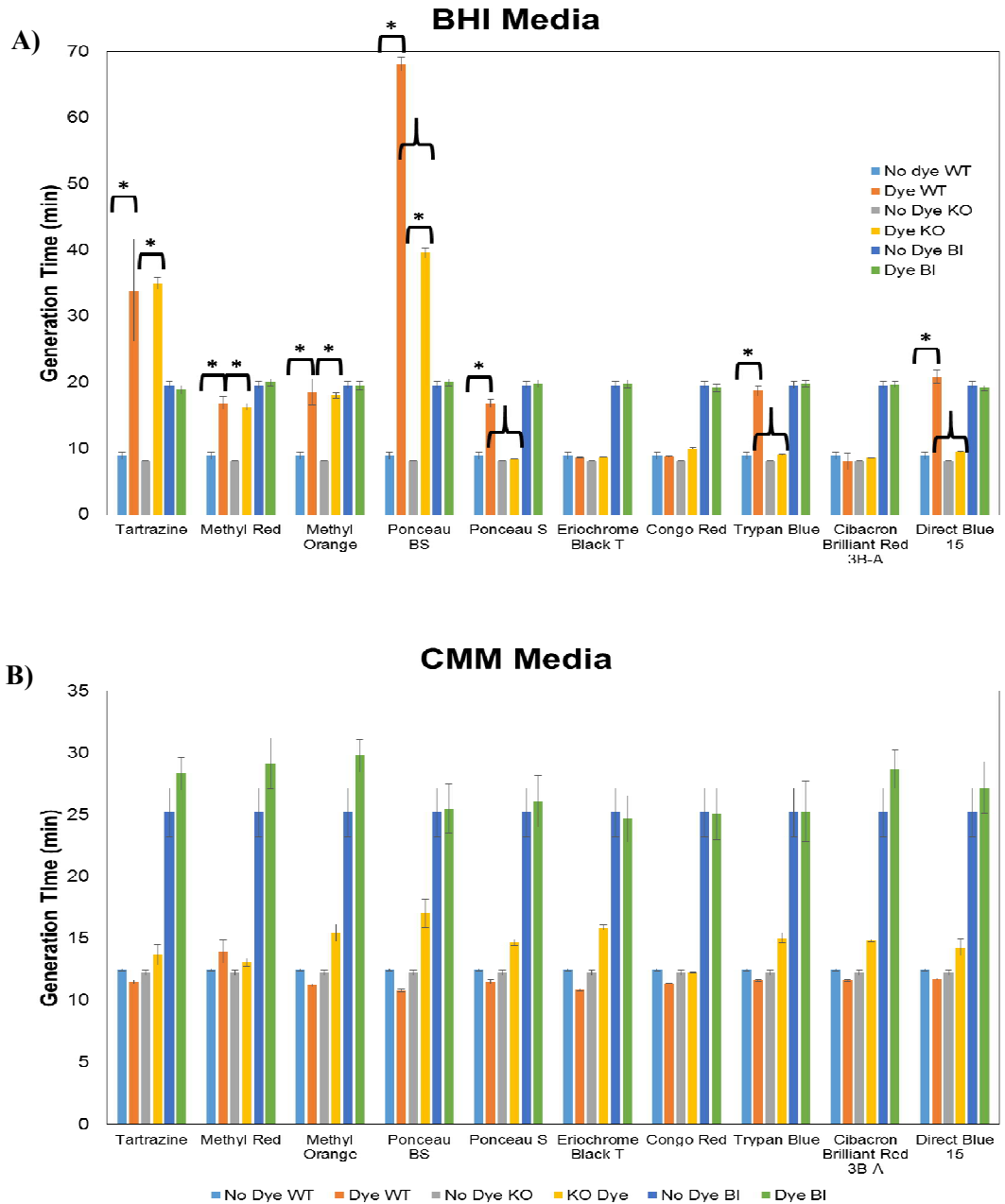


Figure 40. Generation Time of *C. perfringens* Wild Type, *C. perfringens* Δ azoC Knockout Mutant and *B. infantis* in Different Media Types. **A)** BHI media, **B)** CMM media. “WT” is the *C. perfringens* Wild Type, “KO” is the *C. perfringens* Δ azoC knockout mutant and “BI” is *B. infantis*. Samples are listed as either being “No Dye”, meaning that this represents the growth of the bacteria in the absence of dye, or “Dye”, meaning that the bacteria are grown in the particular dye, to give a direct comparison of the effect of the dye on the generation time of the three different bacteria. Errors bars represent the standard deviation of triplicate samples (n=3). For **A)**, a bracket with a star (*) signifies that the comparison of the cell type with and without dye is significant (p-value <0.05, 95% confidence). A bracket without a star (“)”) signifies that the comparison of Wild Type with dye to the Δ azoC knockout with dye is significant (p-value <0.05, 95% confidence).

When azo dyes are added to BHI, the situation changes. Looking first at the effect of azo dye addition on the *C. perfringens* Wild Type cells, it can be seen that the addition of Tartrazine, Methyl Red, Methyl Orange, Ponceau BS, Ponceau S, Trypan Blue and Direct Blue 15 all cause a significantly increased generation time over the no-dye containing BHI control media (p-value <0.05, 95% confidence) (Figure 40A). All 7 of these dyes are highly reduced by *C. perfringens* Wild Type cells, suggesting dye-induced toxicity to growth.

For the *C. perfringens* Δ azoC knockout cells, the situation is slightly different. In this case, Tartrazine, Methyl Red and Methyl Orange exposure for the *C. perfringens* Δ azoC knockout cells is no different than that of the *C. perfringens* Wild Type cells (p-value >0.05, 95% confidence) (Figure 40A). Both strains show approximately the same increased generation time (p-value >0.05, 95% confidence). However, for the azo dyes which AzoC is known to reduce (Table 10), we see significant differences in the generation time changes in the *C. perfringens* Δ azoC knockout cells (p-value <0.05, 95% confidence). Ponceau BS showed a huge increase in generation time for the Wild Type cells, but the generation time for the *C. perfringens* Δ azoC knockout cells is significantly decreased (p-value <0.05, 95% confidence) (Figure 40A). Additionally, Ponceau S, Trypan Blue and Direct Blue 15 no longer show an increased generation time over the no-dye containing control BHI media, suggesting that, in the absence of the *azoC* gene, the increased generation time is no longer seen (Figure 40A).

Looking at the minimal (CMM) media, it can be seen that the *C. perfringens* Wild Type has an increased generation time over what was seen in the rich media (BHI), at around 13 minutes (p-value <0.05, 95% confidence) (Figure 40A and 40B). The absence of the *azoC* gene (*C. perfringens* Δ azoC knockout mutant) does not have a significant effect on generation time over the Wild Type in the absence of dye, confirming what was seen in the rich media, that AzoC does not play a role in basic growth processes (Figure 40B). In the absence of dye, the generation time of *B. infantis* is significantly higher than that of *C. perfringens* at around 25 minutes (p-value

<0.05, 95% confidence) (Figure 40B). Significant generation time effects are not seen in any case with *B. infantis* in BHI media (p-value >0.05, 95% confidence) (Figure 40B). When azo dyes are added to CMM for the *C. perfringens* Wild Type cells, we surprisingly do not see the increased generation time that we saw in the rich (BHI) media (p-value >0.05, 95% confidence) (Figures 40A and 40B).

As generation times are calculated during log phase, we can take a closer look at the increased generation time seen when azo dyes were added to BHI media, by breaking the generation time up into either an early log phase or a late log phase to garner an idea of when the negative effect on generation time occurs. Table 12 shows that, in all cases where the azo dye and BHI media were shown to negatively affect generation time that the increase in generation time can be linked to late log phase.

In addition, for the azo dyes which were shown to negatively affect generation time in the Wild Type, but not in the $\Delta azoC$ mutant, as highlighted in Table 12, we can see that the difference yet again comes during late log phase. For example, Ponceau BS showed a significantly increased generation time with the Wild Type (~70 minutes), but was reduced in the $\Delta azoC$ mutant (~40 minutes). Looking at the fold increase for late log phase over early log phase, in the Wild Type this ratio is 54 whereas in the $\Delta azoC$ mutant this ratio is only 12.3, showing the significantly reduced effect of Ponceau BS on the mutant cells over the Wild Type (p-value <0.05, 95% confidence). Besides Ponceau BS, Ponceau S, Trypan Blue and Direct Blue 15 also show significantly reduced generation time effects in the $\Delta azoC$ knockout (p-value <0.05, 95% confidence) (Table 12).

Table 12. Early and Late Log Phase Comparison for BHI Media for Both *C. perfringens* Wild Type Cells and *C. perfringens* Δ azoC Knockout Mutant. Generation time is shown for the Wild Type and Δ azoC mutant calculated both during early and late log phase. “ \pm ” values represent the standard deviation of triplicate samples. The “Fold Increase” was calculated as the increase of the generation time at Late Log Phase over that at Early Log Phase, to give the increase in generation time. The “No dye control” represents the generation time calculated without any dye present in the media. Highlighted rows show statistically significant reduced effects on generation time in the Wild Type versus the Δ azoC knockout (p-value <0.05, 95% confidence).

	Generation Time (min)					
	Wild Type BHI	Wild Type BHI	Δ azoC BHI	Δ azoC BHI	Wild Type BHI	Δ azoC BHI
	Early Log Phase	Late Log Phase	Early Log Phase	Late Log Phase	Fold Increase	Fold Increase
No dye control	10.3 \pm 0.73	64.6 \pm 0.95	8.30 \pm 0.16	54.9 \pm 3.62	6.3	6.6
Tartrazine	39.7 \pm 5.72	298 \pm 24.8	39.2 \pm 1.41	320 \pm 21.3	7.5	8.2
Methyl Red	23.0 \pm 1.74	63.2 \pm 1.06	22.5 \pm 1.03	59.2 \pm 1.32	2.7	2.6
Methyl Orange	23.9 \pm 3.00	84.5 \pm 3.67	23.3 \pm 0.54	80.2 \pm 1.76	3.5	3.5
Ponceau BS	64.5 \pm 4.48	3461 \pm 7930	9.85 \pm 0.09	121 \pm 9.82	54	12.3
Ponceau S	21.7 \pm 0.71	75.1 \pm 3.99	11.0 \pm 0.15	37.3 \pm 1.40	3.5	3.4
Eriochrome Black T	9.81 \pm 0.10	74.4 \pm 2.04	13.1 \pm 0.20	25.6 \pm 0.70	7.6	2.0
Congo Red	9.75 \pm 0.02	86.1 \pm 12.8	11.4 \pm 0.06	83.9 \pm 5.83	8.8	7.4
Trypan Blue	22.5 \pm 0.52	115 \pm 21.4	12.8 \pm 0.75	31.6 \pm 3.40	5.1	2.5
Cibacron Brilliant Red 3B-A	8.91 \pm 1.57	80.0 \pm 5.95	9.70 \pm 0.08	77.1 \pm 4.35	9.0	7.9
Direct Blue 15	24.6 \pm 2.26	145 \pm 30.9	12.7 \pm 0.54	37.9 \pm 6.47	5.9	3.0

Discussion

The goal of this Chapter was to utilize a Δ azoC knockout mutant in *C. perfringens* strain ATCC 3626 to understand both the effect of the AzoC enzyme on the bacteria, as well as to complete a physiological study to understand the effect of azo dye exposure to *C. perfringens* strain ATCC 3626.

AzoC appears to be not be important for the reduction of Methyl Red, Methyl Orange, or Tartrazine. *C. perfringens* Wild Type cells are capable of strong dye reduction of all three dyes (p-value <0.05, 95% confidence) (Table 10A, 10B, 10D). However, in the *C. perfringens* Δ azoC

knockout mutant, the absence of AzoC does not have any effect on the dye reduction capability of the *C. perfringens* cells (p-values >0.05, 95% confidence) (Table 10A, 10B, 10D). This suggests that AzoC is not responsible for reducing these three azo dyes. This is confirmed by looking at pure enzyme data from AzoC, which shows that AzoC is not able to significantly reduce these three azo dyes under pure enzyme conditions (p-values >0.05, 95% confidence) (Table 10A, 10B, 10D). Because *C. perfringens* cells are able to reduce these azo dyes quite readily, there must be other enzymes present which are capable of reducing these azo dyes.

On the other hand, AzoC appears to be principally responsible for the reduction of Eriochrome Black T, Ponceau BS, Congo Red, Ponceau S, Trypan Blue and Direct Blue 15. In all cases, the *C. perfringens* Wild Type cells were able to significantly reduce these dyes (p-values <0.05, 95% confidence) (Table 10C, 10E, 10F, 10G, 10H and 10I). When the *azoC* gene was knocked out, though, dye reduction was significantly decreased compared to that of the Wild Type cells (p-value <0.05, 95% confidence) (Table 10C, 10E, 10F, 10G, 10H and 10I). This suggests that AzoC is primarily responsible for the reduction of these azo dyes. The reduction of these azo dyes was not eliminated, however, but rather slowed (Table 10C, 10E, 10F, 10G, 10H and 10I). In all cases, the dye reduction ability of the *C. perfringens* Δ *azoC* knockout mutant was able, over time, to recover and reduce these azo dyes to the full amount that the Wild Type could (Table 10C, 10E, 10F, 10G, 10H and 10I). This suggests that, while AzoC appears to be primarily responsible for the reduction of these azo dyes, it is not the only enzyme that can reduce these dyes. The results suggest that there is another enzyme (or enzymes) present that, upon exposure to the azo dyes, is able to be produced to recover the dye reduction ability for these azo dyes.

Interestingly, it seems as though AzoC preferentially reduces larger azo dyes, Eriochrome Black T, Ponceau BS, Congo Red, Ponceau S, Trypan Blue and Direct Blue 15, but does not break down the smaller azo dyes, such as Methyl Red, Methyl Orange and Tartrazine. Other azoreductases that have been studied, such as AzoR (*E. coli*) and AzoM (*E. faecium*),

preferentially reduce Methyl Red and Methyl Orange, but do not reduce larger azo dyes (Chen *et al*, 2004; Nakanishi *et al*, 2001). Using the AzoC, AzoR (*Escherichia coli*) and AzoM (*Enterococcus faecium*) nucleotide sequences, the known *C. perfringens* ATCC 3626 genome was analyzed by BLAST and three potential new azoreductase sequences were identified. The first, we will call AzoC2, is listed as a putative NADPH-dependent FMN reductase and shows a 20% identity to the AzoC studied here. The second and third, called AzoC3 and AzoC4, are listed as flavodoxin family proteins and show 24-30% identity to AzoM and AzoR. AzoC3 and AzoC4 share only 10% identity with the AzoC studied here and AzoC2, suggesting that they may be structurally and functionally unique when compared to the AzoC studied here and AzoC2. Overall, the coupled physiology study results with the genome BLAST results suggest that there are additional azoreductases present in *C. perfringens* strain ATCC 3626 that may be both structurally and functionally unique, supporting variable dye specificities. The preliminary data here supports the need for additional protein studies to fully understand the mechanism of all azoreductases in this important bacterium, as azoreductases may play an important role in the physiological response in *C. perfringens*.

Cibacron Brilliant Red 3B-A appears to be a unique case for an azo dye amongst those tested here. Results with this azo dye suggest that its reduction is favorable under any condition, including in a bacteria that is not capable of azo dye reduction (*B. infantis*). This, coupled with findings from Chapter 3, suggests that Cibacron Brilliant Red 3B-A is strongly reduced under non-enzymatic conditions and its use as an azo dye for azoreduction testing should be taken with caution (Morrison & John, 2013).

In almost all azo dye cases, the strongest dye reduction activity was seen in rich media (BHI), while the minimal media (CMM) showed a slowed dye reduction activity rate. This suggests that, because growth is slower in the minimal media as compared to the rich media, that the azoreductases are still being produced, just at a reduced rate as well. This is further

exaggerated by the growth arrest (PBSG) media, which shows dye reduction occurring at an even slower pace. Because the *C. perfringens* cells are not actively growing the PBSG media, it can be reasoned that any dye reduction seen is the result of the already produced azoreductases. Thus, azoreductase production is constitutive in the *C. perfringens* cells.

There is also a significant effect of azo dyes on *C. perfringens* growth. This phenomenon only seems to occur when the cells are grown in rich media (BHI). In the case of Ponceau BS, the generation time is increased 7-fold as compared to Wild Type cells grown in the absence of the dye (p-value <0.05, 95% confidence) (Figure 40A). The same increase is not seen when the cells are grown in minimal media (p-value >0.05, 95% confidence) (CMM) (Figure 40B). From the dye reduction studies, it is shown that Ponceau BS is readily reduced by the *C. perfringens* Wild Type cells, so along with the Ponceau BS dye, there are metabolites in the mix as well. It is hypothesized that, because rich media is undefined, that there may be components of the media that are interacting with the dye metabolites, creating this increased generation time that is seen here. If this is the case, in the defined minimal media, it would be hypothesized that the increased generation time would not be seen, as is the case. Thus it is thought that the complex undefined media and its interaction with the specific azo dye metabolites are what is causing the increased generation time.

When the generation time is observed throughout log phase, it is noticed that the increased generation time tends to occur during later log phase (p-value <0.05, 95% confidence) (Table 12). This is consistent with the hypothesis that the metabolites are interacting with the rich media. As time goes on, more metabolites are being produced to interact with the media, causing a build-up of products which in turn can cause a further increase in generation time. In addition, *B. infantis* does not show any generation time related effects in the presence of all of the azo dyes tested (p-value >0.05, 95% confidence). Because *B. infantis* does not readily break down these

dyes, the hypothesis holds. Without the metabolites present to interact with the rich media, the *B. infantis* cells are unaffected.

In addition to this, for the dyes which AzoC is capable of reducing (Ponceau BS, Ponceau S, Trypan Blue, Direct Blue 15), we see that the increase in generation time in rich media with the *ΔazoC* mutant is significantly decreased over that of the Wild Type (p-value <0.05, 95% confidence) (Figure 40A). This also supports the hypothesis that the azo dye metabolites are interacting with the rich media to cause the toxicity seen. These four azo dyes are readily reduced by the Wild Type. However, when the *azoC* gene is knocked out, dye reduction is slowed significantly (p-value <0.05, 95% confidence), meaning that fewer metabolites are produced for these azo dyes; less metabolites being produced can equal less toxicity for the hypothesis previously stated. In addition, for these four azo dyes, the late log phase generation time effect is fold differences lower than that of the Wild Type (Table 12).

The azo dyes which show an increased generation time are Tartrazine, Methyl Red, Methyl Orange, Ponceau BS, Ponceau S, Trypan Blue and Direct Blue 15. All of these dyes have varying structures, degrees of polarity and sizes, making it difficult to understand why these azo dyes influence generation time, and not Eriochrome Black T, Congo Red or Cibacron Brilliant Red 3B-A. However, to date, azo dyes themselves have not been found to be toxic to microorganisms (Brown & Devito, 1993). It is also difficult to predict whether the increased generation time is coming from the azo dye, the metabolites, or further metabolic breakdown products, or a combination of any of the above with the components of the undefined rich media (Brown & Devito, 1993). Additional research will need to be completed to understand the mechanism that is increasing the generation time.

In conclusion, this study provides the first look at the physiology of *C. perfringens* upon azo dye exposure and the effect of the azo dyes on bacterial growth.

CHAPTER VII

FINAL DISCUSSION

Azo dyes are ubiquitous in nature, being found in industries spanning foods and beverages to pharmaceuticals and textiles to cosmetics. Azo dyes are constantly coming into contact with both our bodies and the environment. The toxicity of the parent azo dyes is known and has been well-studied, especially those for human consumption. However, the enzymes that are capable of breaking these azo dyes down into aromatic amines and the affect these dyes have on bacteria are not quite so black-and-white. Thus, the study of azoreductase enzymes and azo dyes is important from both a human health and environmental standpoint.

Clostridium perfringens is a strictly anaerobic inhabitant of both the human gastrointestinal tract, as well as the environment and is thus a good candidate to study for this important enzyme. It has been confirmed here that *C. perfringens* does produce an azoreductase enzyme, with several other additional azoreductase enzymes proposed as well. This azoreductase enzyme, AzoC, is very different from other well-studied azoreductases which originate from aerobic bacteria. Sequentially, the nearest neighbor to AzoC shares only 13% identity. In addition, AzoC contains an FAD cofactor, whereas other azoreductases contain an FMN cofactor. Also, AzoC is trimeric in structure, being held together by disulfide bonding, which is also unique amongst azoreductases. AzoC also has a distinctively different substrate preference in that it prefers to reduce larger, sulfonated azo dyes (i.e. Direct Blue 15), whereas other azoreductases

have a preference for the opposite, smaller azo dyes (i.e. Methyl Red). In addition, AzoC has been found to function extracellularly. Despite the large breadth of work presented here on AzoC, there is still much lacking from the field of azoreductase research in general. The major literature gap concerns a lack of information regarding the true substrate of AzoC as well as other azoreductases. Because azo dyes have only been recently introduced into our bodies and into the environment as anthropogenic pollutants, it is highly unlikely that the true substrate of these enzymes is an azo dye, as there is only one naturally occurring compound with an azo bond (4,4'-dihydroxyazobenzene) (Stolz, 2001). Recent work with aerobic bacteria has shown dual functionality of azoreductase and quinone reductase (Liu *et al*, 2009; Ryan *et al*, 2010). Therefore, it is likely that azoreductases have a larger purpose, rather than azo dye reduction, as enzymes under the larger classification of oxidoreductase (a group of which azoreductase is included) have many different functions (Kultz, 2005).

The first dual function azoreductase/quinone reductase studied was AzoR of *E. coli* (Liu *et al*, 2009). The researchers developed the idea that dual enzymatic function was present after a homology alignment of AzoR found significant homology to structurally-known quinone reductases, such as ChrR of *Pseudomonas putida* (Liu *et al*, 2009). In their 2009 manuscript detailing the dual functionality of the azoreductase enzyme, the authors showed AzoR is specifically involved in the two-electron reduction scheme of quinone reduction in which reactive oxygen species are linked to glutathione and excreted (Liu *et al*, 2009). They have linked this process, in *E. coli*, to the avoidance of oxidative stress by the creation of a mutant strain which showed significant impaired growth under the presence of quinones without the quinone reductase gene (Liu *et al*, 2009). Because the overall mechanism for the elimination of oxidative stress in *C. perfringens* is largely unknown to date, we hypothesize that a similar mechanism is present within this medically-relevant bacterium which would largely contribute to the ability of *C. perfringens* to resist the oxidative stress of the host innate immune response, increase the

bacterial survivability and pathogenicity under this condition, as well as detoxify reactive oxygen species produced by fluoroquinone antibiotics, leading to the development of antibiotic resistance.

General quinone reductase activity has been shown in another *Clostridium* species, *C. tyrobutyricum* (Petitdemange *et al*, 1980). Despite this lack of information on a quinone reductase in *C. perfringens*, a BLAST of the available genome shows that this important bacterium contains genes required to support the quinone reductase activity such as a glutathione biosynthetic system that is capable of producing glutathione to detoxify and eliminate reactive oxygen species (Copley & Dhillon, 2002; Fahey *et al*, 1978; Kino *et al*, 2007). Specific genes identified include the glutathione gamma glutamyl cysteine synthetase, glutathione synthetase peroxidase and glutamate cysteine ligase. Initial studies within the laboratory suggest that AzoC possesses the ability to reduce quinone compounds (menadione, lawsone, 1,4-naphthoquinone, 2,6-dichloroquinone and 1,4-dihydroxynaphthalene), as measured by the oxidation and subsequent loss of signal at 430nm for NADPH.

The possible role of azoreductase enzymes in stress response has also been supported by a recent transcriptomics analysis looking at the transcriptomes of enterohemorrhagic *E. coli* O157:H7 under many different environmental conditions (Landstorfer *et al*, 2014). Specifically, the authors found that the azoreductase gene of *E. coli* (AzoR) was upregulated when found on radish sprout roots (Landstorfer *et al*, 2014). The authors suggested the role of this enzyme in stress response, specifically as an enzyme involved in the detoxification of secondary plant metabolites (Landstorfer *et al*, 2014).

In conclusion, although much has recently been discovered about azoreductases and AzoC, much is still yet to be discovered in the field. The upcoming discoveries may prove to be the most beneficial to human and environmental health.

REFERENCES

- Abraham KJ, John GH (2007) Development of a classification scheme using a secondary and tertiary amino acid analysis of azoreductase gene. *Journal of Medical and Biological Sciences* **1**: 1-5
- Ahmad N, Drew WL, Plorde JJ (2010) *Sherris Medical Microbiology*, Fifth edn. New York: The McGraw Hill Companies.
- Alam SI, Bansod S, Kumar RB, Sengupta N, Singh L (2009) Differential proteomic analysis of *Clostridium perfringens* ATCC13124; identification of dominant, surface and structure associated proteins. *BMC Microbiology* **9**: 162-174
- Angelotti R, Hall HE, Foter MJ, Lewis KH (1962) Quantitation of *Clostridium perfringens* in foods. *Applied Microbiology* **10**: 193-199
- Arrondo JLR, Muga A, Castresana J, Goni FM (1993) Quantitative studies of the structure of proteins in solution by fourier-transform infrared-spectroscopy. *Progress in Biophysics & Molecular Biology* **59**: 23-56
- Arumugam M, Raes J, Pelletier E, Le Paslier D, Yamada T, Mende DR, Fernandes GR, Tap J, Bruls T, Batto JM *et al* (2011) Enterotypes of the human gut microbiome. *Nature* **473**: 174-180
- Axley MJ, Fairman R, Yanchunas J, Villafranca JJ, Robertson JG (1997) Spectroscopic properties of *Escherichia coli* UDP-N-acetylenolpyruvylglucosamine reductase. *Biochemistry* **36**: 812-822
- Bafana A, Chakrabarti T, Devi SS (2008) Azoreductase and dye detoxification activities of *Bacillus velezensis* strain AB. *Applied Microbiology and Biotechnology* **77**: 1139-1144
- Bardi L, Marzona M (2010) Factors affecting the complete mineralization of azo dyes. In *Biodegradation of Azo Dyes*, Erkurt HA (ed), Vol. 9, pp 195-210. Berlin: Springer Verlag
- Barth A, Zscherp C (2002) What vibrations tell us about proteins. *Quarterly Reviews of Biophysics* **35**: 369-430
- Beebe JS, Mountjoy K, Krzesicki RF, Perini F, Ruddon RW (1990) Role of disulfide bond formation in the folding of human chorionic gonadotropin beta subunit into an alpha beta dimer assembly competent form. *Journal of Biological Chemistry* **265**: 312-317
- Bendtsen JD, Kiemer L, Fausboll A, Brunak S (2005) Non-classical protein secretion in bacteria. *BMC Microbiology* **5**: 58-70

- Berks BC, Palmer T, Sargent F (2005) Protein targeting by the bacterial twin-arginine translocation (Tat) pathway. *Current Opinion in Microbiology* **8**: 174-181
- Berman HM, Westbrook J, Feng Z, Gilliland G, Bhat TN, Weissig H, Shindyalov IN, Bourne PE (2000) The protein data bank. *Nucleic Acids Research* **28**: 235-242
- Bin Y, Jiti Z, Jing W, Cuihong D, Hongman H, Zhiyong S, Yongming B (2004) Expression and characteristics of the gene encoding azoreductase from *Rhodobacter sphaeroides* ASI.1737. *FEMS Microbiology Letters* **236**: 129-136
- Blumel S, Knackmuss HJ, Stolz A (2002) Molecular cloning and characterization of the gene coding for the aerobic azoreductase from *Xenophilus azovorans* KF46F. *Applied and Environmental Microbiology* **68**: 3948-3955
- Blumel S, Stolz A (2003) Cloning and characterization of the gene coding for the aerobic azoreductase from *Pigmentiphaga kullae* K24. *Applied Microbiology and Biotechnology* **62**: 186-190
- Borriello SP (2000) Microbial flora of the gastrointestinal tract. In *Microbial Metabolism in the Gastrointestinal Tract*, Hill MJ (ed), pp 1-19. Boca Raton, FL: CRC Press
- Bradford MM (1976) Rapid and sensitive method for quantitation of microgram quantities of protein utilizing principle of protein-dye binding. *Analytical Biochemistry* **72**: 248-254
- Bragger JL, Lloyd AW, Soozandehfar SH, Bloomfield SC, Marriott C, Martin GP (1997) Investigations into the azo reducing activity of a common colonic microorganism. *International Journal of Pharmaceutics* **157**: 61-71
- Brown MA, Devito SC (1993) Predicting azo dye toxicity. *Critical Reviews in Environmental Science and Technology* **23**: 249-324
- Bruggemann H, Baumer S, Fricke WF, Wiezer A, Liesegang H, Decker I, Herzberg C, Martinez-Arias R, Merkl R, Henne A *et al* (2003) The genome sequence of *Clostridium tetani*, the causative agent of tetanus disease. *Proceedings of the National Academy of Sciences of the United States of America* **100**: 1316-1321
- Bukau B, Horwich AL (1998) The Hsp70 and Hsp60 chaperone machines. *Cell* **92**: 351-366
- Bulbulyan MA, Figs LW, Zahm SH, Savitskaya T, Goldfarb A, Astashevsky S, Zaridze D (1995) Cancer incidence and mortality among beta-naphthylamine and benzidine dye workers in Moscow. *International Journal of Epidemiology* **24**: 266-275
- Caldwell DR (2000) *Microbial Physiology and Metabolism*, Second edn. Belmont, CA: Star Publishing Company.
- Carlsson F, Stalhammar-Carlemalm M, Flardh K, Sandin C, Carlemalm E, Lindahl G (2006) Signal sequence directs localized secretion of bacterial surface proteins. *Nature* **442**: 943-946

- Cartwright RA (1983) Historical and modern epidemiological-studies on populations exposed to N-substituted aryl compounds. *Environmental Health Perspectives* **49**: 13-19
- Chang JS, Chou C, Chen SY (2001) Decolorization of azo dyes with immobilized *Pseudomonas luteola*. *Process Biochemistry* **36**: 757-763
- ChemAxon. (2014) ChemAxon. In Chemicalize.org (ed.).
- Chen CY, Kuo JT, Cheng CY, Huang YT, Ho IH, Chung YC (2009) Biological decolorization of dye solution containing malachite green by *Pandoraea pulmonicola* YC32 using a batch and continuous system. *Journal of Hazardous Materials* **172**: 1439-1445
- Chen HZ (2006) Recent advances in azo dye degrading enzyme research. *Current Protein & Peptide Science* **7**: 101-111
- Chen HZ, Feng JH, Kweon O, Xu HY, Cerniglia CE (2010) Identification and molecular characterization of a novel flavin-free NADPH preferred azoreductase encoded by *azoB* in *Pigmentiphaga kullae* K24. *BMC Biochemistry* **11**: 13-22
- Chen HZ, Hopper SL, Cerniglia CE (2005a) Biochemical and molecular characterization of an azoreductase from *Staphylococcus aureus*, a tetrameric NADPH-dependent flavoprotein. *Microbiology* **151**: 1433-1441
- Chen HZ, Wang RF, Cerniglia CE (2004) Molecular cloning, overexpression, purification, and characterization of an aerobic FMN-dependent azoreductase from *Enterococcus faecalis*. *Protein Expression and Purification* **34**: 302-310
- Chen Y, Caruso L, McClane B, Fisher D, Gupta P (2007) Disruption of a toxin gene by introduction of a foreign gene into the chromosome of *Clostridium perfringens* using targetron-induced mutagenesis. *Plasmid* **58**: 182-189
- Chen Y, McClane BA, Fisher DJ, Rood JI, Gupta P (2005b) Construction of an alpha toxin gene knockout mutant of *Clostridium perfringens* type A by use of a mobile group II intron. *Applied and Environmental Microbiology* **71**: 7542-7547
- Chung KT (1997) Gastrointestinal toxicology of monogastrics. In *Gastrointestinal Microbiology*, Mackie R, White B, Isaacson RE (eds), Vol. 1, pp 511-582. Springer Science & Business Media
- Chung KT, Cerniglia CE (1992) Mutagenicity of azo dyes - structure activity relationships. *Mutation Research* **277**: 201-220
- Chung KT, Chen SC, Claxton LD (2006) Review of the *Salmonella typhimurium* mutagenicity of benzidine, benzidine analogues, and benzidine-based dyes. *Mutation Research-Reviews in Mutation Research* **612**: 58-76
- Chung KT, Chen SC, Wong TY, Li YS, Wei CI, Chou MW (2000) Mutagenicity studies of benzidine and its analogs: structure-activity relationships. *Toxicological Sciences* **56**: 351-356

- Chung KT, Stevens SE (1993) Degradation of azo dyes by environmental microorganisms and helminths. *Environmental Toxicology and Chemistry* **12**: 2121-2132
- Chung KT, Stevens SE, Cerniglia CE (1992) The reduction of azo dyes by the intestinal microflora. *Critical Reviews in Microbiology* **18**: 175-190
- Claesson MJ, O'Sullivan O, Wang Q, Nikkila J, Marchesi JR, Smidt H, de Vos WM, Ross RP, O'Toole PW (2009) Comparative analysis of pyrosequencing and a phylogenetic microarray for exploring microbial community structures in the human distal intestine. *Plos One* **4**: e6669
- Cole JN, Ramirez RD, Currie BJ, Cordwell SJ, Djordjevic SP, Walker MJ (2005) Surface analyses and immune reactivities of major cell wall-associated proteins of group a *Streptococcus*. *Infection and Immunity* **73**: 3137-3146
- Compton LA, Johnson WC (1986) Analysis of protein circular dichroism spectra for secondary structure using a simple matrix multiplication. *Analytical Biochemistry* **155**: 155-167
- Copley SD, Dhillon JK (2002) Lateral gene transfer and parallel evolution in the history of glutathione biosynthesis genes. *Genome Biology* **3**: 1-16
- Correia B, Chen ZJ, Mendes S, Martins LO, Bento I (2011) Crystallization and preliminary X-ray diffraction analysis of the azoreductase PpAzoR from *Pseudomonas putida* MET94. *Acta Crystallographica Section F-Structural Biology and Crystallization Communications* **67**: 121-123
- Creighton TE (1992) *Proteins: Structures and Molecular Properties*, Second edn. New York: W. H. Freeman and Company.
- Daniels R, Mellroth P, Bernsel A, Neiers F, Normark S, von Heijne G, Henriques-Normark B (2010) Disulfide bond formation and cysteine exclusion in Gram-positive bacteria. *Journal of Biological Chemistry* **285**: 3300-3309
- Decatur SM (2006) Elucidation of residue-level structure and dynamics of polypeptides via isotopically-edited infrared spectroscopy. *Accounts of Chemical Research* **39**: 169-175
- DeDent A, Bae T, Missiakas DM, Schneewind O (2008) Signal peptides direct surface proteins to two distinct envelope locations of *Staphylococcus aureus*. *Embo Journal* **27**: 2656-2668
- Derman AI, Prinz WA, Belin D, Beckwith J (1993) Mutations that allow disulfide bond formation in the cytoplasm of *Escherichia coli*. *Science* **262**: 1744-1747
- Desvaux M, Khan A, Scott-Tucker A, Chaudhuri RR, Pallen MJ, Henderson IR (2005) Genomic analysis of the protein secretion systems in *Clostridium acetobutylicum* ATCC 824. *Biochimica Et Biophysica Acta* **1745**: 223-253
- Dillon D, Combes R, Zeiger E (1994) Activation by cecal reduction of the azo dye D&C Red No. 9 to a bacterial mutagen. *Mutagenesis* **9**: 295-299

- dos Santos AB, Cervantes FJ, van Lier JB (2007) Review paper on current technologies for decolourisation of textile wastewaters: perspectives for anaerobic biotechnology. *Bioresource Technology* **98**: 2369-2385
- Fahey RC, Brown WC, Adams WB, Worsham MB (1978) Occurrence of glutathione in bacteria. *Journal of Bacteriology* **133**: 1126-1129
- Fallingborg J (1999) Intraluminal pH of the human gastrointestinal tract. *Danish Medical Bulletin* **46**: 183-196
- Feng JH, Heinze TM, Xu HY, Cerniglia CE, Chen HZ (2010) Evidence for significantly enhancing reduction of azo dyes in *Escherichia coli* by expressed cytoplasmic azoreductase (AzoA) of *Enterococcus faecalis*. *Protein and Peptide Letters* **17**: 578-584
- Feng JH, Kweon O, Xu HY, Cerniglia CE, Chen HZ (2012) Probing the NADH- and Methyl Red-binding site of a FMN-dependent azoreductase (AzoA) from *Enterococcus faecalis*. *Archives of Biochemistry and Biophysics* **520**: 99-107
- Filippova EV, Wawrzak Z, Kudritska M, Edwards A, Savchenko A, Anderson WF. (2010) Crystal structure of azoreductase from *Bacillus anthracis* str. Sterne. In Diseases CfSGoI (ed.), *PDB.org*.
- Finegold SM, Flora DJ, Attebery HR, Sutter VL (1975) Fecal bacteriology of colonic polyp patients and control patients. *Cancer Research* **35**: 3407-3417
- Forster BM, Marquis H (2012) Protein transport across the cell wall of monoderm Gram-positive bacteria. *Molecular Microbiology* **84**: 405-413
- Frankel MB, Wojcik BM, DeDent AC, Missiakas DM, Schneewind O (2010) ABI domain-containing proteins contribute to surface protein display and cell division in *Staphylococcus aureus*. *Molecular Microbiology* **78**: 238-252
- Fuchs AR, Bonde GJ (1957) The nutritional requirements of *Clostridium perfringens*. *Journal of General Microbiology* **16**: 317-329
- Gandolfi (1991) *Casarett and Doull's Toxicology: The Basic Science of Poisons*, Fourth edn. Highstown, NJ: McGraw Hill.
- Ghosh DK, Ghosh S, Sadhukhan P, Mandal A, Chaudhuri J (1993) Purification of two azoreductases from *Escherichia coli* K12. *Indian Journal of Experimental Biology* **31**: 951-954
- Ghosh DK, Mandal A, Chaudhuri J (1992) Purification and partial characterization of two azoreductases from *Shigella dysenteriae* type 1. *FEMS Microbiology Letters* **98**: 229-233
- Gilbert HF (1990) Molecular and cellular aspects of thiol disulfide exchange. *Advances in Enzymology and Related Areas of Molecular Biology* **63**: 69-172
- Gill M, Strauch RJ (1984) Constituents of *Agaricus-Xanthodermus Geneviev* - the 1st naturally endogenous azo compound and toxic phenolic metabolites. *Zeitschrift Fur Naturforschung C-a Journal of Biosciences* **39**: 1027-1029

- Gill SR, Pop M, DeBoy RT, Eckburg PB, Turnbaugh PJ, Samuel BS, Gordon JI, Relman DA, Fraser-Liggett CM, Nelson KE (2006) Metagenomic analysis of the human distal gut microbiome. *Science* **312**: 1355-1359
- Gingell R, Walker R (1971) Mechanisms of azo reduction by *Streptococcus faecalis*. II. The role of soluble flavins. *Xenobiotica* **1**: 231-239
- Goldin BR (1990) Intestinal microflora - metabolism of drugs and carcinogens. *Annals of Medicine* **22**: 43-48
- Goujon M, McWilliam H, Li WZ, Valentin F, Squizzato S, Paern J, Lopez R (2010) A new bioinformatics analysis tools framework at EMBL-EBI. *Nucleic Acids Research* **38**: W695-W699
- Gray WR (1993) Disulfide structures of highly bridged peptides - a new strategy for analysis. *Protein Science* **2**: 1732-1748
- Gregory EM, Moore WE, Holdeman LV (1978) Superoxide dismutase in anaerobes: survey. *Applied and Environmental Microbiology* **35**: 988-991
- Guarner F, Malagelada JR (2003) Gut flora in health and disease. *Lancet* **361**: 512-519
- Gueimonde M, Delgado S, Mayo B, Ruas-Madiedo P, Margolles A, de los Reyes-Gavilan CG (2004) Viability and diversity of probiotic *Lactobacillus* and *Bifidobacterium* populations included in commercial fermented milks. *Food Research International* **37**: 839-850
- Gupta P, Chen Y (2008) Chromosomal engineering of *Clostridium perfringens* using group II introns. In *Chromosomal Engineering*, Davis G, Kayser KJ (eds), pp 217-228. Totowa, New Jersey: Humana Press
- Hagymasi K, Blazovics A, Lengyel G, Kocsis I, Feher J (2001) Oxidative damage in alcoholic liver disease. *European Journal of Gastroenterology & Hepatology* **13**: 49-53
- Hall HE, Angelotti R (1965) *Clostridium perfringens* in meat and meat products. *Applied Microbiology* **13**: 352-357
- Hanninen O, Lindstromseppa P, Pelkonen K (1987) Role of gut in xenobiotic metabolism. *Archives of Toxicology* **60**: 34-36
- Heap JT, Cartman ST, Kuehne SA, Cooksley CM, Minton NP (2010a) ClosTron-targeted mutagenesis. *Methods in Molecular Biology* **646**: 165-182
- Heap JT, Kuehne SA, Ehsaan M, Cartman ST, Cooksley CM, Scott JC, Minton NP (2010b) The ClosTron: Mutagenesis in *Clostridium* refined and streamlined. *Journal of Microbiological Methods* **80**: 49-55
- Heap JT, Pennington OJ, Cartman ST, Carter GP, Minton NP (2007) The ClosTron: A universal gene knock-out system for the genus *Clostridium*. *Journal of Microbiological Methods* **70**: 452-464

- Hsueh CC, Chen BY (2008) Exploring effects of chemical structure on azo dye decolorization characteristics by *Pseudomonas luteola*. *Journal of Hazardous Materials* **154**: 703-710
- Huang MT, Miwa GT, Cronheim N, Lu AYH (1979) Rat liver cytosolic azoreductase - electron transport properties and the mechanism of dicumarol inhibition of the purified enzyme. *Journal of Biological Chemistry* **254**: 1223-1227
- Humann J, Lenz LL (2009) Bacterial peptidoglycan degrading enzymes and their impact on host muropeptide detection. *Journal of Innate Immunity* **1**: 88-97
- Hwang C, Sinskey AJ, Lodish HF (1992) Oxidized redox state of glutathione in the endoplasmic reticulum. *Science* **257**: 1496-1502
- Idaka E, Horitsu H, Ogawa T (1987) Some properties of azoreductase produced by *Pseudomonas cepacia*. *Bulletin of Environmental Contamination and Toxicology* **39**: 982-989
- Ido Y, Kilo C, Williamson JR (1997) Cytosolic NADH/NAD(+), free radicals, and vascular dysfunction in early diabetes mellitus. *Diabetologia* **40**: S115-S117
- Institute JCV. In Resource TIfGRCM (ed.).
- Ito K, Nakanishi M, Lee WC, Sasaki H, Zenno S, Saigo K, Kitade Y, Tanokura M (2005) Crystallization and preliminary X-ray analysis of AzoR (azoreductase) from *Escherichia coli*. *Acta Crystallographica Section F, Structural Biology and Crystallization Communications* **61**: 399-402
- Ito K, Nakanishi M, Lee WC, Sasaki H, Zenno S, Saigo K, Kitade Y, Tanokura M (2006) Three-dimensional structure of AzoR from *Escherichia coli* - an oxidoreductase conserved in microorganisms. *Journal of Biological Chemistry* **281**: 20567-20576
- Ito K, Nakanishi M, Lee WC, Zhi Y, Sasaki H, Zenno S, Saigo K, Kitade Y, Tanokura M (2008) Expansion of substrate specificity and catalytic mechanism of azoreductase by X-ray crystallography and site-directed mutagenesis. *Journal of Biological Chemistry* **283**: 13889-13896
- Iwasaki K, Murayama N, Koizumi R, Uno Y, Yamazaki H (2010) Comparison of cytochrome P450 3A enzymes in cynomolgus monkeys and humans. *Drug Metabolism and Pharmacokinetics* **25**: 388-391
- Jean D, Briolat V, Reyssset G (2004) Oxidative stress response in *Clostridium perfringens*. *Microbiology* **150**: 1649-1659
- Johansson HE, Johansson MK, Wong AC, Armstrong ES, Peterson EJ, Grant RE, Roy MA, Reddington MV, Cook RM (2011) BTII, an azoreductase with pH-dependent substrate specificity. *Applied and Environmental Microbiology* **77**: 4223-4225
- John DM, Weeks KM (2000) van't Hoff enthalpies without baselines. *Protein Science* **9**: 1416-1419
- Jones DT, Taylor WR, Thornton JM (1992) The rapid generation of mutation data matrices from protein sequences. *Computer Applications in the Biosciences : CABIOS* **8**: 275-282

- Jordan S, Hutchings MI, Mascher T (2008) Cell envelope stress response in Gram-positive bacteria. *FEMS Microbiology Reviews* **32**: 107-146
- Kelly SM, Jess TJ, Price NC (2005) How to study proteins by circular dichroism. *Biochimica Et Biophysica Acta-Proteins and Proteomics* **1751**: 119-139
- Kelly SM, Price NC (2000) The use of circular dichroism in the investigation of protein structure and function. *Current Protein & Peptide Science* **1**: 349-384
- Kino K, Kuratsu S, Noguchi A, Kokubo M, Nakazawa Y, Arai T, Yagasaki M, Kirimura K (2007) Novel substrate specificity of glutathione synthesis enzymes from *Streptococcus agalactiae* and *Clostridium acetobutylicum*. *Biochemical and Biophysical Research Communications* **352**: 351-359
- Korzeniewski C, Callewaert DM (1983) An enzyme-release assay for natural cytotoxicity. *Journal of Immunological Methods* **64**: 313-320
- Kostanski LK, Keller DM, Hamielec AE (2004) Size-exclusion chromatography - a review of calibration methodologies. *Journal of Biochemical and Biophysical Methods* **58**: 159-186
- Kultz D (2005) Molecular and evolutionary basis of the cellular stress response. *Annual Review of Physiology* **67**: 225-257
- Laemmli UK (1970) Cleavage of structural proteins during the assembly of the head of bacteriophage T4. *Nature* **227**: 680-685
- Landstorfer R, Simon S, Schober S, Keim D, Scherer S, Neuhaus K (2014) Comparison of strand-specific transcriptomes of enterohemorrhagic *Escherichia coli* O157:H7 EDL933 (EHEC) under eleven different environmental conditions including radish sprouts and cattle feces. *BMC Genomics* **15**: 1-25
- Lees JG, Miles AJ, Wien F, Wallace BA (2006) A reference database for circular dichroism spectroscopy covering fold and secondary structure space. *Bioinformatics* **22**: 1955-1962
- Lemaire M, Viel A, Moller JV (1989) Size exclusion chromatography and universal calibration of gel columns. *Analytical Biochemistry* **177**: 50-56
- Levine RL, Wehr N, Williams JA, Stadtman ER, Shacter E (2000) Determination of carbonyl groups in oxidized proteins. *Methods in Molecular Biology* **99**: 15-24
- Levine WG (1991) Metabolism of azo dyes - implication for detoxication and activation. *Drug Metabolism Reviews* **23**: 253-309
- Li JH, McClane BA (2008) A novel small acid soluble protein variant is important for spore resistance of most *Clostridium perfringens* food poisoning isolates. *Plos Pathogens* **4**: e1000056-e1000066
- Li JH, McClane BA (2010) Evaluating the involvement of alternative sigma factors sigF and sigG in *Clostridium perfringens* sporulation and enterotoxin synthesis. *Infection and Immunity* **78**: 4286-4293

- Liu GF, Zhou JT, Fu QS, Wang J (2009) The *Escherichia coli* azoreductase AzoR is involved in resistance to thiol-specific stress caused by electrophilic quinones. *Journal of Bacteriology* **191**: 6394-6400
- Liu ZJ, Chen HZ, Shaw N, Hopper SL, Chen LR, Chen SW, Cerniglia CE, Wang BC (2007) Crystal structure of an aerobic FMN-dependent azoreductase (AzoA) from *Enterococcus faecalis*. *Archives of Biochemistry and Biophysics* **463**: 68-77
- Macfarlane GT, Gibson GR (1994) *Metabolic Activities of the Normal Colonic Flora*, London: Springer-Verlag.
- Macwana SR, Punj S, Cooper J, Schwenk E, John GH (2010) Identification and isolation of an azoreductase from *Enterococcus faecium*. *Current Issues in Molecular Biology* **12**: 43-48
- Madigan MT, Martinko JM, Dunlap PV, Clark DP (2009) *Brock Biology of Microorganisms*, Twelfth edn. San Francisco, CA: Pearson Benjamin Cummings.
- Maier J, Kandelbauer A, Erlacher A, Cavaco-Paulo A, Gubitz GM (2004) A new alkali-thermostable azoreductase from *Bacillus sp* strain SF. *Applied and Environmental Microbiology* **70**: 837-844
- Marmion D (1991) *Handbook of U.S. Colorants: Foods, Drugs and Cosmetics, and Medical Devices*, Third edn. New York: John Wiley & Sons.
- Matias VR, Beveridge TJ (2008) Lipoteichoic acid is a major component of the *Bacillus subtilis* periplasm. *Journal of Bacteriology* **190**: 7414-7418
- Mergny JL, Lacroix L (2003) Analysis of thermal melting curves. *Oligonucleotides* **13**: 515-537
- Moller P, Wallin H (2000) Genotoxic hazards of azo pigments and other colorants related to 1-phenylazo-2-hydroxynaphthalene. *Mutation Research-Reviews in Mutation Research* **462**: 13-30
- Moore WEC, Holdeman LV (1974) Human fecal flora - normal flora of 20 Japanese-Hawaiians. *Applied Microbiology* **27**: 961-979
- Morl S (1981) Calibration of size exclusion chromatography columns for determination of polymer molecular weight distribution. *Journal of Analytical Chemistry* **53**: 1813-1818
- Morrison J, Dai S, Ren J, Taylor A, Wilkerson M, John G, Xie AH (2014) Structure and stability of an azoreductase with an FAD cofactor from the strict anaerobe *Clostridium perfringens*. *Protein and Peptide Letters* **21**: 523-534
- Morrison JM, John GH (2013) The non-enzymatic reduction of azo dyes by flavin and nicotinamide cofactors under varying conditions. *Anaerobe* **23**: 87-96
- Morrison JM, Wright CM, John GH (2012) Identification, isolation and characterization of a novel azoreductase from *Clostridium perfringens*. *Anaerobe* **18**: 229-234

- Murataliev MB, Feyereisen R (2000) Functional interactions in cytochrome P450(BM3). Evidence that NADP(H) binding controls redox potentials of the flavin cofactors. *Biochemistry* **39**: 12699-12707
- Myers GS, Rasko DA, Cheung JK, Ravel J, Seshadri R, DeBoy RT, Ren Q, Varga J, Awad MM, Brinkac LM *et al* (2006) Skewed genomic variability in strains of the toxigenic bacterial pathogen, *Clostridium perfringens*. *Genome Research* **16**: 1031-1040
- Nakanishi M, Yatome C, Ishida N, Kitade Y (2001) Putative ACP phosphodiesterase gene (acpD) encodes an azoreductase. *Journal of Biological Chemistry* **276**: 46394-46399
- Nam S, Renganathan V (2000) Non-enzymatic reduction of azo dyes by NADH. *Chemosphere* **40**: 351-357
- Navarre WW, Schneewind O (1999) Surface proteins of gram-positive bacteria and mechanisms of their targeting to the cell wall envelope. *Microbiology and Molecular Biology Reviews* **63**: 174-229
- Nishiya Y, Yamamoto Y (2007) Characterization of a NADH:dichloroindophenol oxidoreductase from *Bacillus subtilis*. *Bioscience, Biotechnology, and Biochemistry* **71**: 611-614
- Oakes J, Gratton P (1998) Kinetic investigations of the oxidation of Methyl Orange and substituted arylazonaphthol dyes by peracids in aqueous solution. *Journal of the Chemical Society-Perkin Transactions 2*: 2563-2568
- Ooi T, Ogata D, Matsumoto K, Nakamura G, Yu J, Yao M, Kitamura M, Taguchi S (2012) Flavin-binding of azoreductase: direct evidences for dual-binding property of apo-azoreductase with FMN and FAD. *Journal of Molecular Catalysis B-Enzymatic* **74**: 204-208
- Ooi T, Shibata T, Matsumoto K, Kinoshita S, Taguchi S (2009) Comparative enzymatic analysis of azoreductases from *Bacillus sp. B29*. *Bioscience, Biotechnology, and Biochemistry* **73**: 1209-1211
- Ooi T, Shibata T, Sato R, Ohno H, Kinoshita S, Thuoc TL, Taguchi S (2007) An azoreductase, aerobic NADH-dependent flavoprotein discovered from *Bacillus sp.*: functional expression and enzymatic characterization. *Applied Microbiology and Biotechnology* **75**: 377-386
- Pallen MJ (2002) The ESAT-6/WXG100 superfamily -- and a new Gram-positive secretion system? *Trends in Microbiology* **10**: 209-212
- Pandey A, Singh P, Iyengar L (2007) Bacterial decolorization and degradation of azo dyes. *International Biodeterioration & Biodegradation* **59**: 73-84
- Patton WF (2002) Detection technologies in proteome analysis. *Journal of Chromatography B-Analytical Technologies in the Biomedical and Life Sciences* **771**: 3-31
- Pelton JT, McLean LR (2000) Spectroscopic methods for analysis of protein secondary structure. *Analytical Biochemistry* **277**: 167-176

- Petitdemange H, Marczak R, Raval G, Gay R (1980) Menadione reductase from *Clostridium tyrobutyricum*. *Canadian Journal of Microbiology* **26**: 324-329
- Pickering BT (1966) Components of the cell wall of *Clostridium welchii* (type A). *The Biochemical Journal* **100**: 430-440
- Pollitt S, Zalkin H (1983) Role of primary structure and disulfide bond formation in beta-lactamase secretion. *Journal of Bacteriology* **153**: 27-32
- Priya B, Uma L, Ahamed AK, Subramanian G, Prabakaran D (2011) Ability to use the diazo dye, CI Acid Black 1 as a nitrogen source by the marine cyanobacterium *Oscillatoria curviceps* BDU92191. *Bioresource Technology* **102**: 7218-7223
- PSI-Plot. PSI-Plot. Poly Software International.
- Punj S, John GH (2008) Physiological characterization of *Enterococcus faecalis* during azoreductase activity. *Microbial Ecology in Health and Disease* **20**: 65-73
- Punj S, John GH (2009) Purification and identification of an FMN-dependent NAD(P)H azoreductase from *Enterococcus faecalis*. *Current Issues in Molecular Biology* **11**: 59-65
- PyMOL. PyMOL Molecular Graphics System. Schrodinger, LLC.
- Rafii F, Cerniglia CE (1990) An anaerobic non-denaturing gel assay for the detection of azoreductase from anaerobic bacteria. *Journal of Microbiological Methods* **12**: 139-148
- Rafii F, Cerniglia CE (1993) Localization of the azoreductase of *Clostridium perfringens* by immunoelectron microscopy. *Current Microbiology* **27**: 143-145
- Rafii F, Cerniglia CE (1995) Reduction of azo dyes and nitroaromatic compounds by bacterial enzymes from the human intestinal tract. *Environmental Health Perspectives* **103**: 17-19
- Rafii F, Coleman T (1999) Cloning and expression in *Escherichia coli* of an azoreductase gene from *Clostridium perfringens* and comparison with azoreductase genes from other bacteria. *Journal of Basic Microbiology* **39**: 29-35
- Rafii F, Franklin W, Cerniglia CE (1990) Azoreductase activity of anaerobic-bacteria isolated from human intestinal microflora. *Applied and Environmental Microbiology* **56**: 2146-2151
- Rafii F, Hall JD, Cerniglia CE (1997) Mutagenicity of azo dyes used in foods, drugs and cosmetics before and after reduction by *Clostridium* species from the human intestinal tract. *Food and Chemical Toxicology* **35**: 897-901
- Rafii F, Smith DB, Benson RW, Cerniglia CE (1992) Immunological homology among azoreductases from *Clostridium* and *Eubacterium* strains isolated from human intestinal microflora. *Journal of Basic Microbiology* **32**: 99-105
- Roberfroid MB, Bornet F, Bouley C, Cummings JH (1995) Colonic microflora - nutrition and health - summary and conclusions of an International Life Sciences Institute (ILSI) [Europe] workshop held in Barcelona, Spain. *Nutrition Reviews* **53**: 127-130

- Roland N, Nugon-Baudon L, Rabot S (1993) Interactions between the intestinal flora and xenobiotic metabolizing enzymes and their health consequences. *World Review of Nutrition and Dietetics* **74**: 123-148
- Rosch J, Caparon M (2004) A microdomain for protein secretion in Gram-positive bacteria. *Science* **304**: 1513-1515
- Roxon JJ, Ryan AJ, Wright SE (1967) Enzymatic reduction of tartrazine by *Proteus vulgaris* from rats. *Food and Cosmetics Toxicology* **5**: 645-656
- Russ R, Rau J, Stolz A (2000) The function of cytoplasmic flavin reductases in the reduction of azo dyes by bacteria. *Applied and Environmental Microbiology* **66**: 1429-1434
- Ryan A, Laurieri N, Westwood I, Wang CJ, Lowe E, Simi E (2010) A novel mechanism for azoreduction. *Journal of Molecular Biology* **400**: 24-37
- Sara M, Sleytr UB (2000) S-Layer proteins. *Journal of Bacteriology* **182**: 859-868
- Saratale RG, Saratale GD, Chang JS, Govindwar SP (2010) Decolorization and biodegradation of reactive dyes and dye wastewater by a developed bacterial consortium. *Biodegradation* **21**: 999-1015
- Saratale RG, Saratale GD, Chang JS, Govindwar SP (2011) Bacterial decolorization and degradation of azo dyes: a review. *Journal of the Taiwan Institute of Chemical Engineers* **42**: 138-157
- Savage DC (1977) Microbial ecology of gastrointestinal-tract. *Annual Review of Microbiology* **31**: 107-133
- Schaeffer AB, Fulton MD (1933) A simplified method of staining endospores. *Science* **77**: 194
- Schneewind O, Missiakas DM (2012) Protein secretion and surface display in Gram-positive bacteria. *Philosophical Transactions of the Royal Society of London Series B, Biological Sciences* **367**: 1123-1139
- Semde R, Pierre D, Geuskens G, Devleeschouwer M, Moes AJ (1998) Study of some important factors involved in azo derivative reduction by *Clostridium perfringens*. *International Journal of Pharmaceutics* **161**: 45-54
- Seronello S, Ito C, Wakita T, Choi J (2010) Ethanol enhances Hepatitis C virus replication through lipid metabolism and elevated NADH/NAD(+). *Journal of Biological Chemistry* **285**: 845-854
- Severin A, Nickbarg E, Wooters J, Quazi SA, Matsuka YV, Murphy E, Moutsatsos IK, Zagursky RJ, Olmsted SB (2007) Proteomic analysis and identification of *Streptococcus pyogenes* surface-associated proteins. *Journal of Bacteriology* **189**: 1514-1522
- Shimizu T, Ohtani K, Hirakawa H, Ohshima K, Yamashita A, Shiba T, Ogasawara N, Hattori M, Kuhara S, Hayashi H (2002a) Complete genome sequence of *Clostridium perfringens*, an anaerobic flesh-eater. *Proceedings of the National Academy of Sciences of the United States of America* **99**: 996-1001

- Shimizu T, Shima K, Yoshino K, Yonezawa K, Shimizu T, Hayashi H (2002b) Proteome and transcriptome analysis of the virulence genes regulated by the VirR/VirS system in *Clostridium perfringens*. *Journal of Bacteriology* **184**: 2587-2594
- Sievers F, Wilm A, Dineen D, Gibson TJ, Karplus K, Li WZ, Lopez R, McWilliam H, Remmert M, Soding J *et al* (2011) Fast, scalable generation of high-quality protein multiple sequence alignments using Clustal Omega. *Molecular Systems Biology* **7**: 539-544
- Smith S, Schaffner DW (2004) Evaluation of a *Clostridium perfringens* predictive model, developed under isothermal conditions in broth, to predict growth in ground beef during cooling. *Applied and Environmental Microbiology* **70**: 2728-2733
- Sneath PHA (1986) *Bergey's Manual of Systemic Bacteriology*, Vol. 2, Baltimore, MD: Williams & Wilkins.
- Song ZY, Zhou JT, Wang J, Yan B, Du CH (2003) Decolorization of azo dyes by *Rhodobacter sphaeroides*. *Biotechnology Letters* **25**: 1815-1818
- Sontag JM (1981) Carcinogenicity of substituted-benzenediamines (phenylenediamines) in rats and mice. *Journal of the National Cancer Institute* **66**: 591-602
- Sorrell MF, Tuma DJ (1985) Hypothesis - alcoholic liver injury and the covalent binding of acetaldehyde. *Alcoholism-Clinical and Experimental Research* **9**: 306-309
- Srinivasan A, Viraraghavan T (2010) Decolorization of dye wastewaters by biosorbents: a review. *Journal of Environmental Management* **91**: 1915-1929
- Stal MH, Blaschek HP (1985) Protoplast formation and cell wall regeneration in *Clostridium perfringens*. *Applied and Environmental Microbiology* **50**: 1097-1099
- Stolz A (2001) Basic and applied aspects in the microbial degradation of azo dyes. *Applied Microbiology and Biotechnology* **56**: 69-80
- Stothard P (2000) The sequence manipulation suite: JavaScript programs for analyzing and formatting protein and DNA sequences. *Biotechniques* **28**: 1102-1104
- Striegel AM, Yau WW, Kirkland JJ, Bly DD (2009) *Modern Size-Exclusion Liquid Chromatography: Practice of Gel Permeation and Gel Filtration Chromatography*, Second edn. Hoboken, NJ: John Wiley & Sons.
- Strober W (2001) Trypan blue exclusion test of cell viability. *Current Protocols in Immunology* **Appendix 3**: Appendix 3B
- Sugiura W, Yoda T, Matsuba T, Tanaka Y, Suzuki Y (2006) Expression and characterization of the genes encoding azoreductases from *Bacillus subtilis* and *Geobacillus stearothermophilus*. *Bioscience Biotechnology and Biochemistry* **70**: 1655-1665
- Suzuki Y, Yoda T, Ruhul A, Sugiura W (2001) Molecular cloning and characterization of the gene coding for azoreductase from *Bacillus sp. OY1-2* isolated from soil. *The Journal of Biological Chemistry* **276**: 9059-9065

- Tamura K, Peterson D, Peterson N, Stecher G, Nei M, Kumar S (2011) MEGA5: molecular evolutionary genetics analysis using maximum likelihood, evolutionary distance, and maximum parsimony methods. *Molecular Biology and Evolution* **28**: 2731-2739
- Tan K, Gu M, Kwon K, Anderson WF, Joachimiak A. (2012) The crystal structure of azoreductase from *Yersinia pestis* CO92 in complex with FMN. In Diseases CfSGoI (ed.), *PDB.org*.
- Tennant JR (1964) Evaluation of the trypan blue technique for determination of cell viability. *Transplantation* **2**: 685-694
- Tiffany ML, Krimm S (1969) Circular dichroism of random polypeptide chain. *Biopolymers* **8**: 347-359
- Tilton RG, Baier LD, Harlow JE, Smith SR, Ostrow E, Williamson JR (1992) Diabetes-induced glomerular dysfunction - links to a more reduced cytosolic ratio of NADH/NAD⁺. *Kidney International* **41**: 778-788
- Tortora G, Funke B, Case C (2012) *Microbiology: An Introduction*, Eleventh edn. San Francisco, CA: Pearson Benjamin Cummings.
- Vazquez-Laslop N, Lee H, Hu R, Neyfakh AA (2001) Molecular sieve mechanism of selective release of cytoplasmic proteins by osmotically shocked *Escherichia coli*. *Journal of Bacteriology* **183**: 2399-2404
- Vineis P, Pirastu R (1997) Aromatic amines and cancer. *Cancer Causes & Control* **8**: 346-355
- Vita N, Hatchikian EC, Nouailler M, Dolla A, Pieulle L (2008) Disulfide bond-dependent mechanism of protection against oxidative stress in pyruvate-ferredoxin oxidoreductase of anaerobic *Desulfovibrio* bacteria. *Biochemistry* **47**: 957-964
- Walker R, Gingell R, Murrells DF (1971) Mechanisms of azo reduction by *Streptococcus faecalis*. I. Optimization of assay conditions. *Xenobiotica* **1**: 221-229
- Walz A, Mujer CV, Connolly JP, Alefantis T, Chafin R, Dake C, Whittington J, Kumar SP, Khan AS, DeVecchio VG (2007) *Bacillus anthracis* secretome time course under host-simulated conditions and identification of immunogenic proteins. *Proteome Science* **5**: 11-20
- Wang CJ, Hagemeyer C, Rahman N, Lowe E, Noble M, Coughtrie M, Sim E, Westwood I (2007) Molecular cloning, characterisation and ligand-bound structure of an azoreductase from *Pseudomonas aeruginosa*. *Journal of Molecular Biology* **373**: 1213-1228
- Wang G, Chen H, Xia Y, Cui J, Gu Z, Song Y, Chen YQ, Zhang H, Chen W (2013) How are the non-classically secreted bacterial proteins released into the extracellular milieu? *Current Microbiology* **67**: 688-695
- Westermeier R, Marouga R (2005) Protein detection methods in proteomics research. *Bioscience Reports* **25**: 19-32
- White K. unfoldprotein.m. MATLAB.

- Whitman WB, Coleman DC, Wiebe WJ (1998) Prokaryotes: The unseen majority. *Proceedings of the National Academy of Sciences of the United States of America* **95**: 6578-6583
- Whitmore L, Wallace BA (2004) DICHROWEB, an online server for protein secondary structure analyses from circular dichroism spectroscopic data. *Nucleic Acids Research* **32**: W668-W673
- Whitmore L, Wallace BA (2008) Protein secondary structure analyses from circular dichroism spectroscopy: methods and reference databases. *Biopolymers* **89**: 392-400
- Wickner W, Schekman R (2005) Protein translocation across biological membranes. *Science* **310**: 1452-1456
- Wilkins MR, Gasteiger E, Bairoch A, Sanchez JC, Williams KL, Appel RD, Hochstrasser DF (1999) Protein identification and analysis tools in the ExPASy server. *Methods in Molecular Biology* **112**: 531-552
- Willardsen RR, Busta FF, Allen CE (1979) Growth of *Clostridium perfringens* in three different beef media and fluid thioglycollate medium at static and constantly rising temperatures. *Journal of Food Protection* **42**: 144-148
- Wright CM (2007) Molecular cloning and expression of a putative FMN-dependent NADH-azoreductase from *Clostridium perfringens*. Masters of Science Thesis, Microbiology and Molecular Genetics, Oklahoma State University, Stillwater, OK
- Xia G, Kohler T, Peschel A (2010) The wall teichoic acid and lipoteichoic acid polymers of *Staphylococcus aureus*. *International Journal of Medical Microbiology* **300**: 148-154
- Xu MY, Guo J, Cen YH, Zhong XY, Cao W, Sun GP (2005) *Shewanella decolorationis* sp nov., a dye-decolorizing bacterium isolated from activated sludge of a waste-water treatment plant. *International Journal of Systematic and Evolutionary Microbiology* **55**: 363-368
- Yamanaka S, Nishihara T, Hattori M, Suzuki Y (1987) Preparation and properties of titania pillared clay. *Materials Chemistry and Physics* **17**: 87-101
- Yan B, Du CH, Xu ML, Liao WC (2012) Decolorization of azo dyes by a salt-tolerant *Staphylococcus cohnii* strain isolated from textile wastewater. *Frontiers of Environmental Science & Engineering* **6**: 806-814
- Zhang R, Gu M, Tan K, Kwon K, Anderson WF, Joachimiak A. (2011) The crystal structure of FMN-dependent NADH-azoreductase from *Bacillus anthracis* str. Ames Ancestor. In Diseases CfSGoI (ed.), PDB.org.
- Zille A, Ramalho P, Tzanov T, Millward R, Aires V, Cardoso MH, Ramalho MT, Gubitz GM, Cavaco-Paulo A (2004) Predicting dye biodegradation from redox potentials. *Biotechnology Progress* **20**: 1588-1592
- Zimmermann T, Gasser F, Kulla HG, Leisinger T (1984) Comparison of two bacterial azoreductases acquired during adaptation to growth on azo dyes. *Archives of Microbiology* **138**: 37-43

Zimmermann T, Kulla HG, Leisinger T (1982) Properties of purified Orange-II azoreductase, the enzyme initiating azo dye degradation by *Pseudomonas* KF46. *European Journal of Biochemistry* **129**: 197-203

VITA

Jessica Marie Morrison

Candidate for the Degree of

Doctor of Philosophy

Thesis: A BIOCHEMICAL, PHYSIOLOGICAL AND STRUCTURAL
CHARACTERIZATION OF *AzoC*, A NOVEL AZOREDUCTASE FROM
CLOSTRIDIUM PERFRINGENS

Major Field: Microbiology, Cell and Molecular Biology

Biographical:

Education:

Completed the requirements for the Doctor of Philosophy in Microbiology, Cell and Molecular Biology at Oklahoma State University, Stillwater, Oklahoma in May, 2015.

Completed the requirements for the Bachelor of Science in Biology at Saginaw Valley State University, University Center, Michigan in 2010.

Completed the requirements for the Bachelor of Science in Medical Technology at Saginaw Valley State University, University Center, Michigan in 2010.

Experience:

Graduate Research/Teaching Associate, Department of Microbiology and Molecular Genetics, Oklahoma State University, Stillwater, Oklahoma.
2010-present

Technical Laboratory Co-op, Dow Corning Corporation, Midland, Michigan.
2007-2010

Professional Memberships:

American Chemical Society (ACS), National Member

American Society of Microbiology (ASM), National and Missouri Valley
Branch Regional Member

Society for the Advancement of Chicanos and Native Americans in Science
(SACNAS), National and Oklahoma State University Chapter Member

Society of Environmental Toxicology and Chemistry (SETAC), National and
Ozark-Prairie Regional Branch Member